THE ROLE OF *CANDIDA ALBICANS* OXIDATIVE STRESS RESPONSES IN TRIGGERING FILAMENT FORMATION AND MACROPHAGE ESCAPE FOLLOWING PHAGOCYTOSIS.

DR. BEATRICE ACHAN, BDS, M. MED (MAKERRE UNIVERSITY),
MRES (UNIVERSITY OF ABERDEEN).

**THESIS SUBMITTED FOR THE DEGREE OF
DOCTOR OF PHILOSOPHY.**

INSTITUTE OF CELL AND MOLECULAR BIOSCIENCES (ICAMB)
FACULTY OF MEDICAL SCIENCES
NEWCASTLE UNIVERSITY, UK.

MAY, 2018.

ABSTRACT

Candida albicans is an important opportunistic fungal pathogen which causes life threatening systemic diseases in immunocompromised people. An important virulence attribute of *C. albicans* is morphological plasticity. Yeasts engulfed by macrophages can transition to a hyphal filamentous morphology which either induce pyroptosis or rupture the phagosomal membrane of the macrophage and evade the toxic reactive oxygen species (ROS) generated by the NADPH oxidase complex of the phagocyte. Recent studies revealed that ROS causes cell cycle arrest resulting in hyperpolarised bud formation in *C. albicans*. Moreover, the ability of this pathogen to mount robust transcriptional responses to ROS is an essential pre-requisite for hyphal filament formation following phagocytosis. Thus, it was hypothesised that macrophage-derived reactive oxygen species (ROS) can inhibit *C. albicans* growth, which is more pronounced in ROS-sensitive mutants resulting in impaired filament formation following phagocytosis. Hence, the aim of this study was to decipher why *C. albicans* responses to ROS are important for filament formation in the phagolysosomal environment of the macrophage.

In vitro, it was examined whether hydrogen peroxide (H_2O_2)-treatment could inhibit serum-induced hyphae formation and whether this was more pronounced in cells lacking the key Cap1 oxidative-stress responsive transcription factor, and its regulators Ybp1 and Gpx3. The results showed that exposure to H_2O_2 inhibited serum-induced hyphae formation. In addition, the inhibition of filament formation was more sustained in the *cap1*Δ, *ybp1*Δ and *gpx3*Δ mutant cells compared to the wild-type strain. A concurrent analysis of cell survival indicated that the mutant cells displayed a longer H_2O_2-induced growth arrest compared to wild-type cells. Hence, to identify regulators of hyperpolarised bud formation and, determine if ROS-resistance is a global requirement for filament formation following phagocytosis, a library of transcription factor mutants was screened for sensitivity to different forms of ROS. The most sensitive mutants; *cap1*Δ, *efg1*Δ, *skn7*Δ, *ndt80*Δ, and *gzf3*Δ were examined for ability to survive and form filaments following phagocytosis using confocal video microscopy. Only *cap1*Δ and *efg1*Δ cells failed to form filaments following phagocytosis. However, the three remaining mutants effectively formed filaments inside the phagosomal environment.

Collectively, these data show that whilst Cap1 is essential for filament formation inside the macrophage, wild-type levels of oxidative stress resistance are not a necessary pre-requisite for this morphological switch following phagocytosis.

DEDICATION

Mummy.

With much fondness, this is for you. Thank you for always being there for me. Your constant encouragement and specially prepared peanut butter (‘*odii*’) always made me feel at home.

ACKNOWLEDGEMENTS.

I would like to thank everyone who contributed to the success of my PhD:

Supervisor; Prof. Janet Quinn and co-supervisor; Prof. Brian Morgan.

On site 'Outside study' advisers; Prof. Lars Erwig and, Prof. Neil Gow, Prof. Alistair Brown, Dr. Donna Maccallum (University of Aberdeen).

Post-doctoral Researchers: Dr. Alison Day (Newcastle University), Dr. Jude Bain, Dr. Louise Walker (University of Aberdeen).

Technician: Susan Badge.

Panel Assessors: Dr. Desa Lilic and Dr. Jeremy Brown.

Postgraduate tutor and Mentor: Dr. Tim Cheek and ICAMB.

Administrative support: Mrs Louise Campbell (Newcastle University), Dr. Karen Mcardle, Dr. Tehmina Amin (University of Aberdeen).

Support provided by the Student Wellbeing services with a special appreciation to Ms Jenny Wallace (Newcastle University) and, Student support services (University of Aberdeen).

IT service desks: Newcastle University and University of Aberdeen.

Home Institutions' leadership support: Dr. Henry Kajumbula (Chair, Department of Medical Microbiology and, Makerere University), Prof. Moses Joloba (Dean School of Biomedical Sciences, Makerere University), Dr. Andrew Kambugu (Infectious Diseases Institute, Makerere University).

Family and friends; Ms Amon Albina (Mummy), Atim Susan, Odokonyero Joseph, Luwum Innocent, Mrs Okello-Olobo Regina & family, Gabriela Campano Alvarez, Eloise Ballard, Ijeoma Okoliegbe, Lucian Duvanage, Dr. Anita Tumwebaze K. Muhumuza, Eva Laker Agnes Odongpiny, Brenda Kitimbo and Sylvia Irene Wanzala.

The project was funded by the Wellcome Trust Strategic Award for Medical Mycology and Fungal Immunology (WTSA-MMFI).

CONTENTS

List of Figures.

List of Tables.

LIST OF ABBREVIATIONS

Acronyms

dH_2O	Distilled H_2O
DIC	Differential interference contrast
DMEM	Dulbeco's Modified Eagle's Medium
FBS	Fetal Bovine Serum
H_2O_2	hydrogen peroxide
IL	Interleaukin
mM	milli Molar
°C	Degrees Celsius
OD_{600}	Optical density at 600 nm
PBS	Phosphate buffered saline
PCR	Polymerase chain reaction
PEG	Polyethylene glycol
SD	Standard deviation
SDS	Sodium dodecyl sulphate
TAE	Tris Acetate
TBS	Tris Buffered Saline
TE	10 mM Tris-HCl, 1mM EDTA
Tris	tris (hydroxymethyl)aminomethane
mM	millimolar
µM	micromolar
µl	microliter

CHAPTER ONE.

1 INTRODUCTION.

1.1 *Candida albicans*.

1.1.1 Taxonomy, nomenclature and history.

Candida albicans is a polymorphic species of yeast which belongs to a class which does not fit the main fungal taxonomic ranks based on sexual reproduction cycles. It is grouped within the '*fungi imperfecti*', deuteromycetes or anamorphic fungi that lack a recognised sexual cycle (Odds, 1987). Some deuteromycetes are related to sexual ascomycetes and others to basidiomycetes (Odds, 1987). The genus *Candida* is characterized by white asporogeneous yeasts which can transition to filamentous morphotypes (Shepherd *et al*., 1985) and are composed of over 150 species of which only 7 or 8 species are of medical importance (Samaranayake, 1990). The most common species which are associated with over 92 % of diseases are *Candia albicans* (65.3 %), *Candida glabrata* (11.3 %), *Candida tropicalis* (7.2 %), *Candida parapsilosis* (6.0 %) and *Candida krusei* (2.0 %). Other rarely isolated species include *Candida dubliniensis, Candida gulliermondii* and *Candida lusitaniae* (Pfaller *et al*., 2010). Furthermore, there are emerging cases of *Candida auris*; a hospital-acquired multidrug resistant species (Chowdhary *et al*., 2017). *C. albicans*; the most commonly isolated species exists predominantly as yeasts (unicellular forms) which are round/ovoid in shape, approximately 4 to 6 µm in size, reproduce by budding that can transition to various morphological forms including filamentous hyphae or pseudohyphae. Over the years there have been over 160 synonyms of which *Oidium albicans* and *Monilia albicans* were the most common names of what is now called *C. albicans* (Yeasts: Characteristics and Identification, 3rd Edition, 2001). First described as an aetiological agent of oral candidiasis in the mid-19th century in 1843, *C. albicans* derives its name from the ancient Roman custom; "*candidatus*" which refers to a *candidate* for public office who dressed in white and "*albico*" also means white. White is depictive of the colour of probable oral thrush for which written descriptions date back to the time of Hippocrates and Galen (Odds, 1987).

A significant increase in the incidence of *C. albicans* infections began in the 1940s due to the widespread use of antibacterial antibiotics. Patients undergoing treatment with antibiotics developed symptoms and signs of thrush including sore mouth and hairy tongue (Woods *et al*., 1951). Growth in the number of cases of systemic candidiasis was

observed in the 1980s due to compromised immune system of individuals with HIV/AIDS and in patients undergoing chemotherapy for cancer, or undergoing immunosuppressive therapy to avoid transplant rejection (Sternberg, 1994). Other factors included advancement in the practice of modern medicine which promotes prolonged hospital stay in the intensive care unit (ICU) that is accompanied by use of medical devices such as in-dwelling catheters (Weinstein, 2005). Since then, the incidence of candidiasis has maintained an upward trend (Pfaller *et al*., 2006). Significantly, *C. albicans* is among the top ten causes of nosocomial blood stream infection (Chowdhary *et al*., 2017).

1.1.2 Epidemiology.

C. albicans exists as a commensal flora of the gastrointestinal tract and the vagina of about 50 to 80% of healthy individuals (Odds, 1987) but it is also the most prevalent opportunistic fungal pathogen (Pfaller *et al*., 2006). Immune-compromisation promotes the transition of *C. albicans* from a harmless coloniser to a pathogen (Pfaller *et al*., 2006, Casadevall, 2014). *C. albicans* can cause a wide spectrum of diseases that range from superficial to invasive candidiasis as dictated by the immune status (Netea *et al*., 2010).

In the setting of defective T cell immunity, clinical observations showed that patients develop superficial candidiasis (Netea *et al*., 2010). Superficial candidiasis can take the form of vulvovaginal candidiasis (VVC), oropharyngeal candidiasis (OPC) and/or chronic mucocutaneous candidiasis (CMC) (van de Veerdonk *et al*, 2010). The most common form of superficial candidiasis is VVC which occurs in about 50 -70 % of women of reproductive age at least once in lifetime (Brown *et al*., 2012). The risk of VVC is increased due to diabetes mellitus, prolonged broad spectrum antibiotic therapy, oral contraceptive use and pregnancy. Notably, in the majority of VVC cases there is no underlying cause (van de Veerdonk *et al*, 2010) . The clinical presentations of VVC include pruritis, dyspareunia and curd like vaginal discharge (van de Veerdonk *et al*, 2010). Nearly 5-8 % of the patients with VVC go on to have recurrences four times annually in what is termed as complicated VVC. In contrast to uncomplicated VVC which is commonly caused by *C. albicans*, complicated VVC is due to species other than *C. albicans* (Sobel *et al*., 2007, Brown *et al.*, 2012). Patients who wear dentures, are receiving broad spectrum antibiotic therapy, infants and HIV/AIDS patients are at increased risk for OPC (Patuwo *et al*., 2015). A common presentation of OPC is thrush which occurs asymptomatically in the oropharynx of up to 90 % of HIV infected patients as AIDS defining illness (Peacock *et al*., 2017). About 50 % of HIV/AIDS patients with OPC show at least one clinical episode which, if untreated can progress to disseminated

candidiasis (Brown *et al*., 2012). Superficial candidiasis can also manifest as heterogeneous, chronic infections of the mucous membranes, skin, hair and nails despite usual adequate therapy, in a condition known as CMC (van de Veerdonk *et al*., 2016). The major risk factor for CMC is T cell primary immunodeficiency (Lilic *et al*, 2003). Over the years, CMC-induced *Candida* esophagitis can be complicated by esophageal stenosis, and disfiguring lesions of the face, nails and alopecia (van de Veerdonk *et al*, 2010).

On the other hand, systemic candidiasis tends to occur when there are defects in phagocytes and due to factors that alter the integrity of the gut epithelium for example, large bowel surgery, or the due to disruption of the skin integrity at the site of indwelling catheter (Netea *et al*., 2010, Kullberg *et al*., 2015). Other risk factors include long term use of immunosuppressive drugs following transplantation, or cancer which also alter the gut epithelium (Pfaller *et al*., 2006, Netea *et al*., 2010). Systemic candidiasis can occur either as a deep-seated infection of hepato-splenic organs, muscle, joints, bones, ocular and/or central nervous systems or more commonly, as candidaemia where it is estimated as the fourth most common nosocomial blood stream infection (BSI) in intensive care units. The highest incidences of candidaemia are at the extremes of age (Wisplinghoff *et al*., 2004, Kullberg *et al*., 2015).

In the laboratory, *C. albicans* can be rapidly identified using the microscopy-based germ tube test (GTT) (Sheppard *et al*., 2008). From the agar plate culture of thrush swab, blood and/or aspirated samples from deep seated infections, a light loopful of inoculum is suspended in 0.5 mL of sterile foetal bovine serum. The culture is incubated at 37˚C for 2-3 hours then a drop is observed with low power field microscopy. *C. albicans* form germ tubes which are identifiable as parallel sided filaments without constrictions between the mother and daughter cells (Sheppard *et al*., 2008). But as some species of *Candida* can also form germ tubes, *C. albicans* can be further identified by its ability to assimilate of a panel of sugar substrates (Miramón *et al*., 2017) and its distinctive light green colonies on ChromCandida agar (Ghelardi *et al*., 2008) .

Treatment of superficial candidiasis is primarily based on topical application of nytstatin, while topical clotrimazole and miconazole are alternatives. Oral itraconazole can be used for refractory cases. Oral fluconazole or the extended azole family such as voriconazole can be used for treatment of chronic, persistent CMC cases (Bondaryk *et al*., 2013). The treatment of systemic candidiasis is based on three classes of drugs. The intravenously administered Amphotericin B deoxycholate and its more efficacious liposomal form (Ambisome) remain the drug of choice for systemic candidiasis. The azoles (fluconazole and

voricozole) and the intravenous echinocandins (caspofungin) are as affective as Amphotericin B and have reduced side effects (Kullberg et al., 2015, Pappas *et al*., 2015). Unlike superficial candidiasis, systemic candidiasis is associated with a high mortality rate which can approach 50 % despite antifungal therapy, mainly due to late initiation of treatment. In some cases, antifungal therapy is complicated by drug resistance (Pfaller *et al*., 2006).

Resistance of *C. albicans* to the antifungal agents are emerging due to mechanisms such as decreased intracellular drug concentration, binding affinity and antagonism of the drugs (Schwartz *et al*., 2018). Decreased intracellular drug concentration occurs through upregulation of efflux pumps encoded by *CDR1*, *CDR2* and the *MDR1* genes (Pfaller *et al*., 2011). Decreased drug-binding affinity due to *ERG11* leads to increased minimum inhibitory concentrations, while counteracting the effects of the drugs occurs through upregulation of the target protein, and alteration of the last steps of biosynthesis of ergosterol (Pfaller *et al*., 2011, Schwartz *et al*, 2018). The high burden of *C. albicans* has prompted in depth research into how *C. albicans* evades the host's immune defense system.

1.2 Host defense.

The primary defense against systemic candidiasis is provided by professional phagocytes of the innate immune system primarily; neutrophils and monocytes such as macrophages (van 't Wout *et al*., 1988, Cheng *et al*., 2012, Lehrer, Cline 1969, Qian *et al*., 1994, Erwig *et al*., 2016). Neutrophils employ both oxidative and non-oxidative mechanisms to alleviate *Candida* infections (Aratani *et al*., 1999, Amulic *et al*., 2012). Significantly, neutrophils are the only immune cells which are able to inhibit *C. albicans* yeast to hypha morphogenesis (Fradin *et al*., 2005). Through ROS-dependent death pathway activation, neutrophils can form the neutrophil extracellular traps (NETs) (Brinkmann *et al*., 2004) which trap and kill the fungus (Urban *et al*., 2006). The role of neutrophils in host defence against *Candida* is underscored by the increased incidence of systemic disease in patients with neutropenia (Richardson *et al*., 2009). However, as *Candida* can transition from yeast to hyphae inside the macrophage which are also easily cultivatable in the laboratory and because the macrophage host is the model which was used for my PhD experiments, the following review of host defense is biased towards macrophage-*Candida* interaction.

Phagocytosis; the process by which phagocytes kill *Candida* can be divided into distinct stages. These include migration, recognition, engulfment, phagosome maturation and killing (Rudkin *et al*., 2013). Migration is the process by which phagocytes move to colocalise with *Candida* (Nourshargh *et al*., 2014). Migration is initiated by the recognition of molecular motifs on the pathogen that are collectively called Pathogen Associated

Molecular Patterns (PAMPS) which are evolutionarily conserved within fungi but absent in self (Medzhitov *et al.*, 2002). Macrophages recognize the PAMPS using Pathogen Recognition Receptors (PRRs). Examples of PRR-fungal PAMPS include mannose recognizing receptors, in particular, Dectin 1 and Dectin 2 which are C-type lectin receptors (CLRs) for β-1,3-glucans and α-mannans, respectively (Dambuza *et al*., 2015), NOD-like receptors which recognize chitin and β-1,3-glucans motifs (Wagener *et al*., 2014), (Netea, Brown *et al*., 2008, Romani, 2011) while TLR7 and TLR9 are involved in the intracellular recognition of the fungal DNA (Kasperkovitz *et al*., 2011, Biondo *et al*., 2012). Recognition of *C. albicans* is important for the recruitment of phagocytes to the site of infection and/ or the orchestration of adaptive immune response (Netea *et al*., 2008, Becker *et al*., 2015). Phagocytosis of *C. albicans* involves mainly CR3 (α_M β_2, CD11b/CD18) that binds to opsonins on the surface of the fungus. The CR3 binds to C3b to promote phagocytosis by activating the alternative pathway of complement (Heinsbroek *et al*., 2008).

Upon engulfment, *C. albicans* are confined in phagosomes, which are defined as vacuoles that are derived from the plasma membranes of the phagocyte. The membranes of the phagocytic vacuole, mediated by Rab GTPases, undergo remodeling through fusion and fission followed by activation and production of acidifying hydrolytic enzymes in process called phagosome maturation (Okai *et al*., 2015). Phagosome maturation follows the endocytic pathway for maturation (Okai *et al*., 2015). There is sequential fusion of the phagosomes with the early, late endosomes and lysosomes, including the assembly of actin filaments. The Rab GTPase proteins regulate the biochemical composition and the phagolysosome fusion by determining the fusion partners and lipid composition of the plasma membranes (Fairn, 2012). Characterization of Rab proteins showed that Rab5 rapidly and transiently associates with the phagosomes while Rab7 associates with the phagosomal membrane for interactions is important for late endosome/lysosome fusion (Niedergang *et al*., 2018). Phagosome maturation, also called phagolysosome biogenesis leads to progressive acidification (Fairn, 2012). The acidic pH promotes activities of the hydrolases such as lysozymes for a fungicidal effect (Okai, *et al*., 2015, Vieira *et al*., 2002). Recently, it was shown that Rab14 enhances the maturation of phagosomes with *C. albicans* but is dysregulated in the presence of the hyphal cells allowing fungal survival and escape following phagocytosis (Bain *et al*., 2014). Macrophages use both oxidative and non-oxidative/enzymatic mechanisms of killing (Cheng *et al.*, 2012, Qian *et al*., 1994, Netea *et al.*, 2008). Following phagocytosis, three outcomes are possible. Cells of *C. albicans* may be killed (Krysan *et al*., 2014), or they may escape by non-lytic expulsion in in which both *C.*

albicans and the macrophage remain viable (Bain *et al*., 2012), or following yeast to hyphae transition, *C. albicans* may escape phagocytosis and induce macrophage death *(Patterson et al*., 2013, Uwamahoro *et al*., 2014) (Figure 1).

Macrophages and dendritic cells of the innate immunity mediate adaptive cell-mediated response to *C. albicans* (Verma *et al*., 2015). Following recognition and ingestion of *C. albicans*, activated dendritic cells home to the peripheral lymph nodes (Netea *et al*., 2015). Dendritic cells present the processed exogenous peptide antigens in association with major histocompatibility complex class II (MHCII) to the memory and naïve T cells (Fidel *et al*., 2002) . Both $CD8^+$ T and $CD4^+$ T cells show anti-*Candida* immunity. *In vitro* studies showed that the cytotoxic $CD8^+$ T cells inhibit yeast to hyphae morphogenesis. However, the protective role of $CD4^+$ T cells is the predominant cell mediated immunity to *C. albicans*. This is highlighted by the increased incidence of oropharyngeal candidiasis in HIV/AIDS patients due to $CD4^+$ T cell lymphopenia (Fidel *et al*., 2002) . The naïve $CD4^+$ T cells can differentiate to four different phenotypes depending on the cytokine milieu (Huang *et al*., 2009). The $CD4^+$ T cell production of IL-12/ IFNγ leads to Th1, IL-4 to Th2, IL-1β/IL-6/IL-23 leads to Th17 and IL-2/TGFβ polarizes to T regulatory cell phenotypes (Romani *et al*, 1999). The predominant phenotype determines the outcome of infection. Historically, Th1 showed protective immune response against oral and gut candidiasis (Romani *et al*., 1999) . However, more recent studies indicate that roles of Th17 cells are superior to Th1 cells in for anti-*Candida* immunity. The Th17 cells express chemokine receptors CCR4 and CCR6, and secrete cytokines; IL-17A, IL-17F, IL-22. The IL-17 recruits and activates neutrophils while IL-22 enhances epithelial barrier protection. Therefore, polarization of $CD4^+$ T either to Th1 or Th17 phenotype offer protective anti *Candida* immunity against chronic mucocutaneous candidiasis and systemic disease (Hernández *et al*., 2012). However, the Th2 phenotype predisposes to disseminated Candidiasis (Richardson *et al*., 2015). The T-regulatory cells induce peripheral tolerance by limiting the expansion of Th17 cells to minimize inflammatory-mediated host damage (Whibley *et al*., 2014) . It is noteworthy that the roles of the T helper phenotypes are location specific. For example, although Th1 and Th17 cells offer protective effects along the gastrointestinal tract, the individual is still susceptible to vulvovaginitis (Van De Veerdonk *et al*., 2010). The γδT cells are important for protection against *Candida* vaginitis (Wormley *et al*., 2001).

Humoral immunity to *C. albicans* is important because antibodies are used for opsonisation, complement activation (CR3) and antibody dependent cell mediated cytotoxicity (ADCC). Studies showed that antibodies bind to fungal targets such as

polysaccharides, which are cell wall associated (Lopez *et al*., 2004). Therefore, antibodies can inhibit host-*Candida* interactions such as hypha formation, growth and induce cell death (Casadevall *et al*, 2012). Studies for the use of monoclonal antibodies as therapy are still inconclusive, however, they are promising adjunct therapy for treatment of candidiasis (Moragues *et al*., 2014).

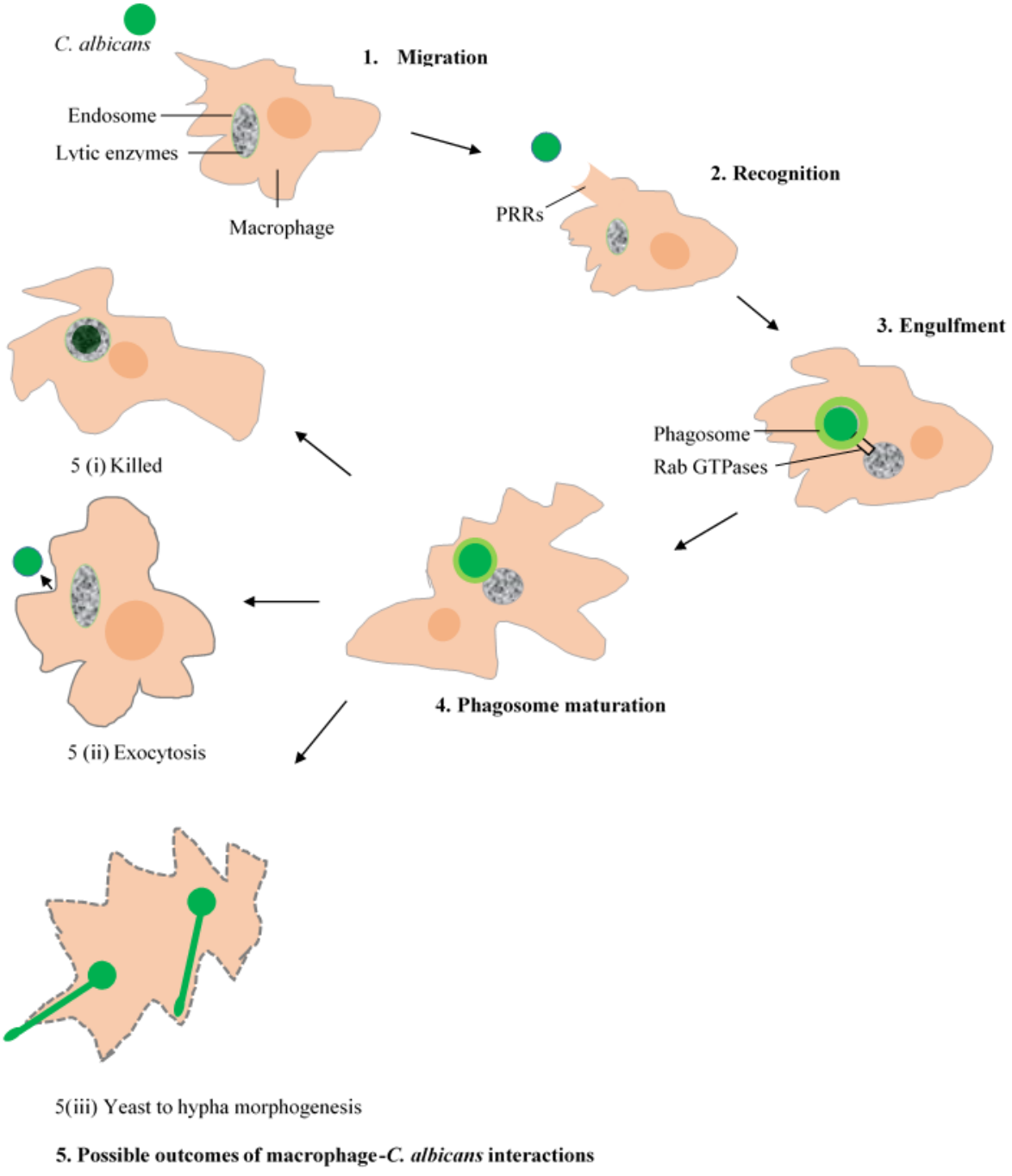

Figure 1: Outcomes of macrophage - *C. albicans* interactions.
Phagocytosis can be divided into distinct steps of; 1. Migration, 2. Recognition, 3. Engulfment, 4. Phagosome maturation and 5. Possible killing or escape. *C. albicans* may (i) be killed but the macrophage remains viable (Krysan *et al*., 2014) (ii) escape by non-lytic expulsion whereby both *C. albicans* and macrophage remain alive (Bain *et al*., 2012) or (iii) survive reactive oxygen species, switch morphology from yeast to hyphae, induce macrophage death and escape phagocytosis (Patterson *et al*., 2013, Uwamahoro *et al*., 2014).

1.2.1 Reactive Oxygen Species (ROS).

In response to phagocytic stimuli such as such as PRR binding to their cognate PAMP, phagocytes rapidly create high hourly oxidative, antimicrobial elements called the oxidative burst (El-Benna *et al*., 2005, Segal *et al*., 2012). The oxidative burst is

catalyzed by the multiunit NADPH-dependent oxidase (Forman, 2002, El-Benna *et al*., 2005, El-Benna *et al*., 2009). The NADPH oxidase is constitutively expressed and active in all cells but inactive in phagocytes which are not activated (Krause, 2004). Phagocytes express PHOX or NOX2 of the phagocyte which play active roles in immune defence (El-Benna *et al*., 2009). The NOX2 complex is composed of p47phox, p67phox, p40phox and RAC1and RAC2 regulatory subunits which after phagocytic activation, assemble at the plasma and phagosomal membranes to generate oxidants (Groemping *et al*., 2005). The ROS are produced by sequential addition of electrons to molecular oxygen to form superoxide anions (Segal *et al*., 2012). Superoxide anions (primary ROS) are highourly reactive with other molecules to generate secondary ROS such as hydrogen peroxide and hydroxyl radicals.

$O_2 + e^- \rightarrow O2^{\cdot -}$

Hydrogen peroxide is produced when two molecules of superoxide react together in a reaction catalyzed by the enzyme superoxide dismutase (Kehrer, 2000). Alternatively, superoxide is decomposed in a reaction that is catalyzed by superoxide dismutase to produce peroxide which is then protonated to produce hydrogen peroxide and oxygen;

$2\ O_2^{\cdot} + 2H^+ \rightarrow \ H_2O_2 + O_2$

Hydrogen peroxide can be further used to generate hydroxyl anions and radicals in Haber Weiss reaction (Kehrer, 2000).

1.2.2 Cellular effects of ROS.

ROS can cause damage to cellular biomolecules including lipids, protein and DNA that can result in growth arrest, senescence or death depending on the level of oxidation. Cellular effects of ROS vary by the target biomolecule (Lambeth *et al*., 2014). The ROS can lead to peroxidation of fatty acids which form components of the lipid bilayer of the cell membrane. Peroxidised fatty acids are unstable molecules that eventually compromise the integrity of the cell (Kwiecien *et al*., 2014). Reaction of ROS with proteins can lead to inactivation of the proteins (Davies, 2005). For example, the oxidation of cysteine through its thiol residue forms a disulfide derivative that is a constituent in many proteins (Alcock *et al*., 2018). Oxidation of methionine can lead to methionine sulfoxide and methionine sulfone which lead to instability and loss of function of the protein (Swaim *et al*., 1988), (Levine *et al*., 2000). The damage caused by ROS on DNA can be either structural or functional. Structural damage to DNA arises from events such as DNA strand breaks, inter/intra-strand and DNA-protein cross-links.

The most detrimental DNA structural damage is double strand breaks because they are difficult to repair (Klaunig *et al*., 2011). Mutated DNA affects the functioning and causes infidelity during replication which is followed by genomic instability and cell death (Olinski *et al*., 2002).

1.3 Pathogenesis.

Even though the macrophage has developed elaborate mechanisms for defense and clearance of *C. albicans*, in an immune compromised host, *C. albicans* can cause diseases dependent on the virulence and fitness attributes and, the organism's ability to avoid immune surveillance and potency.

Virulence factors are fungal factors that interact directly with host components to cause disease (Odds *et al*., 2001, Mayer *et al*., 2013). These include morphological plasticity, adhesins, invasins, hydrolytic enzymes, phenotypic variation (Calderone *et al*., 2001, Mayer *et al*., 2013). In contrast, there are a set of factors which are known as fitness attributes that act indirectly to facilitate the robust response of the fungus to the changing unfavorable host microenvironments (Ene *et al*., 2014). Fitness attributes thus, mediate the adaptation of *C. albicans* to the host. My PhD project was centered on investigating the relationship between oxidative stress responses and morphogenesis. Hence, I have focused mainly on these fitness and virulence attributes, respectively, with a brief description of the remaining determinants.

1.3.1 Virulence Attributes.

1.3.1.1 Morphological Switch.

A distinct virulence attribute of *C. albicans* is pleomorphism. *C. albicans* has the ability to switch among various yeast and filamentous forms. The filamentous forms of *C. albicans* include hyphae, pseudohyphae (Odds *et al*., 1998, Sudbery *et al*., 2004), and hyperpolarised buds (Bachewich *et al*., 2005, Da Silva *et al*., 2010). The morphological forms differ in physical characteristics (Figure 1), cell cycle regulation and gene expression profiles which thus, impact on their roles in pathogenesis and immune recognition (Mukaremera *et al*., 2017).

1.3.1.1.1 Morphological forms.

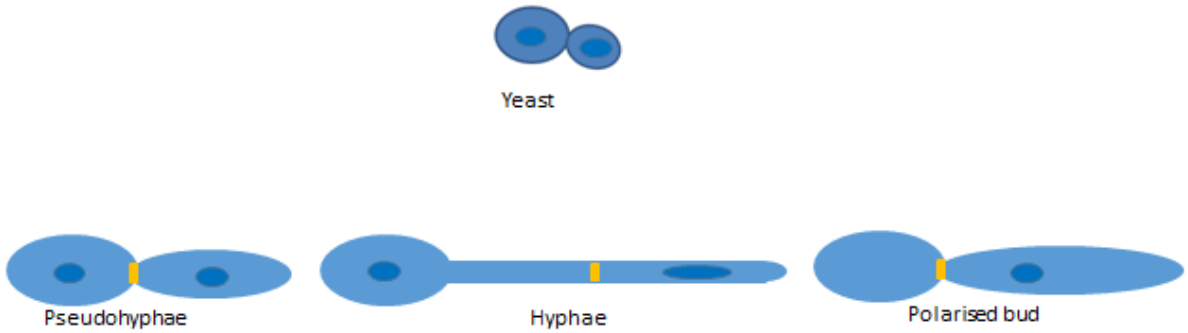

Figure 2: **Morphological forms of *C. albicans*.**
Yeasts are unicellular forms. Pseudohyphae have constrictions at the sites of septation of mother and daughter and are wider in diameter than hyphae. Hyphae are thin with parallel sides and lack constrictions at the sites of septation of the mother and daughter cells (Sudbery, Gow et al. 2004). Another filamentous form that has a constriction at the point of septation of the mother and daughter cells is the hyperpolarised bud which is a single elongated cell characterized by movement of the nucleus from the mother to the daughter cell. Unlike the multicellular hyphae and pseudohyphae which are multi nucleated, hyperpolarized buds have singlet nuclei (Bachewich *et al*., 2005, Da Silva *et al*., 2010).

1.3.1.1.2 Induction of the hyphal/pseudohyphal morphological switch.

Filamentation is induced by different environmental cues that typically mimic the diverse microenvironments in the host. Hypha formation is induced by many factors including, but not limited to serum, neutral pH, 5% CO_2, N- acetyl- D- glucosamine (GlcNAc), growth in microaerophilic atmosphere, temperature of 37^{o}C (Sudbery, 2011) and suppressed by others, for example, quorum sensing farnesol (Lu *et al*., 2014).

Mechanisms of induction of the filamentous forms of *C. albicans* by these factors have been elucidated. Amino acid starvation induces pseudohyphal growth in a Gcn4 dependent manner by upregulating the biosynthesis of amino acid genes (Tripathi *et al*., 2002). Carbon and nitrogen limitation in GlcNAc or Spider media induce hyphae formation through the ammonia permease pathway that causes extrusion of ammonia (Torosantucci *et al*., 1984, Mattia *et al*., 1982). Alkalinisation of pH to neutral from acidity induces hyphae formation (Vylkova *et al*., 2014, Danhof *et al*., 2015). Growth of *C. albicans* in an embedded matrix also induces hyphae formation and the underlying mechanism that was demonstrated was due to contact (thigmotropism) (Brand *et al*., 2009). Carbon dioxide at a partial pressure of 5% in the mammalian host induces pseudohyphal growth through the activation of the core catalytic domain of Cyr1 adenyl cyclase (Hall *et al*., 2010).

Serum which is considered the most potent factor may function in two different ways to trigger hyphae formation. Serum can stimulate Cyr 1(adenyl cyclase) indirectly through Ras1 which is a Cdc24/Cdc42 GTPase (hydrolase) that regulates the signaling pathways for hyphal growth. The Ras1-dependent pathway utilizes the mitogen activated protein kinase (MAPK) pathway. The MAPK is involved in transmitting stimuli from the extracellular environment to the cell by sequential phosphorylation. There are several MAPK pathways in *C. albicans* but the one involved in morphogenesis is the Ras-Raf-MEK-ERK pathway, also shortened as Candida ERK like kinase (Cek1) pathway which has Cph1 as the transcription factor at the end of the pathway (Alonso et al., 2006). Alternatively, serum can directly activate adenyl cyclase through its constituent peptidoglycan. Increased adenyl cyclase activity leads to increase in the intracellular levels of cyclic adenosine monophosphate (cAMP) which in turn, activates protein kinase A (PKA). The PKA induces hyphal growth through activation of hypha-specific transcription factors such as Efg1 and decreased levels of the hyphal transcriptional repressors; Nrg1 and Tup1 (Wang, 2013) (Figure 2). Both the MAPK-Cek1 Ras1-dependent cascade and cAMP PKA Ras1 independent pathways work in parallel.

Except growth in embedded matrix that occurs at 25^{o}C, temperature increase is a central factor in the morphogenesis of *C. albicans* as the transition of yeast to filamentous forms is dependent on elevated temperatures for several of the factors discussed above. For example, serum, pH and CO_2 depend on concurrent rise in temperature to 37^{o}C to induce hyphal growth. In principle, elevated temperature relieves the molecular chaperone HSP90 of its repression of yeast to filament transition (Shapiro *et al*., 2009). Consequently, serum and 37^{o}C coupling is a rapid method to induce formation of hyphae (Shapiro *et al*., 2010). This forms the basis of the germ tube test (GTT) that is used for the diagnosis of *C. albicans* in Clinical Mycology. As the GTT was used for the studies, below is a schematic of the signal transduction pathways for hyphae formation (Figure 2).

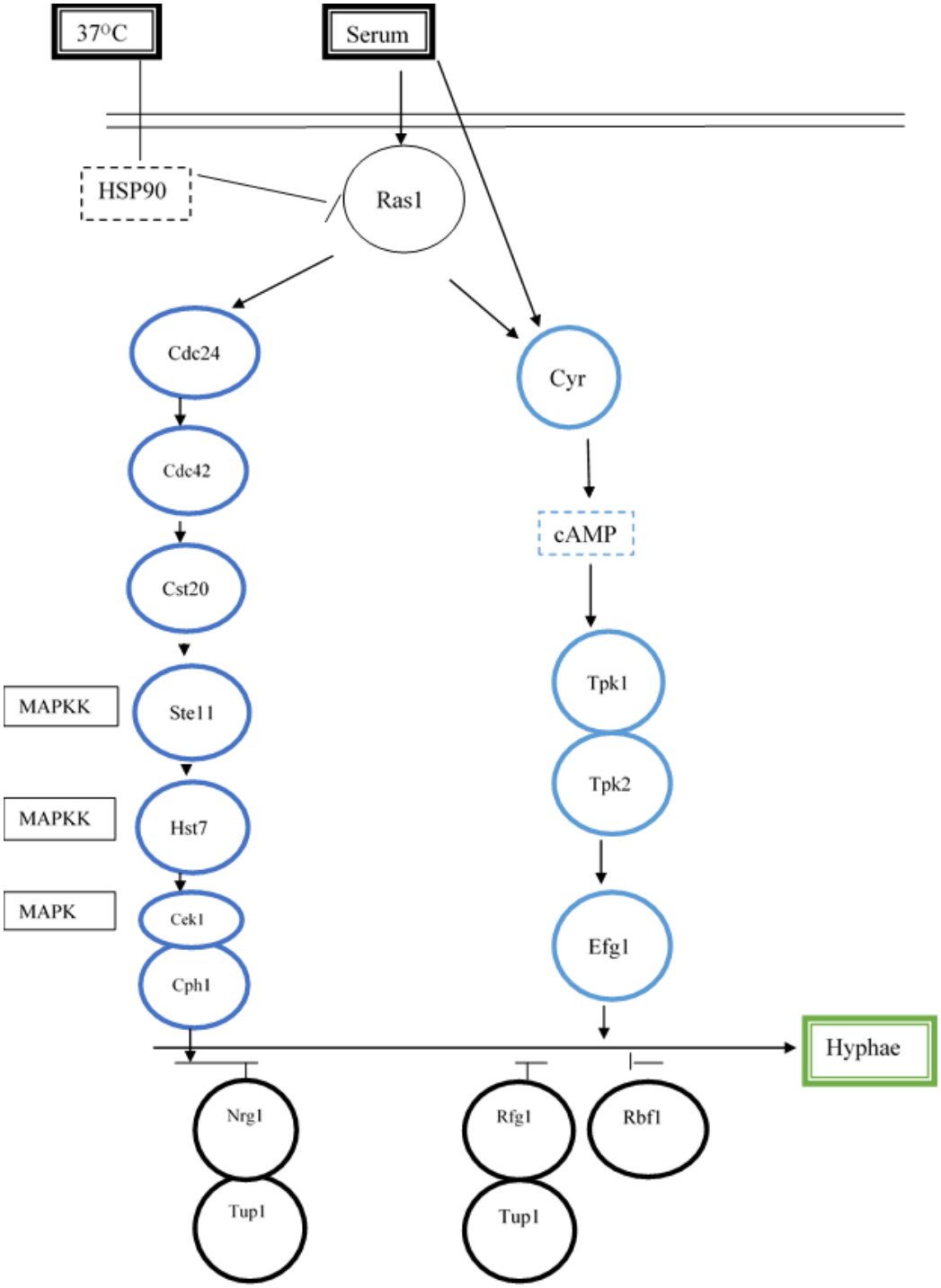

Figure 3*:* Serum and 37°C signal transduction pathways for hyphae induction
Serum can induce hyphae formation in Ras1 dependent or independent fashions. Ras1 independent way follows the cAMP pathway (blue) which is considered the most important pathway. Adenyl cyclase (Cyr) activity plays a pivotal role in the activation of the cAMP pathway as it determines the amount of cAMP produced, which in turn sets the activation cascade of the target transcription factor - Efg1. The Ras1 - dependent serum- induced hyphal growth follows the MAPK pathway (red) which targets Cph1 transcription factor. Temperature increase to 37°C denatures HSP90 which leads to derepression of yeast to hyphae morphogenesis. Negative regulators of hyphae formation include Nrg1, Tup1 and Rfg1 (Adapted from Sudbery *et al.*, 2011).

1.3.1.1.3 Cell cycle regulation of yeasts/pseudohyphae/hyphae.

Yeasts grow by budding, while pseudohyphae grow from cells that divide at the same time which results in cells that appear as co-joined yeasts. In contrast, hyphae grow exclusively by apical extension. After cytokinesis, the mother compartment is in the cell cycle while the emerging germ tube remains in the long Gap 1 phase (G1) (Sudbery *et al*., 2011). During hyphal growth, membrane-bound vesicles are localized at the sites of polarized growth. The vesicles supply the molecules for expansion of the cell membrane and synthesis of a new cell wall that makes up the septum. The localization pattern of the vesicles is suggestive of a structure called Spitzenkorper that drives the tip of filamentous fungi (Brand *et al*., 2009).

1.3.1.1.4 Gene Expression profiles of yeasts/pseudohyphae/hyphae.

The transcription factors Tup1 (Braun *et al*., 1997), Nrg1 and Rox1p (Braun *et al*., 2001) are negative regulators of filamentous growth. Accordingly, *tup1*Δ, *nrg1*Δ and/or *rox1*Δ mutants grow constitutively as filaments but the repression of yeast to hyphae transition is lifted under inducing conditions. Cph1 induce the formation of pseudohyphae although it can also trigger hyphae formation on solid media. Efg1 is considered the main transcription factor that promotes the induction of hyphal growth (Stoldt *et al*., 1997). Unlike the foregoing factors that function under inducing conditions, the expression of *UME6* polarises growth to hyphal morphology under non-inducing conditions (Glory *et al*., 2017).

1.3.1.1.5 Impact of yeast/hyphae/pseudohyphae morphogenesis on pathogenesis.

Yeasts play a crucial role in dissemination and when engulfed by macrophages, they switch to the hyphal morphology that pierces the phagolysomal membrane to aid the escape of *C. albicans* (Lewis *et al*., 2012) Thus, hyphae have a propensity for tissue invasion (Dalle *et al*., 2010, Filler *et al*., 2006). However, more recent studies showed that hyphae formation is essential but not sufficient for aiding macrophage escape (Omeara *et al*., 2015). Another mechanism of hyphae-mediated induction of macrophage death called pyroptosis was described (Wellington *et al*., 2014). Pyroptosis is a type of apoptosis which is activated by binding of Nod-like receptors for example, NLR1, NLR2 and activation of the inflammasome followed by accumulation of the caspase-1 activating adaptor molecule called apoptosis-associated speck-like protein (ASC). Caspase-1 cleaves IL-1β and IL-18 into their

inflammatory forms (Tavares *et al*., 2015). Binding of the adaptor molecule also causes swelling and lysis of the cell (Wellington *et al*., 2014). Further studies showed that both pyroptosis and physical rupture mediate *C. albicans* induction of macrophage death in the first 6-8 h, and from 9 h, respectively (Uwamahoro *et al*., 2014).

Thus, the plastic morphology of *C. albicans* is important for virulence as mutants that are locked in one morphotype show attenuated virulence (Saville *et al*., 2003), (Sudbery *et al*., 2004, Lo *et al*., 1997). However deletion of hyphae-specific cyclin gene (*HGC1*) resulted in cells that grew exclusively in yeast form but still expressed the hypha-specific genes for example, *HWP1* (Zheng *et al*., 2004). These yeast form mutants show attenuated virulence in a model of systemic candidiasis strengthening the view that hyphae formation alone is an important attribute of virulence (Jacobsen *et al*., 2012). Pseudohyphae are usually found together with yeasts and hyphae at the sites of infection but their role in pathogenesis has not been elucidated.

1.3.1.1.6 Induction of hyperpolarized buds.

Another mechanism that induces filamentation in *C. albicans* has been described. Hyperpolarized buds are formed by treatment of *C. albicans* with a range of genotoxic agents (Shi *et al*., 2007). When yeast cells are treated with a DNA synthesis inhibitor (for example, hydroxyurea) or DNA damaging agent such as H_2O_2, they form hyperpolarized buds. Furthermore other mutants including *cdc5*Δ (polo kinase gene) also exhibit hyperpolarized bud filamentous growth. The mechanism underlying formation of hyperpolarized buds includes DNA damage caused by the genotoxic agents which trigger activation of the DNA checkpoint Rad53 kinase (Da Silva *et al*., 2010). Activation of Rad53 kinase occurs via phosphorylation of the conserved threonine-glutamine or serine-glutamine sites that are clustered at specific regions. DNA damage checkpoints are biochemical cellular surveillance mechanisms that monitor the fidelity of DNA during progression in the cell cycle (Finn *et al*., 2012). Activation of DNA check point halts the cell cycle to allow repair mechanisms (Bachewich *et al*., 2005, Finn *et al*., 2012). During cell cycle arrest, there is activation of transcriptional response of genes to initiate DNA repair. At this point, *C. albicans* switches to a filamentous mode of growth (Shi *et al*., 2007).

1.3.1.1.7 Cell cycle regulation of hyperpolarized buds.

Opposed to hyphae and pseudohyphae that are actively dividing cells, hyperpolarized buds are in a state of cell cycle arrest (Bachewich *et al*., 2005). When *C. albicans* is treated with genotoxic agents such as H_2O_2, the cell cycle is arrested as

evidenced by a single nucleus that delocalizes from the mother to the elongating daughter filamentous hyperpolarized bud (Da Silva *et al*., 2010). Previous studies showed that genotoxic stress-induced hyperpolarized bud formation is regulated by Rad9 which is the signal transducer of DNA damage checkpoint, Mrc1; the DNA synthesis checkpoint and Fork Head Associated (FHA) domain on serine/glutamine (SQ) and threonine/glutamine protein clusters at the N terminus which bind phosphopeptides (Shi *et al*, 2007). Specifically, thioredoxin was shown to regulate H_2O_2-induced hyperpolarized bud growth through activation of the Rad53 checkpoint kinase (Da Silva *et al*., 2010).

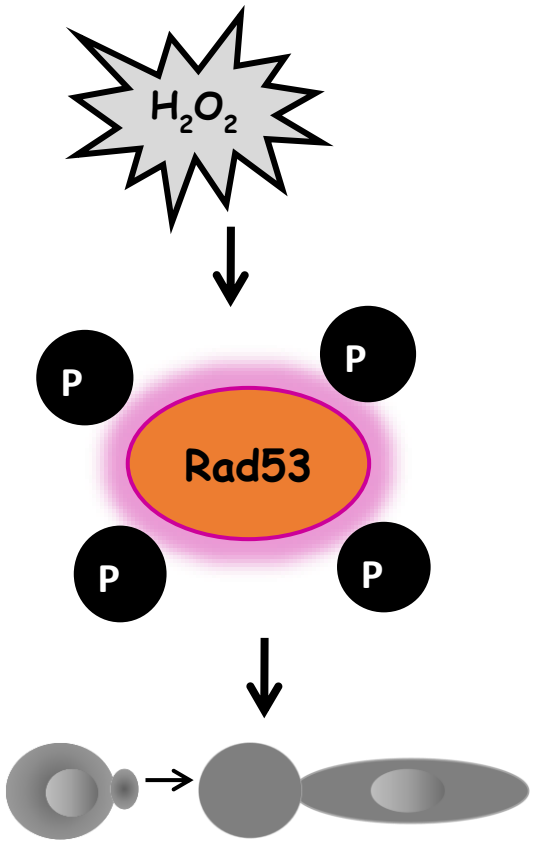

Figure 4: Activation of Rad53 kinase pathway.
Treatment of *C. albicans* with a genotoxic agent for example, H_2O_2, causes activation of DNA damage responsive Rad53 kinase via phosphorylation of the threonine-glutamine or serine-glutamine sites which are conserved and clustered at specific regions of the kinase. Activation of Rad53 kinase leads to cell cycle arrest and morphogenesis of *C. albicans* from yeasts to hyperpolarized buds. Hyperpolarized buds are characterized by translocation of the nucleus from the oval mother to the elongated filamentous hyperpolarized bud (Adapted from Da Silva *et al*., 2010).

1.3.1.1.8 Gene Expression profile.

The formation of hyperpolarized buds does not require the expression of genes for Efg1 or Cph1 but phosphorylation of Rad 53 kinase is essential for formation of H_2O_2 - induced hyperpolarized buds (Da Silva *et al*., 2010). Hyperpolarised buds induced by

treatment of cells with other genotoxic agents, for example, hydroxyurea (HU) and, due to depletion of Cdc5p show expression of numerous hyphae-specific genes, particularly at the end stage elongation. Furthermore, cdc5p depleted cells expressed more hyphae-specific genes than following HU treatment (Bachewich *et al*., 2005). Therefore, towards the later stages of elongation, hyperpolarized buds express hyphae specific-specific genes and the level depends on the method of induction (Bachewich *et al*., 2005).

1.3.1.1.9 Role of hyperpolarised buds in pathogenesis.

The role of hyperpolarized buds in pathogenesis of *C. albicans* is not yet known, but they may be important because they express hypha and virulence-specific attributes during the course of elongation (Bachewich *et al*., 2005). Furthermore, it has been suggested that since the expression of the hypha and virulence genes consumes a lot of resources, it is plausible that the pathogen induces formation of hyperpolarized buds for stress adaptation and survival in the host (Shareck *et al*., 2011).

1.3.1.2 Adhesins.

Adhesins are molecules on the surfaces of *C. albicans* for adherence to host tissues to allow colonization (Sundstrom, 1999, Staab *et al*., 1999). Examples are agglutinin like sequence proteins (ALS). The ALS proteins are an eight-member glycosylated family of proteins (Families 1-7 and 9) that are homologous to the *S. cerevisiae* alpha-agglutinnins that are involved in cell- cell recognition during mating. Als1 is essential for virulence in a haematogeneously disseminated murine model of candidiasis as mutants are attenuated in virulence (Hoyer *et al*., 2008, Hoyer, 2001). Intergrin like proteins (*Int1p*) bind to several extracellular matrix (ECM) ligands. *INT1* plays important roles in adherence and filamentation of *C. albicans* as null mutants were less effective in performing such roles. *Mnt1p* is a type II membrane protein that is required for O and N- mannosylation in fungi. Mannans are a major constituent of the outer cell wall of fungi therefore form the first point of contact between the fungus and the host. They are important for host recognition to initiate immune response (Hostetter, 1994). The hyphal wall protein 1 (*Hwp1*) was originally isolated as the outer mannan proteins of germ tubes and hyphae. It is used for adhesion to the human buccal epithelial cells and is important in the systemic model of infection (Staab *et al*., 1999). During the infection process, yeast to hyphae transition is associated with an increase in the number and distribution of adhesins (Ryan *et al*., 2012) further, demonstrating their roles in the disease process.

1.3.1.3 Secretion of hydrolytic enzymes.

Are enzymes that are necessary for tissue penetration and for the fungus to forage nutrients. They have also been shown to attack host immune cells and have thus, been implicated in evasion of immune system (Naglik *et al*., 2003). They include secreted aspartyl proteinases (SAPs) and phospholipases (PLP) and lipases. SAPs are important in *C. albicans* virulence as clinical isolates have been shown to be more proteolytic in murine models of vaginal candidosis than *sap*Δ/Δ mutant counterparts (Monod *et al*., 1994). PLB1p has been described in hyphal tips during tissue penetration and it is important in murine models of systemic candidiasis (Ryan *et al*., 2012, Schaller *et al*., 2005). More recently, a novel toxin was described in *C. albicans*. Candidalysin is a toxin which is secreted by hyphal cells and causes damage to epithelial membranes. A peptide toxin, it has positively charged carboxy terminals which allow entry of current and influx of calcium ions and causes cytolytic damage to the epitheial cells. This leads to activation of damage associated pathway and induction of mucosal immunity (Moyes e*t al*., 2016).

1.3.1.4 Phenotypic switching.

A basic prowess of *C. albicans* as a pathogen appears to be due to the diversity of its phenotype. *C. albicans* can spontaneously and reversibly switch between numerous phenotypes at a high frequency as demonstrated by colonial morphology on laboratory agar. Up to seven colonial phenotypes including white (smooth) to opaque (stipple) switches smooth, star, ring, irregular, wrinkled, stipple, fuzzy, and hat morphologies have been described (Slutsky *et al*., 1987, Soll, 1992). When cells from the smooth colonies were removed, they comprised exclusively of budding yeasts. In contrast, cells from the other types of morphology exhibited both budding and hyphal morphologies (Soll, 1992). The phenotypic diversity of *C. albicans* may account for many of its features including the ability to invade multiple host niches, evade antibiotic therapy, immune system and to infect a diverse spectrum of hosts (Mayer *et al*., 2013).

1.3.2 Fitness Attributes.

In this subsection, I will give succinct descriptions of how *C. albicans* adapts to stresses upon phagocytosis but with emphasis on oxidative stress response as this is one of the themes of my PhD research.

Responses of *C. albicans* to phagocytosis (Lorenz *et al*., 2004) have been studied by DNA microarrays (Fradin *et al*., 2003) and proteomics (Fernández *et al*., 2007) and they have revealed various types of stress that are imposed. *C. albicans* responses to

stress can either be core to multiple stresses or specific to a particular stress (Enjalbert *et al*., 2006).

1.3.2.1.1 Metabolic adaptation.

Carbohydrate starvation during phagocytosis causes *C. albicans* to induce alternative pathways for utilization of carbon including gluconeogenesis, glyoxylate cycle and β-oxidation. Amino acid deprivation induces *C. albicans* to upregulate genes that are necessary for amino acid biosynthesis in a GCN4-dependent fashion. Furthermore, during nitrogen starvation usually leads to the upregulation of the ammonia permease *MEPI* genes (Lorenz *et al*., 2004).

Trace metal deprivation in the intracellular environment of macrophages up regulates the expression of genes that are involved in homoeostasis of levels of metals for example, *CTR1* for copper and *ZRT2* for zinc, ferric reductase genes *FRE3* for iron and the use of high affinity iron permease to scavenge iron (Lorenz *et al*., 2004, Ramanan, 2000).

1.3.2.1.2 pH regulation.

C. albicans is faced with fluctuating pH in the diverse host niches it inhabits. The pH levels of the GIT and vagina that *C. albicans* occupies during commensalism are acidic; 2 in the stomach, 4.5 in the vagina and 6 in the oral mucosa. But as a bloodstream pathogen, *C. albicans* has to grow at the alkaline pH range of 7. 35 to 7. 45 (Sherrington *et al*., 2017). The variation in the pH of the host niches and ability of *C. albicans* to adapt mean that *C. albicans* has proven adept at maintaining homeostasis of the pH of its environment by using several mechanisms. Two pH regulated proteins concerned with cell wall cross-linking Phr1 and Phr2 are expressed in neutral to alkaline and acidic pH, respectively (Mühlschlegel *et al*., 1997, Calderon *et al*., 2010). Homozygous deletion mutants of *phr1* and *phr2* mutants show defects in morphogenesis and cause inverse patterns of virulence. The *phr1* mutant shows attenuated virulence in mouse model of systemic candidiasis but can still cause vaginitis, while the *phr2* mutant is avirulent in vaginal model of infection but can cause systemic candidiasis (Calderon *et al*., 2010, De Bernardis *et al*., 1998). Additionally *C. albicans* can regulate the pH of its extracellular milieu through alkalinisation. During nutrient starvation, it induces biosynthesis of amino acids (especially arginine) and polyamines which lead to production of ammonia that is split into other constituents including urea. Urea raises the pH to neutrality and leads to induction of hyphae (Vylkova *et al*., 2011).

1.3.2.1.3 Pathways for responses to stresses.

During interaction with the host, *C. albicans* encounters a number of stresses to which it must adapt to survive. The pathways which were initially characterized in the model *Saccharomyces cerevisiae* model yeast have largely diverged in *C. albicans* (Brown *et al*., 2014).

The heat shock factor 1-heat shock elements (Hsf1-HSE) pathway responds to acute thermal stress (Alonso *et al*., 2006). The heat shock proteins and the associated signaling pathways are also responsive to heavy metal and oxidative forms of stress (Gong *et al*., 2017). When the pathway is triggered, Hsf1 becomes phosphorylated and the HSEs induce the expression of heat shock proteins. To promote adaptation to the thermal stress, the protein undergoes refolding or degradation depending on the extent of damage. Expression of polyubiquitin is essential for resistance to thermal stress (Alonso *et al*., 2006). Mutations of the Hsf1-HSE regulon were shown to lead to attenuation of virulence of *C. albicans*. (Nicholls *et al.*, 2011). Significantly, the Hsf1-HSE regulon is important for maintaining *C. albicans* thermal homeostasis as it is activated in febrile patients (Nicholls *et al*., 2009). The heat shock proteins are potential antifungal targets (Gong *et al*., 2017).

Responses to cell wall damaging agents such as ecchinocandin antifungal agents and chemicals such as calcoflour white are mediated by Hog1, MAPK Cek1 and MAPK Mkc1 stress pathways which are evolutionarily conserved in other fungi (Alonso *et al*., 2006). The Hog1 signaling is a core pathway of three protein kinases that is conserved in all eukaryotes (Nikolaou *et al*., 2009). In *C. albicans*, it is composed of MAPKK kinase (MAPKKK) (Ssk2), MAP kinase kinase (MAPKK) (Pbs2) and MAP kinase (MAPK) (Hog1). Sequential phosphorylation of each preceding kinase sets an activation cascade initiated by Ssk2 which receives the input signals and, ending with MAPK (Hog1), is activated by the Pbs2 kinase to generate output signals to activate the protein kinase (Cheetham *et al*., 2007). In *C. albican*s, the MAPK Hog1 is activated in response to diverse stresses including cell wall, osmotic/cationic stress and oxidative stress (Smith *et al*., 2004), (Smith *et al*., 2010). The MAPK Cek1 pathway is activated by the Msb2 sensor. The components of MAPK Cek1 includes MAPKKK Ste11, MAPKK Hst7 and MAPK Cek1 signaling molecules. Mutants of Cek1 pathway are unable to undergo yeast to filamentous morphological transition and show attenuation in virulence. The mediator for the MAPK Mkc1 pathway is protein kinase C. The Mkc1 pathway comprises of MAPKKK Bck1, MAPKK Mkk1 and MAPK Mkc1. Disruption of the Mkc1 pathway results in increased sensitivity to cell wall stresses and attenuated virulence.

When *C. albicans* cells are exposed osmotic or cationic stress, there is phosphorylation, nuclear accumulation of Hog1 and induced biosynthesis of glycerol for adaptation (Alonso *et al*., 2006).

1.3.2.1.4 Oxidative stress responses.

1.3.2.1.4.1 Detoxification of ROS.

The molecules involved in oxidative stress response can be classified by enzymatic and non-enzymatic mechanisms.

Non-enzymatic mechanisms to detoxify ROS in *C. albicans* include the use of trehalose (Martínez, *et al*., 2007) and glutathione (Yadav *et al*., 2011). The accumulation of the non- reducing disaccharide sugar trehalose through the action of trehalose-6-phosphatase has been demonstrated to prolong survival by protecting *C. albicans* from macrophage induced injury (Martínez *et al*., 2007). Additionally, *C. albicans* can use the protein glutathione to detoxify ROS. Glutathione exists in both oxidized (GSSG) and non- oxidized (GSH) forms. The reduced form is able to donate electrons to ROS resulting in neutralization of ROS (Yadav *et al*., 2011).

Enzymatic mechanisms involve the use of a number of catalytic proteins. Superoxide is broken down by enzymes known as superoxide dismutases (SODs) that are divided into five types; Sod1, Sod2, Sod4 and, Sod5 and Sod6. Sod1 and Sod2 are located in the intracellular compartment while Sod4 and Sod5 are membrane-associated. Sod1 is needed for innate resistance to macrophages (Chaves *et al*., 2007, Lorenz *et al*., 2004, Fernández *et al*., 2007) and its expression is up-regulated upon interaction with macrophages and is protective in a murine model of systemic candidiasis, (Chaves *et al*., 2007), (Hwang *et al*., 2002). In contrast to Sod1 and Sod2 that are constitutively expressed to macrophages, the expression of Sod 4 and 5 in *C. albicans* are morphotype associated; yeast cells express Sod4 while hyphae express Sod5. Sod 5 is particularly pivotal to protection as deficiency leads to the accumulation of extracellular ROS which renders *C. albicans* prone to phagocytic killing (Frohner *et al*., 2009).

Detoxification of superoxide yields hydrogen peroxide (H_2O_2) which is still reactive to produce profound damaging effects on the cell. Following, *C. albicans* uses a number of enzymes to detoxify H_2O_2. Catalase1 (Cat1) is the major detoxification enzyme. The expression of *CTA1* is increased following phagocytosis. Catalase splits H_2O_2 into H_2O and O_2. However, a recent study showed that although high basal catalase levels enhance resistance to peroxide stress, *cat1*Δ did not display attenuated virulence in a mouse model of

systemic candidiasis (Pradhan *et al*., 2017). Another enzyme that detoxifies H_2O_2 is the glutathione peroxidase of which the interaction of *C. albicans* with phagocytes is also key. Glutathione peroxidase 3 (Gpx3) catalyzes the oxidation of the Cap1 transcription factor to initiate the production of antioxidative enzymes. Null mutants of glutathione peroxidase are sensitive to macrophage-mediated killing (Patterson *et al*., 2013).

Thioredoxin peroxidases encoded by genes (*TSA1*) are another form of peroxide detoxification systems which use thioredoxin as an electron acceptor. Protein oxidation plays an important role in the activation of oxidative stress responsive signaling pathways (Berlett, 1997). Thioredoxins (Trx1) play several important roles in reversing protein oxidation. Thus, the observations that mutation of *trx*Δ lead to H_2O_2-induced Hog1 (Enjalbert *et al*., 2006), Cap1 (Patterson *et al*., 2013) and Rad53 (Da Silva *et al*., 2010) illustrate that Trx1 is needed for the correct regulation of all the three Hog1, Cap1 and Rad53 pathways. Trx1 is important is important for survival of *C. albicans* within the host in murine models of systemic candidiasis.

1.3.2.1.4.2 Signalling pathways in oxidative stress response.

The signaling mechanisms that induce the above responses are controlled by three pathways. The stress activated protein kinase (SAPK) Hog1 signaling is a core pathway of three protein kinases that is conserved in all eukaryotes (Nikolaou *et al*., 2009). In *C. albicans*, it is composed of MAPKK kinase (MAPKKK) (Ssk2), MAP kinase kinase (MAPKK) (Pbs2) and MAP kinase (MAPK) (Hog1). Sequential phosphorylation of each preceding kinase sets an activation cascade initiated by Ssk2 which receives the input signals and, ending with MAPK (Hog1), is activated by the Pbs2 kinase to generate output signals to activate the protein kinase (Cheetham *et al*., 2007). In *C. albican*s, the MAPK Hog1 is activated in response to diverse stresses including oxidative stress (Smith *et al*., 2004), (Smith *et al*., 2010). It is not yet clear what happens downstream following activation of Hog1 but oxidative stress transcripts are activated in a Hog1-independent fashion (Enjalbert *et al*., 2006). Hog1 is important in oxidative stress response as mutants show attenuated virulence in mouse models of systemic candidiasis in the face of oxidants even when other types of stress are absent. But the stress responses regulated by Hog1 which are important for virulence are not known (Alonso *et al*., 1999, Cheetham *et al*., 2011).

However, the expression of genes encoding antioxidants is mainly dependent on the response regulator Skn7 and Cap1p. Cap1 is an AP-1 transcription factor that is orthologous to Yap1 and Pap1 in *Saccharomyces cerevisiae* and *Schizosaccharomyces pombe*, respectively (Alarco *et al.*, 1999). When *C. albicans* cells are in non-oxidative stress

conditions, Cap1 and Ybp1 form a complex in the cytoplasm to inhibit Cap1 degradation but facilitates H_2O_2-induced oxidation by Gpx3 peroxidase. The Cap1-Ybp1 complexes freely shuttle between the cytoplasm and the nucleus (Zhang *et al*., 2000). However, following oxidative stress due to treatment with hydrogen peroxide, there is Gpx3/Ybp1 mediated oxidation of Cap1 at redox-sensitive cysteine residues within two cysteine rich domains (Zhang *et al*., 2000). This leads to accumulation of Cap1 in the nucleus due to masking of the nuclear export sequence. Nuclear accumulation of Cap1 causes induction of target genes for oxidative stress response via promoter binding of Yap1 response elements. These include genes that are involved in the production of enzymes that detoxify oxidants such as *CAT1*, *SOD1*, genes for glutathione synthesis (*GCS1*), homeostasis of redox and oxidative induced damage (glutathione reductase and thioredoxin: *GLR1* and *TRX1*) enzymes (Wang *et al*., 2006, Znaidi *et al*., 2009). The desired outcome of Cap1 activation is detoxification of ROS and, adaptation of *C. albicans* to the stress which is modulated by the redox regulator thioredoxin (Trx) (Da Silva *et al*., 2010). As can be discernible, inactivation of Cap1, down regulates the expression of the antioxidative genes which result in increased sensitivity of *C. albicans* to oxidative stress (Alarco *et al*., 1999). Furthermore, nuclear accumulation of Cap1 causes dissolution of Cap1-Ybp1 complex which initiates proteasome-mediated degradation of Cap1 actions (Patterson *et al*., 2013).

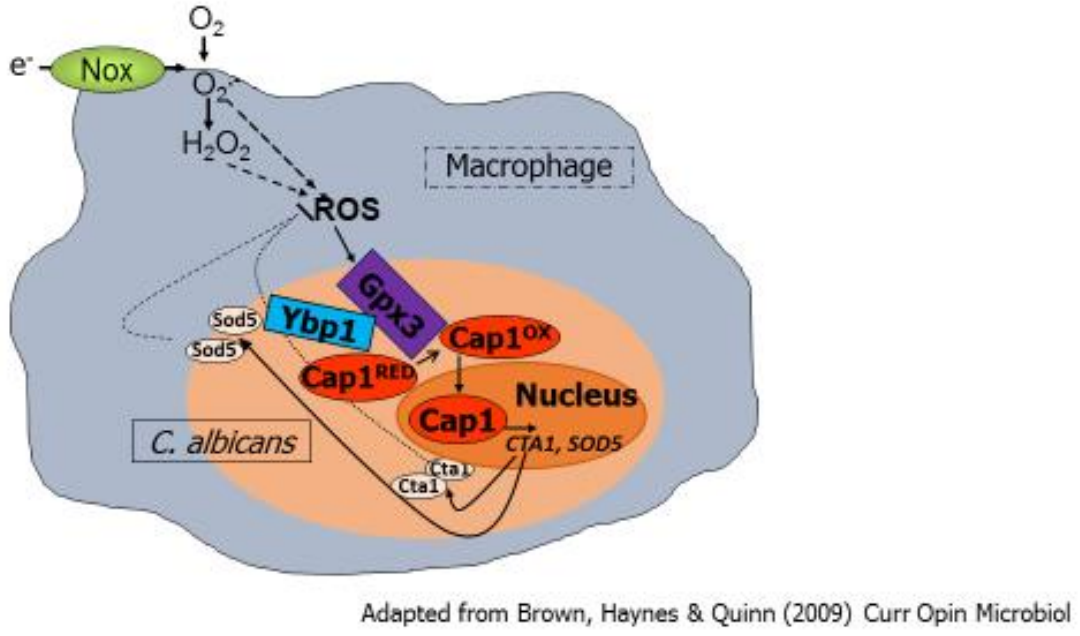

Figure 5*: C. albicans* oxidative stress response pathway.
Phagocytes for example, macrophages present the first line of defence against *C. albicans*. Upon activation of NADPH oxidase complex, and through sequential electron transfer from molecular oxygen, macrophages produce ROS such as superoxide and H2O2. To counter the effects of ROS, *C.*

albicans using Cap1 which is the major transcription factor and its co- regulators Gpx3 and Ybp1 will induce the expression of antioxidative enzymes (Patterson *et al*., 2013). The antioxidative enzymes include catalase, superoxide dismutase.

Another pathway that responds to oxidative stress has been described. Exposure of *C. albicans* to genotoxic agents such as hydroxyurea, menadione and hydrogen peroxide activates cell cycle checkpoints (Shi *et al*., 2007). Cell cycle checkpoints are monitoring mechanisms that ensure systematic progression of the cell cycle events such as formation of buds, DNA synthesis, and segregation of chromosomes (Hartwell *et al*., 1989). When these events are impaired, the checkpoint pathway halts the cell cycle to allow corrective measures. For example, inactivation of thioredoxin by H_2O_2 has been shown to trigger activation of the Rad53 checkpoint pathway. It has been shown that following activation, there is phosphorylation of Rad 53 kinase to induce formation of hyperpolarized buds. The downstream events following, however, are not known. Cells lacking Rad53 show increased sensitivity to H_2O_2 although the role of Rad53 kinase in virulence is also not known (Da Silva *et al*., 2010) (Pathway described in Figure 4).

1.3.2.1.4.3 Filamentation of *C. albicans* within the phagosome.

C. albicans in the phagosomal environment are able to form hyphal filaments in response to oxidative stress as an evasion mechanism. The hyphal cells can cause macrophage death in two ways. The hyphae either induce macrophage pyroptosis or disrupt the membranes of the phagosome to cause lysis of the macrophage (Uwamahoro *et al*., 2014). Following hyphae formation, there is induction of caspase1-dependent-IL1β. This is followed by the cleavage of IL-1β to its bioactive inflammatory form that induces the macrophages to undergo pyroptosis or inflammatory apoptosis (Tavares *et al*., 2015, Wellington et al., 2014). Pyroptosis occurs in the first 6 to 8 h of phagocytosis. But from 9 to 24 h after phagocytosis, *C. albicans* hyphae can pierce and cause rupture of macrophages to undergo death (Uwamahoro *et al*., 2014). Although it is not yet clear what causes filamentation of *C. albicans* inside the macrophage, mutants lacking key antioxidant enzymes or oxidative stress responsive signaling pathways (e.g. Hog1, Cap1) and co-regulators of Cap1 such as Gpx3 and Ybp1 have been shown to fail to filament within macrophages (Patterson *et al*., 2013) and yet are able to form hyphae when induced *in vitro*. Additionally, the oxidative stress sensitive mutants can form H_2O_2-induced hyperpolarized buds but cannot filament inside the macrophage (Da Silva *et al*., 2010).

Therefore, these data show that oxidative stress responses in *C. albicans* are tightly coupled with filamentation and macrophage escape. However, despite these guiding leads, many questions regarding H_2O_2-mediated cell cycle arrest in *C. albicans* remain unanswered. The overall aim of my PhD study was to investigate the importance of H_2O_2 -induced cell cycle arrest and oxidative stress resistance in mediating *C. albicans* evasion of phagocytosis.

1.4 Study Objectives.

(1) Investigation into whether oxidative stress impairs serum induced hyphae formation *in vitro* and whether the impairment is more sustained in oxidative stress regulatory mutants.

(2) Screening of a *C. albicans* transcription factor deletion library for mutants that display impaired H_2O_2-induced hyperpolarised bud formation or H_2O_2 resistance.

(3) Investigation into the role of oxidative stress resistance in promoting *C. albicans* survival following phagocytosis.

CHAPTER TWO.

2 MATERIALS AND METHODS.

2.1 General materials and equipment.

The chemical reagents were purchased from Sigma (Sigma-Aldrich, Dorset, UK) and alcohols and acids were from Fisher (Fisher Scientific, Leicestershire, UK) unless stated. Media ingredients were purchased from Oxoid (Oxoid, Hampshire, UK) and/or Difco (Difco Laboratories, Surrey, UK).

Media and solutions were prepared using deionised water at 18.2 MΩ which was produced by the Milli-Q water purification system (Millipore). Media and stock solutions were sterilised by autoclaving at 121°C for 15 min at 103.4 kPa (15 p.s.i) in a Prestige autoclave (Prestige, Lancashire, UK) or filter-sterilisation using 0.22 µm pore size Stericup disposable filtration units (Millipore, Massachusetts, USA).

Incubation of liquid cultures was performed in Infors HT (Infors HT, Surrey, UK) or an Innova^{4430} (New Brunswick Scientific, Hertfordshire, UK) incubators. Optical densities of cultures were measured in a Helios Unicam Spectrophotometer (Spectronic Unicam, Cambridge, UK).

Centrifugation of samples that were less than 1.5 ml was carried out in an Eppendorf MiniSpin centrifuge (Eppendorf, Hamburg, Germany) or Eppendorf 5804R centrifuge (Eppendorf) if larger volumes of samples were centrifuged. Static cultures were incubated in a static incubator (Laboratory thermal equipment Ltd., Oldham, UK).

2.2 Strains.

Strain	Genotype	Source
JC747	SN148+CIp30 (*URA3, HIS1, ARG4)*	(Patterson *et al*., 2013)
JC 842	*cap1::loxP-HIS1-loxP/cap1::loxP-ARG4-loxP,* CIp20 *(HIS1, URA3)*	(Da Silva *et al*., 2010)
JC 807	*cap1::loxP-HIS1-loxP/cap1::loxP-ARG4-loxP,*CIp20-*CAP1 (HIS1, URA3)*	(Da Silva *et al*., 2010)
JC 917	*ybp1::loxP-HIS1-loxP/ybp1::loxP-ARG4-loxP,* CIp20 *(HIS1, URA3)*	(Patterson *et al*., 2013)
JC 809	*ybp1::loxP-HIS1-loxP/ybp1::loxP-ARG4-loxP,*CIp20-*YBP1 (HIS1,URA3)*	(Patterson *et al*., 2013)
JC 1317	*gpx3::loxP-HIS1-loxP/gpx3::loxP-ARG4-loxP* CIp20 *(HIS1, URA3)*	(Patterson *et al*., 2013)
JC 1346	*gpx3::loxP-HIS1-loxP/gpx3::loxP-ARG4-loxP* CIp20-*GPX3 (HIS1, URA3)*	(Patterson *et al*., 2013)
205 (BWP17)	*ura3Δ::λimm434/ura3Δ::λimm434 his1Δ::hisG/his1Δ::hisG arg4Δ::hisG/arg4Δ::hisG*	(Wilson *et al*., 1999)
707 (SN148)	*arg4Δ/arg4Δ,leu2Δ/leu2Δ,his1Δ/his1Δ,ura3Δ::imm434/ ura3Δ::imm434 iro1Δ::imm434/iro1Δ::imm434*	(Noble *et al*., 2005)
1133 (*hgc1*Δ)	*hgc1*Δ::*ARG4*/*hgc1*Δ::*HIS1, URA3*	(Zheng *et al*., 2004)
1393 (*hgc1*Δ + HGC1)	*hgc1*Δ::*ARG4*/*hgc1*Δ::*HIS1, HGC1 URA3*	(Zheng *et al*., 2004)
1488 (SC5314)	Clinical isolate from Dr Sneh Lata Ranwar School of Life Sciences, Jawaharlal Nehru University, New Delhi -110067, India	
WYS3 (*rad53*Δ)	BWP17 *rad53*Δ::*ARG4*/*rad53*Δ::*URA3*	(Shi *et al*., 2007)
WYS3.1 *RAD53* + *rad53* Δ	BWP17 *rad53*Δ::*ARG4*/*rad53*Δ::*URA3 RAD53*:*HIS1*	(Shi *et al*., 2007)
BWP17+ Clp30	BWP17+Clp30 (HIS1, ARG4, URA3)	Megan Lenardon, unpublished
JC 711 (*cap1*Δ)	*(SN148) cap1Δ::loxP-HIS1-loxP/cap1Δ::loxP-ARG4-loxP*	(Noble *et al*., 2005)
JC987 (*SN148 + pACT1*)	*arg4Δ/arg4Δ,leu2Δ/leu2Δ,his1Δ/his1Δ,ura3Δ::imm434/ ura3Δ::imm434 iro1Δ::imm434/iro1Δ::imm434 + pACT1*	This study
JC1398 (*cap1Δ+pACT1*)	*(SN148) cap1Δ::loxP-HIS1-loxP/cap1Δ::loxP-ARG4-loxP +pACT1*	This study
JC987 + *CAT1*	*arg4Δ/arg4Δ,leu2Δ/leu2Δ,his1Δ/his1Δ,ura3Δ::imm434/ ura3Δ::imm434 iro1Δ::imm434/iro1Δ::imm434 + pACT1 + CAT1*	This study
JC1398 + *CAT1*	*(SN148) cap1Δ::loxP-HIS1-loxP/cap1Δ::loxP-ARG4-loxP +pACT1+ CAT1*	This study
TF 001 to TF 165	Null mutant strains of *C. albicans* transcription library	(Homann *et al*., 2009)

Table 1: Strains of *C. albicans* used in this study.
Wild type cells, *cap1*Δ and co-regulators; *gpx3*Δ and *ybp1*Δ, *ACT1* +/- *CAT1* expressing strains, transcription factor deletion library mutants, Hgc1 and Rad53 deletion strains of *C. albicans* were used.

2.3 Media.

C. albicans strains were grown in Yeast Peptone Dextrose (YPD) broth (1% yeast extract, 2% mycological peptone, 2% glucose) (Sherman, 2002) at 30ºC with shaking at 180 rpm overnight. For transformations, SD (minimal) media were used.

2.4 Growth conditions to induce filament formation.

The overnight cultures were diluted 1: 100 in a working volume of 50 ml. Cultures were treated with serum, H_2O_2, NaCl, or serum plus H_2O_2, and serum plus NaCl combinations.

Hypha formation was induced by the standard and rapid procedure for inducing hyphae under laboratory conditions by treating cells from 24-h overnight culture with 10% foetal bovine serum and incubating the culture at 37°C. Cells were treated with 10% foetal bovine serum by adding 5 mL to 45 mL of the culture volume. To test the effect of H_2O_2 on serum-induced hyphae formation, H_2O_2 was added to the serum- treated cells at various concentrations. The following concentrations of H_2O_2 were used; 0.2, 0.4, 0.6, 0.8 1.0, 3 and 5 mM. For H_2O_2 growth arrest control, cells were treated with H_2O_2 alone at the same concentrations that were added to serum-treated cells.

To assess the effect of osmotic stress, sodium chloride (NaCl) at a concentration of 0.5M was added to the serum treated cells induced to form hyphae in the liquid culture.

All cultures were incubated at 37°C with shaking at 180 rpm and samples collected hourly for 5 h. Then 900 µL samples were added to 100 µL of formaldehyde stock for fixation. Cells were rotated at room temperature for approximately 30 minutes, and stored at 4◦C until processed for characterization of morphology by microscopy. Each experiment was repeated at least three times.

2.5 Impact of removal of H_2O_2 on cell growth.

To determine whether H_2O_2-mediated inhibition of hyphae formation was reversible, stationary 24-hour culture cells were diluted 1:100 with YPD and treated with 10% foetal bovine serum + 2 mM H_2O_2. The culture was grown for 3 h at 37ºC in a working volume of 150 mL. Formation of hyperpolarised buds was confirmed by microscopy before continuing with the experiment. Then two lots of 50 mL were removed, gently centrifuged and suspended in 50 mL of pre-warmed media plus serum alone, and another one in 50 mL pre-warmed media with serum plus H_2O_2 treatment. This ensured the dilution of the cells were not changed. The remaining 50ml was cultured as the untreated control. Cells were collected at hourly intervals and stored as before for assessment microscopy. Each experiment was repeated at least three times.

2.6 H_2O_2 survival assay.

To determine the survival of *C. albicans*, cells treated with H_2O_2 in the presence or absence of serum were taken hourly for 3 h, serially diluted in fresh YPD broth and plated on YPD agar to visualise colony forming units. Plates were incubated at 30◦C for at least 24 hours, and survival was expressed as percentage of zero time samples. Each experiment was repeated at least three times and one-way ANOVA was used to calculate the *p-value* of significance.

2.7 Transcription factor library screening.

A transcription factor library consisting of 16 mutants of *C. albicans* (Homann *et al*., 2009) was screened for impaired formation of hyperpolarized buds. Briefly, stationary phase cells from overnight cultures were diluted to an OD_{660} = 0.15 and allowed to grow to exponential phase at OD_{660} = 0.5 – 1.0. Cultures were then treated with 5 mM H_2O_2 and incubated at 30°C with shaking at 180 rpm for 6 h, before analysis by light microscopy for hyperpolarised bud formation. Strains that showed defects in formation of hyperpolarised buds were retested and images captured by microscopy.

2.8 Microscopy.

Cells fixed in formaldehyde were washed three times in PEM (100 mM (PIPES) piperazine-*N*, *N*′-bis (2-ethanesulfonic acid), pH 7.6, 1 mM EGTA, 1 mM $MgSO_4$), and spread onto air dried poly-L-lysine-coated microscope slides. A drop of 5 µL of the mounting medium Vectashield containing 1.5 mg/ml DAPI (4′-6-diamidino-2-phenylindole) (Vector Laboratories, Burlingame, CA) was applied to each slide. Cover slips were then mounted onto the slides and sealed with varnish. Differential interference contrast (DIC) images and DAPI fluorescence images were captured using a Zeiss Axioscope with a 63× oil immersion objective and the Axiovision imaging system. Images were exported as JPEG onto power point slides for data analysis.

The morphological phenotypes of the filamentous cells were characterised as thin diameter, parallel-sided hyphae (H) (Sudbery, 2011) or thick-diameter hyperpolarised buds (HPB) (Da Silva *et al*., 2010). And, to determine the predominance of cell morphology in each cell treatment, upon resumption of filamentation, the number of each cell morphology (H or HPB) was counted. The cell number was expressed as a percentage of the total number of filamentous cells per high power field. At least 50 cells were counted per experiment.

2.9 Spot tests.

To identify transcription factors essential for resistance to reactive oxygen species, quantitative fitness analysis (QFA) was performed on the transcription factor deletion collection to identify the panel of mutants most sensitive to H_2O_2. Then spot tests were performed using the top 10 hits from this screen.

Agar plates containing different forms of oxidative stress agents were prepared. Hydrogen peroxide (H_2O_2) was prepared from a stock concentration of 8.82 M to working concentrations of 2 mM and 3 mM. Tert butyl hydroperoxide (tBOOH) was prepared from a stock solution of 100 mM and tested at diluted concentrations of 1 mM and 2 mM. Menadione which is a superoxide generator was prepared from a stock concentration of 100 mM (dissolved in dimethyl sulfoxide (DMSO) to working solutions of 200 µM and 300 µM. Diamide (glutathione depleting agent) was prepared from 100 mM stock and added to agar at a working concentration of 2 mM.

Stationary phase cells from overnight cultures were grown to mid-exponential phase, diluted back to an OD_{660} = 0.15, and this and two further serial 10-fold dilutions, were spotted (using a metal cell replicator) onto agar plates containing the different forms of oxidative stress. Cells were incubated at 30˚C overnight.

2.10 Molecular Biology.

2.10.1 *CAT1* over expression.

The *CAT1* gene was initially over expressed from the *pPGK* plasmid promoter of *C. albicans* to assess the impact on H_2O_2-induced inhibition of filamentation.

2.10.2 Cloning strategy.

The *CAT1 Bam*HI restricted PCR product was ligated into *Bam*HI restricted *pPGK* or *pACT1*. The subsequent *pPGK-CAT1* and *pACT1-CAT1* plasmids were linearised at the *Stu*I restriction site in the *RSP10* gene, which targets recombination of the plasmids at this locus in *C. albicans*. Transformation of linearized p*PGK-CAT1* into wild-type and *cap1*Δ cells generated strains AB1 and AB2 whereas transformation of *pACT1-CAT1* into wild-type and *cap1*Δ cells generated strains AB3 and AB4. Correct integration at the *RPS10* locus was confirmed by PCR and DNA sequencing. The cloning strategy is illustrated below.

i) Polymerase Chain Reaction (PCR) amplification of the *CAT1* gene.

The *CAT1* gene was amplified from genomic DNA using the oligonucleotide sequences that incorporated *Bam*HI sites.

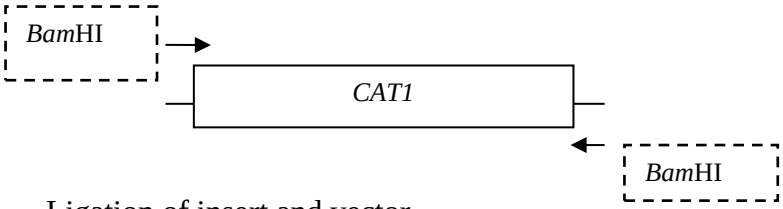

ii) Ligation of insert and vector

The resulting *Bam*HI PCR product was digested with *Bam*HI and ligated into the *Bam*HI site of *pPGK1* to generate the plasmid pPGK-*CAT1*.

The digestion mixture consisted of 30 µL PCR product, 147 µL nH_2O, 20 µL 10X buffer E, and 3 µL of BamHI. The contents were gently mixed, spun briefly in a microcentrifuge and incubated at 37˚C overnight. The ligase reaction based on the insert: plasmid ration of 3:1. It consisted of 2 µL plasmid, 6 µL insert, 1.5 µL 10X buffer, 4.5 µL H_2O, and 1 µL ligase.

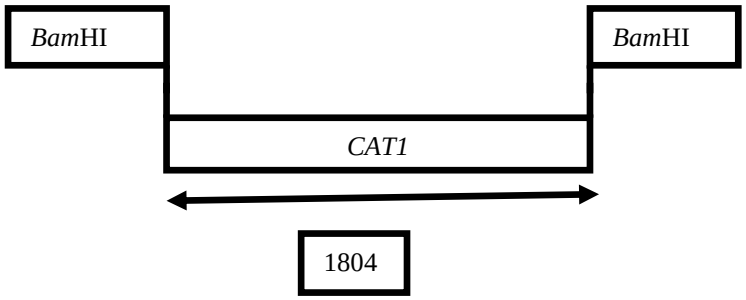

iii) Plasmid *pPGK- CAT1* was linearised at the *Stu*I restriction site in the *RSP10* locus.

iv) Transformation of linearized pPGK-*CAT1* into wild-type and *cap1*Δ cells. The linearized vector- insert combination was introduced into the *RPS10* locus of *C. albicans*.

v) Correct integration at the *RPS10* locus was confirmed by PCR and DNA sequencing.

However, *CAT1* expression from the p*PGK* promoter was not successful. Following, the *CAT1* gene was expressed from the constitutive expression *pACT1* promoter using the same cloning strategy as described previously.

2.10.3 PCR conditions.

PCR of *C. albicans CAT1* gene was performed using the following primers: F1 (Forward Primer) 5'- ATGGCTCCAACATTTACGAATTCTAACG-3', and F2 (Reverse Primer) 5'- GTTTGCACTTTGAGTCAGGCAAGACC-3'. The PCR reaction mixture contained 10 µL of 5X High Fusion (HF) buffer, 1µL of concentrated dNTPS, 2 µL of chromosomal DNA, 2 µL (25pmol/ µL) of each primer, 1.5 µL DMSO and 0.5 µL Phusion. The PCR cycles included initial denaturation at 98°C for 30s, denaturation at 98°C for 10s, primer annealing at 50°C for 30s, elongation at 72°C for 2 minutes, final elongation at 72°C for 10 minutes and final hold 4°C for 10 minutes. A total of 35 PCR cycles was run between denaturation, primer annealing an elongation. PCR for the correct integration of *CAT1* was performed using the following primers: Cat1BamHIF- 5' TAGCGCGGATCCATGGCTCCAACATTTACGAATTCTAACG-3' and Cat1BamHIR- 5' TAGCGCG GATCCGTTTGCACTTTGAGTCAGGCAAGACC-3' The PCR reaction mixture contained 10 µL of 5X High Fusion (HF) buffer, 1µL of concentrated dNTPS,, 2 µL of chromosomal DNA, 2 µL (25pmol/ µL) of each primer, 1.5 µL DMSO and 0.5 µL Phusion. The PCR cycles included in itial denaturation at 98°C for 30s, denaturation at 98°C for 10s, primer annealing at 50°C for 30s, elongation at 72°C for 2 minutes, final elongation at 72°C for 10 minutes and final hold at 4°C for 10 minutes. A total of 35 PCR cycles was run between denaturation, primer annealing an elongation.

2.10.4 Transformation

2.10.4.1 *E. coli* transformation.

E.coli transformation was performed using the following protocol. Two round-bottomed tubes were pre-chilled on ice. The SOC/LB medium was pre-heated to 42°C. The Sure competent cells for transformation were thawed on ice. When thawed, the cells were gently mixed and 100 µl of cells aliquoted into each of the pre-chilled tubes. The tubes were incubated on ice for 10 min with gentle swirling every 2 min. The plasmid alone ligation was added to one tube (control tube), and plasmid plus insert ligation added to the second tube (test tube). The tubes were swirled gently. The tubes were incubated on ice for 30 min. Then the tubes were incubated in a water bath at 42°C for 45s. The tubes were further incubated on ice for 2 min. Samples of 900 µl of preheated (42°C) SOC or LB was added and the mixture incubated at 37°C for 1 h with shaking at 225 -250 rpm. The mixture was centrifuged at 6, 000 rpm for 1 minute and 800 µl of the supernatant removed. Cells were then suspended gently in the remaining medium and plated onto LB-ampicillin agar (100 µg/ml) plates. The plates were incubated at 37°C overnight.

2.10.4.1.1 Plasmid extraction from *E. coli* (Mini prep).

The alkali lysis (‘dirty’) method for mini prep included the following reagents. Solution 1 (Prepared by adding 1.25 ml 1 M Tris HCl pH 8.0 to 1 ml 0.5 M EDTA, and 2.5 ml 1 M glucose), 70% ethanol, phenol- chloroform, 100% ethanol, solution 2 (1 ml 2 M NaOH, 1 ml 10% sodium dodecyl sulfate, Solution 3 (3M potassium acetate, pH 4.8).

Cells were grown in 5 ml of liquid LB plus ampicillin at 37˚C. The cells were spun at 3, 000 rpm for 4 min. The cells were suspended in 100 µl of solution 1 then 200 µl of solution 2 was added. The mixture was gently inverted 4-6 times and left to stand for 5 min. Then 150 µl of solution 3 was added and the cells inverted 4 –times. Cells were spun at 13, 000 rpm for 10 min. The supernatant was transferred to a fresh Eppendorf, and an equal volume of phenol-chloroform added. Cells were vortexed to mix (in the fume hood). Cells were centrifuged at 13, 000 rpm for 3 min. The upper clear phase was transferred to a fresh Eppendorf tube and 2.2 volumes of 100% ethanol was. The mixture was incubated at -20 ˚C for 30 min. The DNA was pelleted by centrifugation at 13, 000 rpm for 15 min. The ethanol was aspirated and the pellet washed in 200-300 µl of 70% ethanol. The tube was centrifuged at 13,000 rpm for 4 min. The ethanol was aspirated and the pellet allowed to air dry. The dried pellet was suspended in 1x TE solution + RNase. Then 5 µl of the digested plasmid was digested on 1% agarose gel.

2.10.4.2 *C. albicans* transformation.

C. albicans transformation was performed by the lithium acetate procedure. Cells from an overnight growth plate were grown in 200 ml culture to OD_{660} 1.0- 3.0. Cells were pelleted by centrifugation at 2, 000 rpm for 2 min. Cells were washed in 20 ml sterile lithium acetate/TE solution and suspended in 1 ml lithium acetate/TE solution. Then 10 µl of boiled (at 100˚C for 5 min) salmon sperm DNA (10 mg/ml) was added to the cells. About 0.5 -5 µg transforming DNA fragment was added. After mixing, 700 µl of PEG mix was added. The mixture was incubated at 30 ˚C for 3 h. Following, heat shock was performed 42 ˚C for 45 min. Cells were pelleted at 8, 000 rpm for a minute resuspended in 200 µl YPD. The cell suspension was plated onto selective SD-Ura plates and incubated at 30˚C.

2.10.4.2.1 Chromosomal DNA extraction from *C. albicans*.

Cells from an overnight culture were suspended in 1 ml distilled water. Cells were spanned and suspended in 200 µl of breakage buffer. 200 µl of glass beads (enough to soak up the liquid) and 200 µl of phenol-chloroform were added. The beads were beaten for 20s. The mixture was centrifuged for 5 min in a microfuge. The supernatant which

was about 150 µl was removed to a fresh tube. Then 15 µl ($1/10^{th}$ volume of the supernatant) of 3 M sodium acetate and 2 volumes of ethanol were added to the supernatant. The mixture were incubated at -20 ◦C for 30 min. The mixture centrifuged in a microfuge at 13,000 rpm for 15 min. The supernatant was removed and the pellet was washed in 400 µl of 70 % ethanol. The pellet was allowed to dry a little before suspending in 100 µl of distilled water.

2.10.4.3 Agarose gel electrophoresis.

The DNA PCR product was separated by electrophoresis on 1% agarose gel; which was prepared by dissolving 0.7 g of agarose (Melford Laboratories, Ipswich, UK) in 70 ml of 1 x Tris-acetate (TAE) pH 8 (0.484 M Tris base, 1.25 N glacial acetic acid and 1 mM Na_2EDTA) solution. After cooling until the flask was not hot to the touch, 50 µL of 0.625 mg/ml ethidium bromide was added to the molten agarose to achieve a concentration of 0.5 µg/ml ethidium bromide. For easy visualisation of each sample during loading and migration during agarose gel electrophoresis, 6x loading dye (0.4% orange G, 0.03% bromophenol blue, 0.03% xylene cyanol FF, 15% Ficoll 400, 10 mM Tris-HCl (pH 7.5) and 50 mM EDTA (pH 8.0) (Promega Ltd., Hampshire, UK) was added to each sample. The gels were run using TAE as the running buffer at 8 V cm^{-1}. DNA was visualised under UV light using a GENE FLASH Syngene Bio Imaging system (TopoGEN, Florida, USA). The size of the DNA band was determined by comparing to a DNA 1 kb ladder (Promega) that was run alongside the samples as a control.

2.10.4.4 DNA Sequencing.

The sequencing was done at GATC biotech using Sanger sequencing.

2.11 Macrophage-*Candida* culture.

2.11.1 Macrophage cell culture and growth conditions.

Cell line of J774 murine macrophages were used in the study. The macrophages were obtained from the European Collection of Cell cultures (ECACC), HPA, Salisbury, UK. The macrophages were maintained in tissue culture flasks in Dulbeco's Modified Eagle's medium (DMEM) (Lonza, Slough, UK) supplemented with 10% (v/v) heat inactivated foetal calf serum (FCS; Biosera, Ringmer, UK), 2% (w/v) penicillin and streptomycin (Invitrogen Ltd, Paisley, United Kingdom) and 1% (w/v) L- glutamine (Invitrogen) at 37^oC with 5% of CO_2. The supplemented DMEM medium is here forth referred to as complete DMEM medium.

2.11.2 Preparing macrophages from liquid nitrogen.

The macrophages were stored as 1 ml aliquots in liquid nitrogen. For use, the macrophages were thawed at 37◦C for 2 min. The thawed 1ml of macrophages was added to 9

ml of pre-warmed complete DMEM medium. The mixture was centrifuged at 1000 rpm for 5 min. The supernatant was discarded while the pellet was suspended in 1 ml of the DMEM medium and added to 19 ml of the DMEM medium in a tissue culture flask. The macrophages were incubated at 37˚C with 5% CO_2 overnight. On day two, the DMEM medium in the flask was aspirated and replaced with fresh DMEM medium. The macrophages grew until they had become confluent which was an indication that they were ready for splitting.

2.11.3 Splitting of macrophages.

Macrophages were maintained by splitting regularly. Macrophages were split to prevent overcrowding and in preparation for experiments. Prior to splitting, the macrophages in the tissue flasks were checked by a microscope to confirm whether they had formed a confluent monolayer which was an indication that they were ready for splitting. If the macrophages had formed a confluent monolayer, they were removed from the bottom of the tissue culture flask using a cell scrapper, and centrifuged. The cell pellet was suspended in 1- 10 ml of fresh pre-warmed DMEM. A volume of the concentrated suspension was added to flasks containing fresh medium (20 mL) using the following dilution factors;

Table 2: Splitting of macrophages.

Dilution	Vols of suspension (ml)	Monolayer ready approximately
1:4	5 ml (add to 15 ml fresh)	After 1 day
1:10	2 ml (add to 18 or 20 ml fresh)	After 2 days
1:20	1 ml (add to 20 ml fresh)	After 3 days
1:40	0.5 ml (add to 20 ml fresh)	After 4 days
1:80	0.25 ml (add to 20 ml fresh)	After 5 days

Table 2: Dilution factors used for splitting of macrophages.
Macrophage cultures which had formed confluent monolayers were diluted and suspended in fresh medium for incubation for the number of days as shown.

2.11.4 Seeding macrophages.

Macrophages were seeded onto a tissue culture slide in preparation for phagocytosis assays. The protocol for splitting cells described in the previous section was followed to generate about 2 ml suspension of cells in pre-warmed complete DMEM medium. The cells in the suspension were stained using trypan blue stain to count the number of viable cells.

A two-fold dilution of the macrophage suspension was made and enumerated by a haemocytometer. Only viable cells (white) were counted within the 10 sets of 16 small squares. The required number of macrophages for phagocytosis assay was 1x 10^5 cells per ml. Thus, the calculated volume of the macrophage suspension containing 1x 10^5 per ml was added to the well. Pre-warmed supplemented DMEM medium was added to make up a total well volume of 300 µl in the well. For confocal spinning disc video microscopy, the macrophages were seeded onto the 8-well slide. The seeded macrophages were incubated at 37^o C with 5% CO_2 overnight before the spinning disc confocal microscopy the following day. On the day of the experiment, immediately prior to setting the assay, DMEM medium was replaced with 290 µl pre-warmed supplemented CO_2-independent medium (Gibco, Invitrogen, Paisley, UK) suspended with *Candida* cells.

2.11.5 Preparation of *C. albicans*.

Single colonies from agar plates stored at 5°C were cultured in 5 ml YPD broth medium; 1% w/v yeast extract (Duchefa Biochemie, Haarlem, Holland), 2% mycopeptone (Oxoid, Cambridge, UK), 2% w/v D-glucose in distilled H_2O) and incubated overnight at 30°C, 200 rpm. Following, 500 µl of the overnight culture was pipetted into a microfuge and centrifuged at 6000 rpm for 1 min. After centrifuging, the supernatant was

removed and put in a waste bottle. The cell pellet was re-suspended in 1 ml of phosphate buffer solution (PBS) (first wash). The mixture was centrifuged as before and re-suspended in 1 ml of PBS (second wash). Then 10 µl of washed cells were pipetted into 990 µl of PBS to make a 1:100 dilution. The diluted cells were counted in a haemocytometer and used at a concentration of 3 x10^5 in 1 ml of the suspension. Additionally for fluorescent confocal video microscopy, LysoTracker Red DND-99 (Invitrogen, Paisley, UK) was added at a ratio of 1 µl per ml of CO_2 independent medium prior to phagocytosis assay.

Alternatively, for phagocytosis assays for *Candida*-macrophage survival experiments, the macrophages were seeded onto 6-well NUNC plates. Maintaining a ratio of 1:3 in the calculations for macrophages: *Candida*, the mixture was used at a total volume of 3, 000 µl per well.

2.11.6 Phagocytosis assay.

2.11.6.1 Confocal video microscopy settings and number of experiments.

The phagocytosis assay was performed in CO_2 independent medium supplemented with 10% heat-inactivated foetal calf serum, 3 mL L- glutamine (Life Technologies, California, USA). The CO_2 independent medium is used for supporting the growth of cells in suspension and adherent, for example, macrophages. It has phenol red, sodium pyruvate but no synthetic buffers thus, lack cytotoxic effects. The working solutions were supplemented 10 % foetal bovine serum. Before the assay, if fluorescent stains (lysotracker Red and Yoyo1 dyes) were used, each was added at 1 µl per ml of CO_2 independent medium. *C. albicans* cells were added to Eppendorf tubes in the required number per well as shown in the calculations previously. Then 290 µl of CO_2 independent medium was added to Eppendorf tubes containing *C. albicans*. The DMEM complete medium was aspirated from the wells of macrophages. Following, DMEM medium was immediately replaced with 290 µl of CO_2 independent medium containing the *C. albicans*.

2.11.6.2 Data acquisition from the confocal videos.

The spinning disc confocal video microscopy utilises the Volocity 6.3 high performance 3D live cell imaging software (http://cellularimaging.perkinelmer.com/downloads/detail.php?id=14). Live cell videos were used to acquire the following data.

a) Macrophage migration speed and directionality.

Migration of the macrophage was tracked using Volocity 6.3 software for 60 min. The outputs

of tracking macrophage migration were displayed in form of tracking diagrams which were used to show the directionality of migration and calculate the tracking velocity (μm/s).

b) Attachment time.

Time of attachment was defined as the time point within the movie that the macrophage and *Candida* made cell-cell contact.

c) *Time of engulfment time*.

Time of engulfment was the time point within the movie when *C. albicans* was completely enclosed within the phagocyte.

d) Time for engulfment time.

Time for engulfment was defined as the difference between the time points in the movie when *Candida*-macrophage cell-cell contact and complete engulfment of *C. albicans* occurred.

e) Rate of Candida engulfment.

The rate of *Candida* engulfment was defined as the average number of *Candida* taken per macrophage per minute.

f) Time to acidification of the phagosome.

Acidification of the phagosome was defined as the time of colocalization of LysoTracker red with *C. albicans* cells (as seen by appearance of a red halo) occurred.

g) Hypha formation.

The length of extracellular (non- engulfed) and intracellular (engulfed) hyphal cells was measured at 30, 60, 90 and 120 min.

h) Macrophage killing.

Macrophage killing by *C. albicans* was determined by counting the number of viable macrophages hourly over the 6 h period of the experiment. Macrophages which had engulfed *C. albicans* and still stained red with Lysotracker Red were counted. Survival of macrophages was expressed as percentage of the original number of macrophages in the field. The findings from Lysotracker Red were compared with DIC appearance of the macrophages.

i) Candida killing.

The macrophage-Candida killing assay was conducted as a separate phagocytosis experiment using a 6-well NUNC plate. After determining the 1:3 Macrophage: *Candida* cell numbers using a haemocytometer as described previously, the phagocytosis assay with incubation at 37°C and 5% CO_2 was set. After 3 h, the slide was removed from the incubator. The

supernatant of each well was put in a labelled tube. Then 4 ml of sterile distilled water was added to each well and left to stand to stand for 5 min for the macrophages to lyse and expel the engulfed *Candida*. The bottom of each well was gently removed using a cell scrapper and the 4 ml of water put in the corresponding labelled tubes. Another 4 ml of water was added to the different wells to obtain 10 ml solution of each sample. 10-fold serial dilutions of each labelled tube was made. Then YPD agar plates were inoculated with 100 µl of each sample in dilution number 3 which was optimised to contain the number of cells that were easily countable.

2.12 Statistical analyses.

Each experiment was carried out at least three times. The exact number of experimental replicates are mentioned in the respective figure legends. Data are shown as mean ± standard deviation (SD). Statistical analysis was performed using one-way analysis of variance (ANOVA) as there were more than two groups, with Bonferroni correction for the multiple comparisons of the means. And p-values ≤ 0.05 were considered as statistically significant.

CHAPTER THREE.

3 INVESTIGATION INTO WHETHER OXIDATIVE STRESS IMPAIRS SERUM-INDUCED HYPHAE FORMATION AND IF THE IMPAIRMENT IS MORE SUSTAINED IN OXIDATIVE STRESS REGULATORY MUTANTS.

3.1 Introduction.

C. albicans is an important fungal pathogen (Brown *et al*., 2012) for which morphological plasticity is key for virulence (Saville *et al*., 2003, Lo *et al*., 1997).

Following phagocytic uptake, toxic armory of reactive oxygen species (ROS) derived from superoxide radicals are generated by the activated NADPH complex (Brown *et al*., 2009). *C. albicans* must survive the ROS to allow the transition of unicellular yeasts to filamentous form which can induce macrophage death and enable fungal escape of the phagocyte (Uwamahoro *et al*., 2014). The scavenging of ROS in *C. albicans* is dependent on the Cap1 AP-1-like transcription factor, and its co-regulators Ybp1 and Gpx3 (Patterson *et al*., 2013) which promote the expression of genes involved in antioxidative mechanisms (Alarco *et al*., 1999, Jain, Pastor *et al*. 2013). Oxidative stress sensitive mutants, such as cells lacking Cap1, are locked in the yeast form inside the macrophage despite the ability to form hyphae *in vitro* (Patterson *et al*., 2013). As ROS induce growth arrest through the activation of the DNA damage checkpoint Rad53 kinase (Da Silva *et al*., 2010) , I hypothesized that ROS prevent filamentation of oxidative stress sensitive mutants in the macrophage due to sustained growth arrest (Da Silva *et al*., 2010, Lowndes *et al*., 2000). To test this hypothesis, experiments were conducted to compare the impact of H_2O_2 -mediated growth arrest on serum-induced hyphae formation in wild-type cells and oxidative stress-sensitive mutants *in vitro*. Cells of Cap1, Gpx3 and Ybp1 mutants were chosen for analysis because they are important for transcriptional responses to oxidative stress and are vital for filamentation within the phagosomal environment (Patterson *et al*., 2013).

3.2 H_2O_2 delays filamentation in a concentration dependent fashion.

I aimed to optimize the concentration of H_2O_2 which could inhibit serum-induced morphogenesis in *cap1*Δ cells using *WT* control but without causing cell death. Hyphae formation was induced by treating cells with serum at 37°C which is the standard procedure for inducing hyphae under laboratory conditions. The ability of H_2O_2 to prevent formation of hyphae was tested by the addition of a range of H_2O_2 concentrations because it was previously demonstrated that the onset and duration of H_2O_2 induced cell cycle arrest is concentration dependent. At lower levels of H_2O_2, cell cycle arrest is rapidly induced, but at

higher levels it is more sustained (Da Silva *et al*., 2010). This could be easily visualized by the formation of hyperpolarized buds; a filamentous form which is distinct from hyphae (Figure 1, Chapter 1), that is characteristic of growth arrest in *C. albicans*. Hyphae are thin with parallel sides and lack constrictions at the sites of septation of the mother and daughter cells (Sudbery *et al*., 2004) while a hyperpolarised bud is a thick diameter, elongated single cell characterized by one nucleus (Da Silva *et al*., 2010). As the concentration of H_2O_2 in the macrophage is not known, cells were exposed to arbitrary concentrations of H_2O_2 in the concentration range of 0.2, 0.4, 0.6, 0.8, 1, 3 and 5 mM in the presence of the hyphae inducing conditions of serum and 37^{o}C. Controls included cells treated with H_2O_2 alone, and serum alone at 37°C, so the kinetics of hyperpolarized bud formation and hyphae formation, respectively, could be followed. All cell treatments were carried out for 5 hours and images were taken as described in Materials and Methods.

The results showed that H_2O_2 causes delay in filamentation of *C. albicans* in a concentration-dependent fashion. Treatment of null *cap1*Δ cells with levels of H_2O_2 up to 1 mM had no impact on serum-induced hyphae formation (Figure 5) hence the concentration was increased to 3 mM. For both the *WT* and *cap1*Δ cells, the serum control induced hyphae formation rapidly, with germ tubes being evident in the first hour. However, for both the WT and *cap1*Δ cells, exposure to 3 mM H_2O_2 delayed serum induced morphogenesis. The serum plus H_2O_2 treatment triggered hyperpolarised bud formation. This was more pronounced with *cap1*Δ cells (Figure 6, white arrow), as serum plus H_2O_2 treatment showed a longer delay in serum-induced hyphae filamentation for 3 hours in *cap1*Δ cells compared to the *WT* was delayed for only 1 hour (Figure 6). In addition to initiation of hyphae after the delay, the H_2O_2 control also induced formation of hyperpolarised buds in both *WT* and *cap1*Δ cells. The difference in the rates of serum-induced hyphae formation of *cap1*Δ and *WT* cells prompted the testing of the ability of a higher concentration of H_2O_2 at 5 mM to inhibit serum-induced hyphae formation.

At 5 mM H_2O_2 concentration, both *WT* and *cap1*Δ strains formed germ tubes after 1 h. However, in serum plus H_2O_2 treatment, the formation of serum-induced hyphae in *WT* cells was delayed for 2 hours while the *cap1*Δ cells did not form any hyphae throughout the 5 hour experiment. And both the *WT* and *cap1*Δ cells treated with H_2O_2 formed hyperpolarised buds from 3 h (Figure 7).

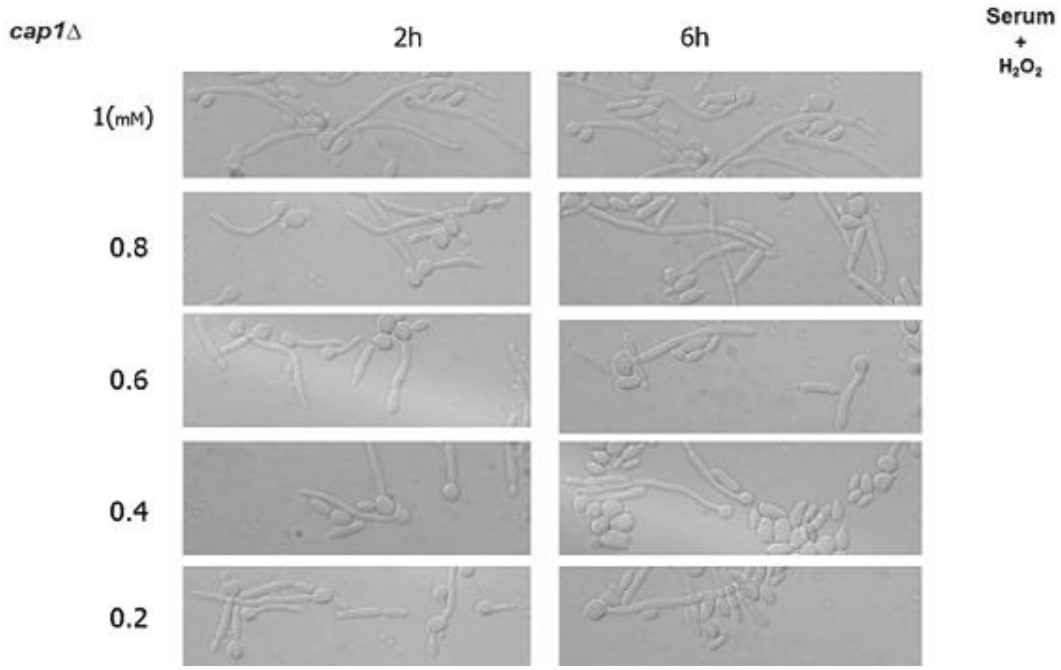

Figure 6: **Impact of 0.2-1 mM H_2O_2 on serum induced filamentation in *cap1*Δ cells.**
Stationary phase cells were diluted 1:100 and treated with 1, 0.8, 0.6, 0.4 or 0.2 mM H_2O_2 plus 10% serum. The cells were incubated at 37˚C with shaking at 180 rpm. The cells were collected after 2 h and 6 h of incubation, fixed, and the DIC microscopy morphology observed using 63X oil immersion objective at each time point shown.

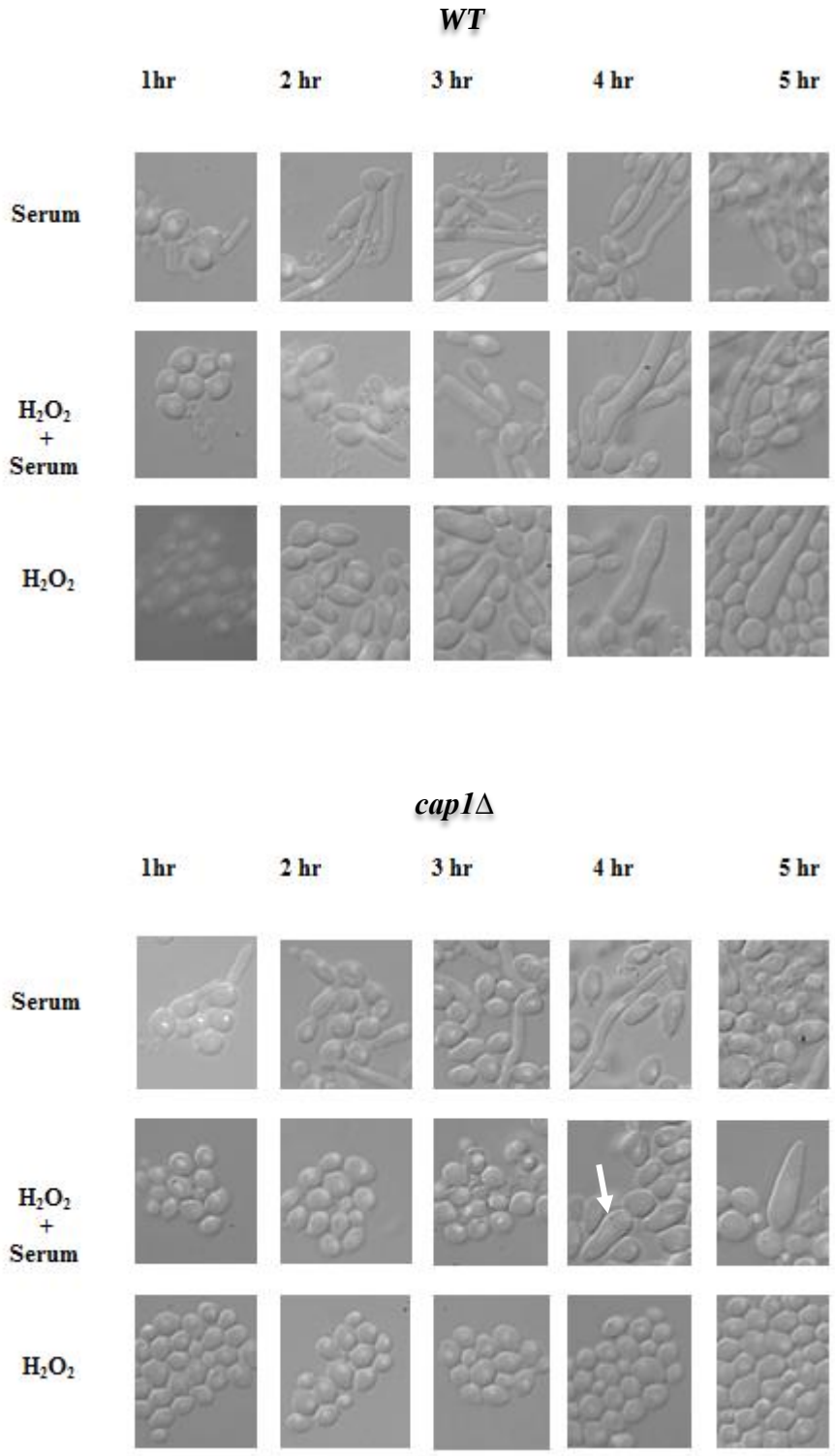

FIGURE 7. Impact of 3mM H_2O_2 on serum induced filamentation in *WT* cells and *cap1*Δ cells. Stationary cells were diluted 1:100 and treated with 10 % serum, 3mM H_2O_2 plus 10% serum, and 3mM H_2O_2. The cells were incubated at 37˚C with shaking at 180 rpm. Cells were collected at hourly intervals for 5 hours and the morphology at each time point shown. Each experiment was repeated at least four times.

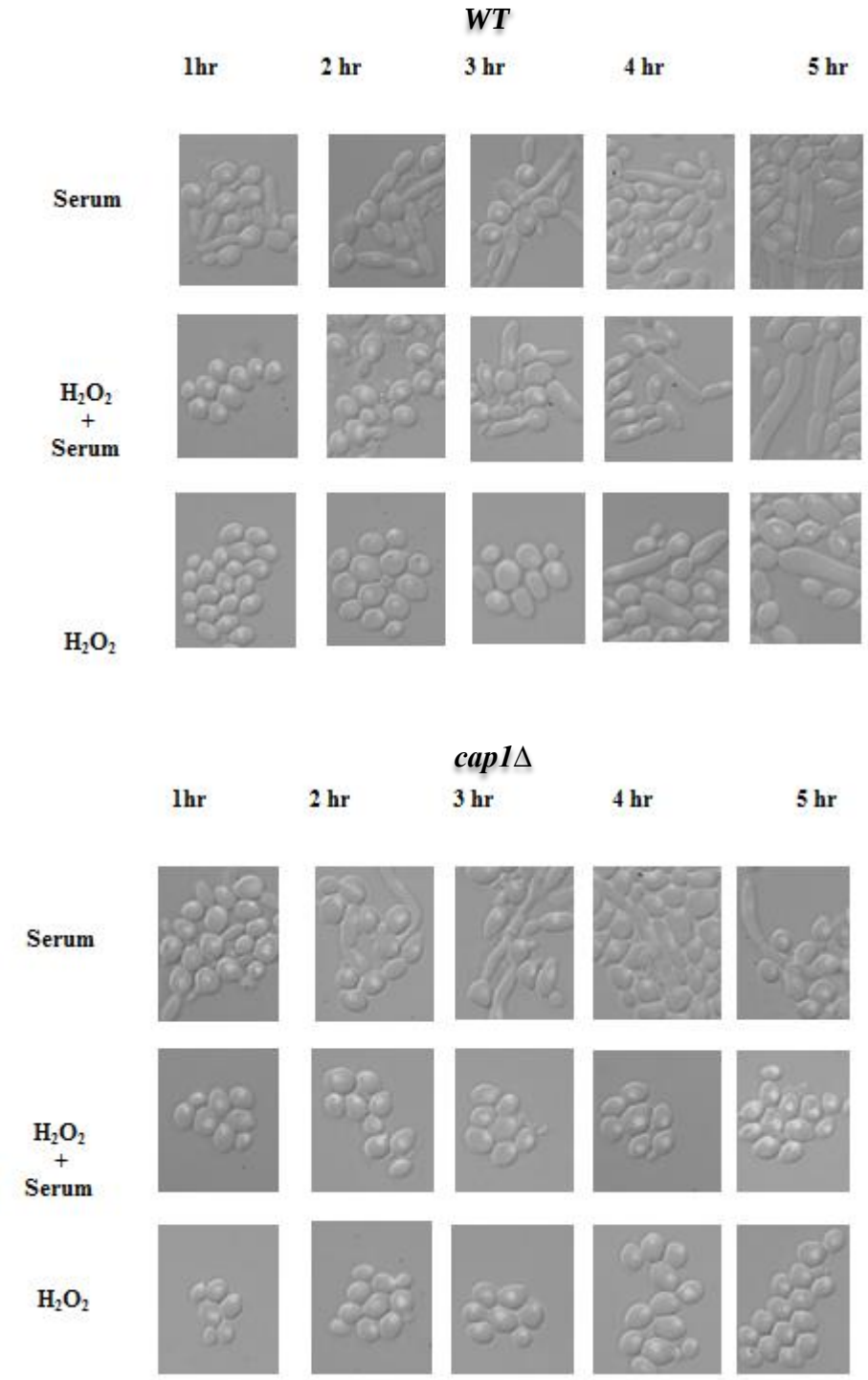

FIGURE 8: Impact of 5 mM H_2O_2 on the filmentation of WT and *cap1*Δ cells.
Stationary cells were treated with 10 % serum, H_2O_2 plus 10% serum, and H_2O_2. The cells were incubated at 37 ˚C with shaking at 180 rpm. The cells were collected at hourly intervals for 5 hours and the morphology induced at each time point shown. Each experiment was repeated at least four times.

3.3 Delay in filamentation is due to growth arrest.

The previous results in figures 5, 6 and 7 above revealed that *cap1*Δ cells were more sensitive to H_2O_2 induced inhibition of serum-induced hyphae formation than *WT* cells. As *cap1*Δ cells are more sensitive to H_2O_2 than WT cells (Patterson *et al*., 2013), it was possible that the enhanced H_2O_2 mediated inhibition of serum induced filamentation of *cap1*Δ cells could be due to cell death. To explore this, growth assays were performed to determine cell survival. Briefly, *WT* and *cap1*Δ cells treated with 3 mM H_2O_2, and H_2O_2 plus serum, were taken at various time points and plated onto YPD agar to determine *Candida* survival over 3-hour period. Following 3 h, the filamentous morphology of the cells makes it impossible to calculate cell survival and it was reasoned that any impact of H_2O_2 on cell viability would be captured within a 3 h time period. The plates were incubated at 30˚C for 24 h. Cell survival was expressed as a percentage of time zero sample.

3.3.1 Cells remained viable in 3 mM H_2O_2 during delay of serum-induced hyphae formation.

The results revealed that when cells were treated with 3 mM H_2O_2, both WT and *cap1*Δ cells showed no significant reduction in the percentage of the colony forming units (Figure 8). Treatment of *WT* cells (left side) with H_2O_2 plus serum, and H_2O_2 showed that within the first hour, cell survival dropped to approximately 90 %, after which it was followed by increasing number of cells from 2 h. The increasing trend indicates that the cells were starting to divide. Treatment of *cap1*Δ cells (right side) with H_2O_2 plus serum showed a decrease in cell survival to about 90 % which was sustained for 2 h. In contrast, there was a significant reduction in cell number following H_2O_2 treatment alone to approximately 60 % which was also sustained for 2 h. From 3 h there was an increasing number of cells over time which means the cells were beginning to divide. Generally, within the first three hours, there was no significant increase in the number of *cap1*Δ cells compared to the WT counterpart that started increasing in number in the second hour. These periods in which there was no increase in number correspond to the duration of the delay of filamentation as shown in the previous data in figures 3 and 4. The lack of marked death of cells ($p > 0.05$) treated with H_2O_2 plus serum and the delay in cell division of *cap1*Δ cells compared to *WT* cells indicates that H_2O_2 induces more sustained growth arrest in *cap1*Δ cells than WT cells and this may underlie the previous observations in Figure 2. Additionally, there was more survival of cells treated with H_2O_2 plus serum compared to cells treated with H_2O_2 alone especially in *cap1*Δ ($p < 0.031$). This suggests that serum offers protective effect from H_2O_2-induced cell death in

C. albicans. The finding is consistent with a study that showed that serum raises the pH of the YPD media which gives a protective effect against ROS.

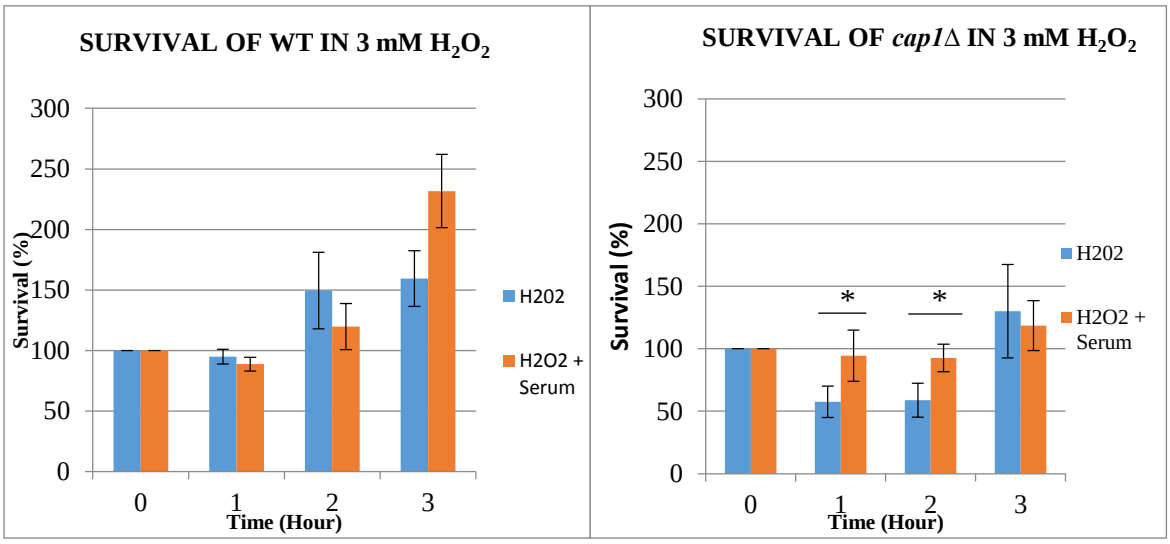

Figure 9: Impact of 3 mM H_2O_2 exposure on cell viability.
WT (left) and *cap1*Δ (right) cells were treated with H_2O_2, and H_2O_2 plus serum. Hourly survival of cells was calculated as a percentage of the original 0 hour number of cells for 3 hours. Each experiment was repeated three times and the error bars show the Standard Deviation (SD). * $p = 0.031$.

3.3.2 Cell death caused the lack of filamentation of *cap1*Δ when treated with 5 mM H_2O_2

When *cap1*Δ cells were treated with 5 mM H_2O_2 and also H_2O_2 plus serum, cell survival drastically decreased to 38 % in the first hour and the downward trend continued over time until there were almost 0 % of the cells by the last time point at 3 h. This is different from 3 mM in which about 90 % and 60 % of the *cap1*Δ cells survived following treatment with H_2O_2 plus serum and H_2O_2 alone, respectively, by 3 h. Serum did not provide any protection from H_2O_2-induced killing which is inconsistent with the observation made with 3 mM treatment of *cap1*Δ cells (Figure 9, Right hand side). In contrast, when *WT* cells were treated with the higher concentration of 5 mM, in H_2O_2 treatment alone decreased to 80% while H_2O_2 plus serum treated cells reduced to about 85 % after 1 hour. There was decreased survival for the H_2O_2 treated cells to 82 % and 75 % for H_2O_2 plus serum treatment after the 2nd hour. Then there was increase to approximately 107 % for cells treated with H_2O_2 alone and 110 % for H_2O_2 plus serum treatment after 3 h. As in the previous *WT* treatment with 3 mM, cells treated with H_2O_2 in the presence of serum had better survival than cells treated with H_2O_2 alone (Figure 9, Left hand side). These results indicate that at 5 mM H_2O_2 treatment when *cap1*Δ did not filament throughout the 5-hour experiment, the cells

were dead as evidenced by the sharp decrease in the number of viable cells over time. However, the H_2O_2 sensitivity assays showed that the lack of filamentation for 2 hours in the *WT* cells was due to growth arrest as seen by no significant change in the number of viable cells. Furthermore, the results showed there was protective effect of serum from H_2O_2 mediated killing in the *cap1*Δ cells (Figure 10).

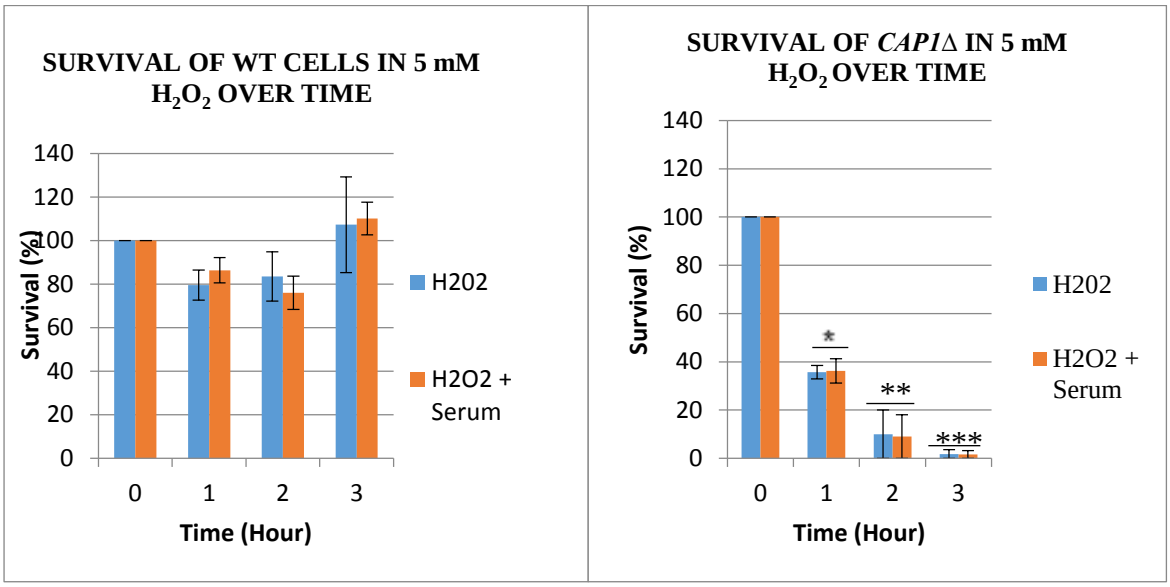

Figure 10: Impact of 5 mM H_2O_2 exposure on cell viability.
Cells were treated with 5 mM H_2O_2 and their survival in H_2O_2 alone and H_2O_2 plus serum. Survival was calculated at hourly intervals for 3 hours for both the *WT* (left) and *cap1*Δ (right) cells. Each experiment was repeated three times and the error bars were drawn using SD. The *p-values* show pairwise comparison of survival of H_2O_2, H_2O_2 plus serum treated cells at 0 h versus 1 h, 0h versus 2 h and 0 h versus 3 h; *p* = * 0.032, 0.032, ** 0.018, 0.018, *** 0.0013, 0.013.

3.4 Osmotic stress had no effect on filament formation.

The previous findings indicate that H_2O_2 inhibits serum-induced hyphae formation in a mechanism that likely involves prolonged growth arrest. However, during phagocytosis, *C. albicans* is also exposed to an armory of other stresses. One of such insults is cationic stress that also causes growth arrest (Kaloriti *et al*, 2014). Hence, it was important to examine whether cationic stress imposition could also inhibit serum-induced hyphae formation. Therefore, the aim was to test the impact of cationic stress on serum-induced hyphae formation of *C. albicans*. Similar to that described for H_2O_2 in section 3.1 above, morphology studies were performed after treating *WT* cells with 10 % fetal bovine serum in the presence or absence of 0. 35M NaCl which was chosen because a previous study had shown that it was within the range which caused low levels of *C. albicans* killing (Duch *et al*., 2012) but the alteration in gene expression levels were sufficient to be studied (Kaloriti, *et al*., 2012). However, the results showed that NaCl did not inhibit serum-induced hyphae

formation. Consistent with serum induced hyphal growth control, the serum plus NaCl cell treatment grew without any inhibition (Figure 10). This means that that this concentration of NaCl was probably not sufficient to cause significant growth arrest.

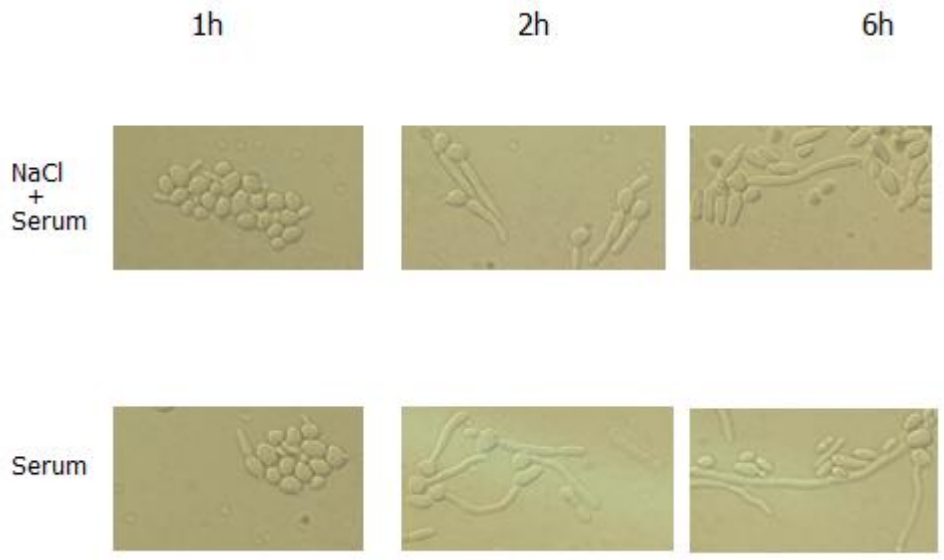

Figure 11: Impact of NaCl on serum- induced hyphae formation in WT cells.
WT cells were treated with NaCl plus serum and, serum as shown in each panel. Morphology was observed for each cell treatment over time as indicated.

3.5 Examination of the role of Cap1 regulatory proteins Ybp1 and Gpx3 in H_2O_2-mediated delay of serum-induced morphogenesis and growth arrest.

The scavenging of ROS in *C. albicans* is dependent on the Cap1 AP-1-like transcription factor, and its co-regulators Ybp1 and Gpx3. Ybp1 forms a complex with Cap1 in the cytoplasm to prevent its degradation and to facilitate its oxidation by the Gpx3 thiol peroxidase (Smith *et al*., 2004) As the previous experiments showed that H_2O_2 caused sustained inhibition of serum-induced morphogenesis in the oxidative stress sensitive *cap1*Δ null mutant, I included mutants of Gpx3 and Ybp1 and the reconstituted strains as controls with the aim to assess for reversal of H_2O_2- mediated inhibition serum-induced morphogenesis and sensitivity in the null mutants in further experiments.

Using 3 mM concentration of H_2O_2 which did not significantly ($p > 0.005$) kill the cells when percentage survival of the cells were compared from 1 h through 3 h to the 0 h for the H_2O_2 plus serum and H_2O_2 treated cells , I determined the effect of ROS on serum-induced hyphae formation as described before.

The results showed that exposure to H_2O_2 did inhibit serum-induced hyphae formation in *C. albicans* which was more prolonged in the oxidative stress sensitive null mutants but reversed in the reconstituted strains. Wild type cells treated with serum rapidly formed germ tubes in one hour, and then hyphae grew progressively longer over the 3 h period. In contrast, when the *WT* cells were treated with serum in the presence of H_2O_2, there was no formation of germ tubes for 1 h. The lack of hyphae formation was more sustained in the oxidative stress sensitive *cap1*Δ, *gpx3*Δ and *ybp1*Δ cells for at least 2 h. However, *WT* cells initiated hyphae formation after 1 h. Similarly, the reconstituted strains *cap1*Δ+ *CAP1*, *gpx3*Δ + *GPX3*, *ybp1*Δ + *YBP1* strains started forming hyphae after 2 h. All cells treated with H_2O_2 remained in the yeast form but started forming filaments at the 3rd hour time point (Figures 11, 12, and 13). The filamentous morphology that was later observed in the mutants following H_2O_2 plus serum treatment was different from the hyphae seen in the *WT* and reconstituted strains.

Therefore, each filamentous cell morphology was identified as hyphae (Sudbery *et al*., 2004) or hyperpolarised buds (HPB) (Da Silva *et al*, 2010), counted and expressed as a percentage of total of the two morphology types per high power field. At least 50 cells were counted per experiment which was repeated at least three times. The number of each filamentous cell type was expressed as a percentage of the total number of filamentous cells.

The results revealed that after 3 h treatment with serum in the presence of H_2O_2, hyphal cells predominated with wild type cells whereas hyperpolarised buds were formed in the oxidative stress sensitive mutants. The filamentous *WT* cells comprised of 95 % hyphal cells while the filamentous *cap1*Δ cells were composed of 98 % hyperpolarised buds. In another comparison, filamentous *WT* cells were 83 % hyphae while filamentous *gpx3*Δ strains were composed of 93 % hyperpolarised buds. Furthermore, the filamentous *WT* cell morphology was 89 % hyphal type while filamentous *ybp1*Δ cells were 79 % hyperpolarised buds (Figure 14). The predominance of hyperpolarised buds in oxidative stress sensitive mutants is further evidence of sustained cell cycle arrest compared to hyphal cells in *WT* cells. This means that H_2O_2 treatment leads to sustained growth arrest which was demonstrated by formation of hyperpolarized buds in the oxidative stress sensitive mutants versus hyphae of actively growing wild type cells.

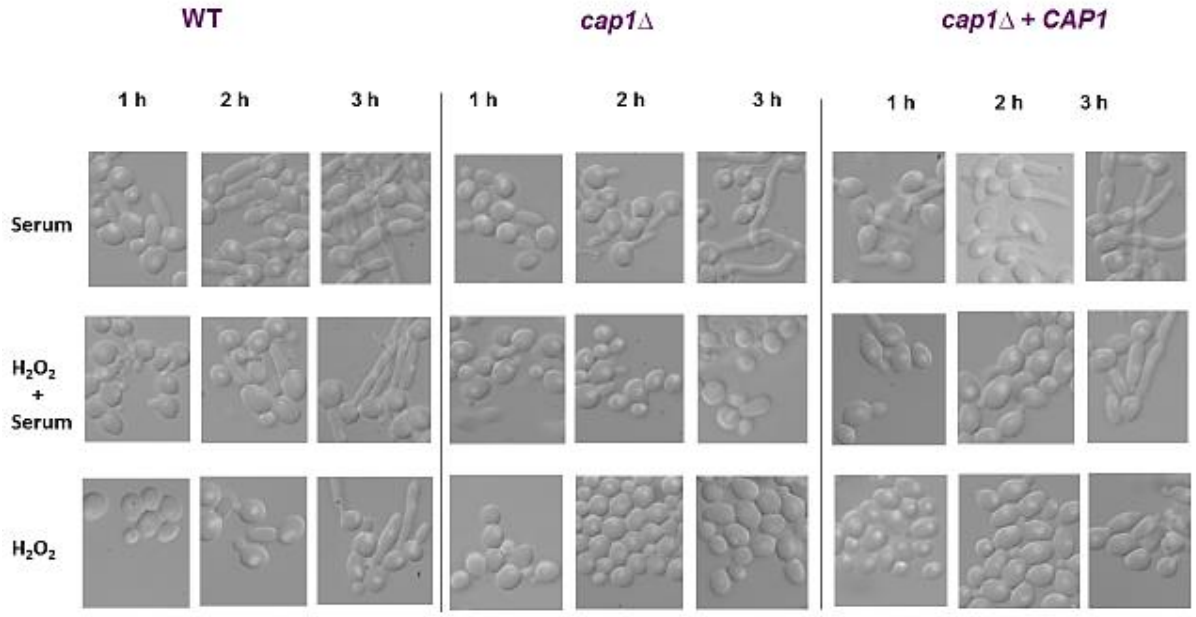

Figure 12: Impact of H_2O_2 on serum-induced filamentation on WT, *cap1*Δ & *cap1*Δ + *CAP1*. Cells were treated with serum, H_2O_2 plus serum, and H_2O_2 as indicated in the panels. Cells were collected at hourly intervals for 3 h and the morphology at each time point shown. Each experiment was repeated at least three times.

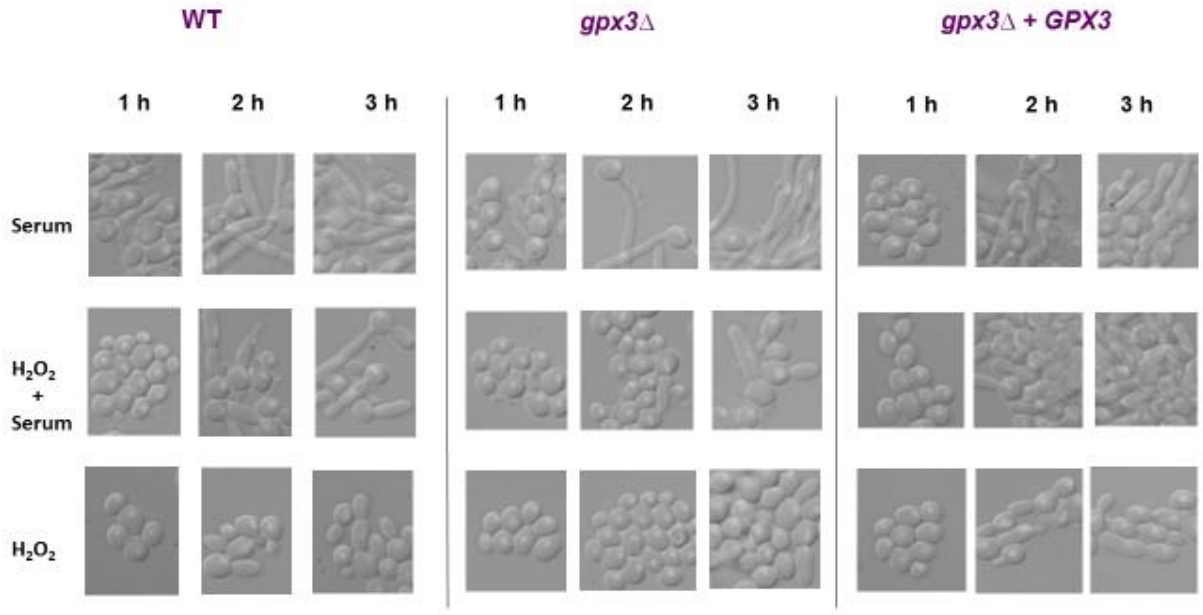

Figure 13: Impact H_2O_2 on serum-induced filamentation in *WT, gpx3*Δ and *gpx3*Δ + *GPX3 cells*. Cells were treated with serum, H_2O_2 plus serum, and H_2O_2 as indicated in the panels. Cells were collected at hourly intervals for 3 h and the morphology at each time point shown. Each experiment was repeated at least three times.

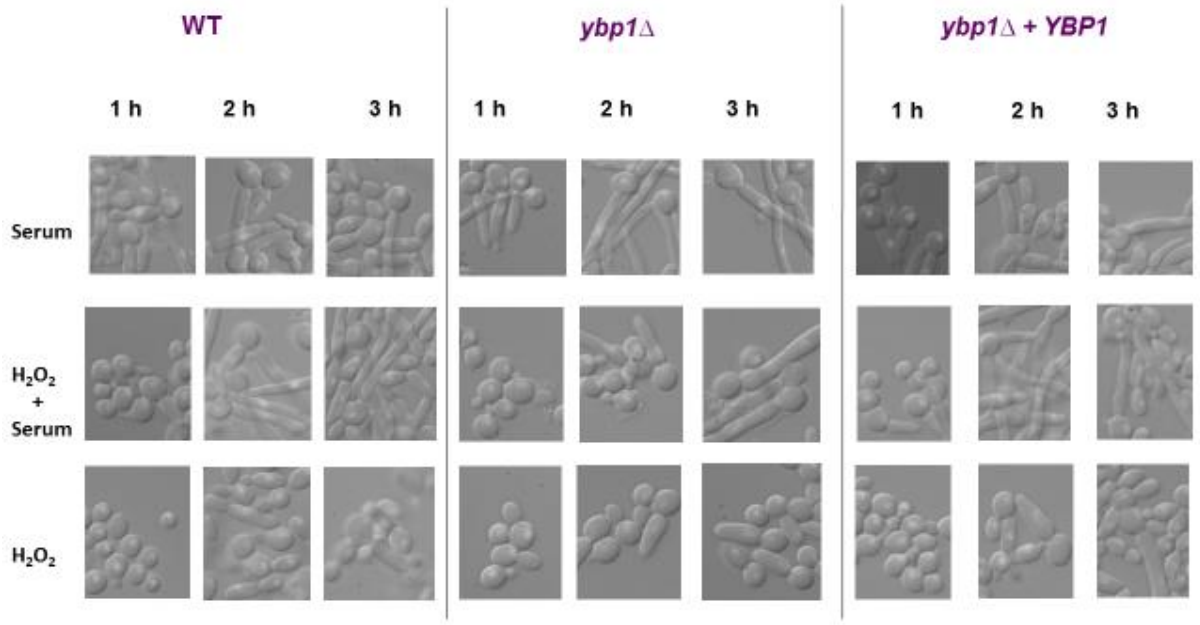

Figure 14: Impact of H_2O_2 on serum induced filamentation in WT, *ybp1*Δ and *ybp1*Δ + *YBP1*.
Cells were treated with serum, H_2O_2 plus serum, and H_2O_2 as indicated in the panels. Cells were collected at hourly intervals for 3 h and the morphology at each time point shown. Each experiment was repeated at least three times.

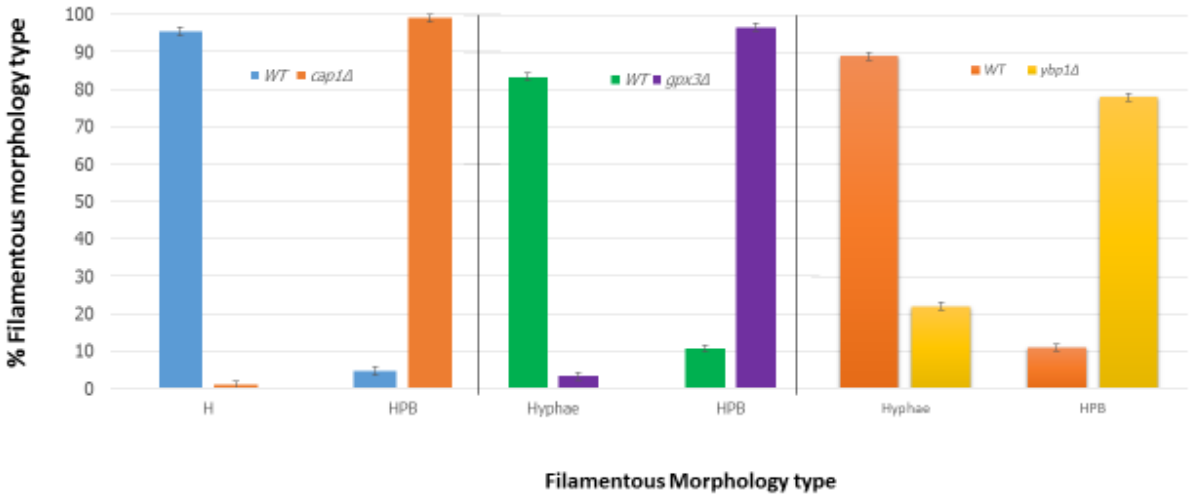

Figure 15: Morphology of *WT*, *cap1*Δ, *ybp1*Δ *and gpx3*Δ cells following treatment with H_2O_2 and serum at 3 h time point.
The morphology of cells treated with serum and H_2O_2 was characterised upon resumption of filamentation at the 3rd hour time point. Each filamentous cell morphology was identified as hyphae or hyperpolarised bud (HPB), counted and expressed as a percentage of the total number of the two types of morphology per field. At least 50 cells were counted per experiment which was repeated at least

three times. The number of each filamentous cell type was expressed as a percentage of the total number of filamentous cells.

3.5. H_2O_2 inhibition of serum-induced morphogenesis was due to growth arrest which was prolonged in oxidative stress sensitive mutants.

The previous experimental data revealed that oxidative stress sensitive *cap1*Δ, *gpx3*Δ, *and ybp1*Δ cells showed a more sustained H_2O_2-induced inhibition of filamentation than *WT* cells. Additionally, upon resumption of filamentation, the phenotypes differed; with hyperpolarized buds being more predominant in the oxidative stress sensitive mutants than *WT* cells. These data suggest that the delay in serum-induced hyphae formation in the oxidative stress sensitive mutants was due to growth arrest. Therefore, based on the previous data, it was expected that the delay in filamentation of cells treated with serum plus H_2O_2 was due to prolonged growth arrest and not cell death. To explore this, survival assays were performed as before.

Briefly, cells treated with H_2O_2, and H_2O_2 plus serum were taken at hourly time points and plated onto YPD agar to determine the impact of H_2O_2 on cell survival over 3 h period. The plates were incubated at 30°C for 24 h. Cell survival was expressed as a percentage of time zero sample.

The findings showed that treatment of *WT* cells did not significantly affect cell survival when compared with *cap1*Δ cells (Figure 15). Following H_2O_2 treatment, cell survival reduced to 80 % while for H_2O_2 plus serum, the cells reduced to about 75 % after 1 h. After 2 h, cells treated with H_2O_2 reduced to 75 % while H_2O_2 plus serum treated cells increased to 100 %. This was then followed by increasing number of cells to over 150% for H_2O_2 treatment, and 130 % for H_2O_2 plus serum treatment at 3 h. In contrast, in *cap1*Δ cells there was decreased survival to 65 % when treated with H_2O_2 and 70% following H_2O_2 plus serum treatment after 1 h. There was still decreased survival of cells to about 68% and 75 % due to treatment with H_2O_2 and H_2O_2 plus serum, respectively after 2 h. In the 3 h time point, the H_2O_2 plus serum treated cells increased to about 130% while in H_2O_2 treatment, they increased to 150 %. However, in the *cap1*Δ + *CAP* cells, there was no decrease in the number of cells. In the 1 h time point, both H_2O_2 and H_2O_2 plus serum treated cells slightly increased to about 113 %. Then the cells treated with H_2O_2 increased to 130 % while the cells in H_2O_2 plus serum treatment increased to 160 %. And after 3 h, cell following both H_2O_2 and H_2O_2 plus serum treatment, the cells increased to 170 % (Figure 15). The findings on the comparison of survival of H_2O_2 plus serum treated cells mean that there was a more prolonged growth arrest in *cap1*Δ cells than the reconstituted *cap1*Δ + *CAP* and *WT* cells.

The H_2O_2 survival assay analysis of *WT* and *gpx3*Δ showed a temporary slow growth followed by increasing trend in the number of cells over time (Figure 16). After 1 h in the *WT* cells treated with H_2O_2, there was no loss in viability of cells but there was a slight increase to about 110% while there was a slight reduction in survival to 95 % in H_2O_2 plus serum treatment. At 2 h time point, the *WT* cells increased in number to 130 % and 220 % following H_2O_2 and H_2O_2 plus serum treatment, respectively. Then the cells increased to 128 % in H_2O_2 and 170% with H_2O_2 plus serum treatments. In contrast for the *gpx3*Δ cells, after 1 h there was decreased survival of H_2O_2 treated cells to 65 % and 60 % after H_2O_2 plus serum treatment. The 1 h decrease in the survival of *gpx3*Δ was overcome in the reconstituted strain of *gpx3*Δ + *GPX3* control which showed no decrease in cell viability which remained at 100 % for 1 hour for H_2O_2 plus serum treatments and 80 % after H_2O_2. In the 2nd hour, the cells increased to 120 % following both H_2O_2 and H_2O_2 plus serum treatment. Then after 3 h, the cells increased to 170 % and 130 % after H_2O_2 and H_2O_2 plus serum treatment (Figure 16). The results mean that there was a prolonged growth arrest of *gpx3*Δ than *gpx3*Δ + *GPX3* and *WT* cells.

Consistent with the data for *gpx3*Δ, H_2O_2 survival assay analysis of *WT* and *ybp1*Δ also showed that the survival of wild type cells increased over time from 1 h to 3 h (Figure 17). In the *WT* cells, the first hour was characterized by slow growth with only about 10% increase in the number of cells treated with H_2O_2 while cells treated H_2O_2 plus serum treatment increased by 20 %. This was followed by a gradual increase in the number of cells to about 130 % and 150 % following H_2O_2 and H_2O_2 plus serum, respectively after 2 h. After 3 h, the cells increased to 140 % in H_2O_2 and 175 % after H_2O_2 plus serum treatment. However, there was a decrease in the viability of *ybp1*Δ cells to 75% for and 70 % after 1 h of H_2O_2 and H_2O_2 plus serum treatment, respectively. This was followed by an increasing trend to 100 % for and 120% for cells treated with H_2O_2 and H_2O_2 plus serum, respectively after 2 h. After the 3rd hour, the cells treated with H_2O_2 increased to 200 % and 180 % after H_2O_2 plus serum treatment. In the reconstituted *ybp1*Δ + *YBP1* strain, the 1 h reduction in the survival of *ybp1*Δ was overcome, which similar to *WT*, showed an increasing trend throughout 3 h of the assay. After 1 h treatment the cells remained at 100 % and increased to 110 % following H_2O_2 and H_2O_2 plus serum treatment respectively. In the 2nd hour, the cells increased to 230 % and 155 % after H_2O_2 and H_2O_2 plus serum treatment respectively. After 3 h of treatment in H_2O_2 and H_2O_2 plus serum treatment the cells increased to 120 % and 180 %, respectively (Figure 17). Therefore, there was a more prolonged growth arrest of *ybp1*Δ than *ybp1*Δ + *YBP1* and *WT* cells.

Common to all these survival assays data (Figures 15, 16 and 17), the periods in which there was no increase in the surviving number of cells correspond to the duration of inhibition of serum induced hyphae formation as shown in the previous data (Figures 11, 12 and 13). There was no significant decrease in survival of the mutants and the *WT* cells following H_2O_2 plus serum treatment (p = 0.0598, 0.1429, 0.0523 for *WT* versus *cap1*Δ, *gpx3*Δ and *ybp1*Δ). Although there was no significant loss of survival of mutant cells during inhibition of serum-induced hyphae formation, the increases in percentage viability of the mutants took longer than *WT* in the early time points of 1 h (for *gpx3*Δ and *ybp1*Δ) and 2 h *cap1*Δ after treatment with H_2O_2 plus serum. These mean that the cells were in a more prolonged state of growth arrest compared to wild type cells. The increasing number of cells from 2 h suggests that the cells were coming out of the H_2O_2 mediated growth arrest. But, similar percentage survival for *WT* and the mutants after 3 h suggests that then filamentation was preventing accurate count of cell number.

There was a variability between the findings of the assays with the *WT* cells. There was decreased survival of *WT* cells in the assay conducted with *cap1*Δ and *cap1*Δ + *CAP1* cells following H_2O_2 treatment. However, there was increased survival of H_2O_2 treated *WT* cells when the assay was conducted with *gpx3*Δ and *gpx3*Δ + *GPX3* cells. The difference could have arisen from using an old stock of H_2O_2. Although, the laboratory stock of H_2O_2 was changed regularly and stored in the fridge, H_2O_2 is an unstable chemical and could have lost potency over 1 month which was reflected in the decreased sensitivity of the *WT* cells.

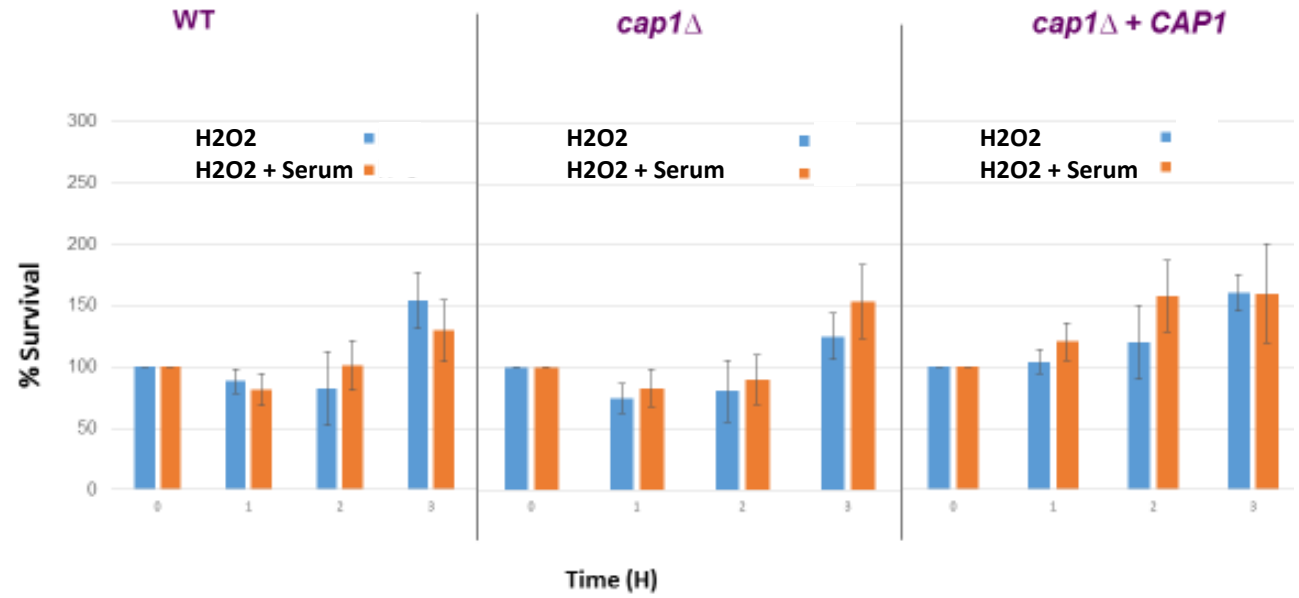

Figure 16: Impact of H_2O_2 exposure on cell viability of *WT*, *cap1*Δ and *cap1*Δ+ *CAP1*. Stationary cells were treated with 2 mM H_2O_2, and 2 mM H_2O_2 plus 10 % serum. The culture was incubated at 37 ˚C with shaking at 180 rpm. Hourly survival of cells was calculated as a percentage of the original 0 hour number of cells for 3 hours. Each experiment was repeated three times and the error bars represent the SD. One way Analysis of variance (ANOVA) was used to determine the statistical significance of Cap1 for H_2O_2 survival comparing *cap1*Δ, *cap1*Δ+ *CAP1* and the wild type cells over time: *p = 0.0598.*

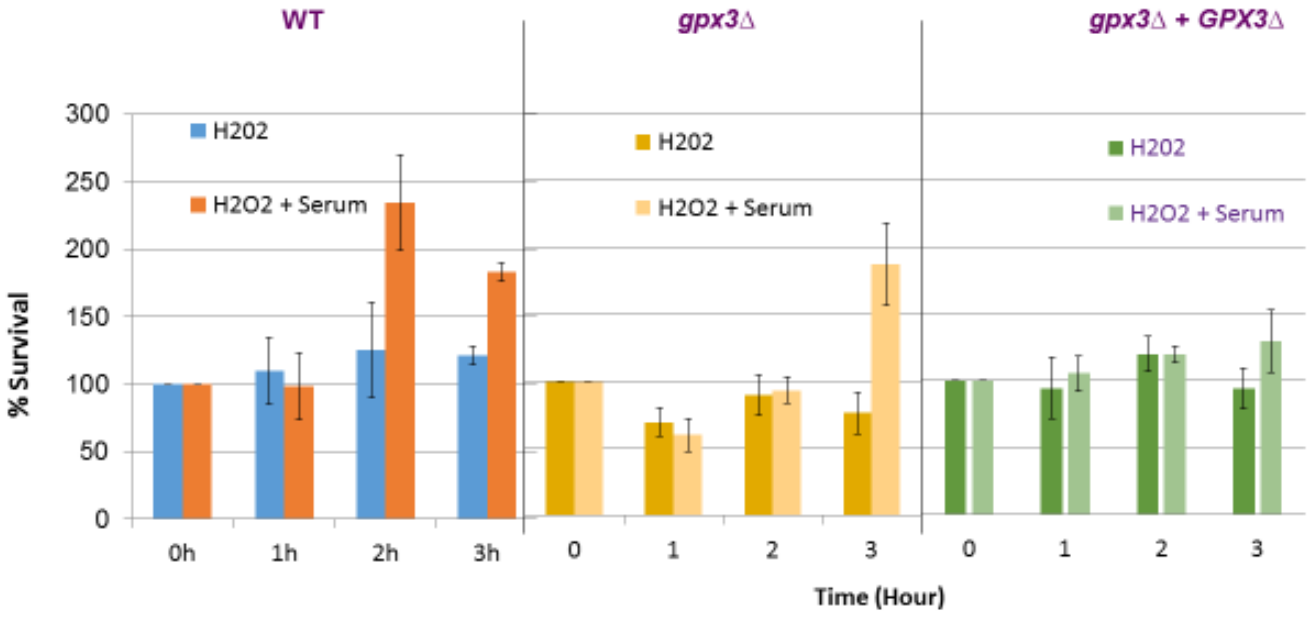

Figure 17: Impact of H_2O_2 exposure on cell viability of *WT*, *gpx3*Δ and *gpx3*Δ+ *GPX3.* Stationary cells were treated with 3 mM H_2O_2, and 3 mM H_2O_2 plus 10 % serum. The culture was incubated at 37˚C with shaking at 180 rpm. Hourly survival of the cells was calculated as a percentage of the original 0 hour number of cells for 3 hours. Each experiment was repeated three times and the error bars represent the SD. One way ANOVA was used to determine the statistical significance of comparison of survival of WT versus *gpx3*Δ versus *gpx3*Δ+ *GPX3* cells for H_2O_2 and H_2O_2 plus serum treated cells over time: *p – value = 0.1429.*

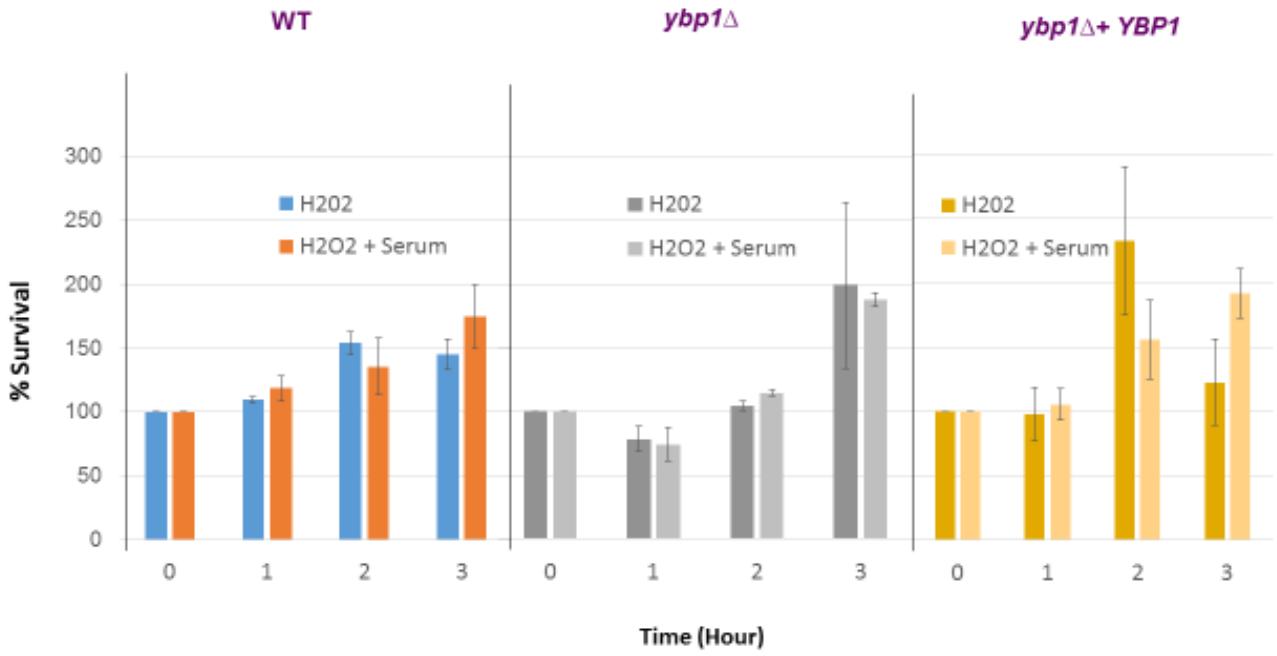

Figure 18*:* Impact of H_2O_2 exposure on cell viability of *WT*, *ybp1*Δ and *ybp1*Δ+ *YBP1*.
Cells were treated with H_2O_2, and H_2O_2 plus serum. Hourly survival of cells was calculated as a percentage of the original 0 hour number of cells for 3 hours. Each experiment was repeated three times and the error bars represent the SD. One way ANOVA was used to determine the statistical significance of Ybp1 for H_2O_2 survival comparing *ybp1*Δ, *ybp1*Δ+ *YBP1* and wild type cells over time: $p = 0.0523$.

3.6 Removal of H_2O_2 did not restore cell growth.

In the previous experiments, it was demonstrated that H_2O_2 causes inhibition of serum-induced morphogenesis by causing growth arrest. Furthermore, oxidative stress sensitive mutants demonstrated sustained growth arrest (Figures 11, 12, 13,15, 16, 17) characterized by hyperpolarised bud formation compared to hyphae predominance in *WT* cells (Figure 14). Thus, the aim was to determine if the hyperpolarised buds attained due to inhibition of serum-induced morphogenesis in the oxidative stress sensitive mutants could form hyphae after the removal of H_2O_2. The *gpx3*Δ mutant was chosen as it had shown the greatest level of hyperpolarised bud formation following the serum plus H_2O_2 treatment (Figure 14). Cells lacking *GPX3* were treated with H_2O_2 and serum until hyperpolarised buds were evident, following which cells were washed to remove the H_2O_2, and then re-suspended in fresh medium containing serum. As a control experiment for hyphae formation, untreated cells were washed in the same way and re-suspended in pre-warmed YPD media containing serum.

The results showed that removal of H_2O_2 did not relieve growth arrest as seen by the predominantly hyperpolarized buds cells from 1 h through 3 h. Furthermore, the hyperpolarised buds did not revert to hyphae following treatment with serum at 37°C. This

could be due to the conditions used as in the control experiment, untreated cells also could not form hyphae after the wash step plus serum and 37°C treatment (Fig 16). Thus, it was not possible to determine whether hyphae formation could be resumed following growth arrest using the method of this experiment.

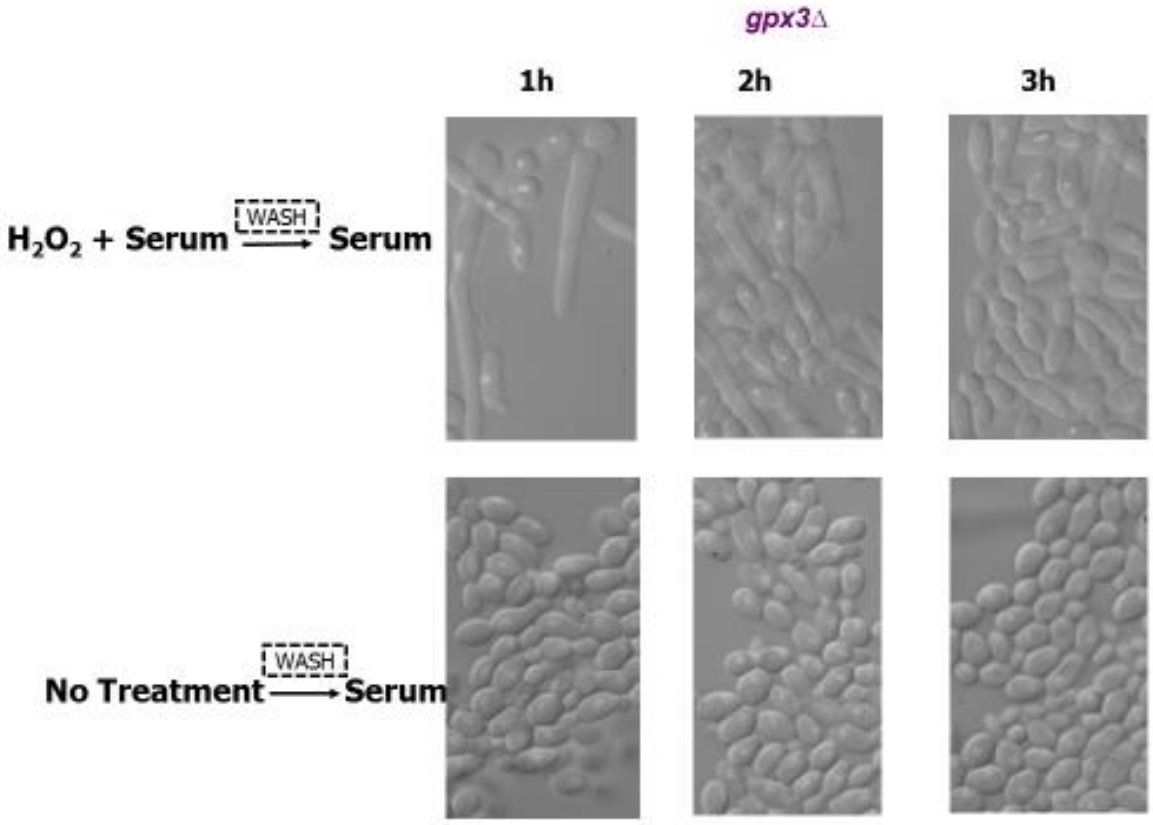

Figure 19: Filamentous morphology of oxidative stress sensitive *gpx3*Δ after removal of H_2O_2 followed by serum treatment.

The data (Sections 3.2-3.5) mean that the ability to mount robust oxidative stress responses is important to prevent sustained ROS - induced cell cycle arrest which in turn inhibits serum-induced morphogenesis.

Taken together, the findings may explain the inability of oxidative stress sensitive mutants of *C. albicans* to filament in the phagolysosomal environment of the macrophage.

3.7 *CAT1* overexpression did not rescue H_2O_2-mediated delay of serum-induced hyphae formation in *cap1*Δ cells.

The antioxidant catalase enzyme is upregulated in peroxide stress (Kaloriti *et al*., 2014), (Kos *et al*., 2016). Following the previous experiments which demonstrated that H_2O_2 causes inhibition of serum-induced filamentation of *C. albicans*, this objective was to

assess the effect of *CAT1*overexpression on H_2O_2-mediated inhibition of serum-induced filamentation. It was hypothesized that *CAT1* overexpression would prevent H_2O_2-induced inhibition of filamentation because the production of high levels of catalase would rapidly detoxify H_2O_2. Consequently, it would be expected that oxidative stress sensitive mutants, overexpressing *CAT1*, would be able to form hyphae following phagocytosis. If successful, these data would support the model that oxidative stress sensitive mutants do not to filament following phagocytosis due to their inability to mount an oxidative stress response.

Plasmid *pACT1+ CAT1* was integrated at the *RPS10* locus in wild-type (BWP13) and *cap1*Δ (BWP13 *cap1::loxP-HIS1-loxP/cap1::loxP-ARG4-loxP*) cells to expresses *CAT1* from the constitutive *ACT1* promoter. The control wild-type and *cap1*Δ cells had the empty vector *pACT1* integrated at the *RPS10* locus. As described before, morphology assays were set to test the abilities of the cells to form hyphae in the presence of 3 mM H_2O_2. Cell treatment was carried out for 3 h.

The results showed that in the *WT+ pACT1* cells, the serum control induced hyphae formation. However, in the serum plus H_2O_2 treated cells there was inhibited hyphae formation for the 3 h treatment (Figure 19). Discerning the impact of *CAT1* overexpression in the wild type cells, both *WT+ pACT1* and *WT+ pACT1+ CAT1* cells formed hyphae in the presence of serum treatment but there was inhibition of hyphae formation in the serum plus H_2O_2 treated cells of *WT+ pACT1* while *WT+ pACT1+ CAT1* formed hyphae. In contrast, in *cap1*Δ cells, there was hyphae formation in the serum treated cells but no induction of hyphae in both the *cap1*Δ + *pACT1* and the *cap1*Δ + *pACT1+ CAT1* cells following serum plus H_2O_2 treatment (Figure 19). The findings mean that *CAT1* overexpression did not reverse H_2O_2-mediated inhibition of serum-induced morphogenesis in the *cap1*Δ cells but did promote hyphae formation in *WT* cells. In the previous experiments where *CAT1* was not overexpressed, hyperpolarized bud formation was prominent in the cells treated with H_2O_2 plus serum in the *cap1*Δ cells. However, in this experiment in which *CAT1* was overexpressed in the cells, only few hyperpolarised buds were seen in the *WT+ pACT1* and none in the *WT + pACT1+ CAT1* cells. This suggests that ectopic expression of catalase improved the oxidase stress resistance of *WT* cells.

There were few hyperpolarized buds in the *cap1*Δ + *pACT1* but none in the *cap1*Δ + *pACT1 + CAT1* cells. The lack of hyperpolarized buds in the *cap1*Δ cells over expressing the catalase enzyme could be because the experiment was conducted for 3 h compared to 5 h in the previous experiments. This experiment was stopped at 3 h because it

was hypothesized that ectopic expression of catalase would overcome H_2O_2- mediated inhibition of serum-induced morphogenesis which was observed within the early time points.

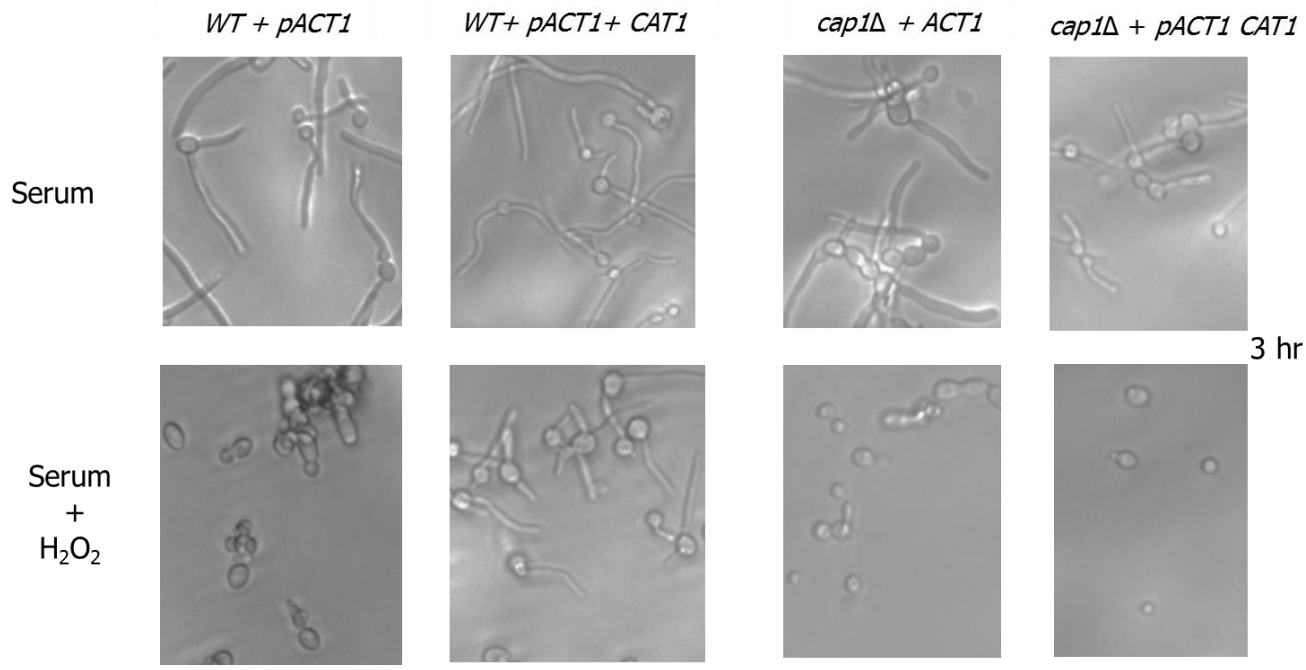

Figure 20: Impact of catalase overexpression on hyphae formation in *WT* and *cap1*Δ cells. Cells of *WT+ pACT1*, *WT+ pACT1+ CAT1*, *cap1*Δ + *pACT1*, *cap1*Δ + *pACT1+ CAT1* strains were treated with serum, serum plus H_2O_2 as shown in each panel. Morphology was observed for each cell treatment after 3h as indicated.

3.8 *CAT1* overexpression did not rescue the sensitivity of *cap1*Δ cells to H_2O_2.

Following *CAT1* overexpression, there was no reversal of H_2O_2-mediated inhibition of serum-induced hyphae formation in the *cap1*Δ cells. I aimed to determine the sensitivity of the *WT* and *cap1*Δ cells which were expressing catalase to H_2O_2.

Stationary phase cells from overnight cultures which were grown to mid-exponential phase, diluted back to OD_{660nm} = 0.15 and two further serial 10-fold dilutions, were spotted onto YPD agar plates containing 2 mM, 3 mM and 5 mM of H_2O_2 concentration range. The concentrations were chosen based on a range below and above 3 mM H_2O_2 which was used for treating the cells in the catalase overexpression morphogenesis experiment for which the finding is presented in Figure 20. The cells were incubated at 30˚C overnight. The results showed that catalase overexpression enhanced the growth of *WT* cells in the presence of 2, 3 and 5 mM H_2O_2. However, the findings revealed that 2 mM, 3 mM H_2O_2 did not affect the survival of *cap1*Δ cells. And even at 5 mM H_2O_2 when the survival of *cap1*Δ cells was decreased, catalase overexpression did not increase the resistance to H_2O_2. These results mean that catalase overexpression increased the resistance of *WT* cells to H_2O_2. However, catalase

overexpression did not increase the resistance of *cap1*Δ cells to H_2O_2. Instead the original *cap1*Δ cells became more resistant to H_2O_2 (Figure 20).

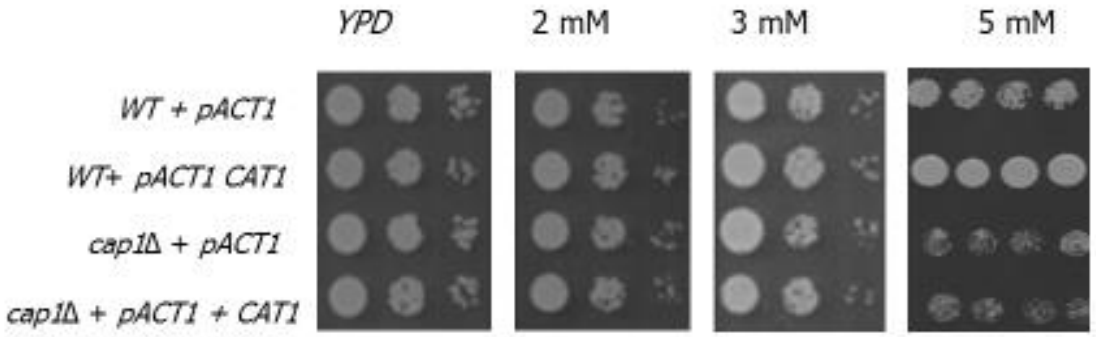

Figure 21: Impact of catalase overexpression on survival of *WT* and *cap1*Δ cells.
Cells of *WT+ pACT1, WT+ pACT1+ CAT1, cap1*Δ *+ pACT1, cap1*Δ *+ pACT1+ ACT1* strains were treated with 2, 3, and 5 mM H_2O_2 as shown in each panel. Growth was observed for each cell treatment after 24 h.

3.9 Summary.

In this chapter 3, the aim was to determine the role of H_2O_2 on serum-induced hyphae formation. Morphogenesis and survival assays where cells were collected at hourly intervals up to 5 h were performed. Then DIC images and, percentage survival CFU were recorded.

The findings showed that H_2O_2 affected serum-induced morphogenesis in a concentration-dependent fashion. Concentrations of H_2O_2 up to 1 mM showed no effect, 3 mM caused delay while 5 mM inhibited serum-induced hyphae formation in the oxidative stress sensitive mutants (Figures 5, 6, 7). The delay in serum-induced morphogenesis was due to growth arrest while inhibition of hyphae formation was caused by cell death of the oxidative stress sensitive mutants when treated with 5 mM H_2O_2. The *WT* cells had shorter delays in serum-induced morphogenesis than the oxidative stress sensitive mutants and the cells remained viable (Figures 8, 9).

Using H_2O_2 concentration which did not cause significant cell death ($p > 0.05$) the findings showed that H_2O_2 caused sustained delay of serum-induced formation of hyphae (Figures 6) due to growth arrest (Figures 8) in the oxidative stress sensitive mutants. Prolonged growth arrest was also shown by the predominance of hyperpolarized buds in the oxidative stress sensitive mutants compared to hyphae in the *WT* cells (Figure 14). The sustained delay in filamentation and growth arrest in the oxidative stress sensitive null mutants were rescued in the reconstituted strains of Cap1 and co-regulators (Figures 11-13, 15-17). Furthermore, growth arrest was not reversible by removal of H_2O_2 from the culture medium (Figure 18). However, overexpression of catalase did not rescue the lack of

filamentation and sensitivity of *cap1*Δ cells (Figures 19, 20). These results mean that the ability to mount a robust oxidative response to ROS is important for serum-induced hyphae formation.

3.10 Discussion.

As oxidative stress sensitive *cap1*Δ and co-regulators failed to filament following phagocytosis (Patterson *et al*., 2013), it was possible that this was due to ROS inhibition of filamentation. Hence, a prediction that ROS might inhibit filamentation in an *in vitro* based filamentation assay was demonstrated.

There was inhibition of filamentation of cells that were treated with H_2O_2 in the presence of hypha-inducing conditions *in vitro* which suggest that ROS could prevent filamentation and macrophage escape of *C. albicans*. A more sustained delay in the filamentation of *cap1*Δ and its co-regulators; *gpx3*Δ and *ybp1*Δ versus *WT* cells which were treated with the various concentrations of H_2O_2 (Figures 6, 7) infers that the ability to mount oxidative stress response is important in triggering filamentation of *C. albicans*.

Notably, the progressive delay in the filamentation of *WT* cells with the increasing concentration of H_2O_2 (Figures 3, 4, 5 and 6) may allude to host factors that determine outcome of infection with *C. albicans*. The major candidacidal mechanism of macrophages is the production of ROS such as H_2O_2. At low levels of ROS, cells are resistant, can adapt to the stress and may escape phagocytosis for example, by forming filaments. At intermediate levels, cells express response genes to overcome the stress and enhance survival for example, by going into a state of growth delay. At a lethal dose, the ROS may overwhelm response elements of the cells which may succumb to the oxidative stress (Pizzimenti *et al*., 2010). The different mechanisms are discernible by the differences in filamentation.

The delay in filamentation of both *WT* and *cap1*Δ cells as evidenced by formation of filaments after some duration of incubation was interpreted to result from growth arrest (Figures 6 and 7). However, treatment of *cap1*Δ mutants with 5 mM H_2O_2 killed the cells as seen by the decreasing survival of cells overtime (Figure 9) and thus, the explanation for the lack of filamentation throughout the 5h experiment (Figure 7). This means that *cap1*Δ are more sensitive to H_2O_2 than *WT* cells and this finding is in agreement with a previous study (Patterson *et al*., 2013). These results provide possible explanations to a previous study that showed that oxidative stress sensitive mutants of Cap1 and co-regulators could not filament inside macrophages even though they were able form hyphae *in vitro*. But it was also observed that serum seemed to confer protection from cell death in the H_2O_2

survival assay (Figures 8). This was particularly noted for *cap1*Δ cells where the number of surviving cells was consistently higher in the H_2O_2 plus serum than H_2O_2 control in all the experiments (Figures 7 and 8). The protective effect of serum from H_2O_2-induced cell death is probably due to its buffer effect. The high pH of serum at 7.35 – 7.45 can neutralize the acidic pH of the YPD medium (pH 6). This observation is consistent with a similar phenomenon that is postulated to trigger phagocytic escape of *C. albicans*. Arginine biosynthesis with its resultant breakdown products such as urea has been suggested to lead to neutralization of the acidic pH of the phagolysosome that triggers filamentation of *C. albicans* (Vylkova *et al*., 2011, Ghosh *et al*., 2009).

C. albicans is also exposed to other forms of stress, including osmotic stress during phagocytosis. However, osmotic stress was not able to inhibit serum-induced hyphal growth as seen by filamentation in the presence of NaCl (Figure 10). This result can be interpreted in three ways. It is possible that NaCl causes transient cell cycle arrest which could be tested by viewing the cells at more frequent time intervals than the hourly timing as was determined. Additionally, it could mean that osmotic stress does not inhibit serum induced hyphal growth or it could also mean that NaCl at a concentration of 0. 35M does not inhibit filamentation of *C. albicans*. Another experiment with a higher concentration of NaCl could have been carried out to make a conclusion, but the focus of the project was on oxidative stress. Furthermore, in the host, various stresses act in combination which lead to enhanced candidacidal effects. For example, a combination of osmotic and oxidative stress was reported to be more potent than osmotic stress alone (Kaloriti *et al*., 2012). The impact of such stresses on hyphae formation *in vitro,* could be examined in further studies.

When the *WT* and null mutants were assessed together with the reconstituted strains of Cap1 and co-regulators, there was restoration of resistance to H_2O_2-mediated inhibition of serum-induced morphogenesis and growth arrest. These further infer that Cap1, Gpx3 and Ybp1 are important for oxidative stress resistance. Oxidative stress sensitive mutants lack transcription factors or signaling pathways that are important in overcoming the effect of oxidants. During physiological non-oxidative stress conditions, Cap1 is freely circulating between the cytoplasm and the nucleus. However, following oxidative stress, Cap1 becomes highly oxidized at its cysteine residues and the nuclear export system is blocked which leads to its accumulation in the nucleus to promote the expression of genes involved in antioxidative mechanisms (Patterson *et al*., 2013, Jain *et al*. 2013). Furthermore, *cap1*Δ was the most sensitive to H_2O_2 as seen by the longest delay in hyphae formation (Figures 9, 10, 11) and growth arrest (Figures 13, 14, 15) of at least 2 h compared

to *gpx3*Δ *and ybp1*Δ cells. This is consistent with previous studies which reported that Cap1 is the main transcription factor for oxidative stress response in *C. albicans* (Alarco *et al*., 1999, Patterson *et al*., 2013, Jain *et al*., 2013).

The relief of growth arrest following removal of H_2O_2 was expected. As H_2O_2 is a genotoxic agent, following DNA damage, it activates DNA checkpoint Rad53 kinase which halts growth arrest to allow for repair (Shi *et al*., 2007). But there was lack of morphogenesis of the formed hyperpolarized buds to yeasts. It was also not possible to induce hyphae formation from the hyperpolarized buds. These were perhaps, because the assay conditions were not conducive for hyphae formation as described above.

There was no reversal of H_2O_2-mediated inhibition of serum-induced hyphae formation in *cap1*Δ following overexpression of catalase perhaps because of increased resistance to H_2O_2 (Figure 19). It is not clear, why the *cap1*Δ strain containing the p*ACT1* promoter showed more resistance to H_2O_2 than the original strain but it is possible that some mutations were introduced during the transformation. But, there was increased resistance of the *WT* cells ectopically expressing catalase which improved serum-induced hyphae formation in the presence of H_2O_2 treatment. This is perhaps, because catalase is important for oxidative stress resistance (Pradhan *et al*., 2017).

CHAPTER FOUR

4 SCREENING OF A *C. ALBICANS* TRANSCRIPTION FACTOR DELETION LIBRARY FOR MUTANTS THAT DISPLAY IMPAIRED H_2O_2-INDUCED HYPERPOLARISED BUD FORMATION OR ROS RESISTANCE.

4.1 Introduction.

Previously in Chapter 3, it was shown that H_2O_2 inhibits serum-induced morphogenesis by causing growth arrest. Studies in the Quinn lab revealed that Rad53 kinase is essential for H_2O_2-induced growth arrest and formation of hyperpolarised buds in *C. albicans* (Da Silva *et al*., 2010). However, the downstream targets of Rad53 kinase remained elusive. It was hypothesised that these would include transcription factors because during growth arrest, there is transcriptional activation of genes to initiate DNA repair (Shi *et al*., 2007). It was further hypothesized that the DNA repair genes may be specific to *C. albicans* as the formation of hyperpolarized buds has not been reported in other yeasts. Thus, the major aim of this chapter was to identify novel transcriptional regulators of Rad53 kinase-induced hyperpolarised bud formation. Building on data in Chapter 3 that oxidative stress regulatory transcription factor mutants, such as *cap1*Δ cells displayed impaired hyphae formation in the presence of ROS, a further aim was to identify other transcriptional regulators necessary for oxidative stress resistance to assess if they similarly, displayed impaired hyphae formation following phagocytosis.

4.2 A screen of the *C. albicans* transcription factor deletion library did not identify transcription factors required for H_2O_2-induced hyperpolarised bud formation.

An initial library screen of 167 mutants of transcription factor (TF) mutants (Homann *et al*., 2009) by incubating exponentially growing cells in 5 mM H_2O_2 did not reveal any mutants that displayed defective H_2O_2 induced hyperpolarised bud formation.

To examine the transcription factor library further, the TF mutants annotated as having defective types of morphology (Homann *et al*., 2009) were retested. The mutants with morphological anomalies included *sfl1*Δ, *tye7*Δ, *mac1*Δ, *ndt80*Δ, *csr1*Δ, *tec1*Δ, *rim101*Δ, *isw2*Δ, *aaf1*Δ, *swi4*Δ, *bcr1*Δ, *cph2*Δ, *efg1*Δ, *rgt1*Δ, *rob1*Δ, *ahr1*Δ, *hms1*Δ, *arg83*Δ, *bas1*Δ, *sfc2*Δ, and *zcf7*Δ. These mutants were chosen as any such morphological anomalies could have been misconstrued as hyperpolarised buds. The mutants were treated with H_2O_2, observed for defective formation of hyperpolarised buds and microscopic images taken as described previously.

The findings from the initial results showed that *sfl1*Δ, *ndt80*Δ, *aaf1*Δ, *sw14*Δ and *sfl2*Δ cells seemed defective in forming hyperpolarised buds (Figure 21). Defective hyperpolarised buds were defined as few, small or indeterminate morphological forms that were similar to hyperpolarised buds. The *sfl1*Δ and *sfl2*Δ mutants formed filamentous cells prior to the addition of H_2O_2; they were filamentous at 0 h time point and the morphology was indeterminate after addition of H_2O_2 at 4 h. In contrast, the *ndt80*Δ cells which were yeasts at 0 h time point remained predominantly comprised of yeast morphology in chains after treatment with H_2O_2 at 4 h. Similarly, *aaf1*Δ and *swi4*Δ cells comprised predominantly of yeast morphology at 0 h time point and after treatment with H_2O_2 at 4 h while some cells had indeterminate morphology.

Following, the five transcription factor mutants; *sfl1*Δ and *ndt80*Δ, *aaf1*Δ, *swi4*Δ and *sfl2*Δ that showed defective formation of hyperpolarised buds were then analysed further at hourly intervals. Briefly, as before, overnight cells which were grown to exponential phase and were treated with 2 mM H_2O_2 and cells collected at hourly intervals for image analysis for formation of hyperpolarised buds. However, closer re-examination of the five mutants at hourly intervals showed that all the mutant cells had formed hyperpolarised buds (Figure 21). Furthermore, the results showed that the *sfl1*Δ strain formed hyperpolarised buds faster than *WT* cells. The other transcription factor mutants; *aaf1*Δ, *sw14*Δ and *sfl2*Δ formed hyperpolarised buds which were comparable to the *WT* cells. The results thus, mean that the transcription factor mutants with morphological defects were not important for formation of hyperpolarised buds.

In addition, as hyperpolarised bud formation is a consequence of growth arrest (Bachewich *et al.*, 2005, Da Silva *et al*., 2010), mutants with known or predicted roles in the cell cycle were examined. These mutants included *mbp1*Δ, *hcm1*Δ and *yox1*Δ. Mbp1 is involved in cell cycle progression from G1 to S phase (Hussein *et al*., 2011), Hcm1 drives S phase activation of genes (Bensen *et al*., 2002) and Yox1 is a homeobox transcriptional repressor (Côte *et al*., 2009). Results from screening of cell cycle regulators showed that all the mutants of cell cycle regulation formed hyperpolarised buds that were comparable to the *WT* cells (Fig. 23). The results mean that none of the transcription factors involved in cell cycle regulation that were examined are important for formation of hyperpolarised buds.

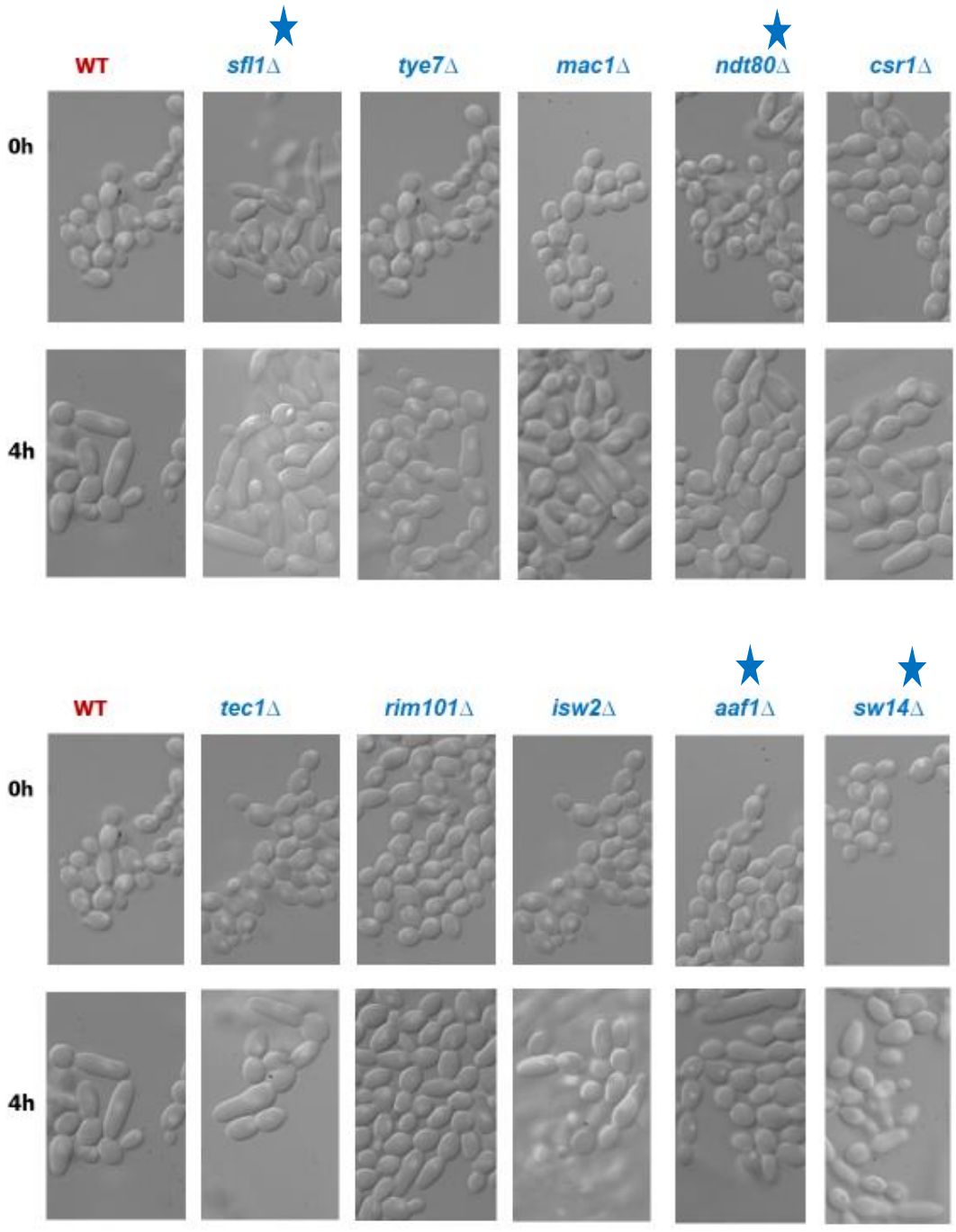
WT
sfl1Δ
tye7Δ
mac1Δ
ndt80Δ
csr1Δ
0h
4h
WT
tec1Δ
rim101Δ
isw2Δ
aaf1Δ
sw14Δ
0h
4h

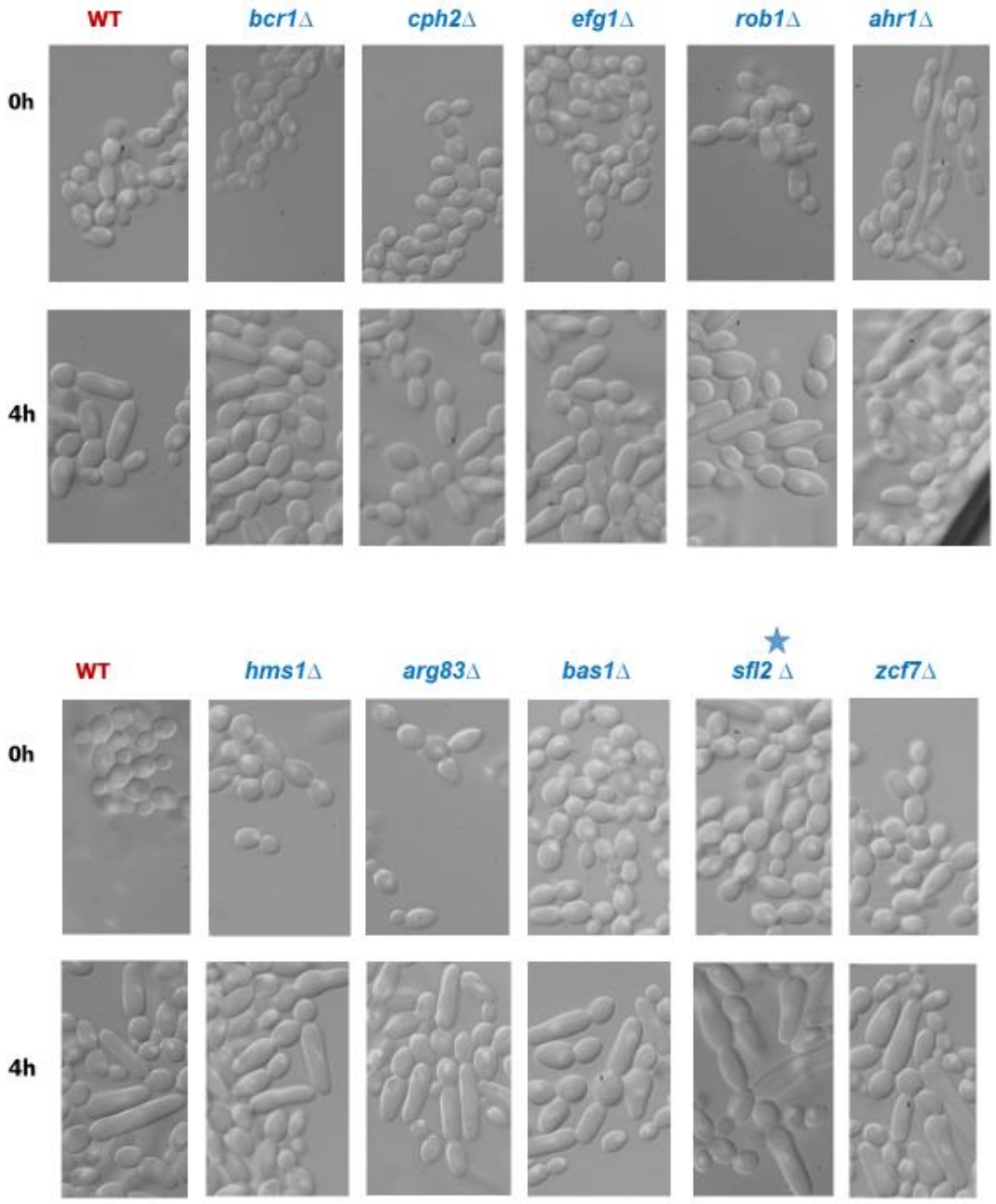

Figure 22: Impact of H_2O_2 treatment of TF mutants with defective colonial morphology. Transcription factor mutants and *WT* cells were treated with 2 mM H_2O_2 and effect on formation of hyperpolarised buds observed at 0 and 4 h as shown. The stars denote transcription factor mutants that formed defective hyperpolarised buds.

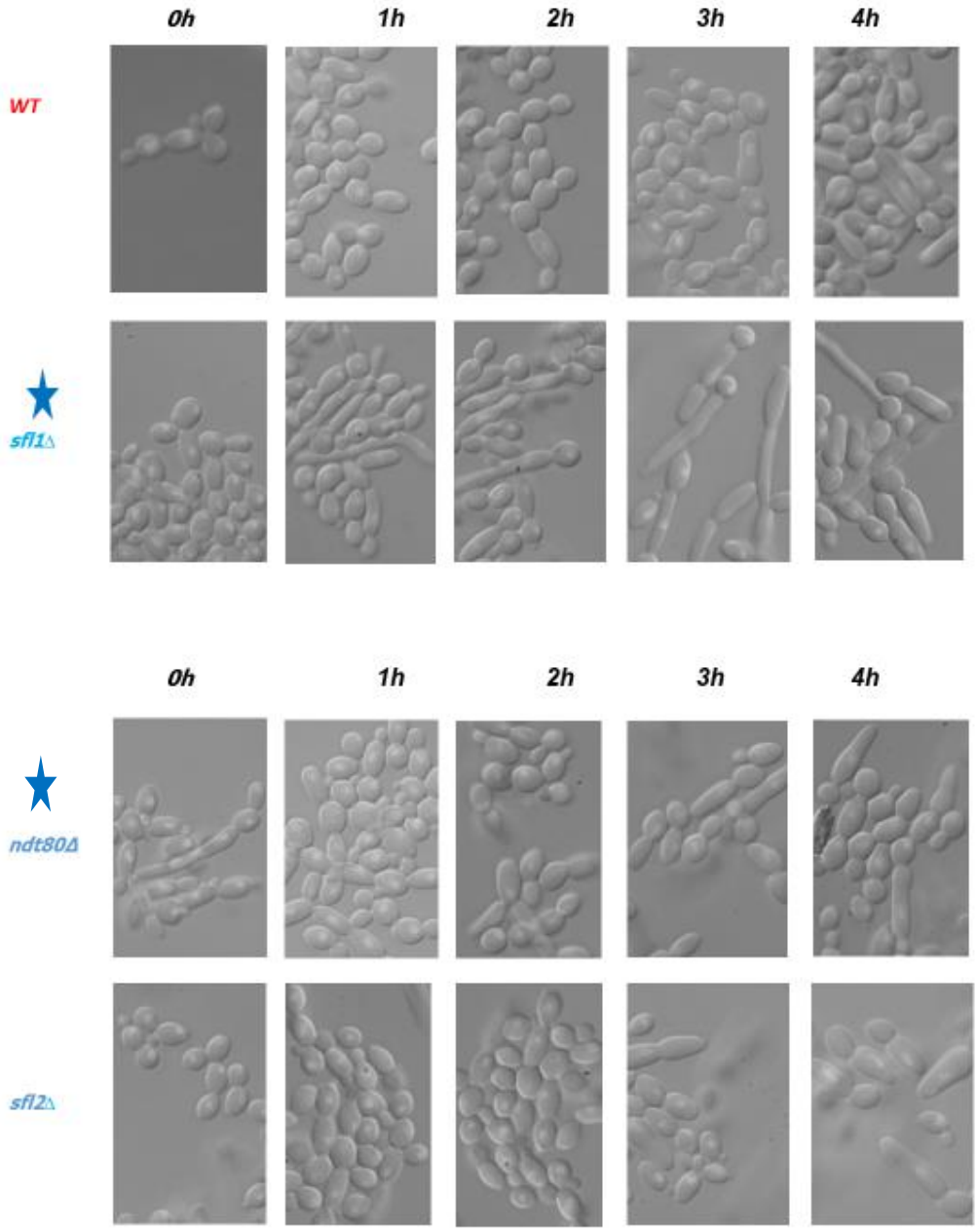
0h
1h
2h
3h
4h
WT
sfl1Δ
0h
1h
2h
3h
4h
ndt80Δ
sfl2Δ

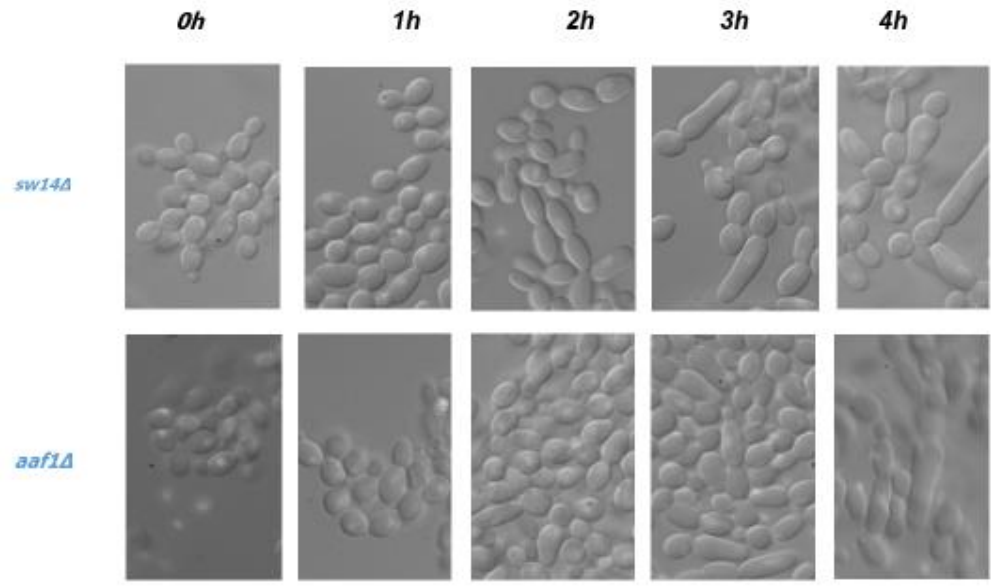

Figure 23: Impact of H_2O_2 treatment on TF mutants that had shown defective formation of hyperpolarised buds.
Exponential phase cells were treated with 2 mM H_2O_2. The cells were incubated at 30˚C with shaking at 180 rpm. Effect on morphology was observed at hourly intervals for 4 hours as shown.

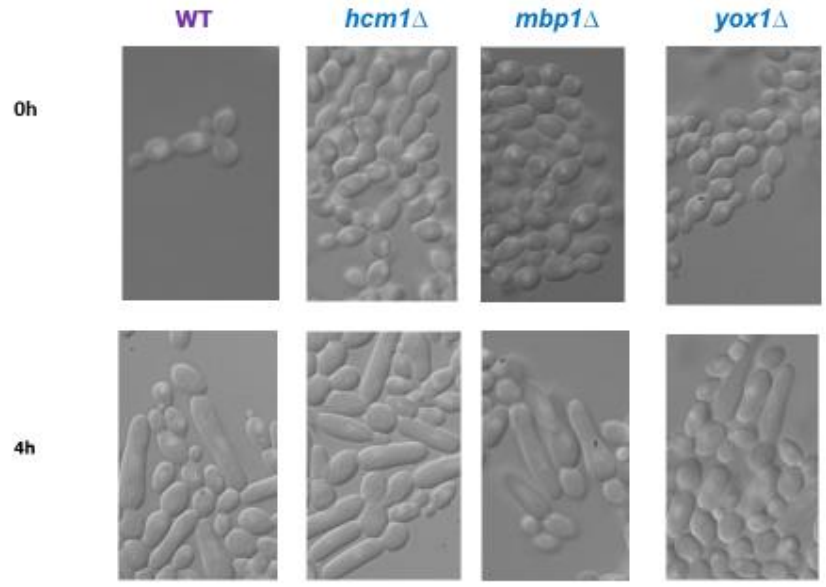

Figure 24: Impact of H_2O_2 treatment of TF mutants that are cell cycle regulators.
Exponential phase cells were treated with 2 mM H_2O_2. The cells were incubated at 30˚C with shaking at 180 rpm. Effect on formation of hyperpolarised buds was observed at 0 and 4 h as shown.

4.3 A screen of the *C. albicans* transcription factor deletion collection revealed that Skn7, Ndt80, Gzf3, Cap1 and Efg1 are important for oxidative stress resistance.

4.3.1 Quantitative fitness analysis (QFA) for transcription factor mutants that were most sensitive to H_2O_2.

To identify transcription factors essential for resistance to H_2O_2, QFA was performed on the transcription factor deletion collection (Homann *et al*., 2009). Exponential cells grown in YPD broth were spotted onto YPD agar with and without 3.5 mM H_2O_2, and growth was monitored by time-course images. The images were processed duplicates and quantitative growth parameters determined by colonyzer software (Figure 24: Data kindly provided by Ikeh *et al*., 2016). The As wild type cells showed reduced fitness in H_2O_2, a multiplicative model was used to assess the fitness of the mutants. In the multiplicative model, the fitness of mutants was expressed relative to the reduced fitness of wild type cells. Then the deviations from the wild type fitness generated a stress interaction score (SIS) of which the lowest value correlated with the most impaired growth in the presence of H_2O_2. The top ten mutants with the lowest SIS scores included *skn7*Δ, *ndt80*Δ, *gzf3*Δ, *cap1*Δ, *efg1*Δ, *cup9*Δ, *fcr1*Δ, *cph2*Δ, *rob1*Δ, *dpb1*Δ and *ash1*Δ (Figure 24: Data kindly provided by Ikeh *et al*., 2016). The QFA assay is more sensitive than the spot test method as it can detect small decreases in fitness.

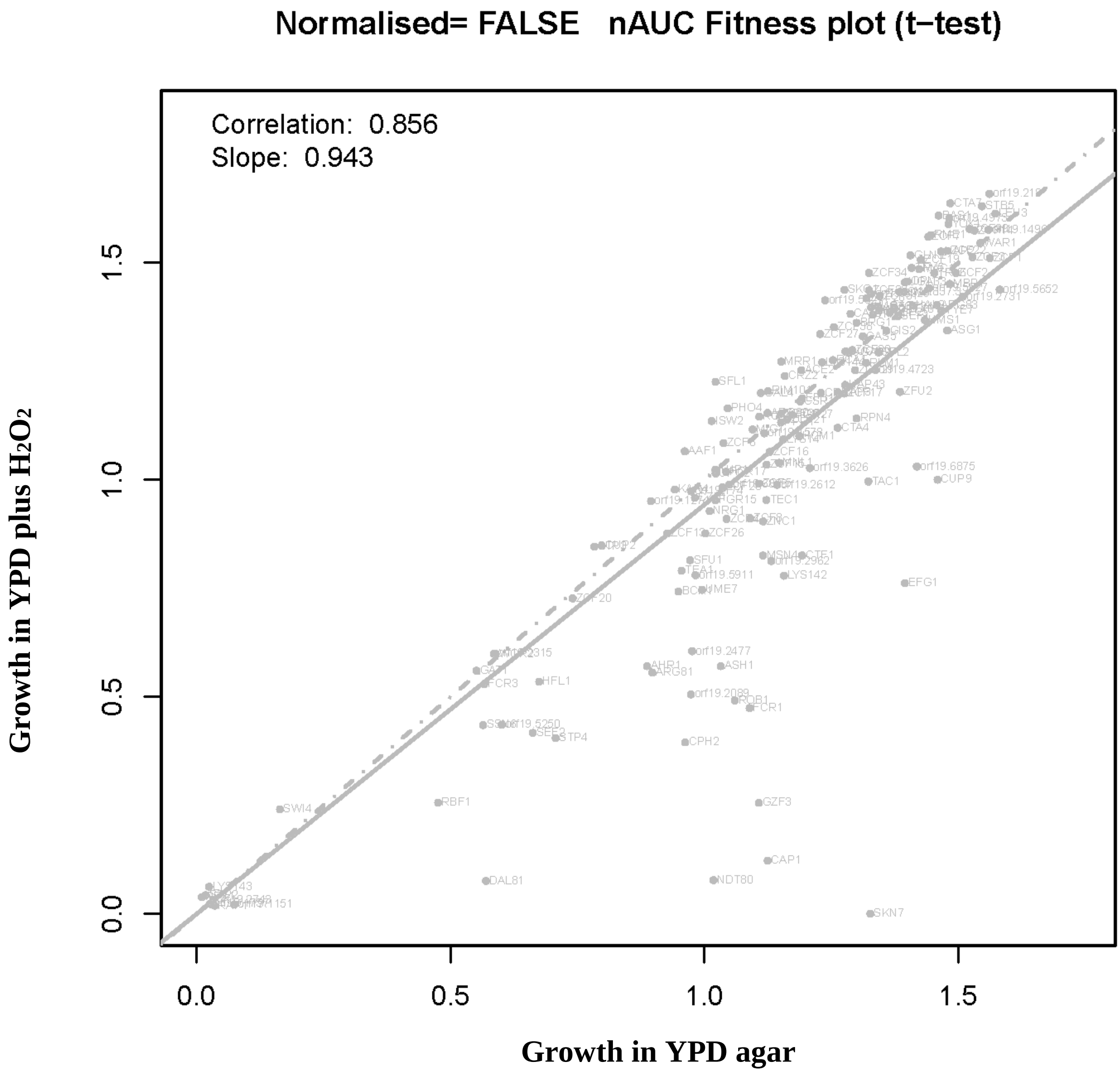

Normalised= FALSE   nAUC Fitness plot (t−test)
Correlation: 0.856
Slope: 0.943
Growth in YPD plus H_2O_2
Growth in YPD agar
0.0
0.5
1.0
1.5
0.0
0.5
1.0
1.5

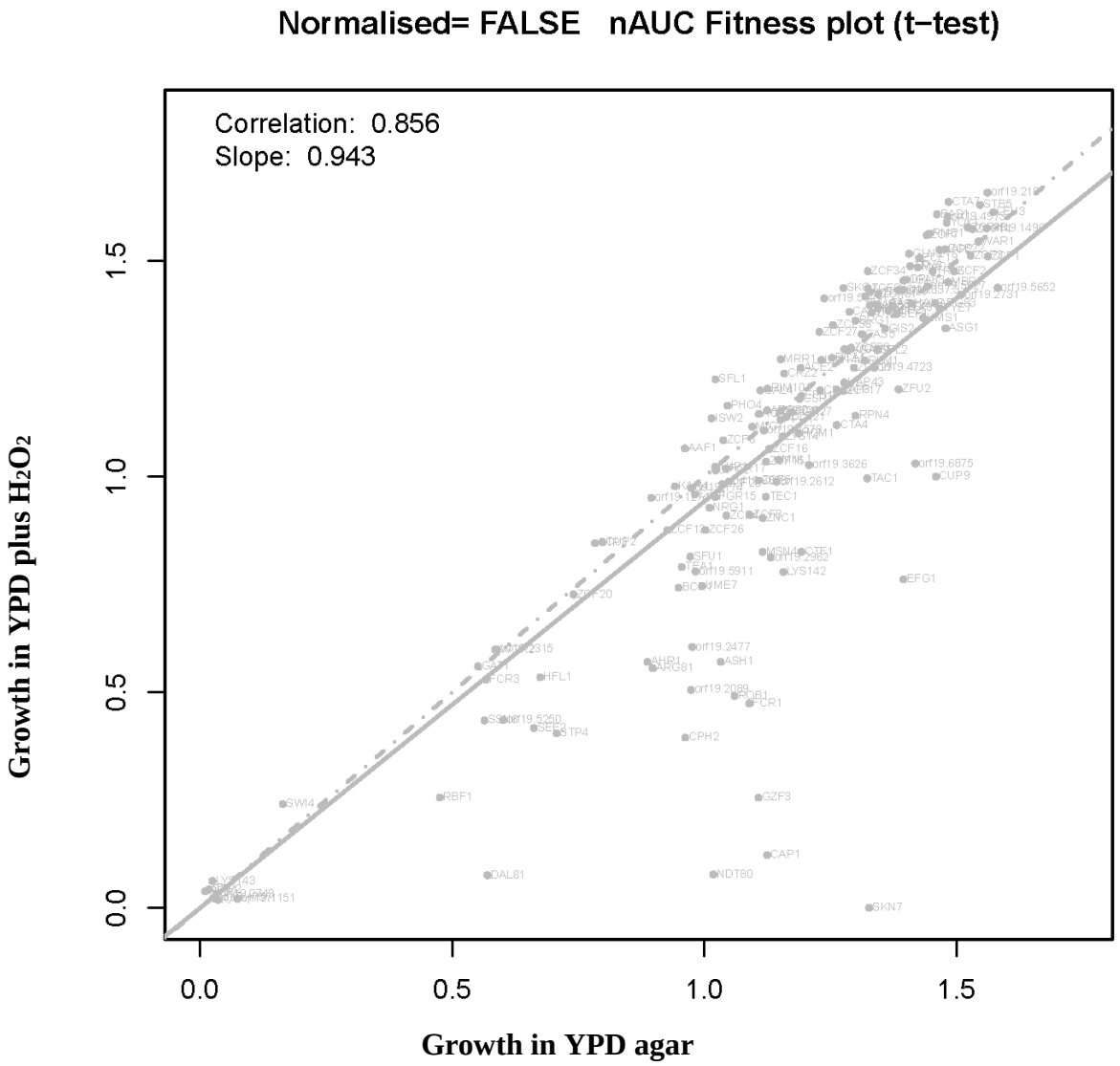

Figure 25: The QFA of the TF mutants in YPD and H_2O_2.
The transcription factor mutants were grown in YPD broth to exponential phase. Then cells were spotted onto YPD (control) and YPD plus H_2O_2 agar. Growth was monitored by time-course images which were processed by colonyzer software to determine quantitative relative fitness of the mutants in YPD, and YPD plus H_2O_2 agar. The Y axis shows quantitative fitness in the various concentrations of H_2O_2 while the X axis denotes quantitative fitness in YPD control (Ikeh et al., 2016).

ORF	Gene	SIS	ORF	Gene	SIS
ORF19.971	SKN7	-1.25116	ORF19.971	SKN7	-1.18974
ORF19.1623	CAP1	-0.93814	ORF19.610	EFG1	-0.97978
ORF19.2119	NDT80	-0.88282	ORF19.1623	CAP1	-0.97106
ORF19.2842	GZF3	-0.78866	ORF19.6514	CUP9	-0.84712
ORF19.610	EFG1	-0.55346	ORF19.2119	NDT80	-0.76149
ORF19.6817	FCR1	-0.55327	ORF19.2842	GZF3	-0.69794
ORF19.1187	CPH2	-0.51255	ORF19.2088	orf19.2089	-0.69215
ORF19.4998	ROB1	-0.50868	ORF19.4998	ROB1	-0.68399
ORF19.3252	DAL81	-0.46207	ORF19.6874	orf19.6875	-0.6035
ORF19.2088	orf19.2089	-0.41283	ORF19.1187	CPH2	-0.59566
ORF19.5343	ASH1	-0.40315	ORF19.6817	FCR1	-0.57967
ORF19.6514	CUP9	-0.37617	ORF19.5343	ASH1	-0.53401
ORF19.2476	orf19.2477	-0.31578	ORF19.2961	orf19.2962	-0.51756
ORF19.4778	LYS142	-0.31241	ORF19.3252	DAL81	-0.51052
ORF19.6874	orf19.6875	-0.3073	ORF19.4869	SFU1	-0.45663
ORF19.1499	CTF1	-0.29928	ORF19.909	STP4	-0.42214
ORF19.4766	ARG81	-0.2907	ORF19.5558	RBF1	-0.36221
ORF19.7381	AHR1	-0.26624	ORF19.1718	ZCF8	-0.35546
ORF19.909	STP4	-0.26265	ORF19.2476	orf19.2477	-0.33523
ORF19.2961	orf19.2962	-0.255	ORF19.6985	TEA1	-0.32049
ORF19.3188	TAC1	-0.25199	ORF19.7381	AHR1	-0.31991

Figure 26: The stress interaction scores of the TF mutants.
Using QFA, the wild type cells showed reduced fitness in both YPD and YPD plus H_2O_2. A multiplicative model in which the fitness of the null mutants was expressed relative to the reduced fitness of the wild type cells. The deviations from wild type fitness generated the SIS of which the lowest meant the least survival. Thus mutants highlighted in red where identified in replicate experiments as having impaired fitness in the presence of H_2O_2 and were examined further.

4.3.2 Transcription factor deletion strains *skn7*Δ, *ndt80*Δ, *gzf3*Δ, *cap1*Δ and *efg1*Δ showed defective growth in the presence of various sources of oxidative stress.

The mutants of transcription factors which were most sensitive to H_2O_2 (Ikeh, *et al*., 2016) were tested for sensitivity to additional forms of oxidative stress. The various sources of oxidative stress which included H_2O_2, tBOOH, menadione, and diamide, were chosen because they have distinct mechanisms of action. A previous study revealed that cell treatment with H_2O_2 leads to activation of DNA checkpoint Rad53 kinase and growth arrest (Da Silva *et al*., 2010). Related to H_2O_2 is tBOOH which is an organic peroxide linked to lipid peroxidation that forms more stable radicals. As can be discernible, the transcription factor mutants showed more sensitivity to tBOOH than H_2O_2 (Figure 4). Menadione; also known as Vitamin K3 causes Glucose-6 Phosphate Dehydrogenase deficiency (G6PD) which

leads to depletion of reduced antioxidative gluthathione and also generates superoxide thus predisposing cells to oxidative stress (Tongul *et al*., 2014, Jan *et al*., 2015). Diamide is a thiol oxidising agent (Hill *et al*., 2009).

The results revealed that null *cap1*Δ showed no growth in 3 mM H_2O_2, 2 mM tert- butyl hydroperoxide (tBOOH), 300 µM menadione and 2 mM diamide, *skn7*Δ showed impaired growth in 3 mM H_2O_2 and 2 mM tBOOH, *efg1*Δ showed defective growth in 2 mM diamide, while *ndt80*Δ showed impaired survival in 2 mM tBOOH and 2 mM diamide, and *gzf3*Δ showed impaired growth in 2 mM tBOOH and 2 mM diamide (Figure 26). The other mutants; *cup9*Δ, *fcr1*Δ, *cph2*Δ, *rob1*Δ, *dpb1*Δ and *ash1*Δ showed wild-type levels of survival to the different forms of ROS.

The findings from the spot tests differed from the results of the QFA screen, as only 5 of the 11 transcriptions factors were found to be sensitive to H_2O_2. The disparity in the findings was probably due to the differences in the methods used. The QFA method is able to identify subtle decreases in fitness in the presence of the stress agents which may not be detected in the less-sensitive spot test assay.

A.

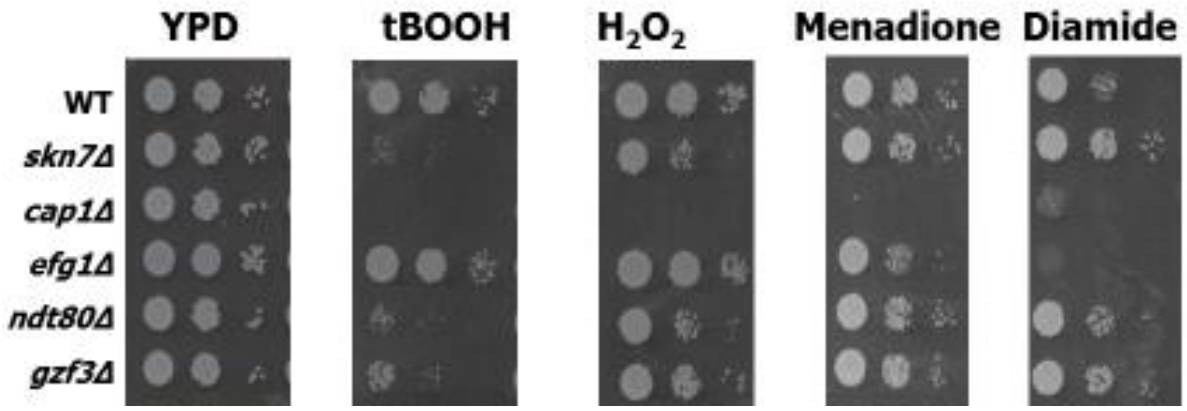

B.

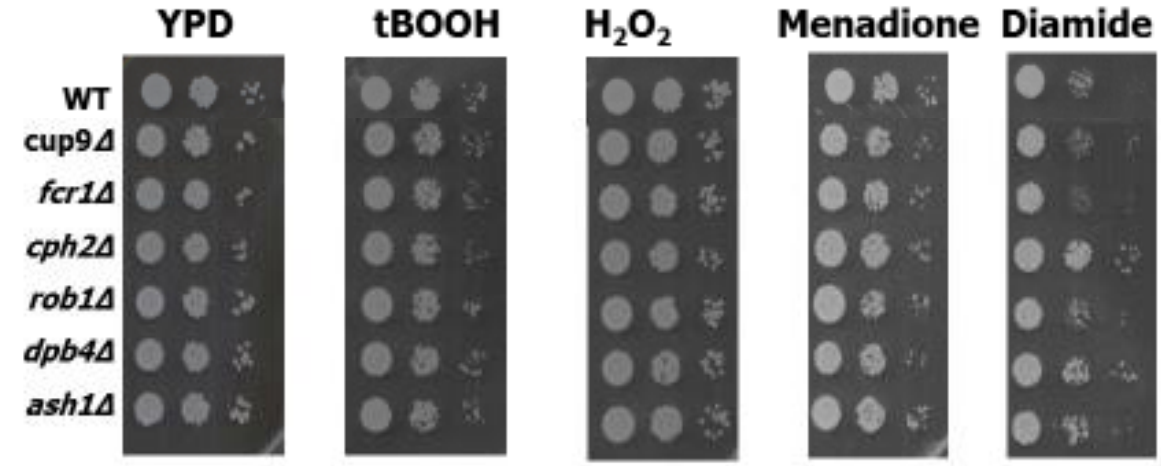

Figure 27: **Spot tests (A and B) survival of the TF mutants in various forms of oxidative stress.** Cells were spotted onto plates containing 2 mM tBOOH, 3 mM H_2O_2, 300 µM menadione, 2 mM diamide and effect on growth observed after as shown.

4.4 Summary.

Following oxidative stress induced DNA damage, the Rad53 checkpoint kinase is activated for DNA damage response and growth arrest to allow for repair mechanisms. Growth arrest can be demonstrable by formation of hyperpolarised buds (Da Silva *et al*., 2010). A library consisting of 167 transcription factor mutants (Homann *et al*., 2009) was screened for defective formation of hyperpolarised buds. The results showed that none of the transcription factor mutants was impaired in forming hyperpolarised buds. Therefore, none of the transcription factors was important for forming hyperpolarised buds.

The AP-1 Cap1 transcription factor is the major regulator for oxidative stress-induced gene expression. To elucidate further regulators of oxidative stress response, a panel of transcription factor mutants which had been identified by QFA as sensitive to H_2O_2 where tested to additional forms of oxidative stress by spot testing. The results showed that *skn7*Δ, *ndt80*Δ, *gzf3*Δ, *cap1*Δ and *efg1*Δ had impaired growth to one or more ROS-inducing compounds. The results mean that the identified transcription factors are important for oxidative stress resistance. Previous studies had shown that the transcription factors Cap1, Gzf3 (Wang *et al*., 2006) and Skn7 (Basso *et al*., 2017) are important for oxidative stress responses. However, Ndt80 and Efg1 were not previously implicated in oxidative stress resistance.

4.5 Discussion.

Phagocytes, primarily neutrophils and macrophages present the first line of defence against *C. albicans* using their effector ROS radicals which impose oxidative stress (Martino *et al*., 1989, Cheng *et al*., 2012, Qian *et al*., 1994, Erwig *et al*., 2016). The Cap1 AP-1 transcription factor is the main oxidative stress response pathway (Wang *et al*., 2006). Following oxidative stress, Cap1 accumulates in the nucleus to induce the expression of ROS-protective enzymes (Patterson *et al*., 2013).

Oxidative stress can cause damage to nucleic acids for example, DNA double strand breaks (DSBs). As in other eukaryotic cells, the budding yeast *Saccharomyces cerevisiae* uses DNA damage check point kinases to arrest the cell cycle progression and allow for DNA repair mechanisms (Pellicioli *et al*., 2001). *S. cerevisiae* DNA damage response includes Mec1, Tel1, Chk1, Rad53, Dun1 and Cdc5 kinases. These work in coordination with Rad9, Rad24, Rad17, Mec3 and Ddc1 kinases (Longhese *et al*., 1998, Rhind *et al*., 1998, Weinert, 1998, Sanchez *et al*., 1999). The *S. cerevisiae* Rad53 DNA checkpoint kinase regulates (Lowndes *et al*., 2000) nine transcription factors; Msn4, Mbp1, Swi6, Swi4, Gcn4, Rfx1, Fkh2, Ndd1 and Mcm1 (Jaehnig *et al*., 2013).

S. cerevisiae and *C. albicans* are closely related but diverged from each other 840 million years ago (Fitzpatrick *et al*., 2006). The regulation of cell cycle might be conserved as there are a number of homologous genes but up to 20 % of the genes are unique to the morphogenetic *C. albicans* (Côte *et al*., 2009). Oxidative stress-induced DNA damage has been associated with morphogenesis. It leads to activation of DNA damage checkpoint Rad53 kinase which halts the cell cycle progression to allow for repair mechanisms during which there is formation of hyperpolarised buds (Da Silva *et al*., 2010). However, there was

limited information on *C. albicans* Rad53 kinase transcriptional regulation of hyperpolarised bud formation. Approximately half of the *S. cerevisiae* Rad53 kinase transcription factor regulators (Msn4, Mbp1, Swi4, and Fkh2) are also present in the *C. albicans* transcription factor library (Pellicioli *et al*., 2001, Côte *et al*., 2009). Therefore, the aim was to determine the transcription factors of *C. albicans* Rad 53 kinase which are essential for formation of hyperpolarised buds.

A screen of 167-transcription factor library of mutants (Homann *et al*., 2009) for defective formation of hyperpolarised buds was performed. However, no novel transcription factor for formation of hyperpolarised buds was identified. As no transcription factor was identified, the results can be interpreted that none of the transcription factors was important for the formation of hyperpolarised buds. Also, as the screening method was a manual, slow process, it is possible that mutants with defective hyperpolarised buds were missed during the microscopic screen. These results suggest that the transcription network downstream of Rad53 kinase in *C. albicans* diverged from that in *S. cerevisiae*.

The 167-transcription factor library of mutants (Homann *et al*., 2009) was also screened by QFA to identify mutants that were sensitive to H_2O_2, and subsequently, the most sensitive mutants were examined for resistance to various oxidative stress-inducing agents. In the original phenotypic screen of the transcription library deletion mutants, sensitivity to 4.5/6.0 mM H_2O_2 and 90 µM menadione was examined (Homann *et al*., 2009). Their findings showed that both *cap1*Δ and *ndt80*Δ cells were sensitive to H_2O_2 and menadione. However, *skn7*Δ and *gzf3*Δ cells were sensitive to H_2O_2 but did not show impaired growth in menadione. And the growth of *efg1*Δ cells was slightly reduced in the presence of menadione but not H_2O_2 (Homann *et al*., 2009).

The findings from this study are inconsistent with the results of the published screen of the TF library which tested the growth of the mutants to menadione and H_2O_2 (Homann *et al*., 2009). In the previous study, *efg1*Δ, *cap1*Δ, and *ndt80*Δ cells showed reduction of growth in the presence of menadione. However, findings from this study showed that only *cap1*Δ and *efg1*Δ cells were sensitive to menadione. The difference in the findings is probably because in the previous study, a lower concentration of menadione of 90 µM was used compared to 300 µM in this study. Furthermore, in the previous study, only *cap1*Δ and *skn7*Δ were sensitive to H_2O_2 while in the current study, all the mutants except *efg1*Δ, showed impaired growth in the presence of H_2O_2. The inconsistency in the findings could be due to the higher 4.5/6.0 mM than 3 mM H_2O_2 concentrations which were used in the previous and, current studies, respectively. Therefore, there was overlap between the previous and current

studies on the findings of the *efg1*Δ cells which showed unimpaired growth in H_2O_2 but slight sensitivity in menadione.

Together, the findings of this study showed that Cap1, Skn7, Ndt80, Gzf3 and Efg1 are transcriptional regulators for oxidative stress resistance in *C. albicans*. In agreement with previous studies, our findings showed that Skn7 is important for survival in H_2O_2 and tBOOH peroxide stress agents (Figure 26). Skn7 is a response regulator which has been reported to induce genes responsive to various stress. Following oxidative stress, Skn7 is activated to upregulate the expression of antioxidative mechanisms (Singh *et al*., 2004), (Basso *et al*., 2017). Null *ndt80*Δ cells were sensitive to both tBOOH and diamide (Figure 26). As both tBOOH and diamide affect the cell growth/division progression, this finding is consistent with the known role of Ndt80 in commitment to meiosis (Winter, 2012). Following cell injury by tBOOH and diamide, the *ndt80*Δ cells were not able to progress through cell division, hence cell death as demonstrable by impaired growth (Figure 26). Furthermore, the finding that null *gzf3*Δ cells were susceptible to tBOOH and diamide is consistent with a previous study which reported increased sensitivity to oxidative stress following loss of Gzf3 (Wang *et al*., 2006). Null *efg1*Δ cells showed slight sensitivity to menadione, perhaps, because the concentration of 300 µM which was used in this experiment was higher than 90 µM used in the previous study (Homann *et al*., 2009). However, the *efg1*Δ cells were clearly sensitive to diamide. As diamide is a thiol oxidising agent, the findings suggest that it was the major pathway affected in the *efg1*Δ cells. As *efg1*Δ cells were resistant to all the other forms of oxidative stress except diamide, it suggests that diamide was the most potent agent. Although *efg1*Δ cells failed to form hyphae due to lack of Efg1 which is essential for hyphae formation (Sudbery *et al*., 2011), the results also mean that *efg1*Δ could fail to filament in the presence of ROS due to its impaired oxidative stress resistance. However, as Efg1 is a key regulator for morphogenesis, it was not possible to dissect this. It is also noteworthy that most mutants were not sensitive to menadione. This is probably because mendione has a nutritional value but toxic in higher doses. Furthermore, the finding that *cap1*Δ cells were sensitive to all forms of oxidative stress is in agreement with the previous studies which showed that Cap1 is the major transcription factor for oxidative stress resistance (Alarco *et al*., 1999, Wang *et al*., 2006). The wild type cells were resistant to all forms of stress which further infer that the identified transcription factors are important for resistance to oxidative stress in *C. albicans*. Following the identification of the transcription factors sensitive to ROS, the 5 most sensitive mutants were used to determine if resistance to ROS was a global requirement for survival inside the macrophage.

CHAPTER FIVE

5 AN INVESTIGATION INTO THE ROLE OF OXIDATIVE STRESS RESISTANCE IN PROMOTING *C. ALBICANS* SURVIVAL FOLLOWING PHAGOCYTOSIS.

5.1 Introduction.

C. albicans can cause systemic diseases in individuals with impaired immunity (Kullberg *et al*., 2015). Phagocytic cells of the innate immune system provide the primary defence against systemic candidiasis (Martino *et al*., 1989, Qian *et al*., 1994, Cheng *et al*., 2012, Erwig *et al*., 2016) by imposing a number of insults including oxidative stress (Brown *et al*., 2011, Horn *et al*., 2009).

The importance of oxidative stress responses in triggering filament formation and survival of *C. albicans* following H_2O_2 treatment was demonstrated using *in vitro* experiments (Chapters 3). *C. albicans* treatment with H_2O_2 inhibited serum-induced hypha formation, and the inhibition was more sustained in oxidative stress mutants (Figures 6, 11, 12, 13) due to cell cycle growth arrest (Figures 8, 15, 16, 17). The *in vitro* findings indicated that the ability of *C. albicans* to mount robust oxidative stress responses is important in preventing sustained ROS-induced growth arrest that can inhibit serum-induced filamentous growth. However, an *in vitro* culture system is less complex than the natural host milieu in the phagosome which consists of an armoury of various insults that range from nutrient starvation, an adversely low pH and toxic chemicals that could impact on *C. albicans* morphogenetic changes and phagocytic escape (Lorenz *et al*., 2004). Therefore, the major aim of this chapter, was to investigate whether the findings *in vitro* that oxidative stress resistance is important for filament formation and survival of *C. albicans* is also observed in the *ex-vivo* macrophage model of infection following phagocytosis.

Phagocytosis is initiated by migration of macrophages to the site of location of *Candida* (Nourshargh *et al*., 2014). Migration is followed by cell-cell macrophage-*Candida* attachment then engulfment of the *Candida* cell by membrane invaginations of the macrophage to form a phagosome (Rudkin *et al*., 2013). Phagosome maturation occurs through a number of steps to form non-oxidative, nitrosative and oxidative microbicidal milieu (Fairn *et al*., 2012) which can induce *C. albicans* morphogenesis (Lorenz *et al.*, 2004). It was hypothesized that the findings of the *in vitro* findings which showed that ROS causes sustained growth arrest in the oxidative stress sensitive mutants underpinned the previously

documented inability of Cap1 and its co-regulators to form filaments and escape the phagosome following phagocytosis.

Confocal video microscopy was employed to determine the role of oxidative resistance in promoting survival following phagocytosis. Fifteen (15) strains were analysed; the *Wt* and (a) mutants of several transcription factors (TFs) which had shown to have impaired resistance to various forms of ROS *in vitro* (6/15); (b) strains that were ectopically expressing catalase (4/15); and (c) wild type & morphogenetic and DNA damage checkpoint mutants (5/15). *C. albicans* cells were co-cultured with J774 cell line macrophages which were originally derived from mouse BALB/c monocytes. Cell line macrophages were chosen because the background study from which the project was derived was based on using J774 macrophages (Patterson *et al*., 2013) and also because they could be easily maintained (Lam *et al*., 2009)

Macrophages and *Candida* yeast cells were cultured at a ratio of 1:3, then DIC and fluorescent (Lysotracker Red stain) confocal microscopy videos were acquired at 1 min per interval over 6 h of the phagocytosis assay. The videos were analysed using Volocity software; (http://cellularimaging.perkinelmer.com/downloads/detail.php?id=14) for the different parameters of phagocytosis as described in the materials and methods section. Briefly, the parameters measured were times to first point of attachment, complete engulfment, phagosome acidification, the number of *Candida* cells engulfed per macrophage, the rate of engulfment of *Candida* cells, length of hypha formation, *Candida* and macrophage survival.

5.2 Transcription factors Cap1 and Efg1 are important for filament formation but not survival inside the macrophage.

The five transcription factor mutants which had shown the greatest impaired fitness in the presence of different forms of ROS were identified as additional regulators of responses and resistance to ROS. These were *skn7*Δ, *gzf3*Δ, *ndt80*Δ, *cap1*Δ and *efg1*Δ. Null *skn7*Δ, *ndt80*Δ, *gzf3*Δ and *cap1*Δ mutants showed impaired survival in the presence of H_2O_2, tBOOH, menadione and diamide while the growth of *efg1*Δ was inhibited by diamide (Chapter 4: Section 4.3.2, Figure 26). Because oxidative stress sensitive mutants of Cap1 and co-regulators showed impaired growth in the macrophage (Patterson *et al*., 2013), I aimed to investigate whether the transcription factors which had shown impaired growth in the presence of the different forms of ROS, *in vitro*, were important for survival and *C. albicans* mediated killing of macrophages. And because the transcription factor mutants had displayed a range of ROS-related stress phenotypes, I also investigated whether

certain phenotypes were more important than others for survival and *C. albicans* mediated killing of macrophages.

5.2.1 The direction of macrophage migration was most random towards *efg1*Δ cells.

Macrophage migration to localise with *C. albicans* is a prerequisite for phagocytosis. Following stimulation by *C. albicans* PAMPs, there is increased adhesiveness and shape changes of the macrophage which initiate polarised motility of the phagocytes towards the pathogen (Nourshargh *et al*., 2014). The speed and directionality of migration of macrophages to the transcription factor mutants was determined in comparison to wild type cells.

Migration speed of macrophages towards *C. albicans* was determined using the tracking software from the tracking diagrams. The results which compared the macrophage migration speed towards wild type cells and the transcription factor mutants using one way ANOVA showed that the track velocity was 0.02 µm/sec towards all the strains of *C. albicans* ($p = 0.085$) (Table 3). This means that the macrophages migrated at the same speed towards the *Wt* and transcription mutant *C. albicans*.

The directionality of migration of the macrophages was determined using tracking diagrams and meandering indices. Macrophages were tracked per min interval for 60 min for 30 macrophages. Comparison of the tracking diagrams of wild type and transcription factor mutants showed that macrophage migration to towards all the strains was random (Figure 27). Meandering indices were used to assess the directionality of macrophage migration. A meandering index is an indication of the linearity of the migration track. As the meandering index approaches 1, the more linear the migration track is, and thus, the more directional the macrophage migration is. Findings and comparison of the meandering indices of the macrophage migration towards wild type cells and transcription factor mutants using one way ANOVA showed that there were a significant differences among the groups ($p = 0.04$). The post hoc test with Bonferroni correction revealed that the meandering index of macrophages towards *efg1*Δ was the lowest at 0.07 ($p = 0.04$) (Table 3). Therefore, the directionality of macrophage migration was most random towards *efg1*Δ. The least linear migration of *efg1*Δ was also reflected in the tracking diagram where the migration tracks were concentrated at the centres of both the XY axes (known as the centriole) (Figure 27). Because migration is driven by recognition of a pathogen induced stimulus, this suggests that Efg1 is important for *C. albicans* recognition by macrophages. It is not clear how the nature of the target cell influences the direction of migration of macrophages, but it was of interest to note that the migration differed significantly for different prey target cells.

TF	Track Velocity (µm	Meandering Index
WT	0.02 (SD = 0.05)	0.12 (SD = 0.05)
*skn7*Δ	0.02 (SD = 0.00)	0.11 (SD = 0.01)
*ndt80*Δ	0.02 (SD = 0.01)	0.12 (SD = 0.03)
*gzf3*Δ	0.02 (SD = 0.05)	0.11 (SD = 0.03)
*cap1*Δ	0.02 (SD = 0.00)	0.13 (SD = 0.05)
*efg1*Δ	0.02 (SD = 0.00)	0.07 (SD = 0.02)*

Table 3: Macrophage migration speed and directionality towards *C. albicans*.
The wild type and TF mutants, were co-cultured with J774 macrophages. Volocity software was used to track the migration of macrophages at 1 min per interval for 60 min which were displayed as tracking diagrams. The numeric outputs of the tracking diagrams were extracted and macrophage speed (tracking velocity) and directionality (meandering index) were compared. Each experiment was repeated three times. One way ANOVA was used to calculate statistical significance of differences among the groups and post hoc correction with Bonferroni; *$p = 0.04$.

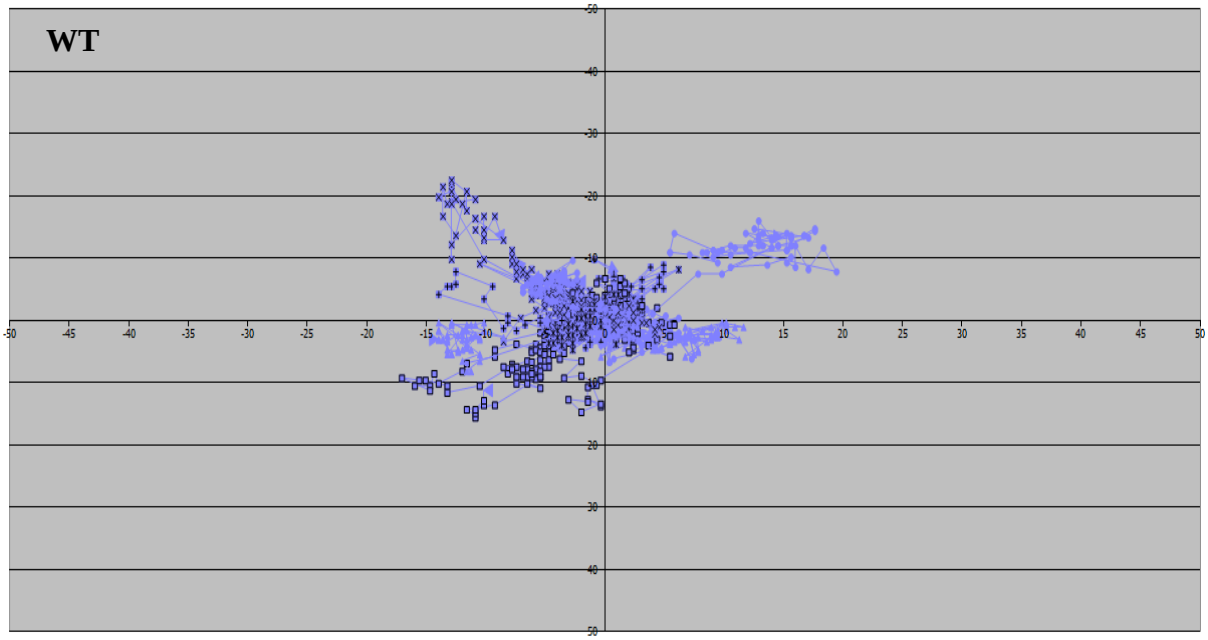
WT

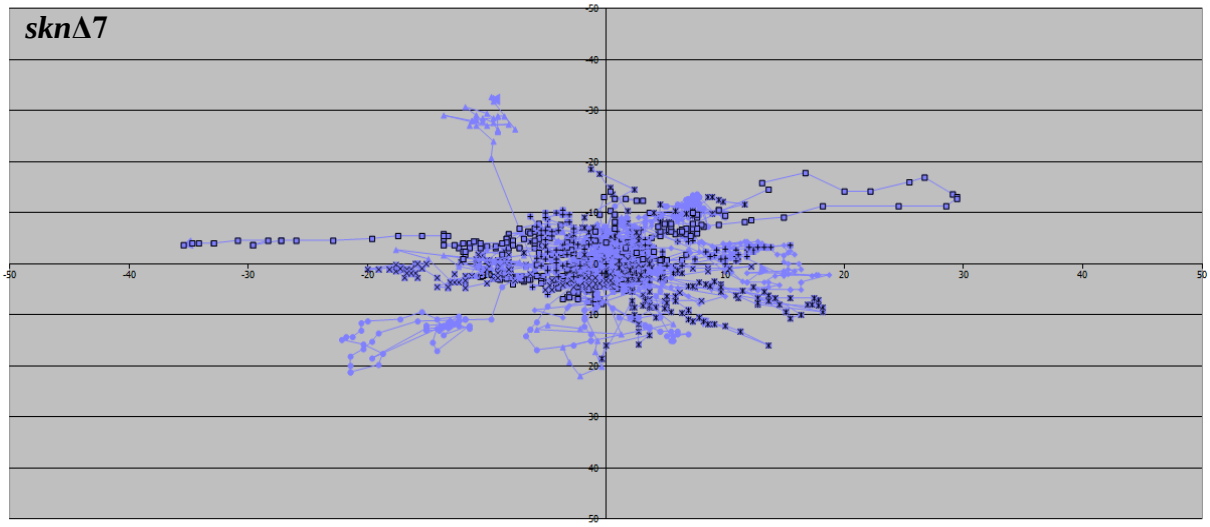
sknΔ7

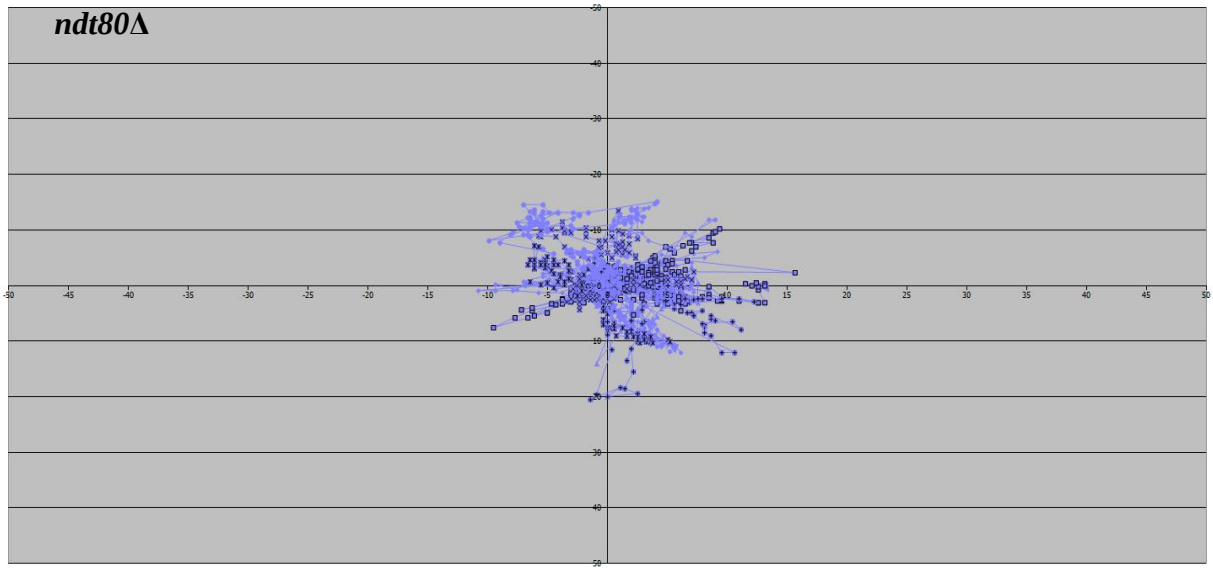
ndt80Δ

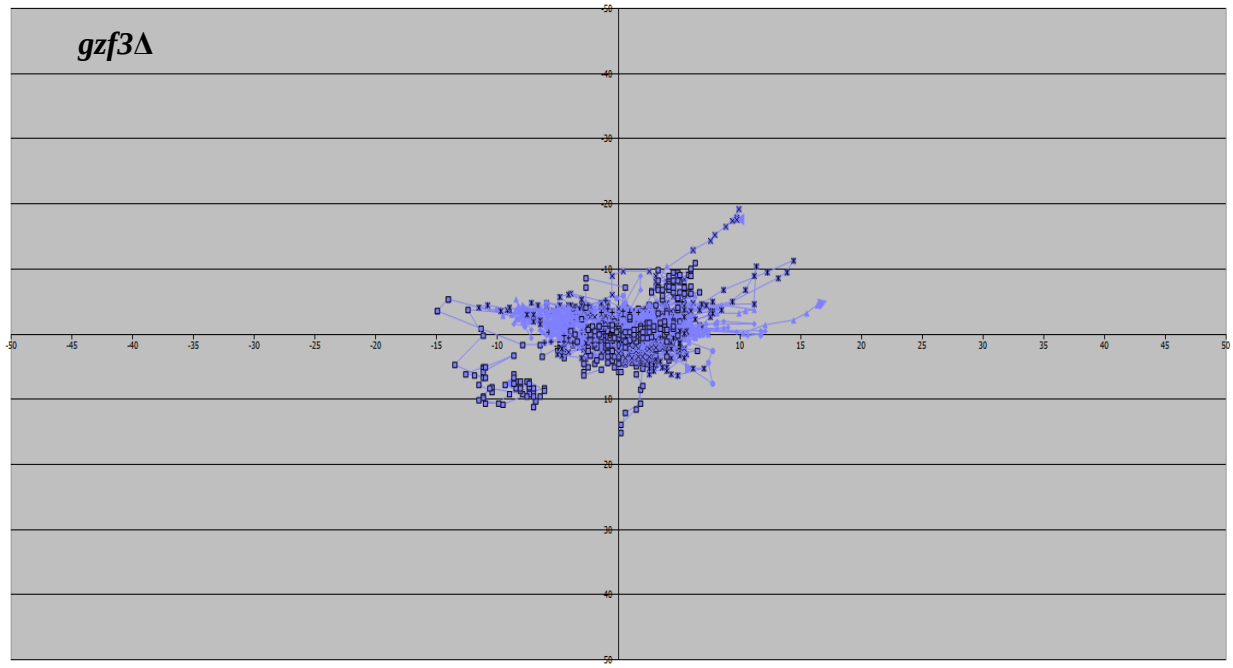
gzf3Δ

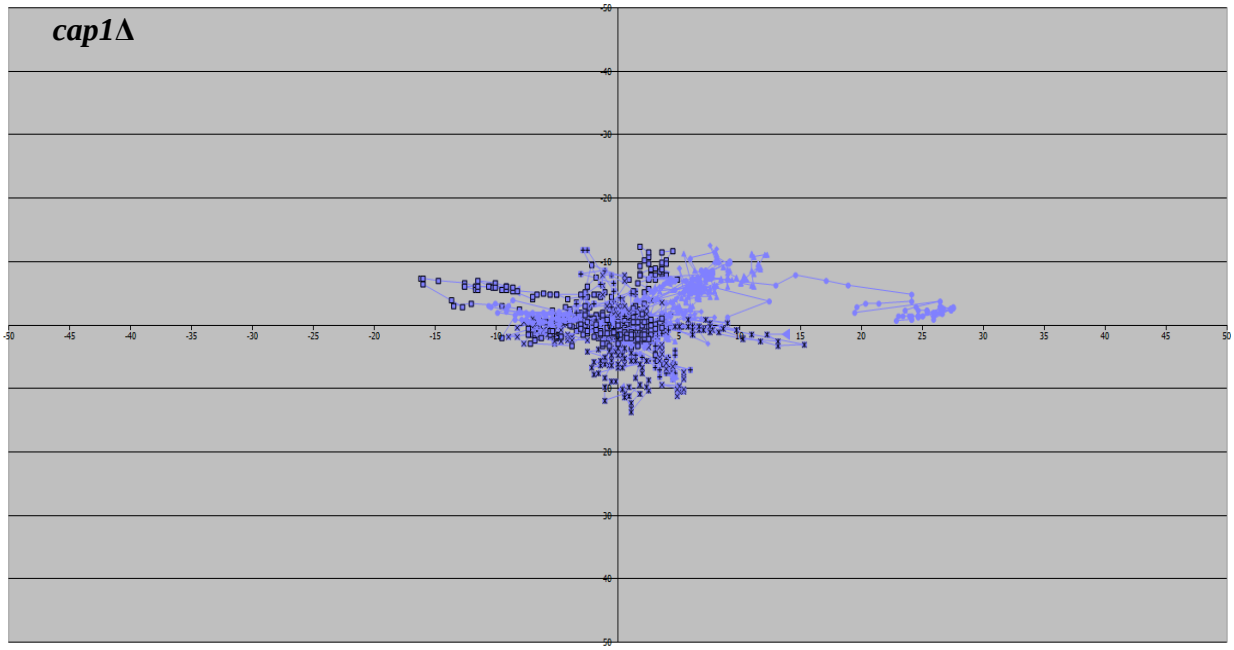
cap1Δ

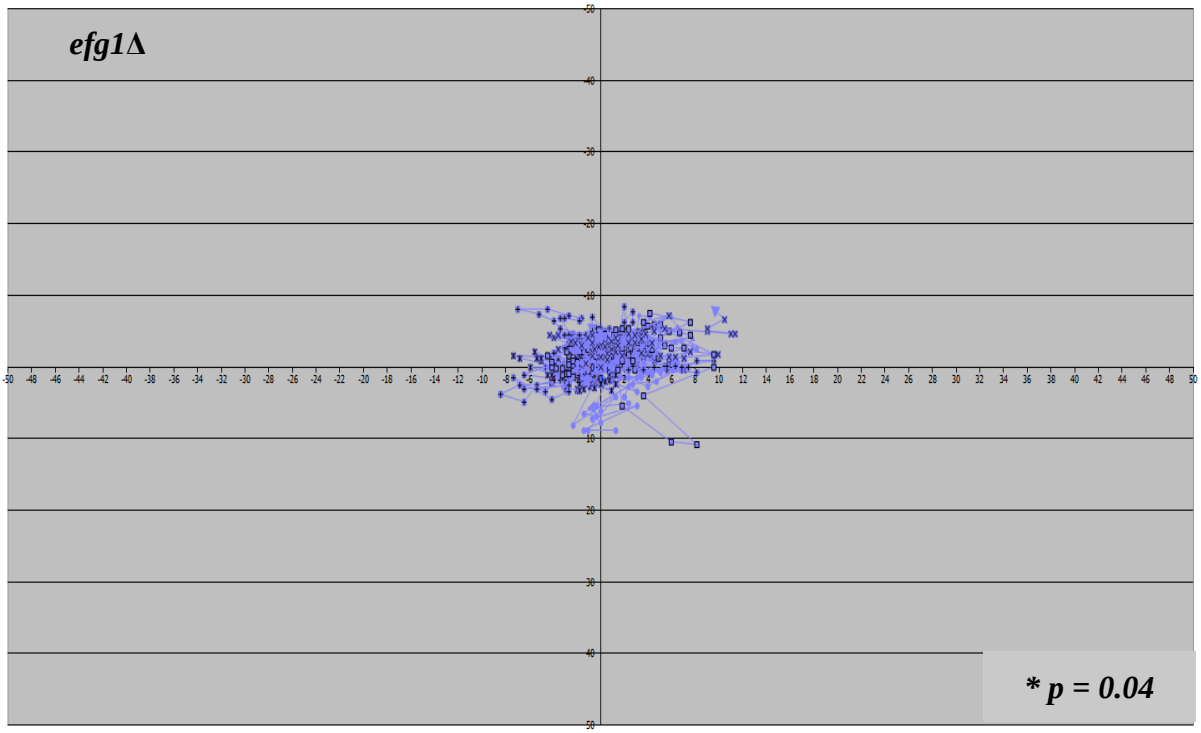

Figure 28: Macrophage migration directionality towards *WT* and TF mutants.
The *WT* and TF mutants' *skn7*Δ, *ndt80*Δ, *gzf3*Δ, *cap1*Δ & *efg1*Δ cells were co-cultured with J774 macrophages. Live cell confocal videos were taken at 1 min per interval for 6 h. Macrophage migration was tracked for 60 min using the tracking software. The tracks indicate the movement of a single macrophage relative to its starting point and the arrows represent directionality of movement. Each experiment was repeated three times. One way ANOVA was used to calculate statistical significance of differences among the groups and post- hoc correction with Bonferroni for pairwise comparisons of a TF mutant to *WT; * p = 0.04*.

5.2.2 Attachment time was latest for *efg1*Δ cells.

Attachment of a macrophage to a pathogen is mediated by pathogen recognition receptors (PRR), for example C-type lectins such as the mannose receptor (MR), dectin-1 and the Pathogen Associated Molecular Patterns (PAMP) such as mannoproteins (Netea *et al*., 2008). The time of attachment of the transcription factor mutants was assessed in comparison to wild type.

Time of attachment was defined as the time within the movie when there was *Candida*-macrophage contact. Because this was determined by microscopy this parameter cannot be taken as being extremely precise. Mean attachment times were;

.

Table 4: Time of attachment of TF mutants

TF mutants	Time of attachment (min) (SD)
WT	18.4 (SD = 3.73)
*skn7*Δ	14.4 (SD = 3.53)
*ndt80*Δ	18.8 (SD = 1.05)
*gzf3*Δ	21.07 (SD = 3.71)
*efg1*Δ	23.91 (SD = 2.53)
*cap1*Δ	15.42 (SD = 19.2)

Table 4: Time of attachment.
The *WT* and *TF* mutants; *skn7*Δ, *ndt80*Δ, *gzf3*Δ, *cap1*Δ & *efg1*Δ were co-cultured with J774 macrophages. Live cell confocal videos were taken at 1 min per interval for 6 h. Macrophage-Candida cell-cell contact time within the movie was recorded for each cell for 30 min for 30 macrophages. Each experiment was repeated three times and the SD calculated.

Comparison of the attachment times of wild type and transcription factor mutants by one way ANOVA showed that there was a significant difference ($p = 0.048$) and the post hoc test with Bonferroni correction indicated that attachment time within the movie was latest for *efg1*Δ ($p = 0.045$) (Figure 29). The other comparisons were statistically non-significant. This means that attachment of *efg1*Δ cells to macrophages was delayed. This could be because *efg1*Δ cells had altered PAMPs exposure as cells with Efg1 are expected to dominantly express hypha-specific genes because it is the main transcription factor for hyphae formation. The cell wall forms the first point of contact with macrophages and other immune cells, therefore, it is likely that the defective PAMP is cell-wall associated. The wide variation in the attachment time of *cap1*Δ is probably because of the predominant yeast morphology in chains. The unicellular yeasts attached early while the multicellular yeasts in chains delayed to attach (Figure 28).

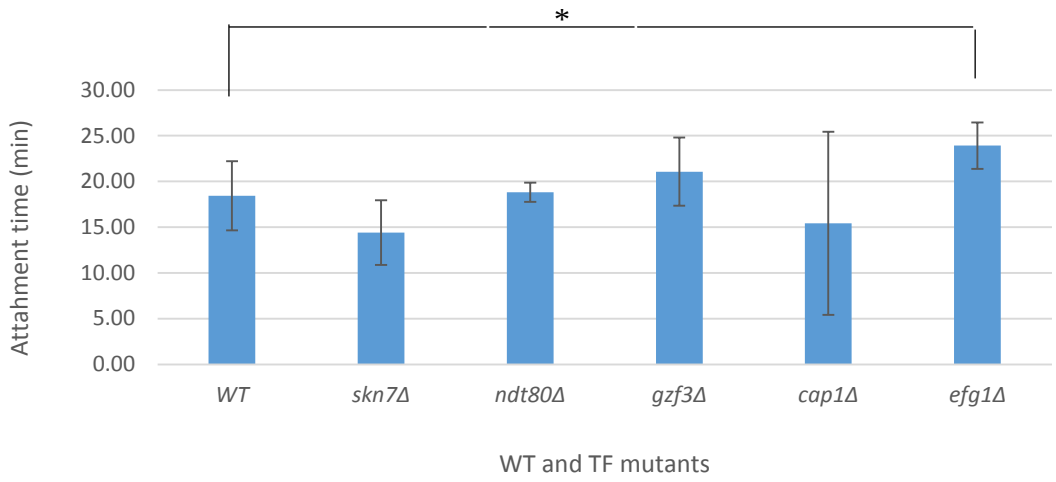

Figure 29: Attachment time.
The *WT* and TF mutants; *skn7*Δ, *ndt80*Δ, *gzf3*Δ, *cap1*Δ & *efg1*Δ were co-cultured with J774 macrophages. Live cell confocal videos were taken at 1 min per interval for 6 h. Macrophage-*Candida* cell-cell contact time within the movie was recorded for each cell for 30 min for 30 macrophages. Each experiment was repeated three times and the error bars calculated from SD. One way ANOVA was used to calculate statistical significance among the groups ($p = 0.048$) and post hoc analysis with Bonferroni; *$p = 0.045$.

5.2.3 Engulfment time was delayed longest for *efg1*Δ cells.

Engulfment is also mediated by macrophage PRRs and *Candida* PAMPs. Engulfment is the enclosure of *Candida* cell within the macrophage pseudopodia. The time of engulfment of TF mutants was determined in comparison to wild type cells.

Time of engulfment was defined as the time within the movie when *Candida* was fully enclosed within the macrophage. Mean engulfment times within the movies were;

Table 5: Engulfment time.

TF mutants	Engulfment time (min), SD.
WT	20.9 (SD = 3.45)
*skn7*Δ	16.61(SD = 2.62)
*ndt80*Δ	21.81(SD = 0.54)
*gzf3*Δ	22.84 (SD = 4.09)
*efg1*Δ	25.90 (SD = 3.05)
*cap1*Δ	19.08 (SD = 10.7)

Figure 5: Engulfment time.
The TF mutants; *skn7*Δ, *ndt80*Δ, *gzf3*Δ, *cap1*Δ, *efg1*Δ & *WT* were co-cultured with J774 macrophages. Live cell confocal videos were taken at 1 min per interval for 6 h. Macrophage engulfment time within the movie was recorded for each cell for 30 min for 30 macrophages. Each experiment was repeated three times and the SD calculated.

Comparison of the times of engulfment for wild type and TF mutants by one way ANOVA showed that there were significant differences ($p = 0.047$) and using

Bonferroni for post hoc analysis revealed that the time of engulfment was latest for *efg1*Δ cells (*p = 0.046*) (Figure 29). Differences between the other TF mutants to *WT* were not significant. This means that *Candida* engulfment time within the movie was delayed for *efg1*Δ prey cells. This is consistent with the delayed attachment time for *efg1*Δ (Figure 28) and, may be associated with its alterations in cell wall PAMPs. The wide variation of the attachment times of *cap1*Δ arose possibly from the yeast cells which were predominantly in chains and attached at different times.

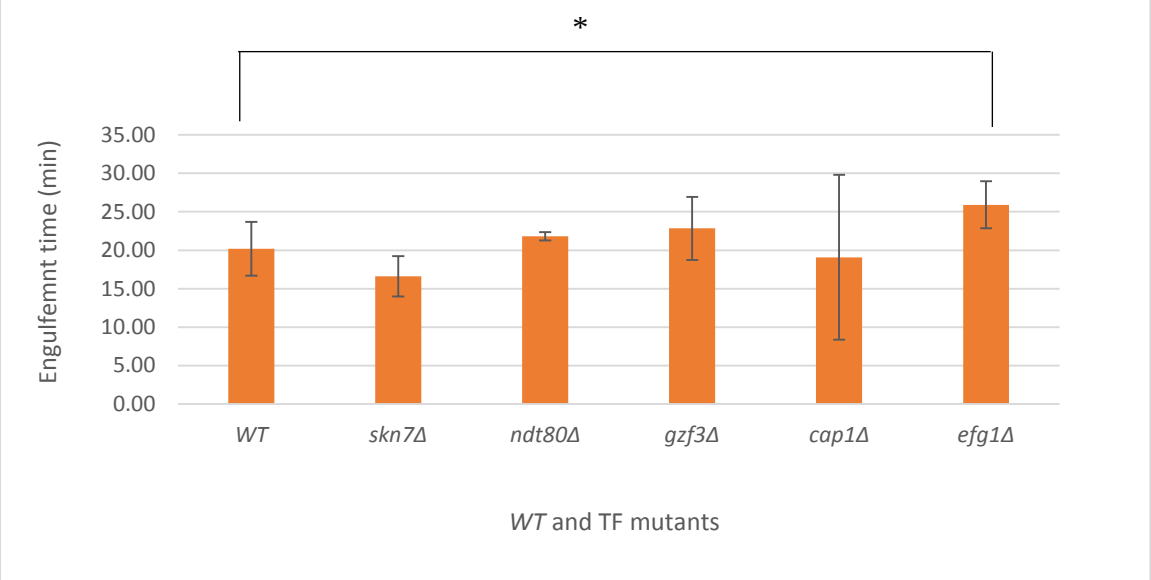

Figure 30: Engulfment time.
The TF mutants; *skn7*Δ, *ndt80*Δ, *gzf3*Δ, *cap1*Δ, *efg1*Δ & *WT* were co-cultured with J774 macrophages. Live cell confocal videos were taken at 1 min per interval for 6 h. Macrophage engulfment time within the movie was recorded for each cell for 30 min for 30 macrophages. Each experiment was repeated three times and the error bars calculated from SD. One way ANOVA was used to calculate statistical significance (*p = 0.047*) and Bonferroni for post hoc analysis **p = 0.046*.

5.2.4 The time it took to engulfment was longest for *cap1*Δ cells.

The time it took for engulfment was defined as the difference between the time of cell-cell contact and when the macrophage fully enclosed *Candida*. The time within the movie when cell-cell contact occurred was subtracted from when engulfment took place. The number of engulfment events observed were from 30 macrophages for 60 min. The time it took for engulfment were;

Table 6: The time it took for engulfment.

TF mutants	Time it took for engulfment
WT	1.75 (SD = 0.34)
*skn7*Δ	2.21 (SD = 0. 91)
*ndt80*Δ	2.99 (SD = 1.22)
*gzf3*Δ	1.76 (SD = 0.59)
*cap1*Δ	3.66 (SD = 2.01)
*efg1*Δ	1.99 (SD = 0.57)

Table 6: **The time it took for engulfment**.
The TF mutants; *skn7*Δ*, ndt80*Δ*, gzf3*Δ*, cap1*Δ, *efg1*Δ & *WT* were co-cultured with J774 macrophages. Live cell confocal videos were taken at 1 min per interval for 6 h of the phagocytosis assay. Duration of engulfment was the difference in time between macrophage-Candida cell-cell contact and engulfment for 30 macrophages. Each experiment was repeated three times and the SD calculated.

One way ANOVA for comparison of the duration of engulfment for wild type and transcription factor mutants showed that there was a statistical difference ($p = 0.04$) and Bonferroni post hoc analysis revealed that it was long for *ndt80*Δ ($p = 0.038$) but longest for *cap1*Δ ($p = 0.035$) (Figure 30). As before, the long duration of engulfment of *cap1*Δ is perhaps related to its morphology. As there was a delay in *cap1*Δ hypha formation (Figure 34), *cap1*Δ cells were predominantly yeasts in chains compared to hyphal cells of *WT*. It is possible that either the long chains of yeasts were physically more challenging for macrophage engulfment or the yeast morphology masks some PAMPs like β-glucan that prevented recognition by macrophages.

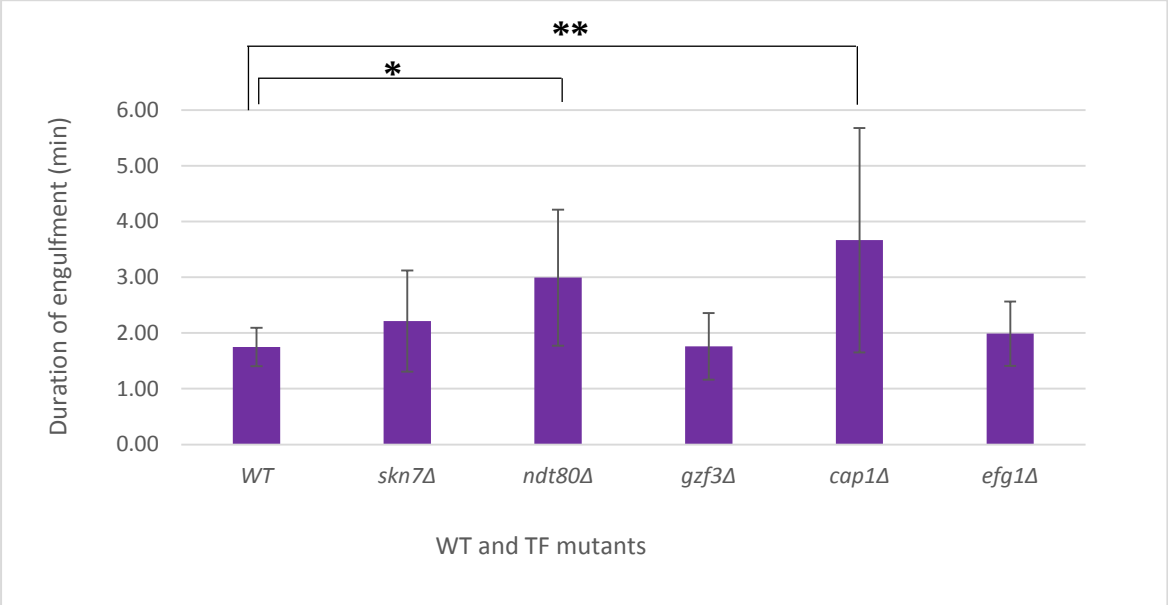

Figure 31: The time it took for engulfment.
The TF mutants; *skn7*Δ*, ndt80*Δ*, gzf3*Δ*, cap1*Δ, *efg1*Δ & *WT* were co-cultured with J774 macrophages. Live cell confocal videos were taken at 1 min per interval for 6 h of the phagocytosis assay. Duration of engulfment was the difference in time between macrophage-*Candida* cell-cell contact and engulfment for 30 macrophages. Each experiment was repeated three times and the error bars calculated from SD. One way ANOVA ($p = 0.04$) and Bonferroni test; $^{**}p = 0.035$, $p = 0.045$ were used to calculate statistical significance.

5.2.5 The number of *Candida* engulfed per minute was highest for *cap1*Δ prey cells.

The number of *Candida* engulfed per macrophage was counted. A total of 30 macrophages was counted per prey cell type. The number of *Candida* engulfed / 60 min were:

Table 7: The number of *Candida* engulfed per minute.

TF mutants	Number of *C. albicans* engulfed /min, SD.
WT	1.09 (SD = 0.07)
*skn7*Δ	0.92 (SD = 0.14)
*ndt80*Δ	1.24 (SD = 0.03)
*gzf3*Δ	1.00 (SD = 0.09)
*cap1*Δ	2.87 (SD = 1.59)
*efg1*Δ	1.01 (SD = 0.13)

Table 7: Number of *Candida* engulfed.
The transcription factor mutants; *skn7*Δ, *ndt80*Δ, *gzf3*Δ, *cap1*Δ, *efg1*Δ and *WT* were co-cultured with J774 macrophages. The movies were at 1 min per interval of the 6 h phagocytosis assay. The average number of *Candida* engulfed were counted for *WT* and the transcription factor mutants. Cells were counted from interval 0 to 60 minutes when most cells were engulfed for 30 macrophages /prey cell type. Each experiment was repeated three times and the SD calculated.

Comparison of the number of *C. albicans* engulfed per minute for wild type and the transcription factor mutants showed that there was a statistical significance ($p = 0.03$) and Bonferroni post-test revealed that the number of cells engulfed per minute was highest for *cap1*Δ ($p = 0.028$) (Figure 31). Pairwise comparison of the number of *Candida* cells engulfed for the other TF mutants to *WT* were not significant. The high number of cells engulfed by *cap1*Δ cells is probably because the cells were yeast morphology some of which had grown in chains as explained previously. Furthermore, the wide variation in the number of *cap1*Δ cells engulfed is possibly because some cells were engulfed singly while other cells were engulfed in chains. The wide variations in *cap1*Δ cells findings consistently affected its uptake throughout the steps of the phagocytosis assay.

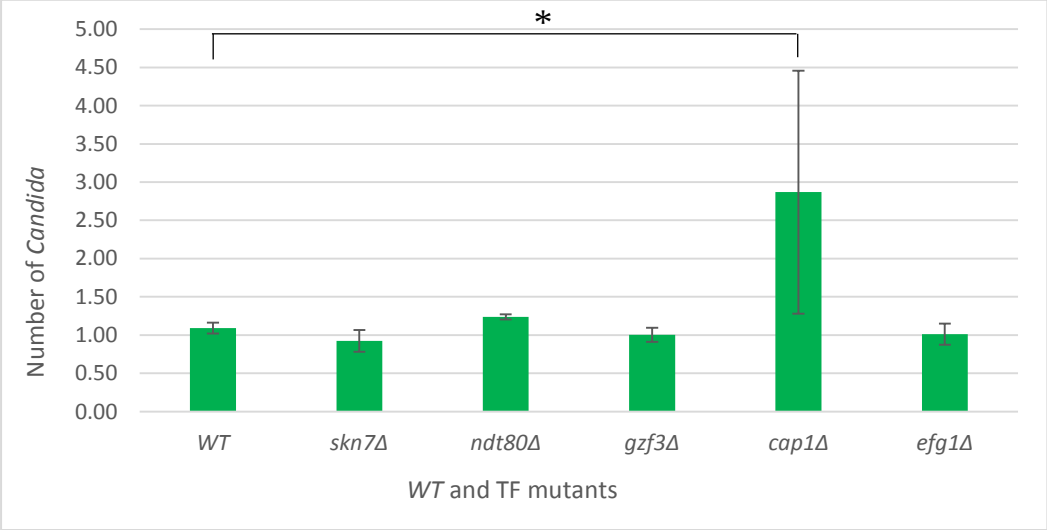

Figure 32: Number of *Candida* engulfed.
The transcription factor mutants; *skn7*Δ, *ndt80*Δ, *gzf3*Δ, *cap1*Δ, *efg1*Δ and WT were co-cultured with J774 macrophages. The movies were at 1 min per interval of the 6 h phagocytosis assay. The average number of *Candida* engulfed were counted for *WT* and the transcription factor mutants. Cells were counted from interval 0 to 60 minutes when most cells were engulfed for 30 macrophages /prey cell type. Each experiment was repeated three times and the error bars calculated are from SD. One way ANOVA was used to calculate statistical significance ($p = 0.03$) and Bonferroni for post hoc analysis: *$p = 0.028$.

5.2.6 The uptake rate increased over time for *efg1*Δ cells.

Uptake rate was defined as the number of *Candida* cells engulfed per min per interval and, expressed as percentage of the total number of cells engulfed over 30 min. Findings on the uptake rates for *WT* and transcription factor mutants when compared using one way ANOVA showed that there was a statistical difference within the group ($p = 0.05$) and the post hoc Bonferroni test revealed that the engulfment of *C. albicans* increased over

time for *efg1*Δ (*p = 0.047*) while it decreased in the *WT* and the other TF mutants cells (Figure 32). The increasing trend of engulfment of *efg1*Δ cells is possibly related to their delayed attachment time (Figure 28). In the early time points when there was no attachment, there was also few uptake of the cells. The uptake of cells therefore increased consistently with the delayed attachment times of the *efg1*Δ cells. In contrast, the *WT* cells and the other transcription factor mutant cells which attached to the macrophages in the early time points, showed a decreasing trend in the engulfment rate because most of the Candida cells were already engulfed (Figure 32, Figure 28).

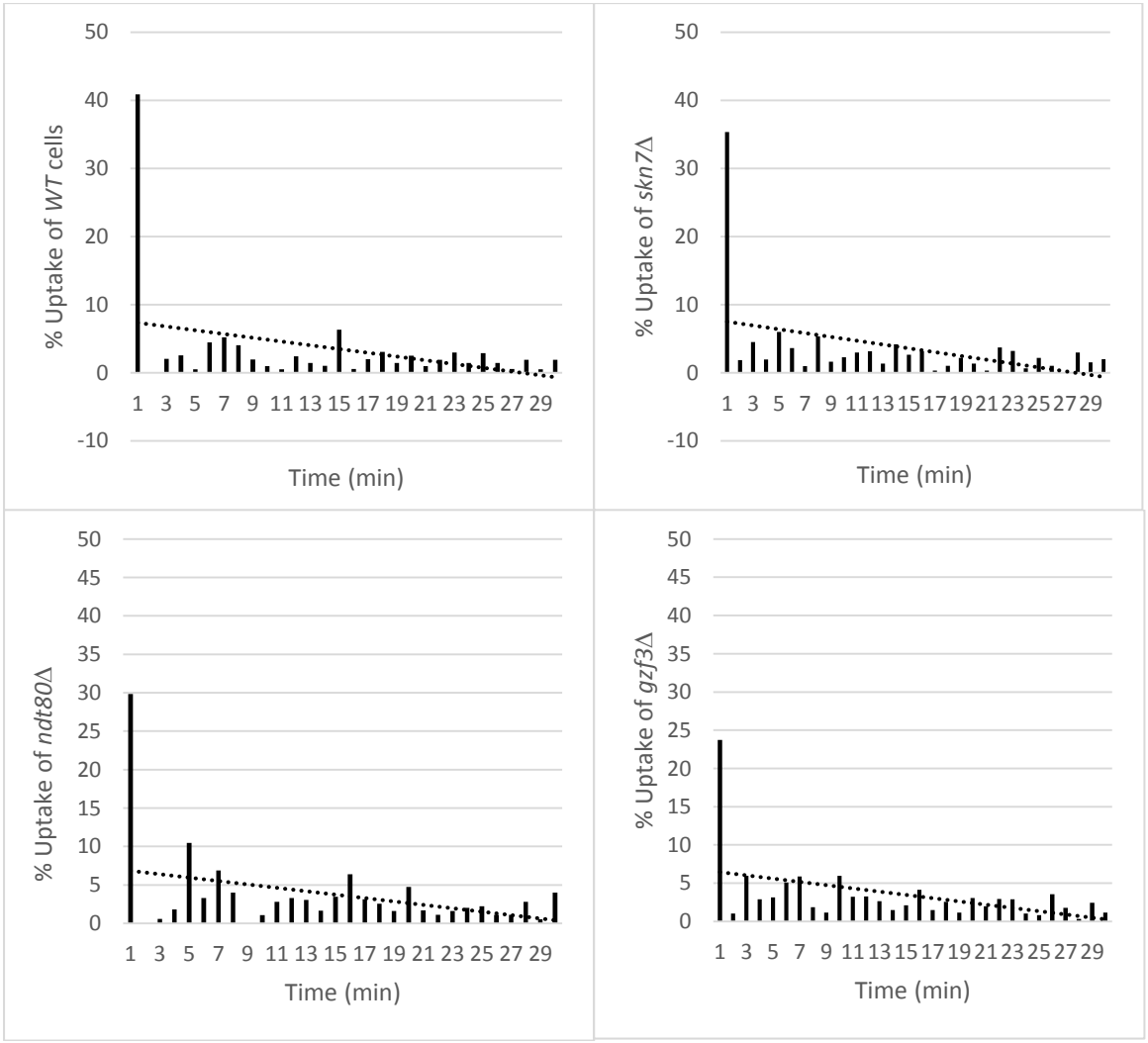

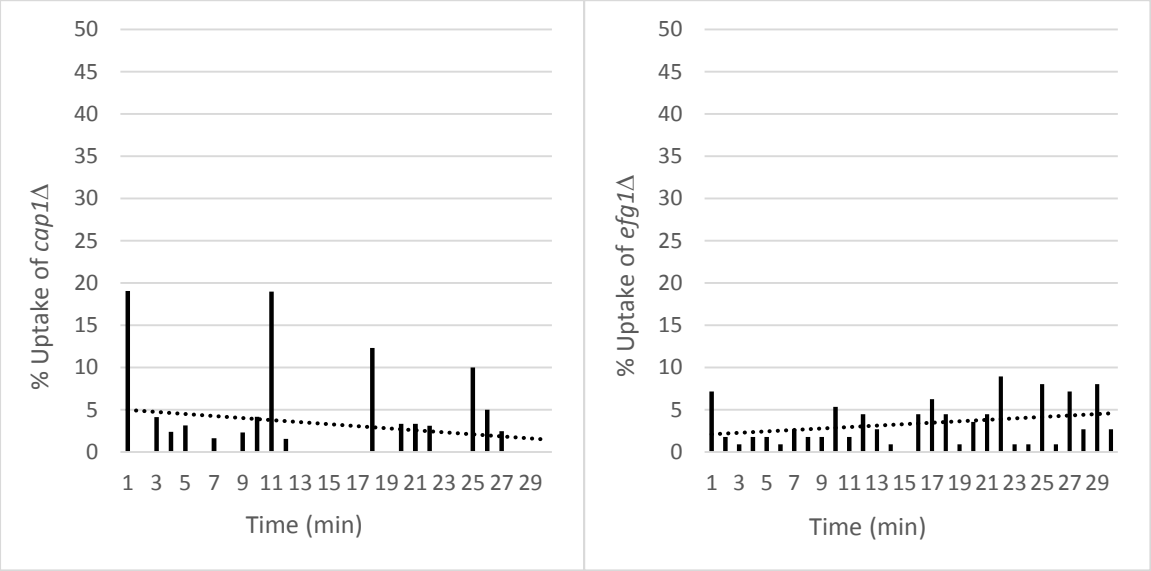

Figure 33: *C. albicans* uptake rate.
The TF mutants; *skn7*Δ*, ndt80*Δ*, gzf3*Δ*, cap1*Δ, *efg1*Δ & WT, were co-cultured with J774 macrophages. Live cell confocal videos were taken at 1 min per interval for 6 h. The number of *Candida* cells engulfed by each macrophage per time interval per minute was counted, calculated and expressed as percentage of the total number of cells engulfed by 30 macrophages over 30 minutes. Each experiment was repeated three times. ANOVA was used to calculate statistical significance: $p = 0.047$.

5.2.7 <u>There were no differences in the time for phagosome acidification for the different transcription factor mutants.</u>

The phagosome is the compartment of the phagocyte which contains the ingested *C. albicans.* Phagosome-lysosome fusion leads to acidification of the phagosome; an integral component of phagosome maturation and for *Candida* killing effects (Bain *et al.*, 2014). The time for phagosome acidification for the transcription factor mutants and wild type cells was assessed.

Phagosome acidification was demonstrable by the appearance of a red halo of the Lysotracker Red stain around engulfed *Candida* cell. Lysotracker Red is a pH-sensitive fluorescent dye which stains red in the acidic environment of the phagolysosome. Time for phagosome acidification was determined by subtracting the time of appearance of the red halo from the time of engulfment of *C. albicans.* The mean time of acidification were;

Table 8: Time to phagosome acidification.

TF mutants	Time to acidification (min)
WT	1.00 (SD = 0.27)
*skn7*Δ	1.64 (SD = 0.26)
*ndt80*Δ	1.06 (SD = 0.24)
*gzf3*Δ	1.27 (SD = 0.24)
*cap1*Δ	1.45 (SD = 0.29)
*efg1*Δ	1.54 (SD = 0.39)

Table 8: Time for phagosome acidification.
The TF mutants; *skn7*Δ, *ndt80*Δ, *gzf3*Δ, *cap1*Δ, *efg1*Δ & WT were co-cultured with J774 macrophages. Live cell confocal videos were taken at 1 min per interval for 6 h. The time for phagosome acidification was calculated as the difference between the time of *Candida* engulfment and first appearance of the red halo of Lysotracker Red stain for 30 macrophages / prey cell type. Each experiment was repeated three times and the SD calculated.

Comparison of the time for phagosome acidification by one way ANOVA for wild type and transcription factor mutants showed that there were no differences ($p = 0.08$) (Figure 33).

Figure 34: Time for phagosome acidification.
The TF mutants; *skn7*Δ, *ndt80*Δ, *gzf3*Δ, *cap1*Δ, *efg1*Δ & WT were co-cultured with J774 macrophages. Live cell confocal videos were taken at 1 min per interval for 6 h. The time for phagosome acidification was calculated as the difference between the time of *Candida* engulfment and first appearance of the red halo of Lysotracker Red stain for 30 macrophages / prey cell type. Each experiment was repeated three times and the error bars show the SD.

5.2.8 There was impaired filamentation of *cap1*Δ and *efg1*Δ cells inside the macrophage.

The ability of *C. albicans* to undergo reversible yeast to hypha morphogenetic switching is an important virulence attribute (Lo *et al*., 1997); formation of hyphae inside the macrophage can mediate macrophage death (Uwamahoro *et al*., 2014). Previously, it was reported that Cap1 and co-regulating oxidative stress sensitive mutants showed impaired hypha formation inside macrophages (Patterson *et al*., 2013). The role ability of the additional oxidative stress sensitive transcription factor mutants to form hyphae and escape phagocytosis was determined.

Hyphal length was measured at 30, 60 and 90 min after which the hyphae were too numerous to measure. The extracellular/intracellular hyphal lengths (µm) were:

Table 9: Extracellular/ Intracellular hyphal length.

TF mutants	Hyphae at 30 min	Hyphae at 60 min	Hyphae at 90 min
WT	6.67 (SD = 2.03), 8.40 (SD = 2.54)	12.73 (SD = 1.93), 14.19 (SD = 2.46)	22.44 (SD = 2.97), 20.47 (SD = 0.074)
*skn7*Δ	5.02 (SD = 0.11), 7.90 (SD = 2.65)	10.44 (SD = 1.34), 13.92 (SD = 2.31)	15.42 (SD = 4.00), 18.57 (SD = 0.34)
*ndt80*Δ	5.31 (SD = 0.25), 7.35 (SD = 1.00)	9.55 (SD = 0.705), 11.43(SD = 1.57)	17.53(SD = 3.28), 16.53 (SD = 0.49)
*gzf3*Δ	5.78 (SD = 2.20), 9.49 (SD = 0.98)	9.55 (SD = 0.705), 11.43(SD = 1.57)	18.79 (SD = 0.27), 20. 21 (SD = 5.84)
*cap1*Δ	0 (SD = 1.00) , 0 (SD = 1.00)	3.84 (SD = 0.83), 0 (SD = 0)	6.54 (SD = 2.27), 0 (SD = 0)
*efg1*Δ	0	0	0

Table 9: Impact of phagocytosis on formation of hyphae.
The transcription factor mutants; *skn7*Δ, *ndt80*Δ, *gzf3*Δ, *cap1*Δ, *efg1*Δ & WT were co-cultured with J774 macrophages. Live cell confocal videos were taken at 1 min per interval for 6 h. Hyphal and pseudohyphal length was measured half hourly at 30, 60 and 90 min.

Comparison of hyphal length inside and outside the macrophage for *WT* cells and the transcription factor mutants showed that there was unimpaired hyphal growth of *skn7*Δ, *ndt80*Δ, and *gzf3*Δ mutants inside the macrophage. Germ tube formation started at 30 min and the length doubled approximately every 30 min up to 90 min when hypha measurement was stopped. Both extracellular and intracellular hypha formation occurred in the cell cultures (Figures 34). There was no visible growth arrest of *WT* cells following phagocytosis possibly because the impact of ROS from the J774 cell line macrophages were not sufficient as the effect is dose dependent. Similarly, there was absence of growth arrest in *skn7*Δ, *ndt80*Δ, and *gzf3*Δ cells which all formed hyphae. Further observations revealed that

engulfed cells formed hyphae faster than cells outside the macrophage. This may be because of the ROS produced inside the macrophage which affect the metabolism of *C. albicans* and causes auto induction of hyphae formation (Lorenz *et al*., 2004). However, *cap1*Δ and *efg1*Δ cells showed delayed formation of hyphae inside the macrophage although outside the macrophage, there was hyphal development by the *cap1*Δ strain and pseudohyphae formation by *efg1*Δ cells (Figure 34). It is noteworthy that after 4 h of the phagocytosis assay, both *cap1*Δ and *efg1*Δ initiated formation of hyphae and pseudohyphae, respectively, inside the macrophage.

Statistical one way ANOVA comparison of hypha formation in *WT* and the transcription factor mutants, extracellular and inside the macrophages showed that there were significant differences ($p = 0.04$) ($p = 0.02$), and with Bonferroni post hoc test, *cap1*Δ showed impaired hypha formation inside the macrophage ($p = 0.001$). There was formation of pseudohyphae in the extracellular environment but not inside the macrophage by the *efg1*Δ cells. There was also a significant difference in pseudohypha formation by *efg1*Δ in the intracellular and extracellular environment ($p = 0.001$). These findings suggest that *cap1*Δ hyphae and *efg1*Δ pseudohyphae formation inside the macrophage were delayed while there was unimpaired filamentation outside the macrophage. Lack of hypha formation by *efg1*Δ was expected because Efg1 is a major transcription factor for the induction of hyphal growth and has previously been shown to be required for filamentation in macrophages (Lorenz *et al*., 2004). Thus, Cap1 and Efg1 were both needed for hypha formation inside the macrophage. Furthermore, the results suggest that Skn7, Ndt80, and Gzf3 are not required for hypha formation inside the macrophage. However, as some of the transcription factors such as Skn7 play known roles in oxidative stress resistance (Basso *et al*., 2017), it was expected that the null mutants would not form hyphae inside the macrophages. The finding in which such cells as *skn7*Δ formed hyphae inside the macrophages suggest that J774 may not have been the appropriate macrophages to inhibit hypha formation as ROS effects are dose-dependent. But the *cap1*Δ cells did not form hyphae inside the J774 macrophages, perhaps, because Cap1 is the ROS responsive transcription factor for *C. albicans*.

A

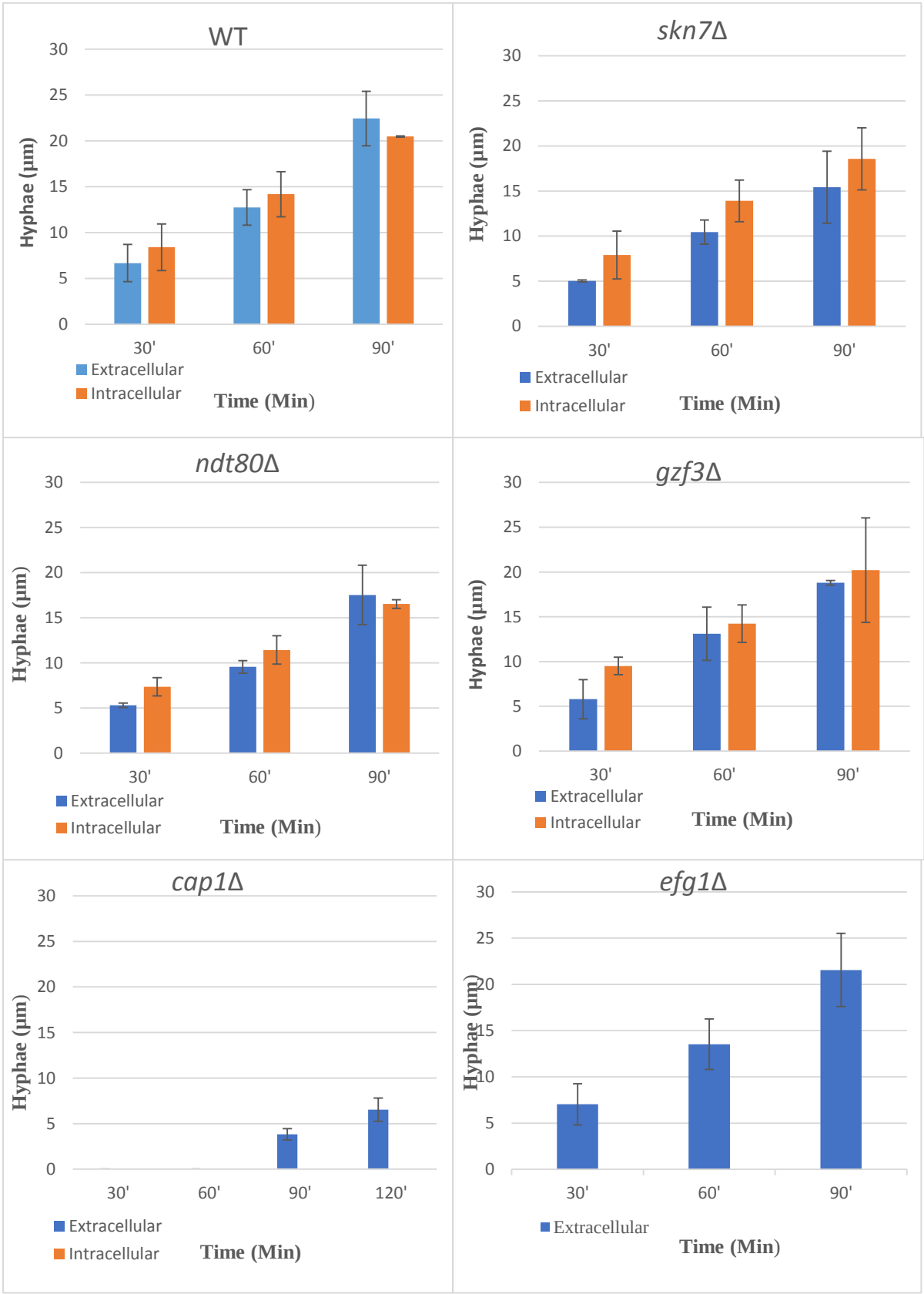
WT
skn7Δ
ndt80Δ
gzf3Δ
cap1Δ
efg1Δ
Hyphae (µm)
Time (Min)
30'
60'
90'
120'
Extracellular
Intracellular

B

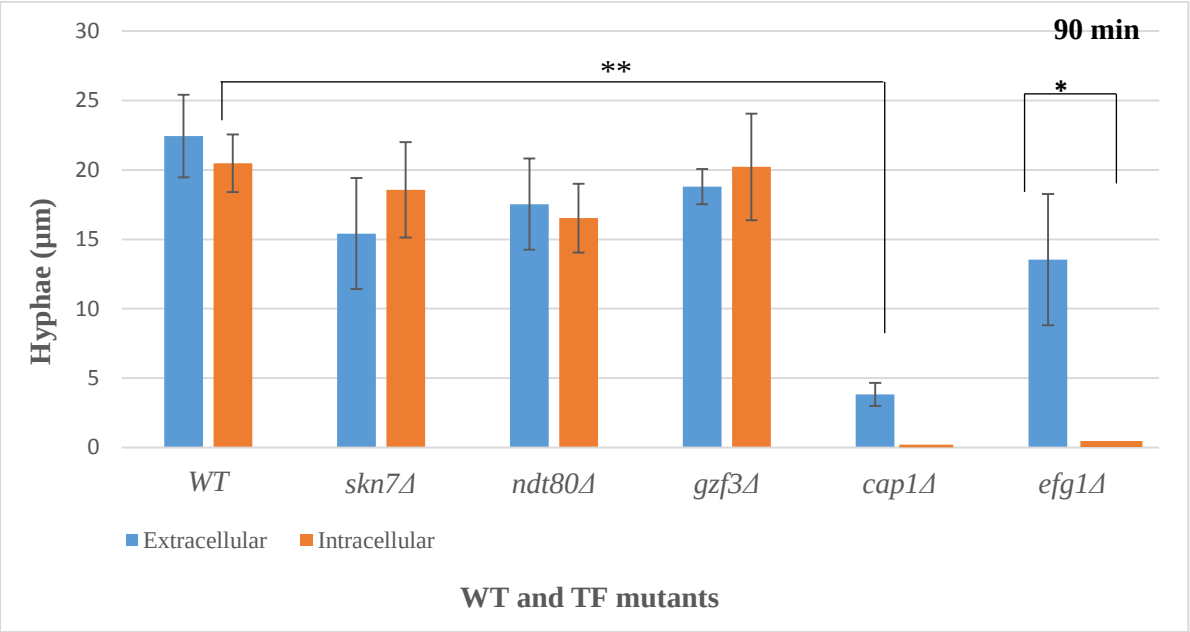

C

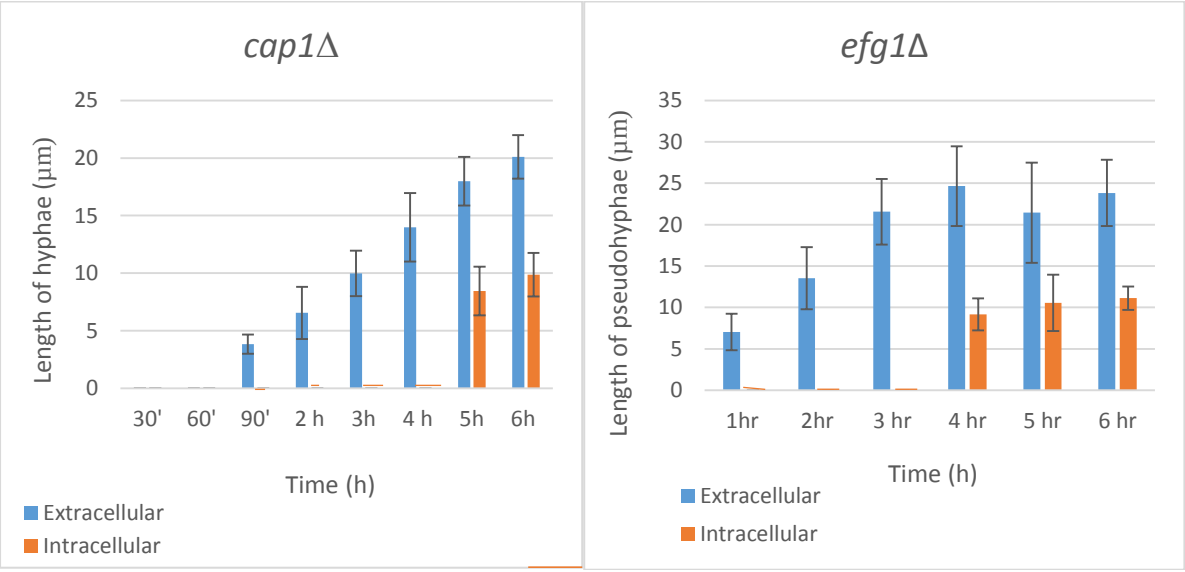

Figure 35: Impact of phagocytosis on formation of hyphae.
The transcription factor mutants; *skn7*Δ, *ndt80*Δ, *gzf3*Δ, *cap1*Δ, *efg1*Δ & WT were co-cultured with J774 macrophages. Live cell confocal videos were taken at 1 min per interval for 6 h. Hyphal and pseudohyphal length was measured half hourly at 30, 60 and 90 min (**A**), at 90 min (**B**), Up to 6h (**C**). Each experiment was repeated three times and the error bars drawn from SD. One way ANOVA and Bonferroni post hoc test was used to calculate statistical significance of differences in extracellular and intracellular hyphal length: ** ($p = 0.035$) ($p = 0.01$), and intracellular and extracellular pseudohyphae * ($p = 0.01$).

5.2.9 Null *efg1*Δ and *cap1*Δ cells remained viable inside the macrophage following phagocytosis.

Similar to previous observations in which *cap1*Δ cells and co- regulators failed to filament following phagocytosis (Patterson *et al*., 2013), cells of *cap1*Δ and *efg1*Δ remained in the yeast form up to 120 min inside the macrophages (Figure 34). It was probable that the cells initially did not undergo morphological transition due to cell death or arrested growth phase because in the later time points, and outside the macrophage, they formed filaments. The survival of the transcription factor mutants following phagocytosis was screened with the Lysotracker Red dye. Lysotracker Red is a vital stain which is excluded from viable cells. Staining characteristics of *Candida* cells (co-cultured with macrophages) with Lysotracker Red was observed at 3 h when the phagocytosis assays were stopped and the cells plated to assess the viable surviving population.

Approximately >90 % of *cap1*Δ and *efg1*Δ cells which did not filament inside the macrophages and did not take up the red Lysotracker Red which formed halos around the cells. Few cells which were < 5% were stained as red, oval/round, opaque bodies inside the macrophages. As cells only become permeable upon compromised integrity of the cell wall, it can be interpreted that at least 90% of *cap1*Δ and *efg1*Δ cells which were engulfed by the macrophages but were not filamenting were remained viable. The images of Lysotracker Red stained cells are shown side by side with the DIC images (Figure 35). These results suggest that *cap1*Δ cells engulfed by macrophages but not forming hyphae were viable.

Alternatively, to ascertain the viability of *Candida* cells engulfed by macrophages, a CFU assay was conducted by culturing the cells with macrophages and, expressing the number of viable cells as percentage of the original number of cells. The CFU assay showed that there was;

Table 10: Percentage CFU survival of TF mutants

TF mutants	% Survival
Wt	87 (SD = 16.2)
*skn7*Δ	95 (SD =18)
*ndt80*Δ	130 (SD = 14.0)
*gzf3*Δ	83 (SD = 22.0)
*cap1*Δ	202 (SD = 8.56)
*efg1*Δ	190 (SD = 5.89)

Table 10: Impact of phagocytosis on *Candida* survival.
The *WT* and transcription factor mutants; *skn7*Δ, *ndt80*Δ, *gzf3*Δ, *cap1*Δ and *efg1*Δ cells were co-cultured with J774 macrophages for 6 h. Viability of the cells was assayed using colony forming units (CFUs). Survival of the cells after 3 h was calculated as a percentage of the original 0 h number of cells for 3 h. Each experiment was repeated three times and the SD calculated.

Comparison of the survival of *WT* and transcription factor mutants by one way ANOVA ($p = 0.039$) and with Bonferroni post hoc test showed that the yeast cells of *efg1*Δ and *cap1*Δ cells had the highest survival rates inside the macrophages ($p = 0.035$) ($p = 0.029$) (Figure 36). There were no statistical differences between the *WT* and the other TF mutants. The observation that there was more survival of *cap1*Δ and *efg1*Δ compared to cells of wild type show that the cells were replicating inside the macrophage as their number doubled in the 3 h. However, it could also be because of the morphological differences of the cells after 3 h of the phagocytosis assay when the cells were plated and, the disadvantage of using CFU assay to assess survival. Unlike yeast cells of *cap1*Δ, hyphal cells of *WT* and the other TF mutants were co-joined and therefore could not be separated. This means that one CFU from a hypha could lead to growth of a single CFU but be based on more than one surviving cell, hence the inferred lower survival of *WT* compared to *cap1*Δ cells. Viable *cap1*Δ and *efg1*Δ non-filamentous cells inside the macrophages suggest that the cells replicated inside the macrophages as was seen by increased CFU numbers. The survival increased to 202 (SD = 8.56) % for *cap1*Δ, and 190 (SD = 5.89) % for *efg1*Δ cells after 3 h of the phagocytosis assay. However, as the accuracy of the CFU assay is affected by morphology type, the percentage survival of the cells cannot be used conclusively to show replication but as a guide to assess viability. Therefore, Cap1 and Efg1 are not important for *C. albicans* survival inside the macrophage following phagocytosis. As there was similar survival of the hyphae forming *skn7*Δ, *ndt80*Δ, and *gzf3*Δ to *WT* cells, it is suggestive that the transcription factors are not important for survival inside the macrophages. However, as explained previously, it is possible that the ROS environment of the J774 cell line macrophages was not sufficiently damaging to inhibit these cells.

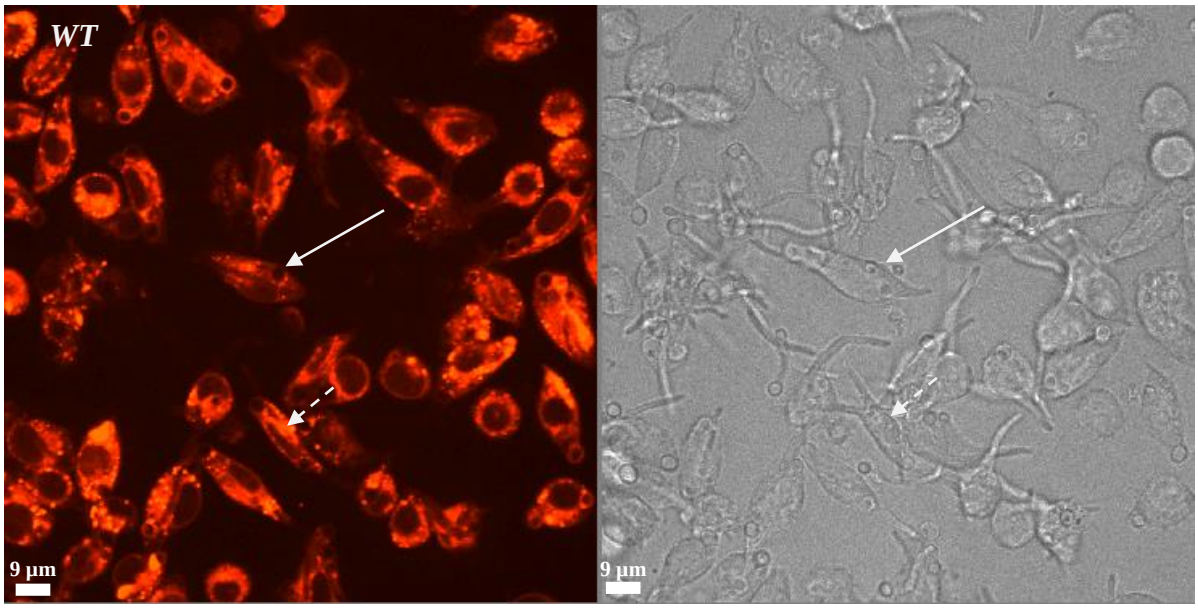
WT
9 µm
9 µm

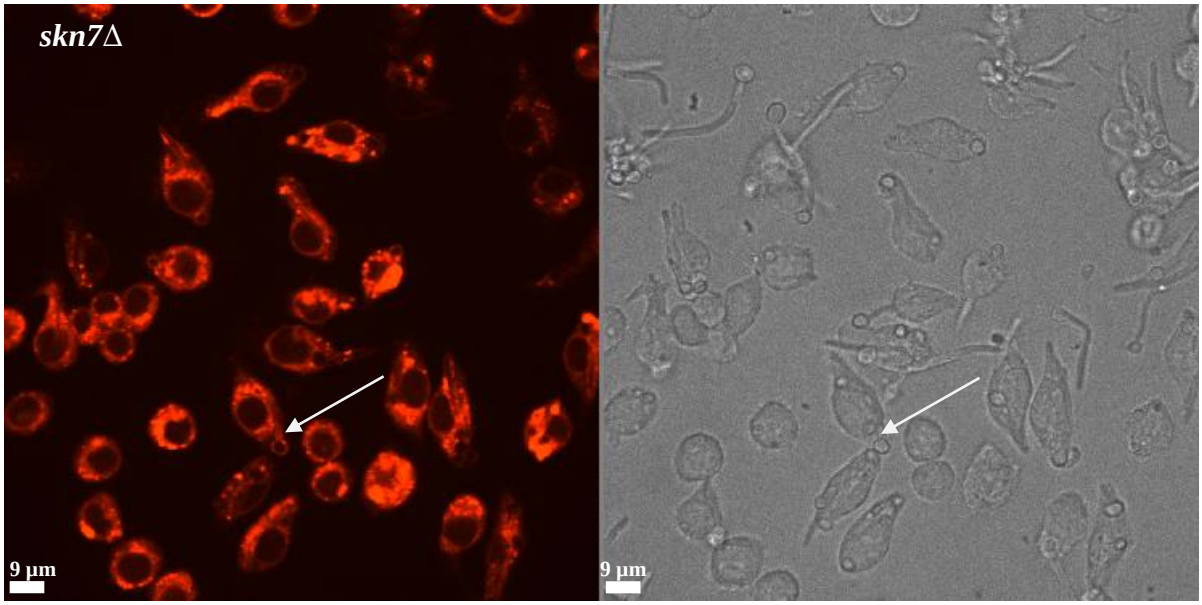
skn7Δ
9 µm
9 µm

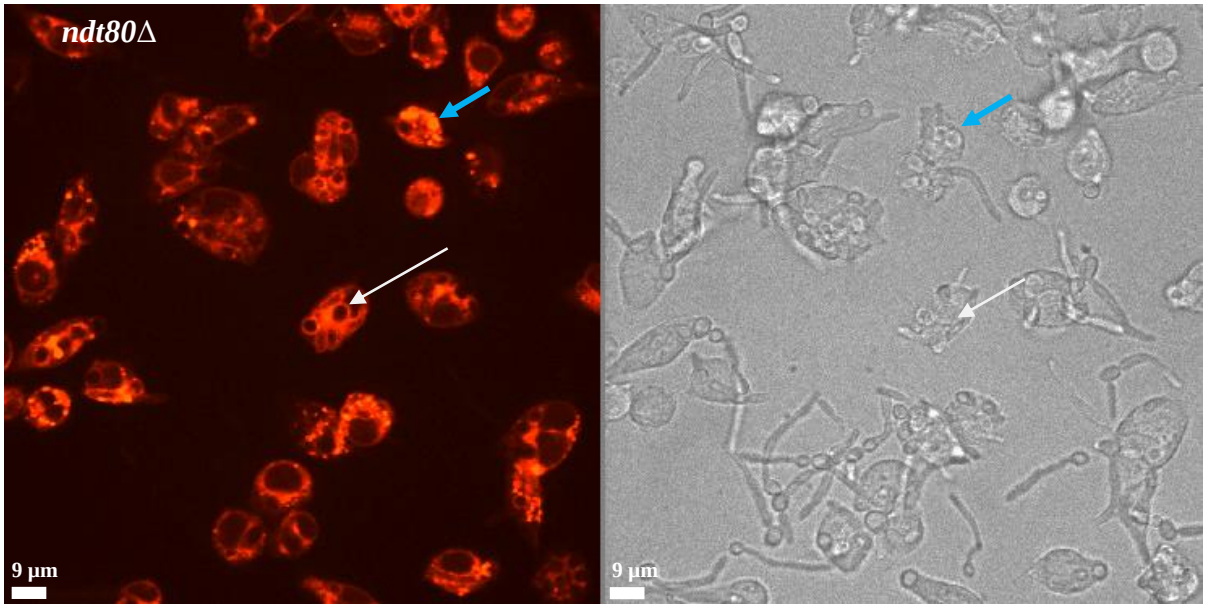
ndt80Δ
9 µm
9 µm

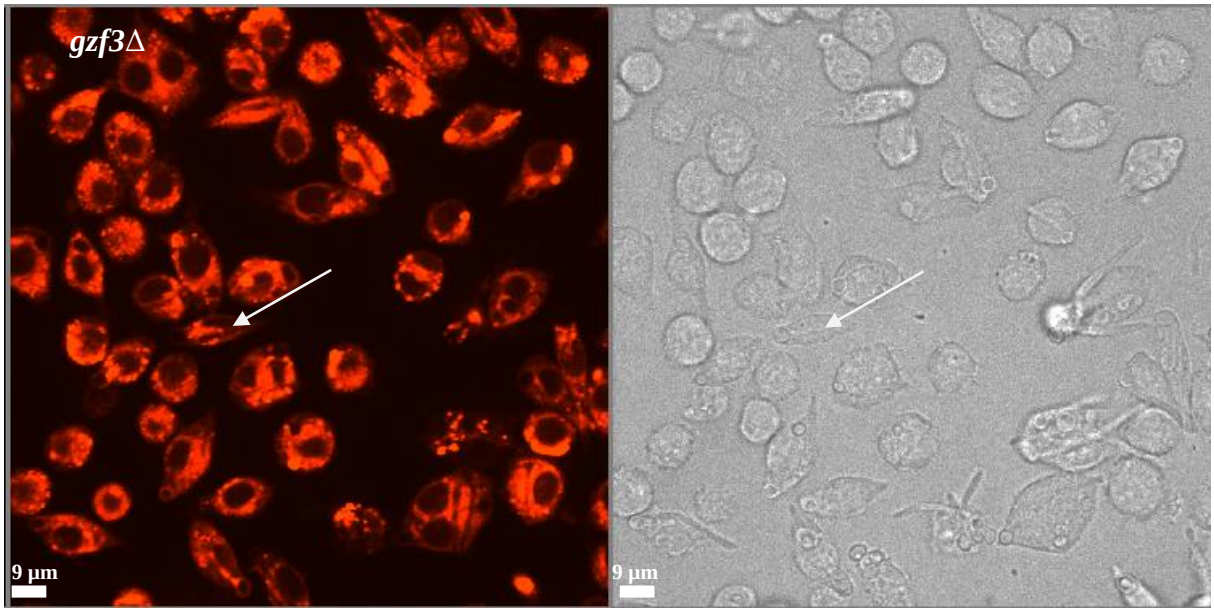
gzf3Δ
9 µm
9 µm

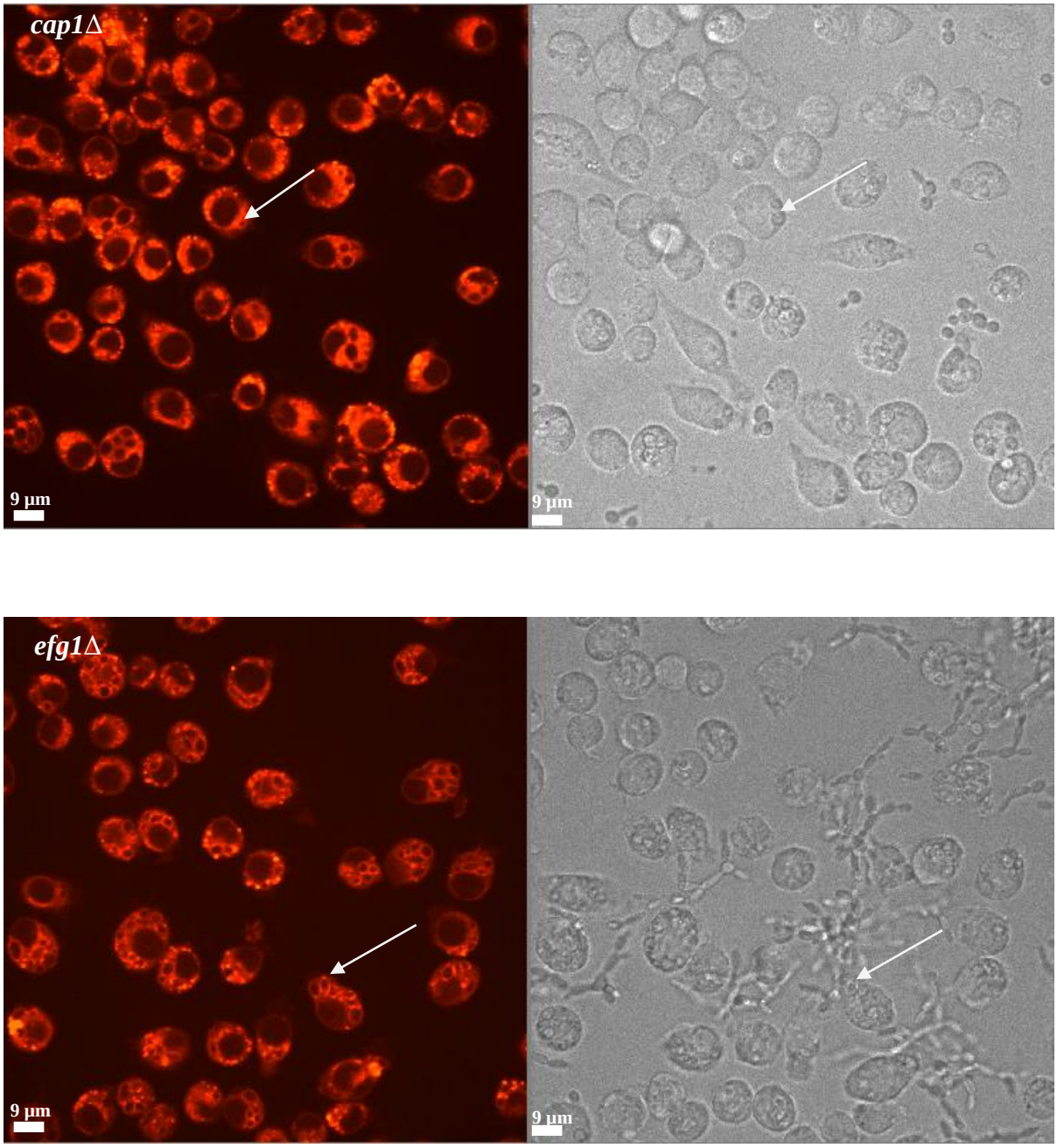

Figure 36: Impact of phagocytosis on *Candida* viability.
The transcription factor mutants; *WT*, *skn7*Δ, *ndt80*Δ, *gzf3*Δ, *cap1*Δ & *efg1*Δ were co-cultured with J774 macrophages for 6 h. Live cell confocal videos were taken at 1 min per interval for 6 h. A snapshot of the Lysotracker Red staining to assess viability of *Candida* was taken after 3 h. *Candida* viability was assessed by exclusion of, and formation of a red halo of the Lysotracker Red dye around the cell. The thin white arrows are pointing to the halos. The thick blue arrows are pointing to dead *Candida* cells. The snap shot images were captured to scale bar = 9.00 µm. Each experiment was repeated three times.

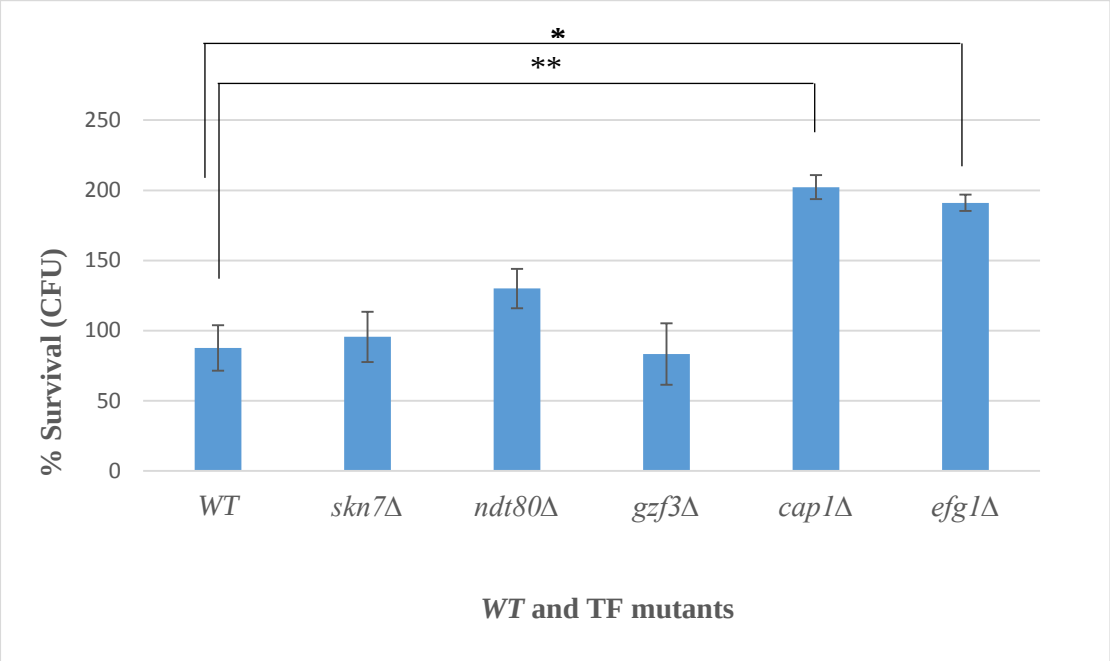

Figure 37: Impact of phagocytosis on *Candida* survival.
The *WT* and transcription factor mutants; *skn7*Δ, *ndt80*Δ, *gzf3*Δ, *cap1*Δ and *efg1*Δ cells were co-cultured with J774 macrophages for 6 h. Viability of the cells was assayed using colony forming units (CFUs). Survival of the cells after 3 h was calculated as a percentage of the original 0 h number of cells for 3 h. Each experiment was repeated three times and the error bars calculated from SD. One way ANOVA (*p = 0.039*) with Bonferroni correction was used to calculate the statistical significance: *p = **0.029, *p = 0.035.*

5.2.10 Macrophages co-cultured with *cap1*Δ and *efg1*Δ survived following phagocytosis.

C. albicans morphological transition from yeast to hypha has been associated with immune modulatory mechanisms (Gow *et al*., 2012), (Erwig *et al*., 2016), (Mukaremera *et al*., 2017), including decreased macrophage survival (Uwamahoro *et al*., 2014). The survival of macrophages following phagocytosis of the transcription factor mutants was determined.

The fluorescent and vital Lysotracker Red pH sensitive dye was used to stain cells for live cell video microscopy. During phagocytosis, viable macrophages retained the colour of the dye while dead macrophages lost the fluorescent signal of the dye. Therefore, the hourly survival of macrophages co-cultured with the transcription factor mutants was determined by counting. Macrophages that retained the red colour of Lysotracker were counted and the number expressed as a percentage of the original number at 0 h. For confirmation, the Lysotracker Red images were compared to the DIC pictures which showed morphological changes of the macrophages. The findings showed that the survival of macrophages co-cultured with *cap1*Δ increased from;

Table 11: Macrophage percentage hourly survival when co-cultured with *C. albicans*.

TF mutants	1h	2h	3h	4h	5h	6h
WT	96.6 (SD = 7.34)	81.57 (SD = 5.87)	50.61 (SD = 9.23)	30.58 (SD = 11.30)	15.6 (SD = 6.8)	7.15 (SD = 2.51)
*cap1*Δ	101.53 (SD = 5.13)	102.3 (SD = 5.21)	105.16 (SD = 5.36)	104.85 (SD = 5.7)	108.3 (SD = 4. 3)	108.3 (SD =10.14
*efg1*Δ	99.42 (SD =0.822)	99.28 (SD = 1.03)	100.58 (SD = 0.822)	102.03 (SD =1.23)	104. (SD = 0.21)	103 (SD = 0.61
*skn7*Δ	99.68 (SD = 13.56)	82.44 (SD =15.13)	61.85 (SD = 10.22)	45.98 (SD = 8.18)	40.51 (SD = 12.36)	26.79 (SD = 6.51)
*ndt80*Δ	100.97 (SD = 12.78)	98.21 (SD = 4.31)	74.59 (SD = 0.57)	57.24 (SD = 5.67)	50.44 (SD = 2.91)	40.44 (SD =11 24)
*gzf3*Δ	95.01 (SD = 4.32)	88.47 (SD = 8.07)	73.44 (SD = 12.83)	44.9 (SD= 14.75)	32.45 (SD =11.77)	18.94 (SD = 8.90)

Table 11: Impact of *C. albicans* uptake on macrophage survival.
The *WT* cells were co-cultured with macrophages. Viability of the macrophages was determined by their ability to retain Lysotracker Red stain. Macrophages which were stained red were counted at hourly intervals to the end of the experiment. The hourly survival was calculated as a percentage of the original 0 h number of macrophages. Each experiment was repeated three times and the SD calculated.

Comparison of the 6 h survival of the macrophages (Figure 38) co-cultured with *WT* , TF mutants and the macrophages showed that there were significant differences ($p = 0.05$). Using post hoc test with Bonferroni, macrophage cultures with yeast cells of *cap1*Δ ($p = 0.015$) and *efg1*Δ (p = 0.02) showed a high survival of macrophages while there was intermediate macrophage survival with *ndt80*Δ ($p = 0.035$) and associated death of macrophages cultured with *WT*, *skn7*Δ and *gzf3*Δ. Poor macrophage survival in the presence of hyphal cells of *Candida*, was noted. Hyphal cells are detrimental to the survival of macrophages and can induce pyroptosis or cause physical rupture which lead to macrophage death (Uwamahoro *et al*., 2014). There was intermediate survival of the macrophages with *ndt80*Δ possibly because the phenotype of some *ndt80*Δ cells was not true hyphae but also composed of pseudohyphae. Therefore, Cap1 and Efg1 are important for *C. albicans*-mediated killing of macrophages during phagocytosis. In contrast, Skn7 and Gzf3 are not important for macrophage killing as demonstrable by the null mutants which formed hyphal cells and caused macrophage death.

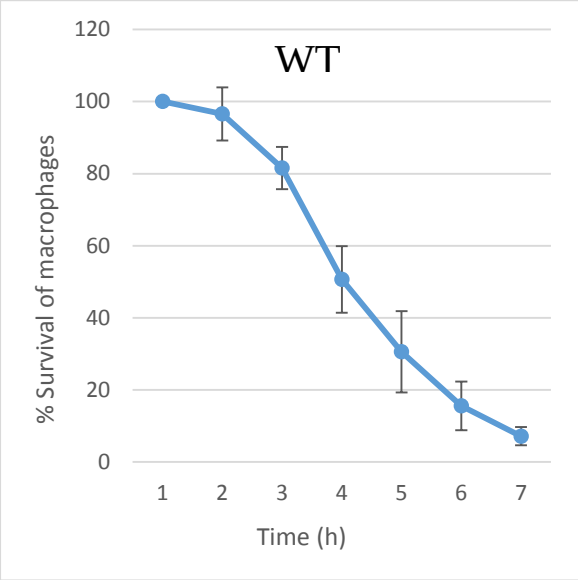
WT
% Survival of macrophages
120
100
80
60
40
20
0
1 2 3 4 5 6 7
Time (h)

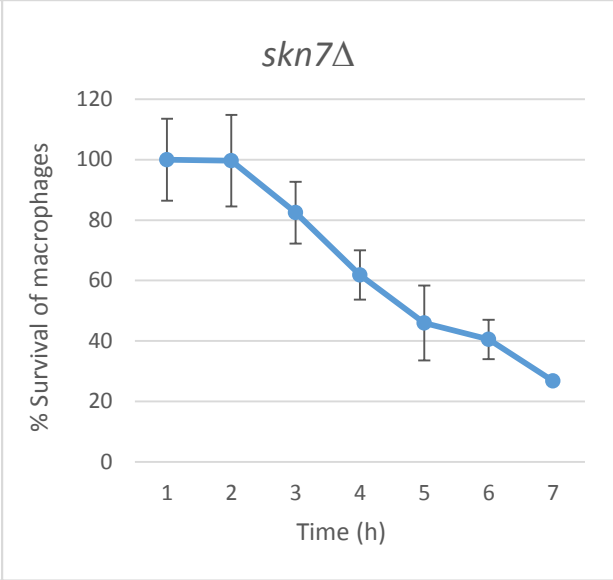
skn7Δ
% Survival of macrophages
120
100
80
60
40
20
0
1 2 3 4 5 6 7
Time (h)

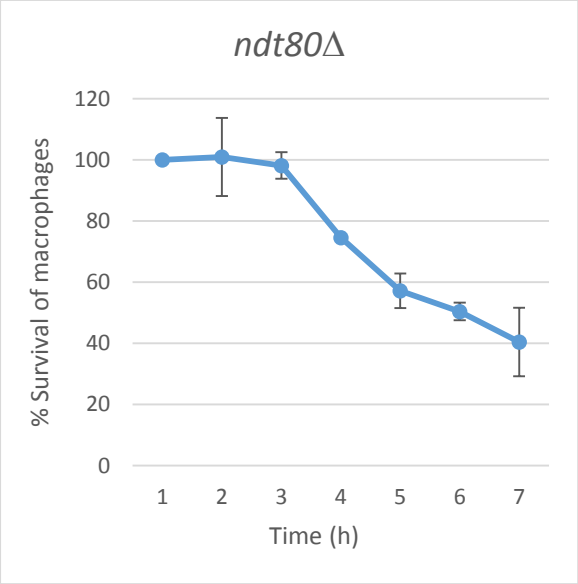
ndt80Δ
% Survival of macrophages
120
100
80
60
40
20
0
1 2 3 4 5 6 7
Time (h)

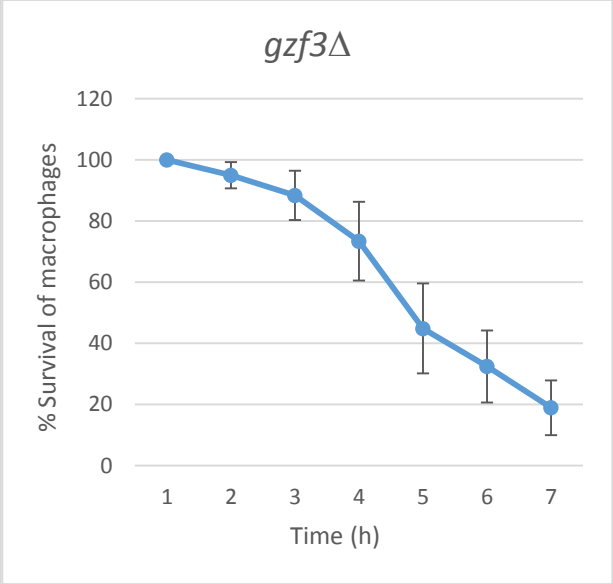
gzf3Δ
% Survival of macrophages
120
100
80
60
40
20
0
1 2 3 4 5 6 7
Time (h)

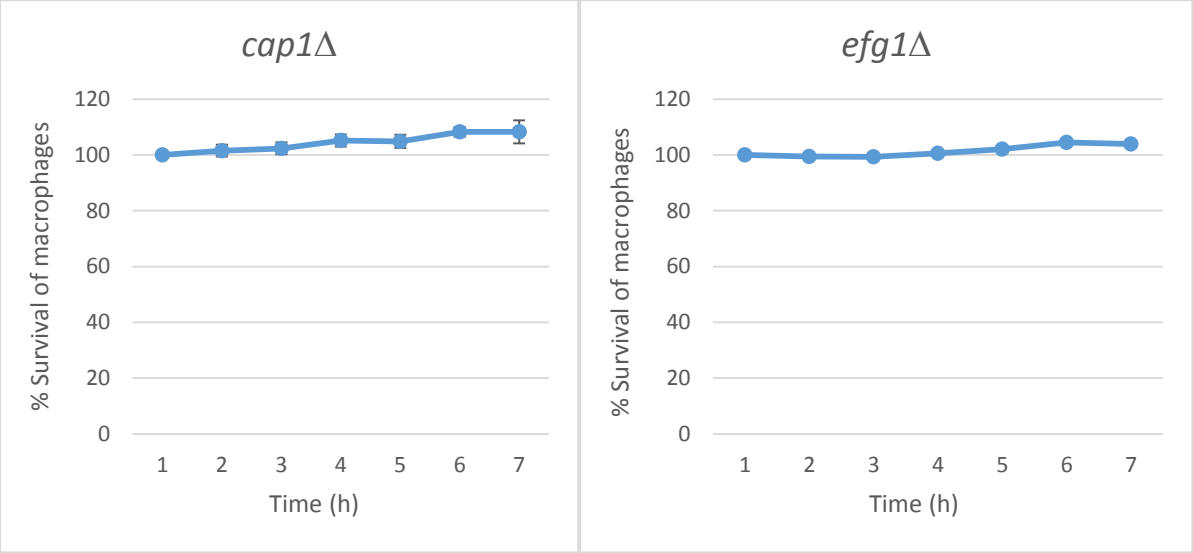

Figure 38: Impact of *C. albicans* uptake on macrophage survival.
The *WT* cells were co-cultured with macrophages. Viability of the macrophages was determined by their ability to retain Lysotracker Red stain. Macrophages which were stained red were counted at hourly intervals to the end of the experiment. The hourly survival was calculated as a percentage of the original 0 h number of macrophages. Each experiment was repeated three times and the error bars calculated from SD.

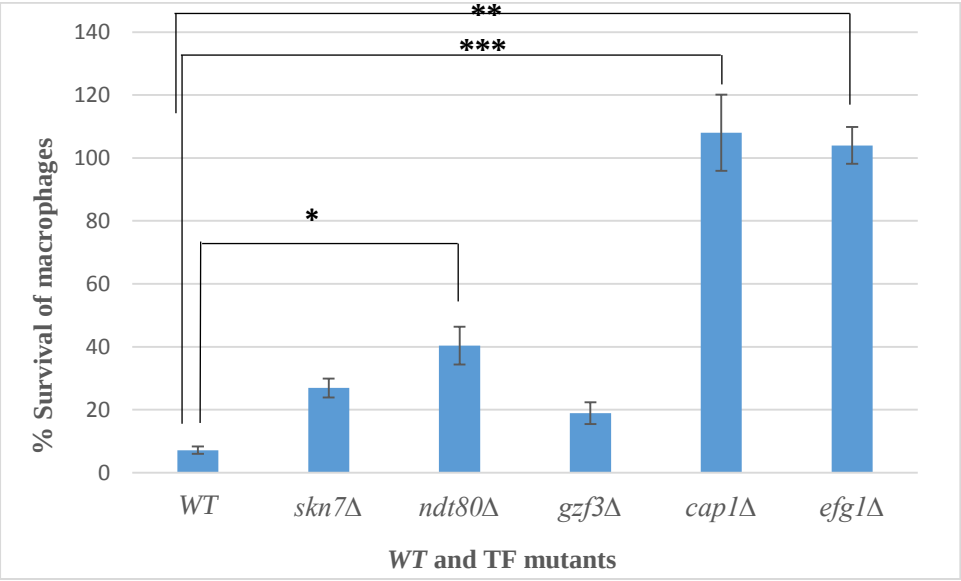

Figure 39: The 6 h survival of macrophages following phagocytosis of *WT* and TF mutants.
The *WT* cells were co-cultured with macrophages. Viability of the macrophages was determined by their ability to retain Lysotracker Red stain. Macrophages which were still stained red were counted at 6 h at the end of the experiment. The 6 h survival was calculated as a percentage of the original 0 h number of macrophages. Each experiment was repeated three times and the error bars calculated from SD. One way ANOVA was used to calculate the statistical significance: *p = ***0.015, **p = 0.02, * p = 0.035.*

5.2.11 Ectopic expression of *CAT1* did not restore hypha formation within macrophages.

Catalase is one of the enzymes involved in the detoxification of H_2O_2 (Brown *et al*., 2014, Kaloriti *et al*., 2014). It was shown that catalase is up-regulated in phagocytes and, disruption of the *CAT1* gene was shown to lead to increased sensitivity to H_2O_2 and attenuated virulence in mouse models of infection with *C. albicans* (Wysong *et al*., 1998). More recently, it was reported that over expression of *CAT1* did not alter virulence of *C. albicans* (Pradhan *et al*., 2017). As oxidative stress sensitive *cap1*Δ cells failed to filament following phagocytosis (Patterson *et al*., 2013), the goal was to determine if ectopic expression of catalase would restore hypha formation in the macrophage model of infection. In Chapter 3, it was demonstrated that ectopic catalase expression did not overcome H_2O_2 mediated inhibition of serum-induced hypha formation in *cap1*Δ cells *in vitro*. Nonetheless, due to differences between *in vitro* and the macrophage *ex vivo* environment, it was possible that *CAT1* overexpression might restore filamentation following phagocytosis.

Plasmid *pACT1+ CAT1* which expresses *CAT1* from the constitutive *ACT1* promoter was integrated at the *RPS10* locus in wild-type (BWP13) and *cap1*Δ (BWP13 *cap1::loxP-HIS1-loxP/cap1::loxP-ARG4-loxP*) cells. As controls, the empty vector *pACT1* was integrated at the *RPS10* locus in both wild-type and *cap1*Δ cells. Then the cells overexpressing catalase were assessed for abilities to form hyphae inside the macrophage. Cells co-cultured with macrophages and measurement of hyphal length every 30 min for 120 min showed that there was hyphal growth inside the macrophage in *cap1*Δ + *pACT1+ CAT1* cells (Figure 39). There was also hyphal growth of the *cap1*Δ + *pACT1* control cells inside the macrophage (Figure 39). Comparison of *cap1*Δ + *pACT1* + *CAT1* to *cap1*Δ + *pACT1* cells showed that hyphal growth was slower in the cells expressing the *ACT1*-driven *CAT1*. This suggests that over expression of catalase imposed a fitness cost on *C. albicans*. As reported previously that overexpression of catalase in the absence of peroxide stress leads to impaired survival of *C. albicans* (Pradhan *et al*., 2017), it is possible that the J774 macrophage environment did not produce sufficient ROS to impose oxidative stress on the *Candida* cells which were overexpressing catalase. Hence, the *ACT1*-driven *CAT1 Candida* cells formed hyphae slower than the control cells minus the *CAT1* gene because they were not exposed to sufficient oxidative stress. When used as an infection model, the cell line J774 macrophages was reported to produce a less robust oxidative burst than primary bone marrow derived macrophages (Andreu *et al*., 2017).

Together, these findings on the role of Cap1 on filamentation and escape show that Cap1 is important for *C. albicans* hypha formation but is dispensable for survival following phagocytosis. Therefore, oxidative stress sensitive mutants like *cap1*Δ were unable to undergo yeast to hypha morphogenesis inside the macrophage (Patterson *et al*., 2013), not because the cells were dead, but due to slow growth which could not be rescued by catalase overexpression. The inability of *CAT1* expression to increase the filamentation of *cap1*Δ cells following phagocytosis is consistent with the *in vitro* results reported in Chapter 3, which showed that ectopic expression of catalase did not restore H_2O_2-mediated inhibition of serum-induced morphogenesis *in vitro* (Figure 39).

It is noteworthy that strains of *cap1*Δ cells used in these experiments were different. The *cap1*Δ cells with *pACT1* integrated at the *RPS10* locus (this study) behaved differently from the original *cap1*Δ cells used in Patterson *et al*., 2013 in which Cip20 was integrated at the *RPS10* locus. The *cap1*Δ cells with *pACT1* integrated at the *RPS10* locus (this study) showed a different phenotype from the transcription factor (TF140) *cap1*Δ cells from the library (Homann *et al*., 2009). These strain differences may explain the inconsistencies observed with the *cap1*Δ cells but a full explanation of these results is still lacking.

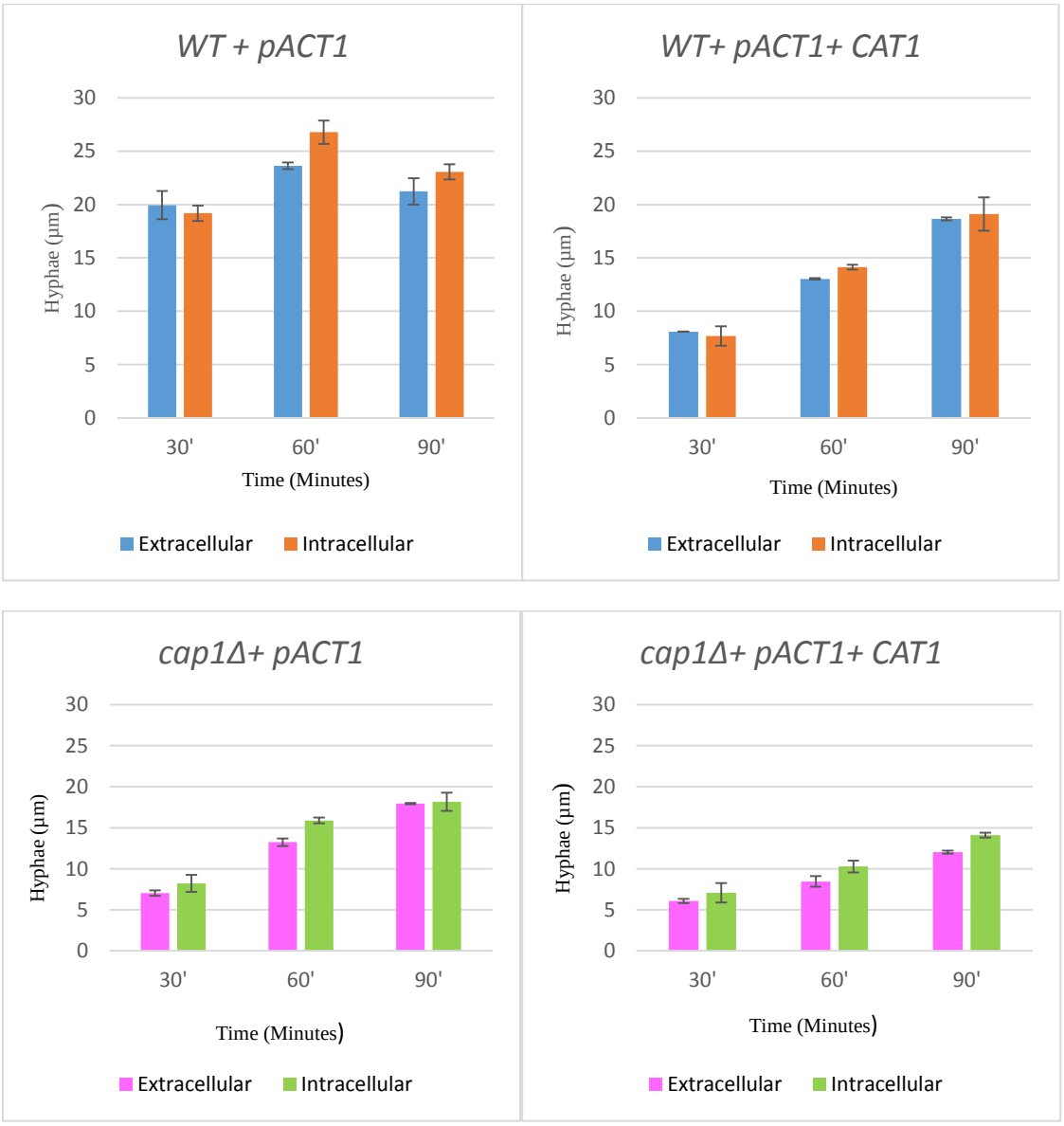

Figure 40*:* Impact of ectopic expression of *CAT1* on hypha formation in WT and *cap1*Δ cells following during phagocytosis.
The *WT + pACT1*, *WT+ pACT1 + CAT*, *cap1*Δ *+ pACT1*, *cap1*Δ *+ pACT1+ CAT1* cells were co-cultured with macrophages. Hyphal length was measured every 30 min for 90 min. Each experiment was repeated three times and the error bars calculated from the SD.

5.3 Both Hgc1 and Rad53 are important for filament formation but only Rad53 is essential for survival following phagocytosis.

Yeast to hypha morphogenesis is mediated by Hgc1 which is a hyphal specific G1 cyclin (Zheng *et al*., 2004). In contrast, DNA damage induced growth arrest is regulated by the Rad53 DNA damage responsive kinase (Da Silva *et al*., 2010). The lack of hypha formation of the oxidative stress sensitive *cap1*Δ and co-regulators inside the macrophage (Patterson *et al*., 2013) was shown to be due to sustained growth arrest *in vitro* (previous chapters 3, 4) and *ex vivo* macrophage (current chapter 5, results). Here, the aim

was to determine the roles of Hgc1 and Rad53 proteins in hypha formation and macrophage escape following phagocytosis. The mutants were used to assess if hypha formation or ROS mediated growth arrest were important for hypha formation and *Candida* survival following phagocytosis.

Null *hgc1*Δ, *rad53*Δ and reconstituted *hgc1*Δ + *HGC1* and *rad53*Δ + *RAD53* cells together with the parental wild type *BWP17 + Cip30* were co-cultured with J774 macrophages.

5.3.1 There was reduced directional migration of macrophages towards *hgc1*Δ cells.

Comparison of the track velocities showed that there were no significant differences in the track velocities of the morphological and growth arrest mutants ($p = 0.06$) (Table 4). One way ANOVA comparison of the meandering indices of the morphogenesis, and growth arrest mutants with *WT* showed that there were significant differences between the groups ($p = 0.05$) and post hoc Bonferroni test revealed that there was a reduced directionality of migration towards *hgc1*Δ ($p = 0.04$) (Table 4, Figure 40). There were no statistical differences in the comparison of the other mutants to *WT*. Therefore, the loss of Hgc1 led to reduced macrophage migration. As macrophage migration is offset by recognition, these findings suggest that there may be low exposure of PAMPs in *hgc1*Δ. The yeast locked *hgc1*Δ may mask some of the PAMPs that are differentially exposed in hyphae such as mannan (Gow *et al*., 2012).

Table 12: Macrophage migration directionality

Controls	Track Velocity (μm/sec)	Meandering Index
***hgc1*Δ**	0.016 (SD = 0.0091)	0.116 (SD = 0.046)*
hgc1*Δ *+HGC1	0.015 (SD = 0.0025)	0.154 (SD = 0.125)
***rad53*Δ**	0.018 (SD = 0.0056)	0.128 (SD = 0.060)
rad53*Δ+*RAD53	0.017 (SD = 0.0072)	0.140 (SD = 0.001)
BWP17+Cip30	0.028 (SD = 0.0060)	0.193 (SD = 0.002)

Table 12: Impact of Rad53 or Hgc1 loss on macrophage migration speed and directionality. *C. albicans hgc1*Δ, *hgc1*Δ *+HGC1, rad53*Δ, *rad53*Δ *+ RAD53 and BWP17 + Cip30* cells were co-cultured with J774 macrophages. Volocity tracking software was used to track the migration of macrophages per min per interval for 60 min. The numeric outputs of the tracking diagrams were displayed inform of speed (tracking velocity (μm/s)) and directionality (meandering index). One way ANOVA was used to calculate statistical significance of differences among the groups and post hoc correction with Bonferroni; *$p = 0.04$.

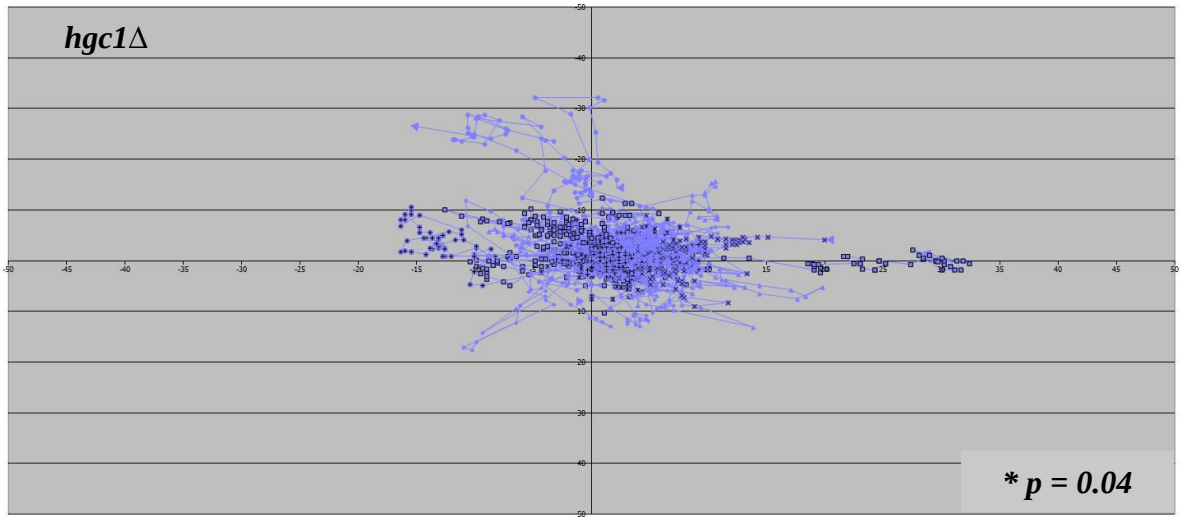
hgc1Δ
* p = 0.04

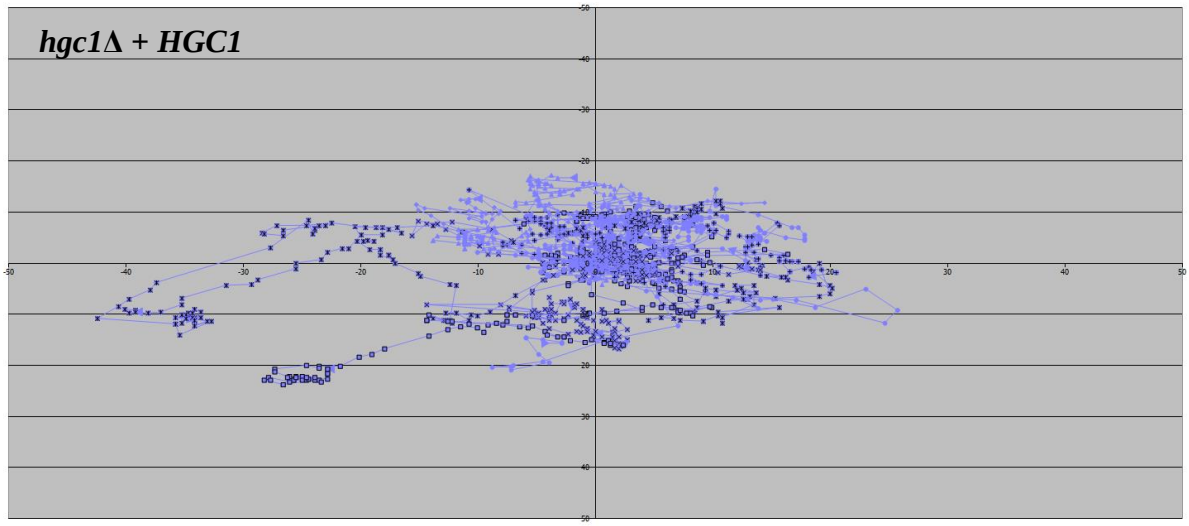
hgc1Δ + HGC1

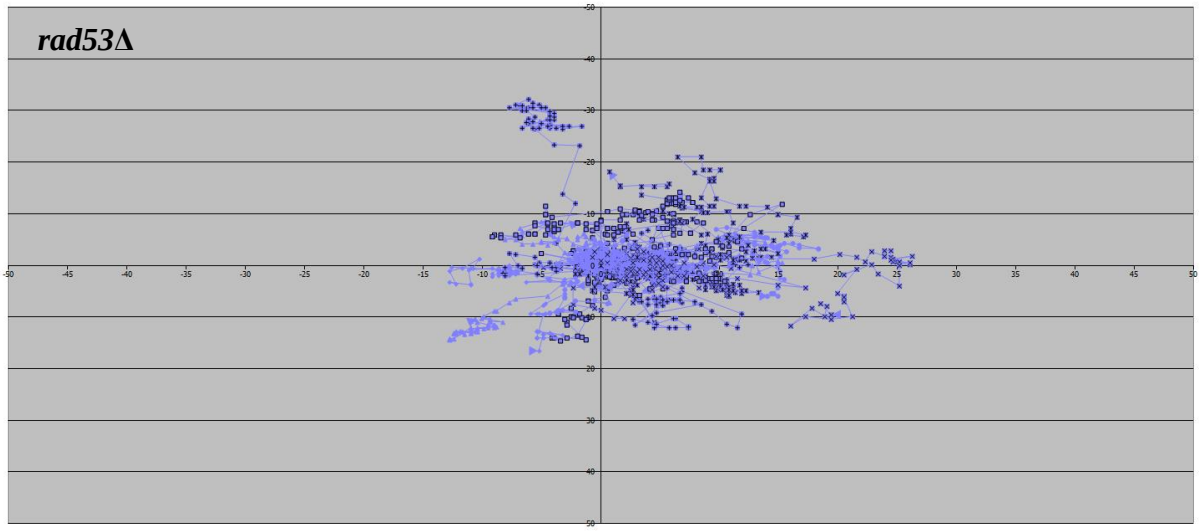
rad53Δ

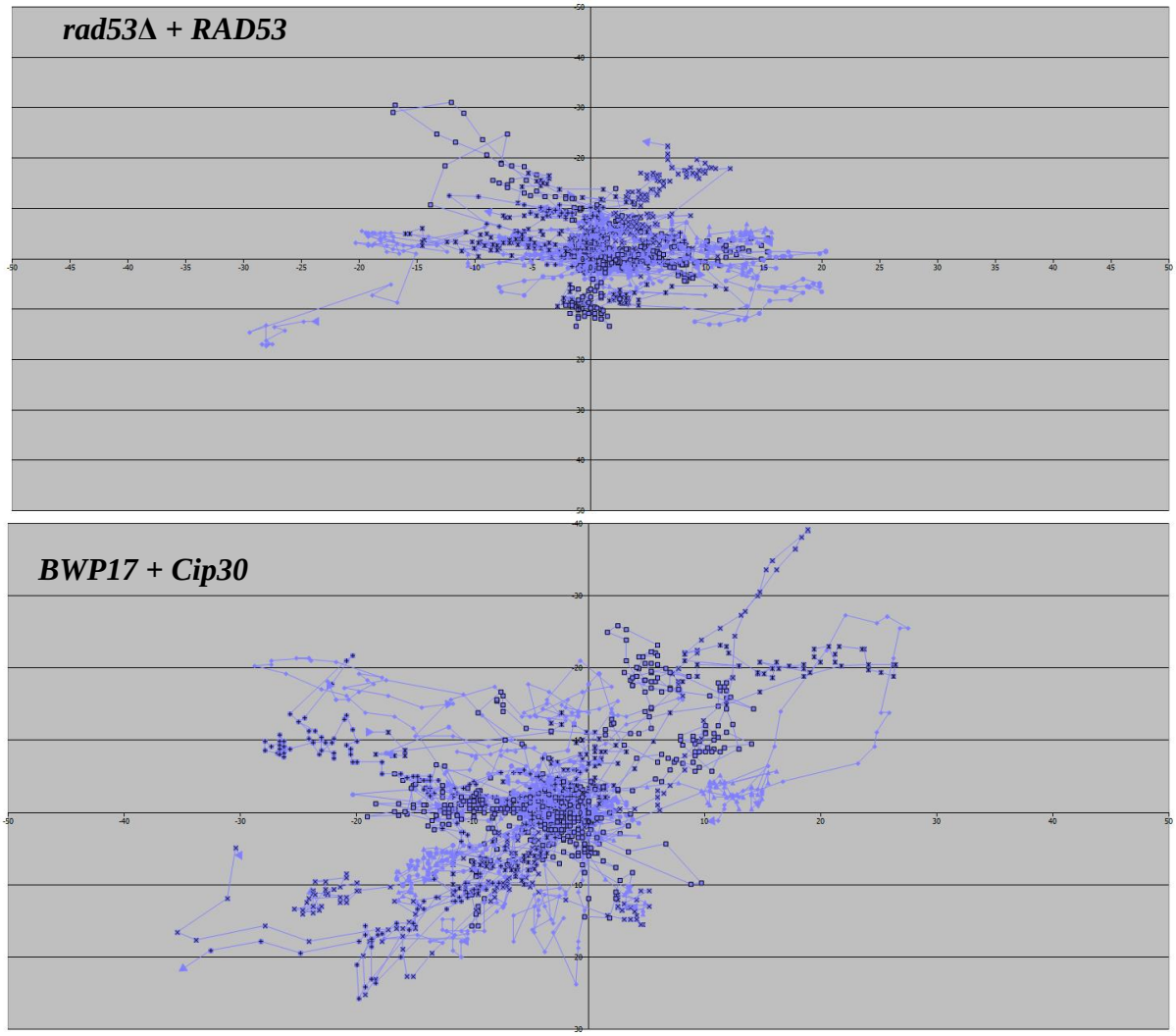

Figure 41: Impact of loss of Rad53 or Hgc1 on macrophage migration directionality.
Cells of *hgc1*Δ, *hgc1*Δ *+HGC*, *rad53*Δ, *rad53*Δ *+ Rad53 and BWP17 + Cip30* were co-cultured with J774 macrophages. Live cell video microscopy was taken at 1 min per interval and tracked using the tracking software for 60 min. The tracks indicate the movement of a single macrophage relative to its starting point and the arrows represent directionality of movement.

5.3.2 The loss of Hgc1 or Rad53 had no impact on attachment time.

The findings showed that attachment times were;

Table 13: Attachment times of the morphogenesis and growth arrest mutants.

Morphogenesis and growth arrest mutants	Attachment times (min)
*hgc1*Δ	12.18 (SD = 2.61)
*hgc1*Δ + *HGC1*	19.22 (SD = 3.54)
*rad53*Δ	16.34 (SD = 1.59)
*rad53*Δ + *Rad53*	14.77 (SD = 4.52)
BWP17 + *Cip30*	19.94 (SD = 2.09)

Table 13: Impact of Rad53 or Hgc1 loss on attachment time.
*C. albicans hgc1*Δ, *hgc1*Δ + *HGC1*, *rad53*Δ, *rad53*Δ + *Rad53*, and *BWP17* + *Cip30* were co-cultured with J774 macrophages. Live cell video microscopy was taken at 1 min per interval for 6 h. Attachment time was the time when macrophage-*Candida* cell-cell contact time within the movie. Each experiment was repeated three times and the SD calculated.

One way ANOVA comparison of the attachment times of the mutants to the wild type cells showed that there were no statistical differences in the attachment times ($p = 0.071$) (Figure 41). Therefore, Hgc1 and Rad53 are not important for *C. albicans*-macrophage attachment.

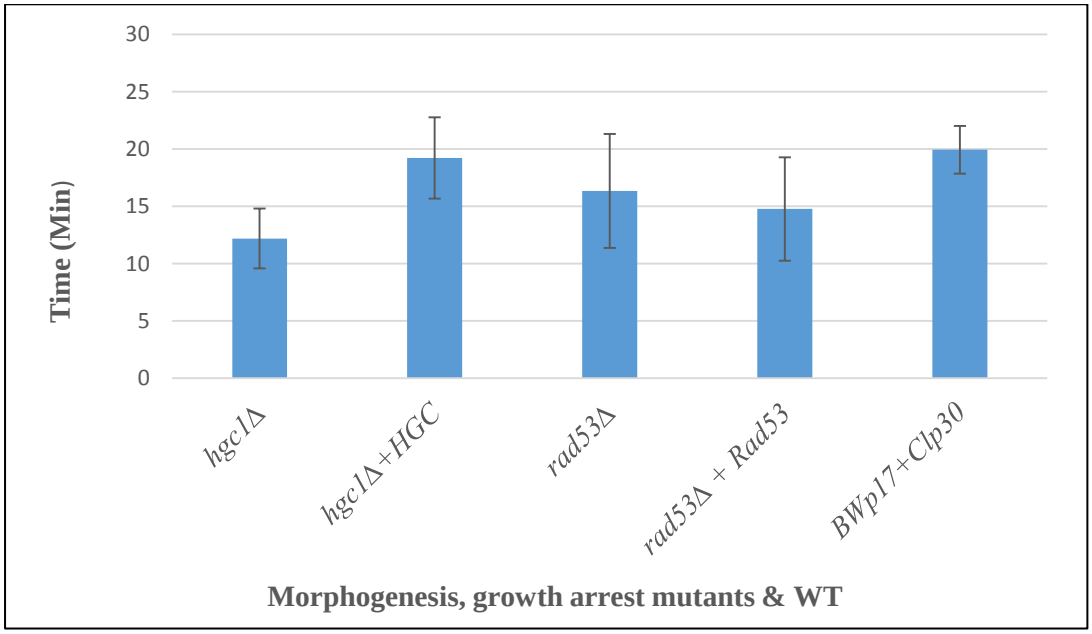

Figure 42 : Impact of Rad53 or Hgc1 loss on attachment time.
*C. albicans hgc1*Δ, *hgc1*Δ + *HGC1*, *rad53*Δ, *rad53*Δ + *Rad53*, and *BWP17* + *Cip30* were co-cultured with J774 macrophages. Live cell video microscopy was taken at 1 min per interval for 6 h. Attachment time was the time when macrophage-*Candida* cell-cell contact time within the movie. Each experiment was repeated three times and the error bars calculated from SD. One way ANOVA was used to calculate statistical significance.

5.3.3 There were no differences in the time of engulfment of *hgc1*Δ and *rad53*Δ cells.

The results showed that the times of engulfment were;

Table 14: Time of engulfment of the morphogenesis and growth arrest mutants.

TF mutant	Time of engulfment (min)
*hgc1*Δ	12.98 (SD = 3.55)
*hgc1*Δ + *HGC1*	20.61 (SD = 3.57)
*rad53*Δ	17.53 (SD = 5.53)
*rad53*Δ + *RAD53*	16.16 (SD = 4.57)
BWP17 + *Cip30*	21.50 (SD = 1.83)

Table 14: Impact of Rad53 or Hgc1 loss on time of engulfment.
*C. albicans hgc1*Δ, *hgc1*Δ + *HGC1*, *rad53*Δ, *rad53*Δ + *Rad53*, and *BWP17* + *Cip30* were co-cultured with J774 macrophages. Live cell video microscopy was taken at 1 min per interval for 6 h. Time of engulfment was the time within the movie when *Candida* was enclosed within the membranes of the macrophage. Each experiment was repeated three times.

Comparison of the engulfment times of the mutants to *WT* cells using one way ANOVA showed that there were no statistically significant differences ($p = 1.00$). Similar times of engulfment was expected because there were no differences in the times of attachment.

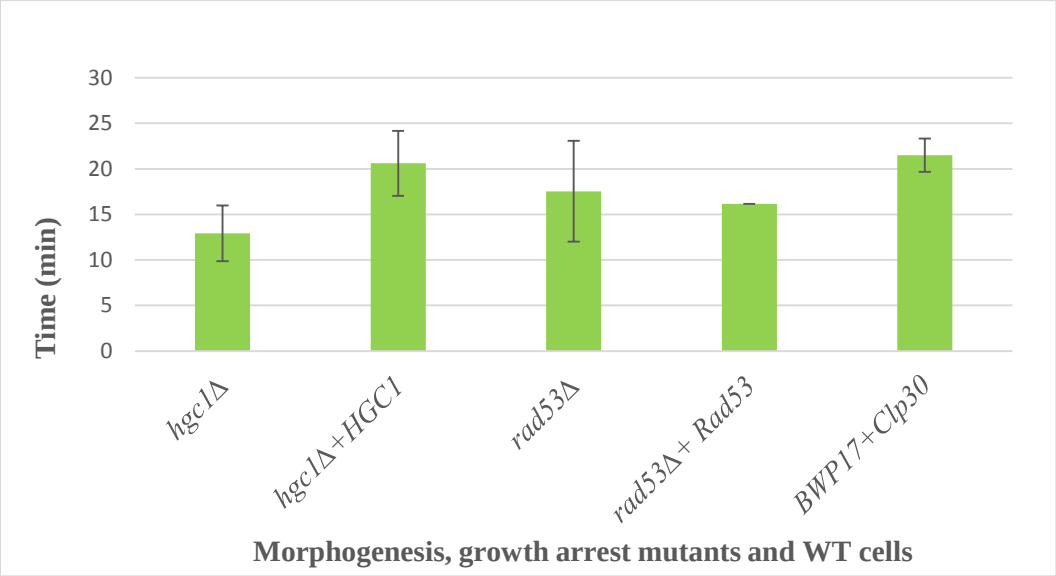

Figure 43: Engulfment time: Impact of Rad53 or Hgc1 loss on time of engulfment.
*C. albicans hgc1*Δ, *hgc1*Δ + *HGC1*, *rad53*Δ, *rad53*Δ + *Rad53*, and *BWP17* + *Cip30* were co-cultured with J774 macrophages. Live cell video microscopy was taken at 1 min per interval for 6 h. Time of engulfment was the time within the movie when *Candida* was enclosed within the membranes of the macrophage. Each experiment was repeated three times and the error bars calculated from the SD. One way ANOVA was used to calculate statistical significance.

5.3.4 The time taken for engulfment was longest for the *rad53*Δ mutant.

The results showed that the durations of engulfment were;

Table 15: Time taken for engulfment.

Morphogenesis, growth arrest mutants and *WT* cells	**Time taken for engulfment (min)**
*hgc1*Δ	0.74 (SD = 0.446)
*hgc1*Δ + *HGC1*	1.39 (SD = 0.025)
*rad53*Δ	3.13 (SD = 2.18)
*rad53*Δ + *RAD53*	1.40 (SD = 0.13)
BWP17 + *Cip30*	1.31 (SD = 0.1)

Table 15: Impact of Rad53 or Hgc1 loss on the time taken for engulfment.
*C. albicans hgc1*Δ, *hgc1*Δ + *HGC1*, *rad53*Δ, *rad53*Δ + Rad53 and *BWP17* + *Cip30* cells were co-cultured with J774 macrophages. Live cell video microscopy was taken at 1 min per interval for 6 h. The time taken for engulfment was calculated as the difference between the times of attachment and engulfment. Each experiment was repeated three times. One way ANOVA was used to calculate statistical significance of the differences of the mutants to *WT* and post hoc Bonferroni test: *(*p = 0.029*).

One way ANOVA comparison of the findings of the wild type, morphogenesis and growth arrest strains showed that the times taken for engulfment were significantly different (*p = 0.04*) and with post hoc Bonferroni test it was longest for *rad53*Δ cells (*p = 0. 029*) (Figure 43). Pairwise comparison of the other mutants to wild type were not significant. The long duration of engulfment of *rad53*Δ is probably related to the higher number of *C. albicans* engulfed (Figure 18). However, it is also possible that *rad53*Δ has defects in the cell wall, therefore masked PAMPs exposure for recognition and engulfment.

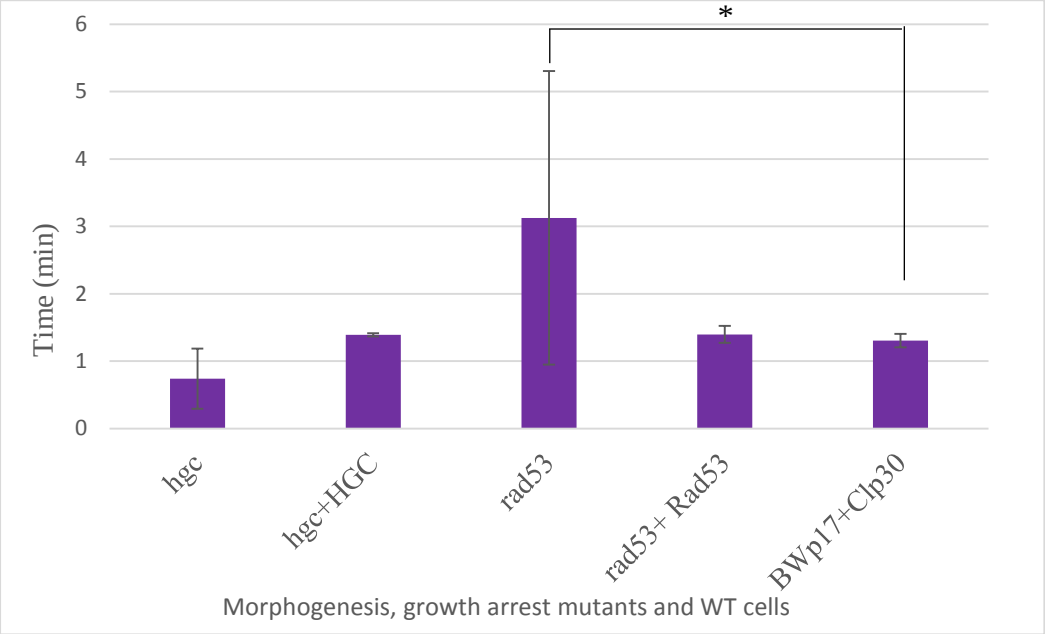

Figure 44: Impact of Rad53 or Hgc1 loss on the time taken for engulfment.
*C. albicans hgc1*Δ, *hgc1*Δ + *HGC1*, *rad53*Δ, *rad53*Δ + Rad53 and *BWP17 + Cip30* cells were co-cultured with J774 macrophages. Live cell video microscopy was taken at 1 min per interval for 6 h. Duration of engulfment was calculated as the difference between the times of attachment and engulfment. Each experiment was repeated three times and the error bars calculated from SD. One way ANOVA was used to calculate statistical significance of the differences of the mutants to *WT* and post hoc Bonferroni test: *(*p = 0.029*).

5.3.5 The loss of Rad53 led to an increase in the number of *C. albicans* engulfed.

The results showed that the number of *C. albicans* engulfed were;

Table 16: Number of *C. albicans* engulfed.

Morphogenesis, growth arrest mutants and *WT* cells	**Time taken for engulfment (min)**
*hgc1*Δ	0.99(SD = 0.01)
*hgc1*Δ + *HGC1*	1.22 (SD = 0.52)
*rad53*Δ	1.43 (SD = 0.56)*
*rad53*Δ + *RAD53*	0.97 (SD = 0.14)
BWP17 + Cip30	1.04 (SD = 0.03)

Table 16: Impact of Rad53 or Hgc1 loss on the number of engulfed *C. albicans*.
*C. albicans hgc1*Δ, *hgc1*Δ + *HGC1*, *rad53*Δ, *rad53*Δ + Rad53 and *BWP17 + Cip30* were co-cultured with J774 macrophages. Live cell video microscopy was taken at 1 min per interval for 6 h. The average number of *C. albicans* engulfed over the first 60 min was calculated. Each experiment was repeated three times and the SD calculated.

Comparison of the number of the cells engulfed by one way ANOVA showed that there were statistical differences (*p = 0.03*) and by Bonferroni test analysis, the number was highest for *rad53*Δ (*p = 0.02*). Comparison of the other mutants was significant (Figure 44). The findings that the loss of Rad53 led to increased number *Candida* engulfment is possibly because they were not readily forming hyphae. Although the cells formed

filamentous morphology there were many yeast cells which were growing as budding forms. Therefore, the *rad53*Δ were engulfed as chains of yeast cells compared to the single yeasts of *hgc1*Δ or hyphae of *rad53*Δ + *RaD53*, *hgc1*Δ + *HGC1* and *BWP17* + *Cip30*.

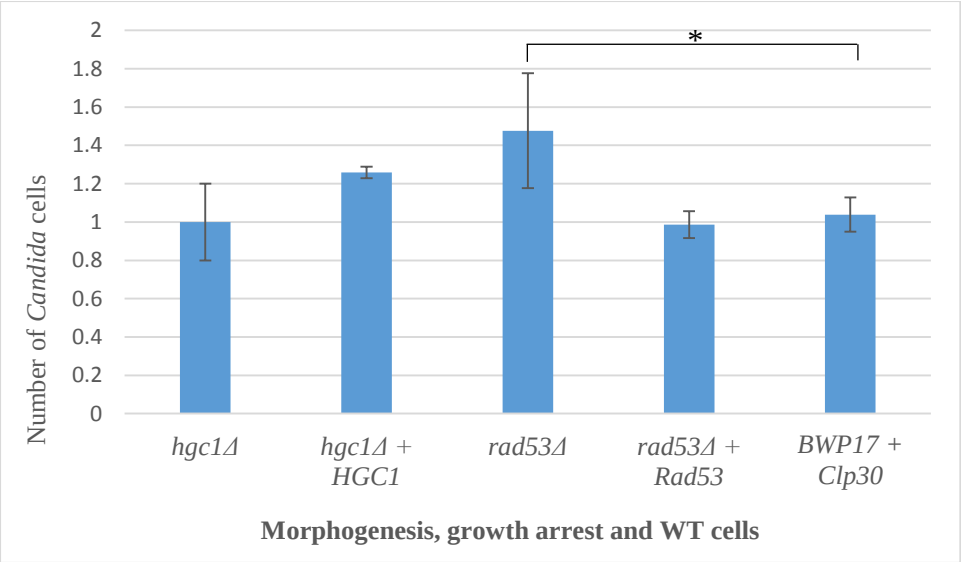

Figure 45: Impact of Rad53 or Hgc1 loss on the number of engulfed *C. albicans*.
*C. albicans hgc1*Δ, *hgc1*Δ + *HGC1*, *rad53*Δ, *rad53*Δ + Rad53 and *BWP17* + *Cip30* were co-cultured with J774 macrophages. Live cell video microscopy was taken at 1 min per interval for 6 h. The average number of *C. albicans* engulfed over the first 60 min was calculated. Each experiment was repeated three times and the error bars calculated from SD. One way ANOVA, followed by Bonferroni post hoc test was used to calculate statistical significance: *$p = 0.02$.

5.3.6 There were no differences in the time of acidification of the phagosome.

The findings revealed that the times of acidification were;

Table 17: Time of acidification of the phagosome.

Morphogenesis, growth arrest mutants and *WT* cells	**Time taken for engulfment (min)**
*hgc1*Δ	1.17 (SD = 0.19)
*hgc1*Δ + *HGC1*	1.05 (SD = 0.16)
*rad53*Δ	0.96 (SD = 0.23)
*rad53*Δ + *RAD53*	0.90 (SD = 0.041)
BWP17 + *Cip30*	1.07 (SD = 0.002)

Table 7: Impact of Rad53 or Hgc1 loss on phagosome acidification.
*C. albicans hgc1*Δ, *hgc1*Δ + *HGC1*, *rad53*Δ, *rad53*Δ + Rad53 and *BWP17* + *Cip30* cells were co-cultured with J774 macrophages. Live cell video microscopy was taken at 1 min per interval for 6 h. The time for phagosome acidification was calculated as the difference between the time when *Candida* was completely engulfed by the macrophage and when the red halo of Lysotracker Red appeared. Each experiment was repeated three times and the SDs calculated. One way ANOVA was used to calculate statistical significance of differences of the mutants to *WT* among the groups.

One way ANOVA analysis of the time to acidification showed that there were no differences in the times of acidification of the mutants compared to the *WT* cells (p =

1.00) (Figure 45). This means that there was no impact of the loss of Hgc1 or Rad53 on the acidification of the phagosome. Therefore, Hgc1 and Rad53 played no role in the acidification of the phagosome.

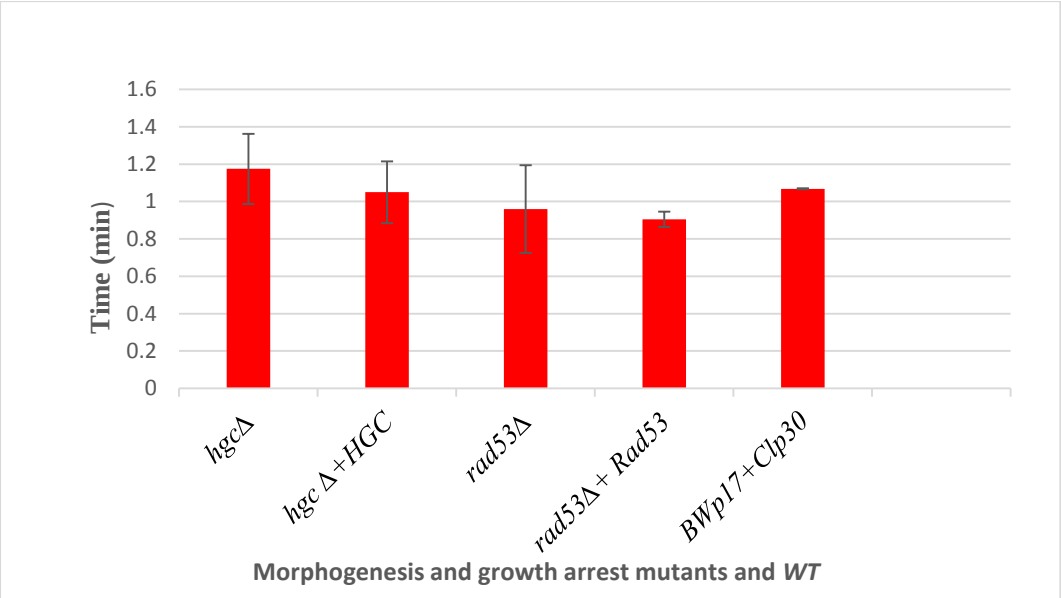

Figure 46: Impact of Rad53 or Hgc1 loss on phagosome acidification.
*C. albicans hgc1*Δ, *hgc1*Δ + *HGC1*, *rad53*Δ, *rad53*Δ + Rad53 and *BWP17 + Cip30* cells were co-cultured with J774 macrophages. Live cell video microscopy was taken at 1 min per interval for 6 h. The time for phagosome acidification was calculated as the difference between the time when *Candida* was completely engulfed by the macrophage and when the red halo of Lysotracker Red appeared. Each experiment was repeated three times and the error bars calculated from SD. One way ANOVA was used to calculate statistical significance of differences of the mutants to *WT* among the groups.

5.3.7 There was no effect of the loss of Hgc1 or Rad53 on uptake rate.

Comparison of the uptake rates of the mutants to *WT* using one way ANOVA showed that that the uptake rate was the same ($p = 1.00$) (Figure 46). This means that uptake rate did not change following the loss of Hgc1 or Rad53 (Figure 20). This finding means that Hgc1 or Rad53 are not important in the uptake of *C. albicans*.

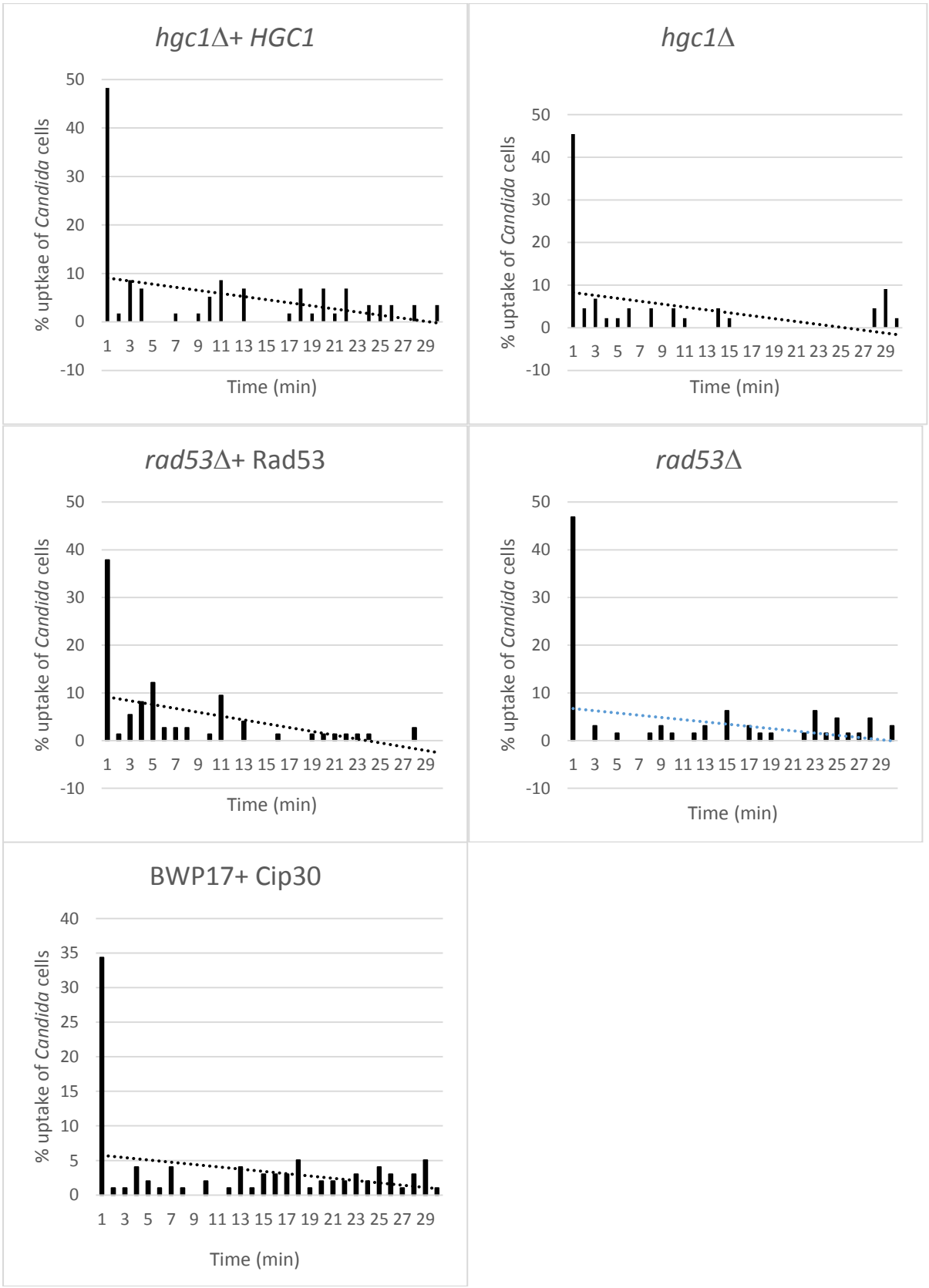

Figure 47: Impact of Rad53 or Hgc1 loss on uptake rate:
Strains of *C. albicans hgc1*Δ, *hgc1*Δ + *HGC1*, *rad53*Δ, *rad53*Δ + *RAD53* and *BWP17 + Cip30* cells were co-cultured with J774 macrophages. Live cell video microscopy was taken at 1 min per interval for 6 h. The number of Candida cells engulfed by each macrophage per time interval per min was calculated and expressed as percentage of the total number of cells engulfed by all macrophages over

30 minutes. Each experiment was repeated three times. One way ANOVA was used to calculate the statistical significance of the differences of the mutants to WT.

5.3.8 Null *rad53*Δ and *hgc1*Δ did not form hyphae inside macrophages.

The cells of *hgc1*Δ+*HGC1*, *rad53*Δ + Rad53 and *BWP17*+ *Cip30* formed hyphae while *rad53*Δ delayed to form intracellular hyphae and *hgc1*Δ remained yeast-locked both intracellularly and outside the macrophages (Figure 48). The length of hyphae were measured at 30, 60 and 90 min. The extracellular/intracellular length (μm) included;

Table 18: Extracellular/Intracellular length and SD of hyphae formed.

Morphogenesis, growth arrest mutants and *WT* cells	Hyphae at 30 min (μm)	Hyphae at 60 min	Hyphae at 90 min
*hgc1*Δ	0 (0), 0 (0)	0 (0), 0 (0)	0 (0), 0 (0)
*hgc1*Δ + *HGC1*	4.56 (0.59), 6.88(0.19)	9.87 (0.08), 10.5 (0.66)	13.35 (0.84), 15.52 (2.02)
*rad53*Δ	5.17 (0.01), 0 (0)	9.32 (0.13), 0 (0)	12.32 (0.11), 0
*rad53*Δ + *RAD53*	4.19 (0.68), 7.25 (0.51)	7.63 (1.16), 12.06 (0.93)	7.75 (0.04), 14.64 (3.75)
BWP17 + *Cip30*	4.14 (0.38), 7.63 (1.86)	7.83 (1.41), 9.79 (0.96)	14.4 (1.15), 13.5 (0.81)

Table 18: Impact of Rad53 or Hgc1 loss on hypha formation.
*C. albicans hgc1*Δ, *hgc1*Δ + *HGC1*, *rad53*Δ, *rad53*Δ + Rad53 and *BWP17* + *Cip30* cells were co-cultured with J774 macrophages. Live cell video microscopy was taken at 1 min per interval for 6 h. Extracellular/intracellular hyphal length was measured at 30, 60 and 90 minutes and the SD calculated.

Comparison of the hyphal length at 90 min using one way ANOVA showed that there were significant differences among the groups ($p = 0.045$). The post hoc analysis with Bonferroni revealed that there were significant differences between extracellular and intracellular hyphal length of *hgc1*Δ cells ($p = 0.00$) ($p = 0.00$) in comparison with *WT*. There were significant differences ($p = 0.04$) ($p = 0.002$) between the extracellular and intracellular hyphal length of *rad53*Δ when compared with *WT*. The results mean that Rad53 is important for formation of hyphae inside the macrophage, whereas *HGC1* is important for hypha formation both inside and outside the macrophage following phagocytosis, which is consistent with the known role of *HGC1* in yeast to hypha transition (Zheng *et al*., 2004). As *HGC1* is important for hypha formation, null *hgc1*Δ are devoid of hypha formation. The Rad53 kinase is needed for growth arrest in response to DNA damage. This indicates that the phagosome presents a DNA damaging environment to the *Candida* cell and that activation of Rad53 is necessary for the cells to stop proliferation

A

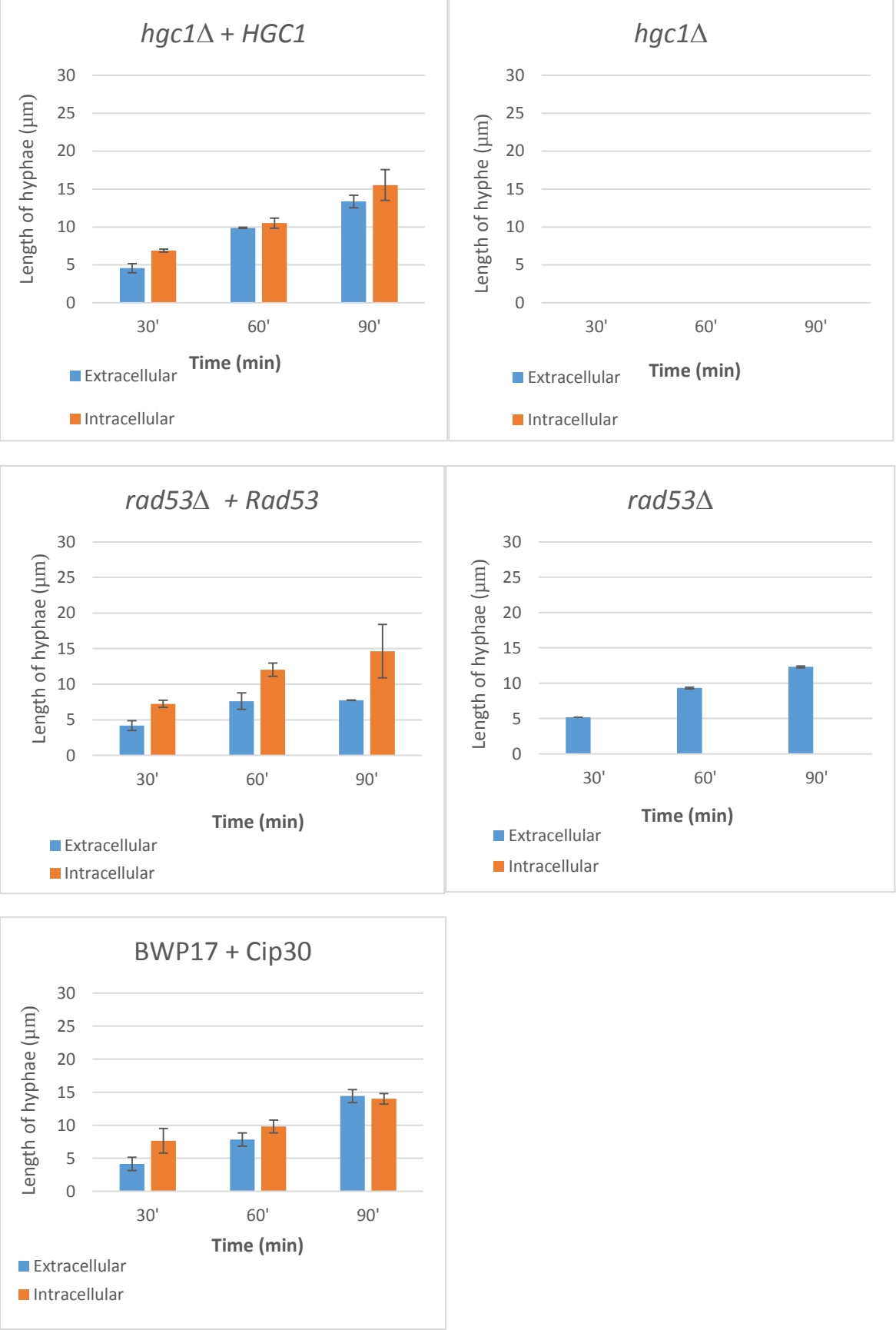
hgc1Δ + HGC1
Length of hyphae (µm)
30
25
20
15
10
5
0
30'
60'
90'
Time (min)
Extracellular
Intracellular
hgc1Δ
Length of hyphe (µm)
rad53Δ + Rad53
rad53Δ
BWP17 + Cip30

B

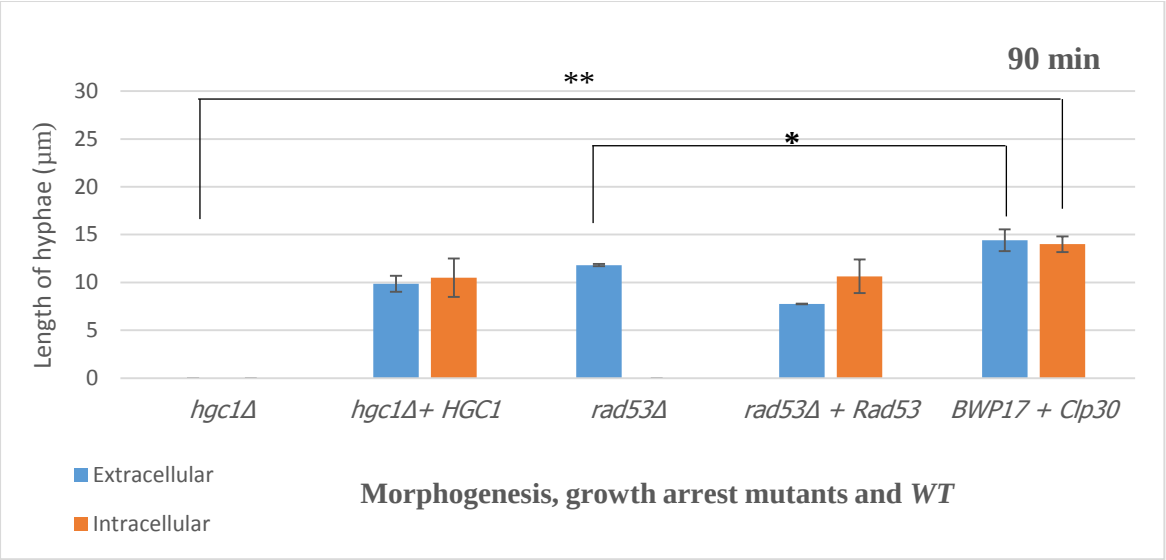

Figure 48: Impact of Rad53 or Hgc1 loss on hypha formation.
*C. albicans hgc1*Δ, *hgc1*Δ + *HGC1*, *rad53*Δ, *rad53*Δ + Rad53 and *BWP17 + Cip30* cells were co-cultured with J774 macrophages. Live cell video microscopy was taken at 1 min per interval for 6 h. Hyphal length was measured at 30, 60 and 90 minutes (**A**). Hyphal length were compared at 90 min (**B**). Each experiment was repeated three times and the error bars calculated from SD. One way ANOVA was used to calculate the statistical significance ($p = 0.045$) and post hoc analysis with Bonferroni for differences in extracellular, intracellular hyphal length compared with WT; * ($p = 0.04$), ($p = 0.002$), ** ($p = 0.00$), ($p = 0.00$).

5.3.9 Null *rad53*Δ showed impaired survival following phagocytosis but loss of Hgc1 did not affect the survival of *C. albicans* inside the macrophage.

As *rad53*Δ did not filament inside the macrophage, but formed hyphal cells in the extracellular environment, it was hypothesised that the cells inside the macrophage were dead because Rad53 kinase is essential for oxidative stress resistance and growth arrest (Da Silva *et al*., 2010). The survival of the morphogenesis and growth arrest mutants following phagocytosis using Lysotracker Red staining and the CFU assay as described previously, was determined.

Results of the Lysotracker Red screen showed that over 90 % of the *hgc1*Δ yeasts and hyphal cells of *hgc1*Δ+*HGC1*, *rad53*Δ + Rad53, and *BWP17+ Cip30* excluded the dye and were stained as red halos inside the macrophages. In contrast ~ 60% of *rad53*Δ cells were stained as red round/oval bodies inside the macrophage (Figure 48). The red oval bodies of *rad53*Δ cells signify that the cells had become permeable to Lysotracker Red stain because of the compromised cell wall following death.

Using the CFU assay, after 3 h of the phagocytosis assay, the *Candida* cells were plated. After 24 h, the CFUs were counted and survival expressed as percentage of the original number of cells. The results showed that the percentage survival of the cells were;

Table 19: Percentage survival CFUs.

Morphogenesis, growth arrest mutants and *WT* cells	**% survival CFUs**
*hgc1*Δ	148.9 (SD = 14.29)
*hgc1*Δ + *HGC1*	176.7 (SD = 22.94)
*rad53*Δ	56.7 (SD = 5.98)
*rad53*Δ + *RAD53*	100 (SD = 20.07)
BWP17 + Cip30	104.4 (SD = 18)

Table 19: Impact of Hgc1 or Rad53 loss on *C. albicans* viability following phagocytosis: *C. albicans hgc1*Δ*, hgc1*Δ *+ HGC1, rad53*Δ*, rad53*Δ *+ Rad53* and *BWP17 + Cip30* cells were co-cultured with J774 macrophages. Viability of the cells was determined using CFUs. Survival of the cells after 3 h was calculated as a percentage of the original 0 h number of cells for 3 h. Each experiment was repeated three times and the SD calculated.

Comparison of the cell survival using one way ANOVA showed that there were significant differences ($p = 0.03$) and Bonferroni test revealed that *hgc1*Δ ($p = 0.03$) and *hgc1*Δ+*HGC1* ($p= 0.028$) strains had increased survival while *rad53*Δ had the lowest survival following phagocytosis ($p = 0.026$) (Figure 49). The increased survival of *hgc1*Δ and *hgc1*Δ+*HGC1* cells is possibly related to their morphology during phagocytosis. Null *hgc1*Δ are yeast- locked while not all *hgc1*Δ+*HGC1* cells formed hyphae. The yeast cells are easy to recover from the tissue culture well for CFU assay as they do not adhere together compared to hyphal cells of *WT*. Together, the results of the Lysotracker Red stain and CFU assay show that *HGC1* is important for hypha formation but not survival of *C. albicans* while Rad53 is important for hypha formation and survival inside the macrophage following phagocytosis. The resistance of *hgc1*Δ to macrophage killing is not surprising because it has a functional Rad53 for growth arrest in the realm of the killing effects of the macrophage environment. Following, it is discernible that *rad53*Δ showed the least survival inside the macrophage which is likely related to its inability to initiate DNA damage induced cell cycle arrest necessary to initiate repair and survival (Da Silva *et al*., 2010).

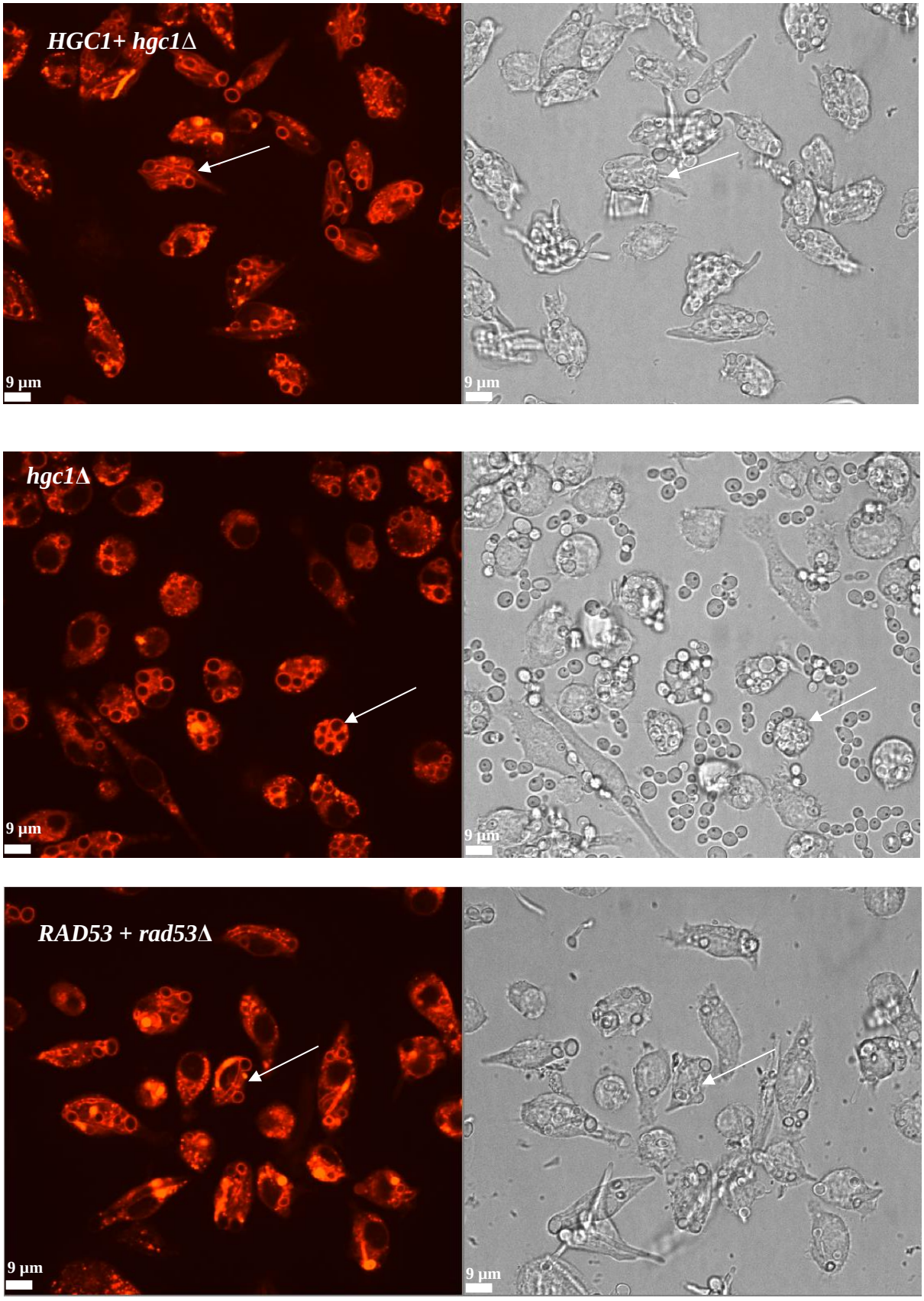
HGC1+ hgc1Δ
9 µm
9 µm
hgc1Δ
9 µm
9 µm
RAD53 + rad53Δ
9 µm
9 µm

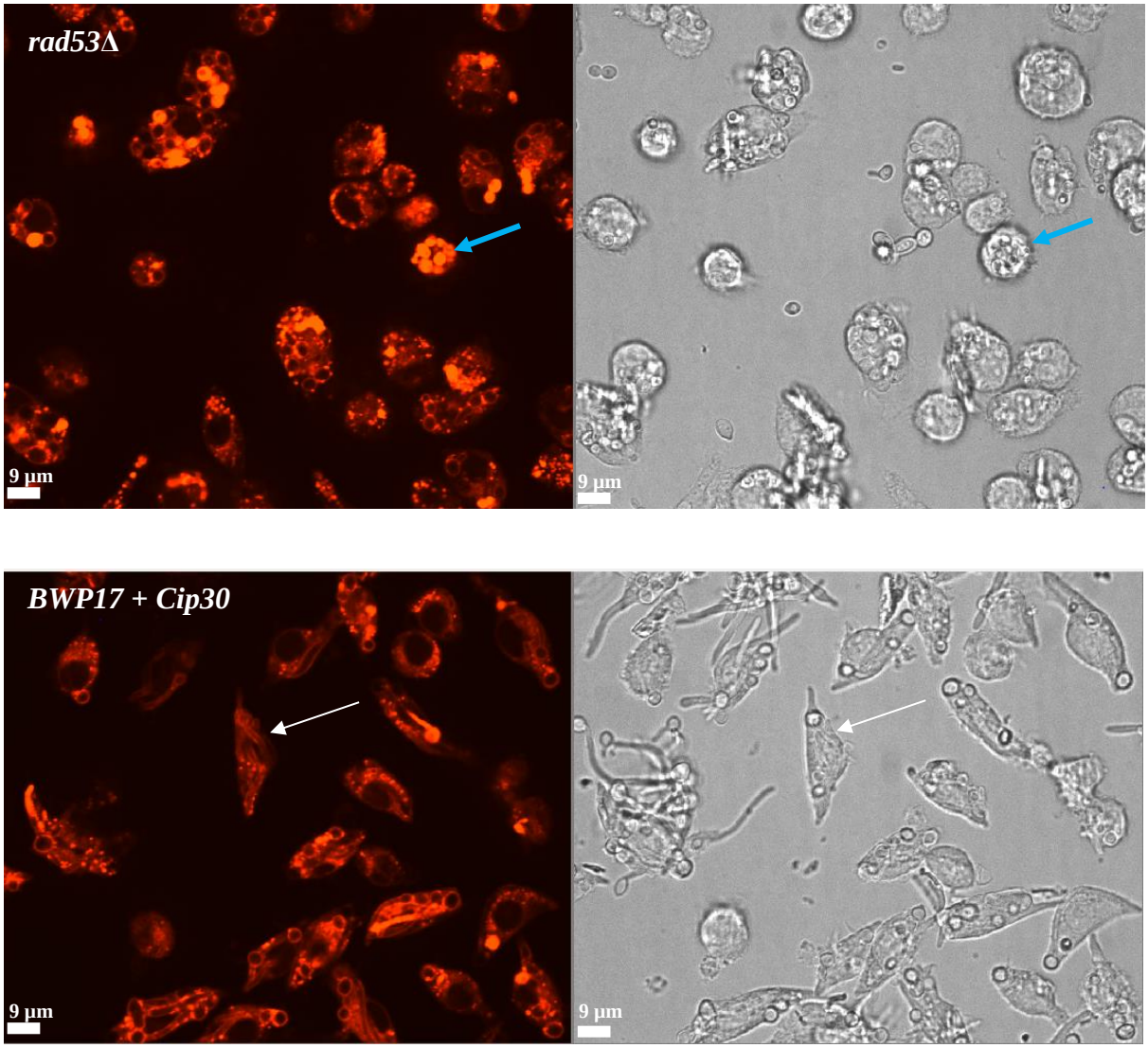

Figure 49: Impact of Hgc1 or Rad53 loss on *C. albicans* viability following phagocytosis.
*C. albicans hgc1*Δ, *hgc1*Δ + *HGC1*, *rad53*Δ, *rad53*Δ + *RAD53* and *BWP17* + *Cip30* were co-cultured with J774 macrophages. Viability of *Candida* after 3h was assessed by exclusion of, and formation of a red halo of the Lysotracker Red dye around the cell. Dead cells were seen as red, oval opaque bodies. The white, thin, long arrows are pointing to viable cells while the blue, thick and short arrows are pointing to dead cells. The images were captured to scale = 9.00 µm. Each experiment was repeated three times.

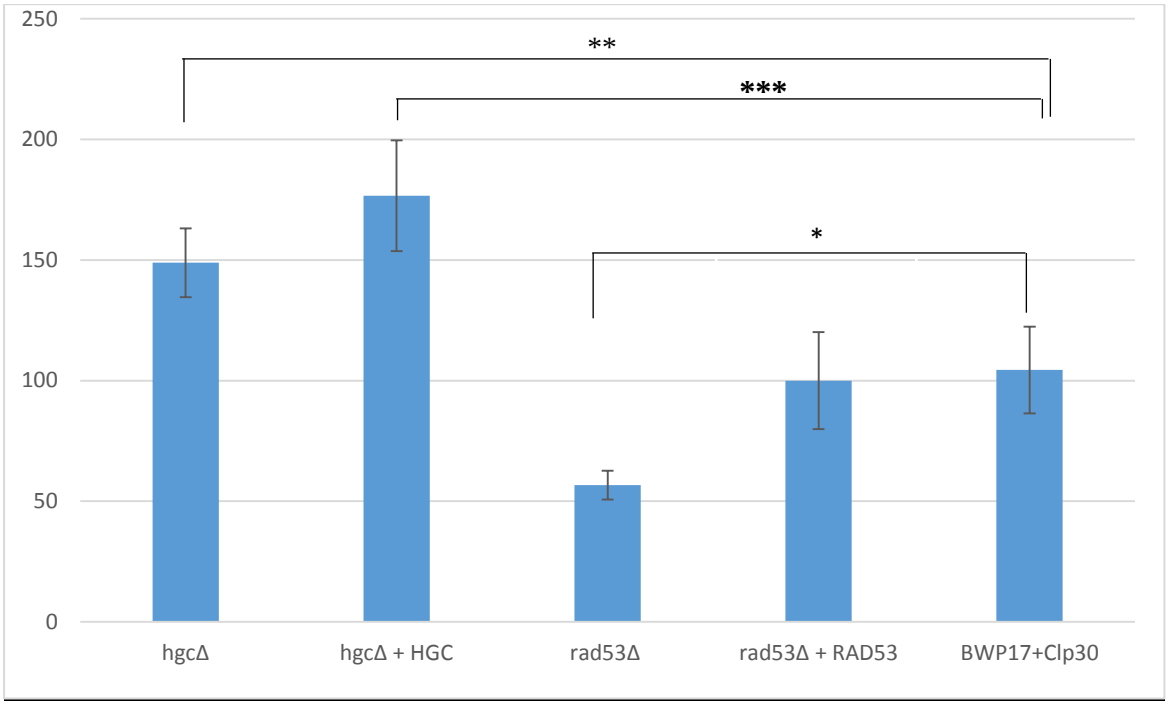

Figure 50*:* Impact of Hgc1 or Rad53 loss on *C. albicans* viability following phagocytosis: *C. albicans hgc1*Δ*, hgc1*Δ *+ HGC1, rad53*Δ*, rad53*Δ *+ Rad53* and *BWP17 + Cip30* cells were co-cultured with J774 macrophages. Viability of the cells was determined using CFUs. Survival of the cells after 3 h was calculated as a percentage of the original 0 h number of cells for 3 h. Each experiment was repeated three times and the error bars calculated from SD. One way ANOVA was used to calculate statistical significance; *p = 0.03* and post hoc test with Bonferroni; * *p = 0. 03*, ** *p = 0.028*, *** *p= 0.026*.

5.3.10 Yeast cells of *hgc1*Δ and *rad53*Δ were non-lethal while hyphal cells of *hgc1*Δ*+HGC1, rad53*Δ *+ Rad53* and *BWP17+ Cip30* killed macrophages.

There was high survival of macrophages co-cultured with cells that maintained yeast morphology following phagocytosis. However, there was decreased survival of macrophages co-cultured with *hgc1*Δ *+ HGC1*, *rad53*Δ + Rad53 and *BWP17+ Cip30* cells which formed hyphae inside the macrophages (Table 20).

Table 20: Macrophage percentage survival following co-culture with Hgc1 and Rad53 mutant strains.

Strains	1 h (%, SD)	2 h (%, SD)	3 h (%, SD)	4 h (%, SD)	5 h (%, SD)	6 h (%, SD)
*hgc1*Δ	104.02 (6.55)	106.32 (4.85)	(113.21 (2.21)	116.09 (10.34)	112.64 (6.06)	112.64 14.1
*rad53*Δ	105.79 (3.41)	105.79 (4.73)	101.45 (5.35)	100.72 (6.75)	90.57 (11.61)	84.78 (10.24)
*hgc1*Δ + *HGC1*	102.86 (9.27)	94.29 (11.49)	51.4 (11.74)	35.71 (12.17)	35.71 (12.17)	34.28 (12.94)
*rad53*Δ + *RAD53*	105 (4.99)	99.29 (4.42)	92.85 (5.74)	77.74 (6.21)	67.85 (6.6)	60.71 (9.21)
BWP17 + Cip30	95.83 (6.36)	79.17 (2.12)	54.16 (2.12)	23.61 (0.7)	4.17 (0.7)	2.78 (1.4)

Table 10: Impact of Hgc1 or Rad53 loss on *C. albicans*-mediated macrophage killing following phagocytosis.
Cells of *C. albicans hgc1*Δ*, hgc1*Δ + *HGC1, rad53*Δ*, rad53*Δ + *Rad53 and* BWP17 + Cip30 were co-cultured with J774 macrophages. Viability of the macrophages was determined by their ability to retain Lysotracker Red stain. Macrophages which were stained red were counted at hourly intervals to the end of the experiment. The hourly survival was calculated as a percentage of the original 0 h number of macrophages. Each experiment was repeated three times and the SD calculated.

Comparison of the results by one way ANOVA showed that there were significant differences ($p = 0.04$). Post hoc analysis by Bonferroni correction showed that cells which remained as yeasts inside the macrophages; *hgc1*Δ ($p = 0.001$) and *rad53*Δ ($p = 0.01$) showed the least killing effects compared to hypha forming *hgc1*Δ+*HGC1* (*0.027)*, *rad53*Δ + *Rad53* ($p = 0.03$) when compared to and *BWP17+ Cip30* cells (Figure 25) (Figure 50). Therefore, *HGC1* and Rad53 are important for *C. albicans*-mediated macrophage killing during phagocytosis, perhaps, due to their roles in hypha formation inside the macrophage (Figure 47). The intermediate survival of macrophages co-cultured with *hgc1*Δ+*HGC1* and *rad53*Δ + *RAD53* is possibly because the filamentous cells formed were not all true hyphae (Figure 47). Some of the filamentous forms looked like pseudohyphae. It is possible that not full rescue is being seen because the cells are heterozygous *hgc1*Δ+*HGC1* and *rad53*Δ + *RAD53* mutants. This is similar to the observation made previously with the transcription factor mutant *ndt80*Δ which did not form true hyphae and showed intermediate killing of macrophages (Figure 37). Therefore, *C. albicans* hypha formation is important for macrophage killing and the finding is consistent with previous reports (Wellington *et al*., 2014, Lewis *et al*., 2012, Uwamahoro *et al*., 2014).

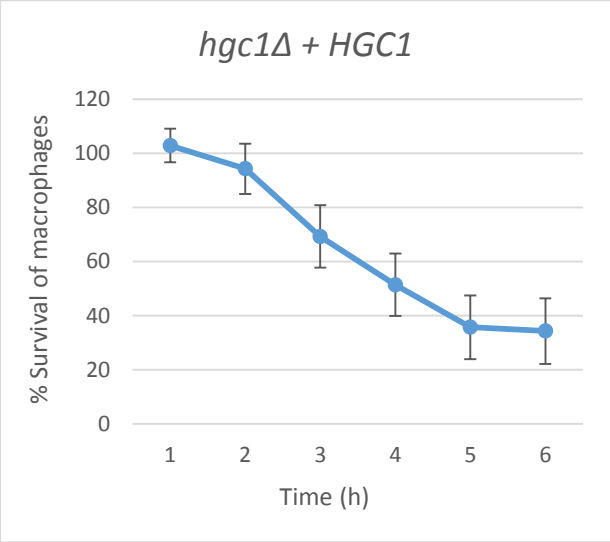
hgc1Δ + HGC1
% Survival of macrophages
120
100
80
60
40
20
0
1
2
3
4
5
6
Time (h)

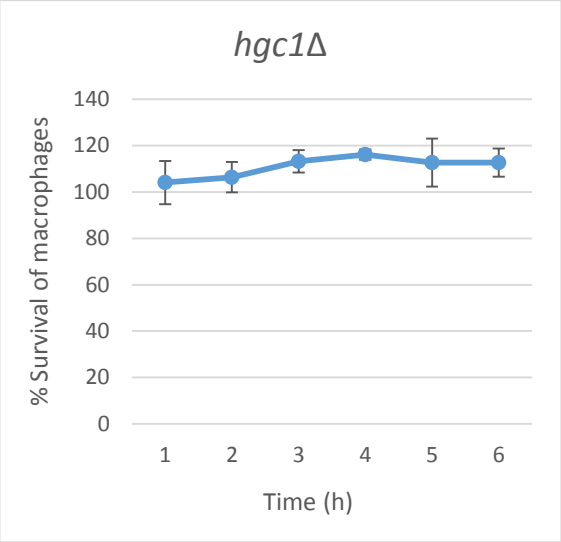
hgc1Δ
% Survival of macrophages
140
120
100
80
60
40
20
0
1
2
3
4
5
6
Time (h)

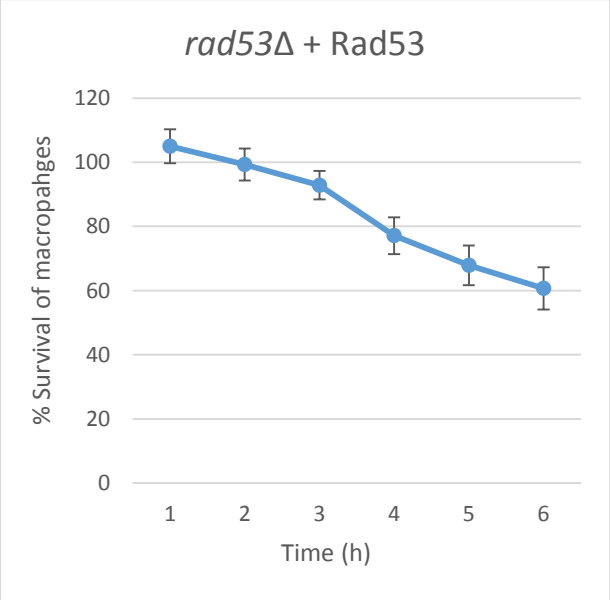
rad53Δ + Rad53
% Survival of macropahges
120
100
80
60
40
20
0
1
2
3
4
5
6
Time (h)

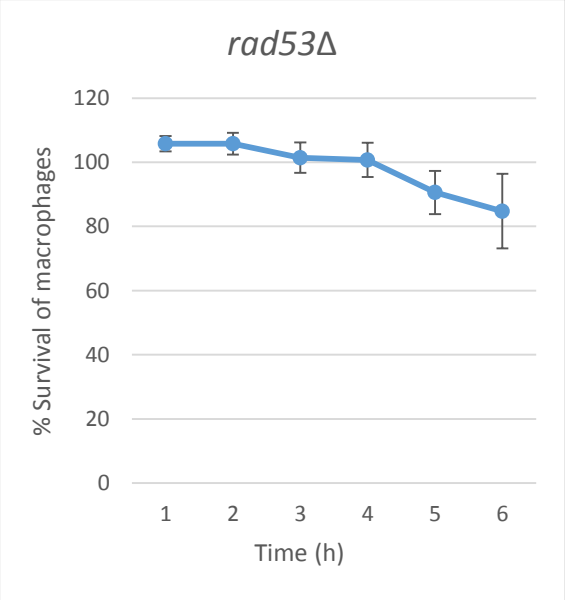
rad53Δ
% Survival of macrophages
120
100
80
60
40
20
0
1
2
3
4
5
6
Time (h)

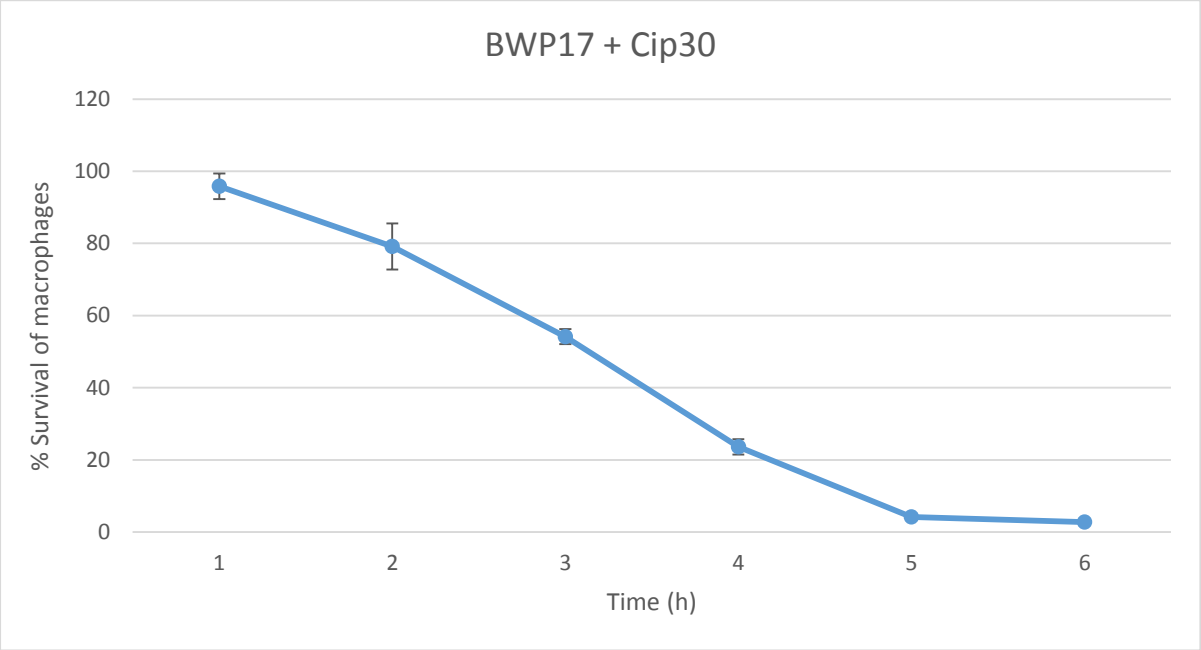

Figure 51: Impact of Hgc1 or Rad53 loss on *C. albicans*-mediated 6 h macrophage killing following phagocytosis.
Cells of *C. albicans hgc1*Δ, *hgc1*Δ + *HGC1*, *rad53*Δ, *rad53*Δ + *Rad53 and* BWP17 + Cip30 were co-cultured with J774 macrophages. Viability of the macrophages was determined by their ability to retain Lysotracker Red stain. Macrophages which were stained red were counted at hourly intervals to the end of the experiment. The hourly survival was calculated as a percentage of the original 0 h number of macrophages. Each experiment was repeated three times and the error bars calculated from SD.

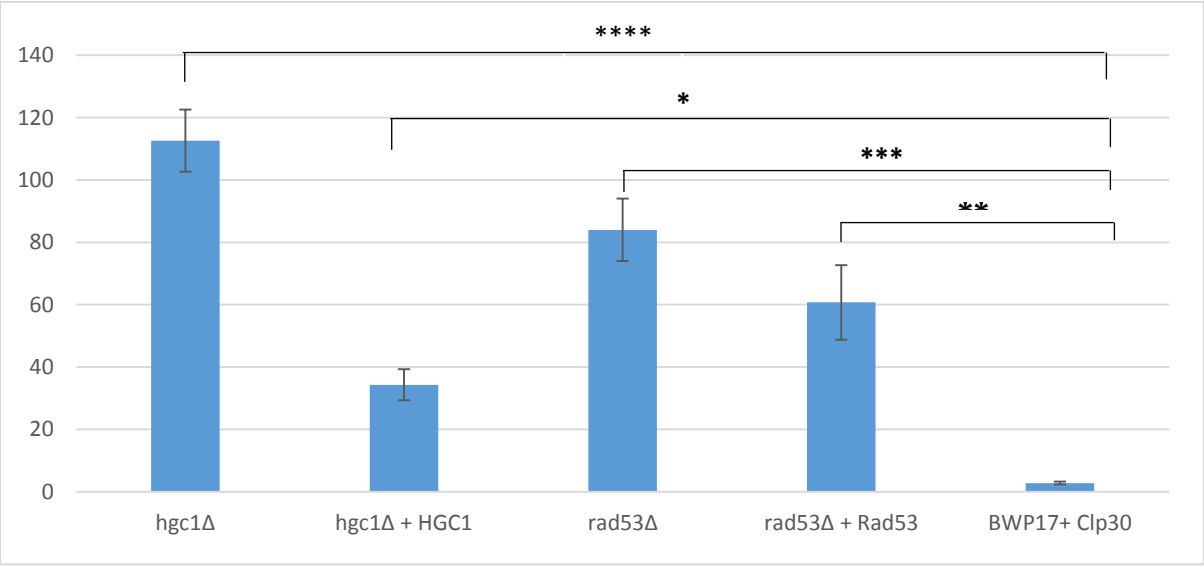

Figure 52: Impact of *C. albicans* phagocytosis on macrophage 6 h survival.
Null *hgc1*Δ, *hgc1*Δ+ *HGC1*, *rad53*Δ, *rad53*Δ + *Rad53* and *BWP17+ Cip30* cells were co-cultured with J774 macrophages. Viability of the macrophages was determined by counting of cells that retained the red colour of Lysotracker Red at 0 and 6 h. Survival of the macrophages after 6 h was calculated as a percentage of the original 0 h number of macrophages. Each experiment was repeated three times and the error bars calculated from SD. One way ANOVA was used to calculate statistical

significance; *p = 0.04*, and post hoc Bonferroni test; **** *p = 0.001*, *** *p = 0.01*, **p = 0.03*, * *p = 0.027*.

5.3.11. SUMMARY.

Table 21: The role of oxidative stress resistance on phagocytosis of *C. albicans*.

STRAINS	MQ Rate	MQ direction	Attachment	Engulfment	Engulfment	Uptake	*Candida*	Acidification	Hyphae***	*Candida* %survival	MQ %survival
Transcription factor mutants											
WT	0.002	0.11	18.4	20.9	1.75	↑	1	1.00	20.47	87	7.15
skn7 Δ	0.002	0.12	14.4	16.61	2.21	↑	1	1.64	18.57	95	26.9
ndt80 Δ	0.002	0.11	18.82	21.81	2.99	↑	1	1.06	16.52	130	40.4
gzf3 Δ	0.002	0.13	21.07	22.84	1.76	↑	1	1.27	20.22	83	18.9
cap1 Δ	0.002	0.12	15.42	19.08	3.66	↑	3	1.45	0.00	200	108.3
efg1 Δ	0.002	0.07	23.91	25.91	1.99	↓	1	1.54	0.00	190	103.9
ANOVA p - value	*0.085*	*0.04*	*0.048*	*0.047*	*0.04*	*0.05*	*0.03*	*0.08*	*0.04*	*0.039*	*0.05*
Figure	*Table 1*	*Table 1, Fig.1*	*Fig. 2*	*Fig.3*	*Fig. 4*	*Fig. 6*	*Fig. 5*	*Fig. 7*	*Figs. 8*	*Fig. 10*	*Fig. 12*
***CAT1* ectopic expression strains**											
WT + pACT1									23.06		
WT + pACT1 + CAT1									19.11		
cap1 Δ *+ pACT1*									18.15		
cap1 Δ *+ pACT1 + CAT1*									14.10		
ANOVA p - value									*N/A*		
Figure									*Fig. 13*		
CONTROLS											
hgc1 Δ	0.02	0.128	12.18	12.92	0.74	↑	1	1.17	0.00	148.9	112.6
hgc1 Δ + HGC1	0.016	0.116	19.22	20.61	1.39	↑	1	1.05	15.5	176.7	34.3
rad53 Δ	0.014	0.151	16.34	17.53	3.13	↑	2	0.96	0.00	56.70	84
rad53 Δ + Rad53	0.018	0.128	14.77	16.16	1.4	↑	1	0.9	14.64	100	60.71
BWP17 + Clp30	0.028	0.193	19.94	21.5	1.31	-	1	1.07	14	104.4	2.8
ANOVA p - value	*0.06*	*0.05*	*0.071*	*1*	*0.04*	*1*	0.03	*1*	*0.045*	*0.03*	*0.04*
Figure	*Table 2*	*Table 2, Fig. 14*	*Fig. 15*	*Fig. 16*	*Fig. 17*	*Fig. 20*	*Fig. 18*	*Fig. 19*	*Fig. 21*	*Fig. 23*	*Fig.25*
KEY											
* Time of engulfment											
** Time taken for engulfment											
***Hyphae @ 90 min											
Statistical difference											
No statisticial difference											
Parameter not assessed											

Table 22: Summary of results on the roles of oxidative stress resistance on phagocytosis.
The TF mutants, stains ectopically expressing catalase, Hgc1 and Rad53 mutants, and wild type cells were co-cultured with macrophages. Live cell video confocal microscopy was taken at 1 min per interval for 6 h. Parameters of phagocytosis were assessed. Each experiment was repeated three times. One way ANOVA +/- post hoc analysis using Bonferroni was used to determine statistical significance; p < /= 0.05.

5.4 Discussion.

Oxidative stress sensitive *cap1*Δ and its co-regulators failed to filament following phagocytosis. As *in vitro* tests had identified the five transcription factor mutants *skn7*Δ, *gzf3*Δ, *ndt80*Δ, *cap1*Δ and *efg1*Δ as ROS-sensitive (Chapter 4), it was hypothesised that they would show impaired hypha formation and survival inside the macrophage following phagocytosis.

The findings showed that there was discordance between *in vitro* ROS sensitivity and *ex vivo* filament formation and macrophage killing. The majority of the ROS sensitive transcription factor mutants were able to form hyphae and kill the macrophages.

Null *skn7*Δ, *ndt80*Δ and *gzf3*Δ cells were unimpaired in forming hyphae and killing the macrophages (Figures 34, 37 and 38). The difference in these observations could have arisen from differences in ROS concentrations *in vitro* and inside the macrophage. While the *in vitro* concentrations of laboratory chemicals used to generate ROS are easily determined, inside the macrophage, the concentration of ROS is not known. Therefore, it is possible that the ROS concentration inside the macrophage was too low to affect *skn7*Δ, *ndt80*Δ and *gzf3*Δ transcription factor mutants which formed hyphae inside the macrophages. Furthermore, some researchers have reported that primary and cell line macrophages showed different responses as infection models, possibly due to low production of ROS by J774 cells (Andreu *et al*., 2017). However, as the study which formed the background of this project utilised J774 cell line macrophages (Patterson *et al*., 2013) , it was appropriate to use similar J774 macrophages for comparison. The disparity in the in ROS sensitivity *in vitro* and *ex vivo* of the macrophage also means that *cap1*Δ and *efg1*Δ which showed impaired filament formation inside the macrophage have very low thresholds for oxidative stress sensitivity.

During *in vitro* testing of the transcription factor mutants, there were two groups of phenotypes. Null *skn7*Δ, *ndt80*Δ, *gzf3*Δ and *cap1*Δ were sensitive to H_2O_2, tBOOH, menadione and diamide while *efg1*Δ was sensitive to diamide only. Findings from the phagocytosis assay did not highlight importance of a particular resistance phenotype. This is perhaps, because the findings from the *in vitro* ROS condition did not directly correlate with the ROS-inducing environment of the macrophage.

The findings that the ROS-sensitive TF mutants including *skn7*Δ did not show impaired growth inside the macrophage is also inconsistent with the recent discovery that Skn7 is key to resistance of oxidative stress and morphogenesis in *C. albicans* (Basso *et al*., 2017). This is probably is due to type of macrophage model used as explained previously.

Further results of assessment of the parameters of phagocytosis showed that there was reduced directional macrophage migration, attachment and engulfment times of *efg1*Δ ($p = 0.04$) (Table 3, Figure 27). As macrophage migration, recognition and engulfment are factors associated with *C. albicans* PAMPs which are mostly cell wall associated, the findings mean that null *efg1*Δ may be defective in the cell wall structure, hence the poor recognition by macrophages. This postulation can be illustrated by the initially slow uptake rate of *efg1*Δ ($p = 0.05$) (Fig. 6). As the *efg1*Δ cells looked oblong to cylindrical in shape compared to the oval/round shape of the other mutants and *WT* cells, it can be expected that the decreased phagocytosis parameters are attributable to defects in the cell wall architecture of *efg1*Δ. These findings are consistent with the known roles of Efg1 in previous studies.

Efg1 is a major regulator of cell wall proteins (Sohn *et al*., 2003) which in turn play important roles in *C. albicans* immunogenicity as the cell wall PAMPs form the first point of contact with the immune cells. Following, cells which lacked Efg1 were defective in modulating the cell wall structure and immunogenicity of *C. albicans* (Zavrel *et al*., 2012).

Furthermore, there was no hypha formation by *efg1*Δ cells although pseudohyphal cells delayed to form inside the macrophage ($p = 0.01$) (Figure 34). Lack of hypha formation by *efg1*Δ was expected because Efg1 is the major transcription factor for formation of hyphae (Sudbery *et al*., 2011). Delayed pseudohyphal growth inside the macrophage is probably because of the oxidative stress sensitivity of *efg1*Δ. As imposed oxidative stress is always robust, pseudohypha formation inside the macrophage occurred in the later time points (Figure 34). Therefore, delayed filamentation of *efg1*Δ inside the macrophage was consistent with the oxidative stress sensitivity and the known role of Efg1 in hypha formation as null *efg1*Δ formed pseudohyphal cells outside the macrophage. As the *efg1*Δ yeast cell survival was 191 %, ($p = 0.035$) (Figures 37, 38) , it can be interpreted that oxidative stress inside the macrophage caused delayed formation of pseudohyphae due to prolonged growth arrest. It is worth mentioning that the CFU assay used for assessing survival of *C. albicans* was not accurate. Hyphal cells which were strongly adherent to each other were difficult to scrape from the bottom of the tissue culture well. Additionally, a hypha which represents more than one cell usually inaccurately grows as one CFU, hence, 'decreased' survival. In contrast, yeast cells showed 'increased' survival because the unicellular cells were easy to retrieve from the tissue culture plate and also grew as single CFUs which make them appear as increasing in number. Furthermore, *efg1*Δ was unable to kill macrophages to escape phagocytosis (Figure 38) which means it had attenuated virulence. This finding is consistent with a previous study which reported attenuation in the virulence of mutants lacking Efg1 (Lorenz *et al*., 2004, Lo *et al*., 1997).

The finding of delayed filamentation of *cap1*Δ *ex- vivo* the macrophage model (Figure 2) is consistent with the previous *in vitro* observations in which there was delayed hypha formation in oxidative stress sensitive mutants (Chapter 3). Comparing with the predominance of hyperpolarised buds in the oxidative stress sensitive mutants in the *in vitro* assay, the few *cap1*Δ hyphal cells in the macrophage model means that *cap1*Δ was in a more prolonged delay of filamentation than wild type. The findings from *Candida* survival assay which showed that the non-filamenting *cap1*Δ inside the macrophage were viable ($p = 0.029$) (Figure 8) was consistent with the findings from the *in vitro* assay. Together, these findings mean that the delay in filamentation in the macrophage was due to prolonged growth

arrest. Therefore, oxidative stress mutants did not fail but delayed to form filaments inside the macrophage following phagocytosis.

Because the findings from the oxidative stress sensitive transcription factor mutants showed that hyphal cells of *skn7*Δ, *ndt80*Δ, *gzf3*Δ and wild type killed macrophages while the yeast cells of *efg1*Δ and *cap1*Δ were avirulent, it means that yeast to hypha morphogenesis is important for macrophage killing following phagocytosis. It is noteworthy that formation of hyphae is more important than pseudohyphae in macrophage killing. Significantly, the findings also mean that *in vitro* oxidative stress resistance does not always translate to impaired growth following phagocytosis.

Catalase overexpression did not reverse the lack of filamentation and oxidative stress sensitivity in *cap1*Δ (Figure 39). Both *cap1*Δ + p*ACT1* and *cap1*Δ + p*ACT1-CAT1* formed hyphae inside the macrophage. As the original *cap1*Δ mutant does not filament inside the macrophage, it is unclear why filamentation was restored in *cap1*Δ + p*ACT1* cells. It is possible that secondary mutations were incorporated upon making this strain. The lack of impact of catalase overexpression suggests that other antioxidant enzymes may be important for reversing the sustained growth arrest in the oxidative stress mutants.

There is a slight difference between the previous (Patterson *et al*., 2013) and the current findings on the responses of *cap1*Δ during phagocytosis. The previous study reported lack of filamentation (Patterson *et al*., 2013) but filament formation inside the macrophage was delayed. The disparity in the findings could be because in the previous study, the duration of the experiment was 3 h, while in this study the phagocytosis assay was allowed up to 6 h which enabled observation of filament formation in the later time points. The study by Patterson *et al,* 2013 reported that *cap1*Δ cells were more sensitive to macrophage-mediated killing while I observed unimpaired survival following phagocytosis. This difference could have arisen from the different strains of *cap1*Δ used in the experiments. Delayed hypha formation in oxidative stress sensitive mutants following phagocytosis is consistent with what is known about the transcriptional programming of *C. albicans* in the phagolysosomal environment. When engulfed by a macrophage, *C. albicans* responds in two successive steps; an initial starvation mode during which it responds to oxidative stress and repairs biomolecules like DNA and, the later growth phase when arginine biosynthesis triggers auto hypha formation (Lorenz *et al*, 2004). As Cap1 is the main transcription factor for oxidative stress response, *cap1*Δ showed a compromised response in the macrophage environment as seen by delayed filamentation due to prolonged growth arrest in the step during which there would have been hyphal growth following phagocytosis. The other

oxidative stress sensitive s*kn7*Δ, *ndt80*Δ and *gzf3*Δ did not show delayed filamentation possibly because the macrophage environment did not affect their transcriptional programming as they may have a higher threshold for ROS. As Efg1 is the main transcription factor for hypha formation, the lack of macrophage killing is likely to be due to impaired hypha formation.

To discern the mechanisms of impaired filament formation and survival inside the macrophages, the effects of the loss of *HGC1* and *RAD53* which are essential genes for morphogenesis and growth arrest, respectively, were determined (in control experiments using the mutants). Broadly, the yeast-locked morphology of *hgc1*Δ inside the macrophage shows that impaired hypha formation in the absence of ROS sensitivity is sufficient to prevent filamentation and macrophage killing. Specifically, the lack of hypha formation by *hgc1*Δ showed that *cap1*Δ and *efg1*Δ did not form filament inside the macrophage because of ROS sensitivity and not defective hypha formation. *HGC1* regulates yeast to hypha morphogenesis (Zheng *et al*., 2004). The death of *rad53*Δ cells inside the macrophage further shows that non-filamentous *cap1*Δ and *efg1*Δ inside the macrophage are in growth arrest rather than death. Both *cap1*Δ and *efg1*Δ have active DNA checkpoint Rad53 kinase, possibly, for a longer time than for the control *WT* cells, hence the observed differences. *C. albicans* is able to withstand the toxic environment of the macrophage when it has an intact growth arrest inducing DNA checkpoint Rad53 kinase (Da Silva *et al*., 2010). Growth arrest enables the cell to undergo repair, for example, of DNA double strand breaks that would not be compatible with cell survival. Therefore, the lack of Rad53 kinase caused cell death which was observed as reduced survival of *rad53*Δ cells. Similar to impaired filamentous *cap1*Δ and *efg1*Δ, there was no macrophage killing by *hgc1*Δ and *rad53*Δ because of lack of hyphal growth and not ROS sensitivity. Therefore, the lack of macrophage killing by *cap1*Δ and *efg1*Δ is not only due to ROS sensitivity but impaired hypha formation. Hyphae have been reported to cause macrophage death through induction of pyroptosis and physical rupture (Wellington *et al*., 2014, Uwamahoro *et al*., 2014).

The findings that the loss of Rad53 did not affect the macrophage migration speed and directionality, times of attachment, engulfment and rates of *Candida* engulfment is suggestive that Rad53 kinase does not have biological functions related to the cell wall which contains a host of PAMPs for recognition by macrophages. Similar to *hgc1*Δ, *rad53*Δ showed less killing of macrophages than wild type cells due to impaired hypha formation inside the macrophages.

Collectively, the findings of the controls confirm that *cap1*Δ and *efg1*Δ did not filament inside the macrophages due to oxidative stress sensitivity which caused more sustained growth arrest compared to the *WT* cells. Therefore, prolonged ROS-induced growth arrest underscores the lack of filamentation of oxidative stress sensitive *C. albicans* inside the macrophages following phagocytosis.

CHAPTER SIX.

6 GENERAL DISCUSSION.

The morphological plasticity of *Candida albicans* is an important virulence attribute (Lo *et al*., 1997). Yeasts cells and hyphae also induce different cytokine responses Mukaremera *et al*., 2017) and only hyphae produce the cytolytic toxin candidalysin (Moyes *et al*., 2016). Yeasts engulfed by macrophages can transition to hyphal filaments, induce macrophage death and escape phagocytosis thereby evading reactive oxygen species ROS generated by the NADPH oxidase complex (Miramón *et al*., 2013, Uwamahoro *et al*., 2014). However, *C. albicans* cells lacking the Cap1 AP-1-like oxidative-stress responsive transcription factor or its co-regulators, Ybp1 and Gpx3, fail to filament inside the macrophage, despite being able to form hyphae when induced *in vitro* (Patterson *et al*., 2013). It has been reported that phagocytosis induces *C. albicans* to switch to a slow growth program while upregulating oxidative stress responses to enhance survival (Lorenz *et al*., 2004). In addition, a previous study showed that the ROS; H_2O_2 causes activation of the DNA checkpoint Rad53 kinase and growth arrest in *C. albicans* (Da Silva *et al*., 2010). Therefore, it was hypothesised that ROS could inhibit the yeast to hypha transition due to growth arrest, and that this would be more pronounced in ROS-sensitive mutants resulting in impaired filamentation, either *in vitro* or in the macrophage.

To test the hypotheses, the role of ROS on hyphae formation *in vitro* was initially investigated. The findings showed that ROS inhibit hypha formation. *In vitro*, treatment with H_2O_2 caused inhibition of serum-induced morphogenesis which was prolonged in cells lacking Cap1 and its co-regulators due to sustained growth arrest. A transcription factor deletion library screen revealed a number of mutants; *skn7*Δ, *cap1*Δ, *efg1*Δ, *ndt80*Δ, *gzf3*Δ, *cup9*Δ, *fcr1* Δ, *cph2*Δ, *rob1*Δ, *dpb4*Δ, *ash1*Δ that were more sensitive to H_2O_2 than wild-type cells. To explore whether impaired ROS resistance *in vitro* correlated with impaired filamentation following phagocytosis, the five most oxidative-stress sensitive mutants; *cap1*Δ, *efg1*Δ, *skn7*Δ, *ndt80*Δ, and *gzf3*Δ were examined. *Ex vivo* in the macrophage host, *cap1*Δ and *efg1*Δ cells failed to filament following phagocytosis. However, the other tested ROS-sensitive mutants, *skn7*Δ, *ndt80*Δ, *gzf3*Δ, formed filaments inside the macrophage which were comparable to wild type cells.

The mechanism that underlies impaired filamentation in *cap1*Δ cells following H_2O_2 exposure *in vitro* and *ex vivo* is perhaps sustained DNA damage checkpoint activation. The presence of DNA damage stimulates phosphorylation of Rad53 protein which

leads to activation of the protein kinase (Shi *et al*., 2007). Normally, in the model yeast *S. cerevisiae*, the phosphorylation and kinase activity of Rad53 disappear at the time the cells resume progression in the cell cycle. However, in mutants which lack the Cap1 transcription factor for oxidative stress resistance, there may be extensive DNA damage that cause the growth arrest to be prolonged to allow for repair (Guillemain *et al*., 2007). Oxidative stress dependent expression of key antioxidant enzymes such as catalase is dependent on Cap1 (Alarco *et al*., 1999). Therefore, it is reasonable to assume that DNA-damaging ROS will not be efficiently removed in cells lacking Cap1. During the period of prolonged growth arrest, Rad53 kinase activity would be predicted to remain elevated. In the future, activation of Rad53 could be examined by Western blotting as the active phosphorylated state has a slower mobility (Da Silva *et al*, 2010). It is predicted that the Rad53 kinase would remain phosphorylated for a longer time in *cap1*Δ cells than in wild type cells.

In addition to looking at Rad53 phosphorylation, further studies to determine Rad53 kinase inactivation following H_2O_2 induced growth arrest would be interesting. A previous study on methylmethanesulfonate (MMS) which imposes genotoxic stress showed that dephosphorylation of Rad53 kinase was an essential perquisite for cell recovery following MMS-induced DNA damage (Wang *et al*., 2012). The decrease in the phosphorylated forms of Rad53 kinase due to decrease in kinase activity and/or increase in phosphatase activity allows for cells to resume growth.

However, the downstream regulators of Rad53 kinase remain elusive. A screen of a *C. albicans* deletion library of transcription factor mutants, to identify downstream regulators of Rad53 kinase did not identify any mutants that were defective in the formation of hyperpolarised buds. The library of transcription factor mutants which also included homologues of mutants regulated by Rad53 in the model yeast *S. cerevisiae* remained competent to undergo H_2O_2-mediated hyperpolarized bud formation. This implies that there may be divergence of regulators downstream of the Rad53 kinase in *C. albicans*. Further experiments to determine the downstream regulators of Rad53 kinase may reveal roles in the induction of hyperpolarised bud formation following oxidative stress.

Whilst *cap1*Δ and *efg1*Δ cells displayed impaired filamentation following phagocytosis, other ROS-sensitive mutants did not. The oxidative stress sensitive transcription factor mutants *skn7*Δ, *ndt80*Δ and *gzf3*Δ, effectively formed filaments inside the phagosomal environment, perhaps because they are less sensitive to ROS and thus, overcome ROS produced in the macrophage. In the *in vitro* spot test used to identify the mutants, the read out for ROS sensitivity was qualitative - growth or no growth in the presence of the

stress agent. Because this assay does not scrutinise differences in the quantity of growth, it is possible that the differences in levels of sensitivity of the different strains was missed in the spot test but were revealed in the phagocytosis assay. Also, the difference between the *in vitro* oxidative stress sensitivity and filamentation of the mutants inside the macrophage could be due to a requirement for specific transcription factors that depend on the type of ROS to which the cells are exposed. The *in vitro* test for oxidative stress sensitivity used various sources of ROS (tBOOH, H_2O_2, menadione and diamide) which differed in chemical properties of stability, reactivity and mechanisms of action. Furthermore, the mutant cells were exposed to a single source of ROS in the *in vitro* assay. In contrast, inside the macrophages, the mutant cells were exposed simultaneously to a range of ROS agents. The contrast between the *in vitro* single sources of ROS compared to combined sources of ROS within the macrophage environment could have also led to differences in the levels of ROS. While the concentrations of ROS imposed *in vitro* were known, the levels generated *ex vivo* is not known. Therefore, such differences could point to variation between the *in vitro* and *ex vivo* macrophage morphogenesis inducing milieu.

Specifically, the ROS-rich environment of the macrophage upregulates arginine biosynthesis from which breakdown products lead to alkalisation of the pH of the medium (Lorenz *et al*., 2004). In the initial starvation phase within the phagosome, *C. albicans* induces arginine biosynthesis. Following the induction of arginase, one of the breakdown products of arginine utilisation is ammonia which raises the pH of the phagosome. Urea is in turn, degraded by amidolyase to produce CO_2 which can acts as a trigger for hypha formation. In the second glycolytic phase, the raised pH and CO_2 sustain hyphal growth (which is also termed auto induction of hypha formation inside the macrophage). The high pH offers a protective mechanism of buffering the acidic milieu of ROS hence faster hyphal growth inside the macrophage compared to the extracellular medium. Moreover, *Candida* cells, and chitin are known to induce macrophage arginase leading to the diversion of arginine away from the iNOS system which is required for a respiratory burst (Wagener *et al*., 2017). Therefore, although serum was also discerned to offer ROS buffering effect H_2O_2 *in vitro* in Chapter 3, it is possible that serum's buffer property would be less than the protective effect of *C. albicans* modulation of arginine metabolism following exposure to various sources of ROS in the continuous culture of the macrophage.

The findings from the *in vitro* and *ex vivo* the macrophage host showed that null mutants of *efg1*Δ cells delayed to form pseudohyphae inside the macrophage compared

to uninhibited pseudohyphal growth outside the macrophage. These suggest that in addition to the oxidative stress signaling AP-1 Cap1 and DNA checkpoint Rad53 kinase pathways, ROS inhibits pseudohyphal growth by a pathway which remains to be investigated.

Therefore, the *in vitro* oxidative stress sensitivity did not translate to impaired filamentation inside the macrophage perhaps because the oxidative stress genes expressed *in vitro* differ from inside the macrophage following phagocytosis.

Collectively, the data show that whilst Cap1 is essential for filament formation inside the macrophage, wild-type levels of oxidative stress resistance are not a necessary pre-requisite for this morphological switch following phagocytosis. This may be related to the fact that *C. albicans* produces ROS at hyphal tips which directs polarised growth (Rossi *et al*., 2017), as previously documented in other filamentous fungi (Ballou *et al*., 2013, Chi *et al*., 2016). This means that ROS may impact both positively and negatively on morphogenesis. Such positive and negative roles of ROS are consistent with many previous studies which showed that at low concentrations, ROS have signaling roles while at high levels they cause cellular damage and growth arrest (Martindale *et al*., 2002, Pizzimenti *et al*., 2010).

An implication of the findings from this research is that drugs which target the oxidative stress responsive and the hypha-inducing Efg1transcription factor might have utility for the treatment of *C. albicans*. As Efg1 is important for oxidative stress resistance and hyphae formation and, yeast to hypha dimorphism is considered to be a *C. albicans* virulence attribute, its inhibition may significantly decrease or ameliorate its pathogenicity. This suggestion is supported by previous studies which showed that non-filamentous strains of *C. albicans* were avirulent (Lo *et al*., 1997). And, because antifungal treatment is unable to sufficiently eliminate fungal diseases in the immunocompromised hosts, such drugs could be designed as adjunctive immune therapies (Casadevall *et al*., 2001). Furthermore, targeting the DNA damage response Rad53 kinase for antifungal development seems feasible. Data from this study showed that that the survival of *rad53*Δ cells was impaired in the macrophage model of infection. The data on impaired survival of *rad53*Δ cells point to the importance of Rad53 kinase in cell survival. Exposure to ROS causes DNA damage which leads to activation of Rad53 kinase to initiate the repair mechanisms and enhance survival of *C. albicans* (Da Silva *et al*., 2010). Conversely, targeting Rad53 kinase will cause its inactivation which means that unrepaired DNA damage caused by ROS could lead to cell death of *C. albicans*.

It is recommended that further studies on this project include comparative determination of transcript profiling data on the effect of ROS on hyphae formation *in vitro* and *ex vivo* the macrophage host. The findings on gene expression profiles would help to

discern which pathway of yeast to hyphae morphogenesis is inhibited by ROS and the genes induced under *in vitro* conditions and inside the macrophage following phagocytosis.

The comparison of results from the *ex vivo* macrophage host and *in vitro* assays also highlighted the advantage of using spinning disc confocal live cell microscopy (SDCM) versus fixed cell imaging. The SDCM has a pair of discs, a scanner fitted to the second disc and, both discs with thousands of pinholes rotate in a spiral fashion. As other types of confocal microscopy, the application of SDCM is based on the principle of elimination of out of focus light to generate wide-field clear images (Gräf *et al*., 2005). The SDCM images are collected in parallel which, together with the high scan speed of up to 360 frames per second, significantly decrease photobleaching and phototoxicity which are major limitations of fixed cell imaging (Wang *et al*., 2005, Cole, 2011). The SDCM live cell imaging allowed for visualisation of the phagocytosis processes in real time which were instrumental in understanding the role of ROS resistance in the survival and filamentation of *C. albicans* following phagocytosis.

Using the SDCM live cell imaging, the phagocytosis process was studied within the different stages i) Migration of the phagocytes, ii) Recognition of *C. albicans* PAMPs by the host PRRs, iii) Engulfment of *C. albicans* by the macrophages and iv) Processing of the engulfed *C. albicans* (Lewis *et al*., 2013). By being able to describe the phagocytic processes into distinct stages, it was possible to observe the delayed attachment of the *efg1*Δ cells. Without live cell imaging, the phagocytosis process would have had to be studied in entirety and there would only be end point findings. Although end point findings are informative, they are lacking in information that at the different stages of phagocytosis. Furthermore, there was high throughput data collection using the SDCM live cell imaging. Eight samples could be processed in a single experiment using the 8-well slide of the SDCM live cell imaging for up to ten parameters of data per sample, compared to one sample per slide for one datum using fixed cell imaging. The advantages described show how live cell imaging has upgraded the study of cells from fixed cell imaging (Bain *et al*., 2015).

A schematic diagram of the key findings.

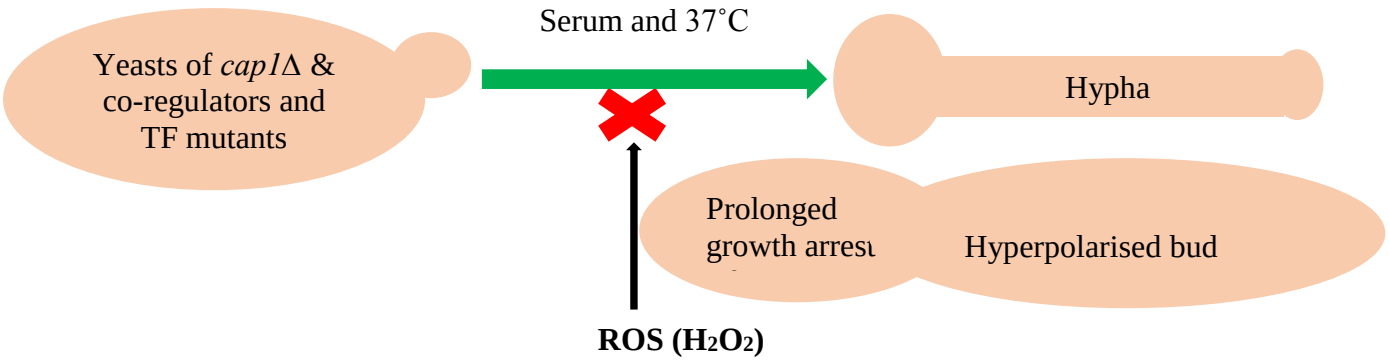

Figure 53: The role of oxidative stress on the filamentation of *C. albicans* following phagocytosis. *C. albicans* oxidative stress sensitive strains were tested for ability to survive and form hyphae in the presence of ROS. *In vitro*, *WT* and oxidative stress sensitive cells of *cap1*Δ & its co-regulators; *gpx3*Δ and *ybp1*Δ were treated with serum at 37˚C in the presence of H_2O_2 to determine the effect of ROS on hyphae formation and survival. The findings showed that ROS inhibit formation of hyphae through growth arrest which is more prolonged in the oxidative stress sensitive mutants. Upon resumption of filamentation, there was predominance of hyperpolarized buds in the oxidative stress sensitive mutants, further demonstrating prolonged growth arrest. To determine if ROS-resistance is global requirement for hyphae formation following phagocytosis, *C. albicans* transcription factory library was tested for sensitivity to ROS. *Ex vivo*, the most ROS sensitive transcription factor mutants *skn7*Δ, *ndt80*Δ, *gzf3*Δ, *cap1*Δ, *efg1*Δ and *WT* cells were co-cultured with macrophages. The cells of *cap1*Δ and *efg1*Δ cells did not form hyphae inside the macrophages due to prolonged growth arrest. However, *skn7*Δ, *ndt80*Δ and *gzf3*Δ cells formed hyphae following phagocytosis. Therefore, although Cap1 is essential for filament formation inside the macrophage, wild type levels of oxidative stress resistance are not a necessary pre-requisite for morphological switch following phagocytosis.

7 BIBLIOGRAPHY.

Yeasts: Characteristics and Identification, 3rd Edition. (2001). *Pediatric dermatology*, **18**, 547-547.

Alarco, A., and Raymond, M. (1999). The bZip transcription factor Cap1p is involved in multidrug resistance and oxidative stress response in Candida albicans. *Journal of Bacteriology*, **181**,700-708.

Alcock, L.J., Perkins, M.V. and Chalker, J.M. (2018). Chemical methods for mapping cysteine oxidation. *Chemical Society Reviews*, **47**, 231-268.

Alonso Monge, R., Román, E., Nombela, C. and PLA, J. (2006). The MAP kinase signal transduction network in *Candida albicans*. *Microbiology*, **152**, 905-912.

Alonso-Monge, R., Navarro-García, F., Molero, G., Diez-Orejas, R., Gustin, M., Pla, J., Sánchez, M. and NOMBELA, C. (1999). Role of the Mitogen-Activated Protein Kinase Hog1p in Morphogenesis and Virulence of *Candida albicans*. *Journal of Bacteriology*, **181**, 3058-3068.

Amulic, B., Cazalet, C., Hayes, G.L., Metzler, K.D. and Zychlinsky, A. (2012). Neutrophil Function: From Mechanisms to Disease. *Annual Review of Immunology*, **30**, 459-489.

Andreu, N., Phelan, J., De Sessions, P.F., Cliff, J.M., Clark, T.G. and Hibberd, M.L. (2017). Primary macrophages and J774 cells respond differently to infection with *Mycobacterium tuberculosis*. *Scientific Reports*, **7**, 42225

Aratani, Y., Koyama, H., Nyui, S., Suzuki, K., Kura, F. and Maeda, N. (1999). Severe Impairment in Early Host Defense against *Candida albicans* in mice deficient in myeloperoxidase. *Infection and immunity*, **67**, 1828-1836.

Bachewich, C. and Whiteway, M. (2005). Cyclin Cln3p links G1 progression to hyphal and pseudohyphal development in *Candida albicans*. *Eukaryotic Cell*, **4**, 95-102.

Bain, J., Gow, N.A.R. and Erwig, L. (2015). Novel insights into host-fungal pathogen interactions derived from live-cell imaging. *Seminars in Immunopathology*, **37**, 131-139.

Bain, J.M., Louw, J., Lewis, L.E., Okai, B., Walls, C.A., Ballou, E.R., Walker, L.A., Reid, D., Munro, C.A., Brown, A.J.P., Brown, G.D., Gow, N.A.R. and Erwig, L.P. (2014). *Candida albicans* hypha formation and mannan masking of ß-Glucan inhibit macrophage phagosome maturation. *mBio*, **5**, 6.

Bain, J.M., Lewis, L.E., Okai, B., Quinn, J., Gow, N.A.R. and Erwig, L. (2012). Non-lytic expulsion/exocytosis of *Candida albicans* from macrophages. *Fungal Genetics and Biology*, **49**, 677-678.

Ballou, E.R., Selvig, K., Narloch, J.L., Nichols, C.B. and Alspaugh, J.A., 2013. Two Rac paralogs regulate polarized growth in the human fungal pathogen *Cryptococcus neoformans*. *Fungal Genetics and Biology*, **57**, 58-75.

Basso, V., Znaidi, S., Lagage, V., Cabral, V., Schoenherr, F., Leibundgut-Landmann, S., d'Enfert, C. and Bachellier-Bassi, S. (2017). The two-component response regulator Skn7 belongs to a network of transcription factors regulating morphogenesis in *Candida albicans* and independently limits morphogenesis-induced ROS accumulation. *Molecular microbiology*, **106**, 157-182.

Becker, K.L., Ifrim, D.C., Quintin, J., Netea, M.G. and Van De Veerdonk, F.L. (2015). Antifungal innate immunity: recognition and inflammatory networks. *Seminars in Immunopathology*, **37**, 107-116.

Bensen, E.S., Filler, S.G. and Berman, J. (2002). A forkhead transcription Factor is important for true hyphal as well as yeast Morphogenesis in *Candida albicans*. *Eukaryotic Cell*, **1**, 787-798.

Berlett, B.S. and Stadtman, E.R. (1997). Protein oxidation in aging, disease, and oxidative stress. *Journal of Biological Chemistry*, **272,** 20313-20316.

Biondo, C., Malara, A., Costa, A., Signorino, G., Cardile, F., Midiri, A., Galbo, R., Papasergi, S., Domina, M., Pugliese, M., Teti, G., Mancuso, G. and Beninati, C. (2012). Recognition of fungal RNA by TLR7 has a nonredundant role in host defense against experimental candidiasis. *European journal of immunology*, **42**, 2632-2643.

Bondaryk, M., Kurza¸Tkowski, W. and Staniszewska, M. (2013). Antifungal agents commonly used in the superficial and mucosal candidiasis treatment: Mode of action and resistance development. *Postepy Dermatologii i Alergologii*, **30**, 293-301.

Brand, A. and Gow, N.A.R. (2009). Mechanisms of hypha orientation of fungi. *Current opinion in microbiology*, **12**, 350-357.

Braun, B.R., Kadosh, D. and Johnson, A.D. (2001). NRG1, a repressor of filamentous growth in *C.albicans*, is down-regulated during filament induction. *EMBO Journal*, **20**, 4753-4761.

Braun, B.R. and Johnson, A.D. (1997). Control of Filament Formation in *Candida albicans* by the transcriptional repressor TUP1. *Science*, **277**, 105-109.

Brinkmann, V., Reichard, U., Goosmann, C., Fauler, B., Uhlemann, Y., Weiss, D.S., Weinrauch, Y. and Zychlinsky, A. (2004). Neutrophil extracellular traps kill bacteria. *Science*, **303**, 1532-1535.

Brown, A.J.P., Budge, S., Kaloriti, D., Tillmann, A., Jacobsen, M.D., Yin, Z., Ene, I.V., Bohovych, I., Sandai, D., Kastora, S., Potrykus, J., Ballou, E.R., Childers, D.S., Shahana, S. and L.M.D. (2014). Stress adaptation in a pathogenic fungus. *Journal of Experimental Biology*, **217**, 144-155.

Brown, A.J., Haynes, K. and Quinn, J. (2009). Nitrosative and oxidative stress responses in fungal pathogenicity. *Current opinion in microbiology*, **12**, 384-391.

Brown, G.D. (2011). Innate antifungal immunity: The key role of phagocytes. *Annual Review of Immunology*, **29**, 1.

Brown, G.D., Denning, D.W., Gow, N.A.R., Levitz, S.M., Netea, M.G. and White, T.C. (2012). Hidden killers: human fungal infections. *Science translational Medicine*, **4**, 165.

Calderon, J., Zavrel, M., Ragni, E., Fonzi, W.A., Rupp, S. and Popolo, L. (2010). PHR1, a pH-regulated gene of *Candida albicans* encoding a glucan-remodelling enzyme, is required for adhesion and invasion. *Microbiology*, **156**, 2484-2494.

Calderone, R.A. and Fonzi, W.A. (2001). Virulence factors of *Candida albicans*. *Trends in microbiology*, **9**, 327-335.

Casadevall, A. and Pirofski, L.A. (2014). Ditch the term pathogen. *Nature*, **516**, 165-166.

Casadevall, A. and Pirofski, L. (2001). Adjunctive immune therapy for fungal infections. *Clinical Infectious Diseases*, **33**, 1048-1056.

Chaves, G.M., Bates, S., Maccallum, D.M. and Odds, F.C. (2007). *Candida albicans GRX2*, encoding a putative glutaredoxin, is required for virulence in a murine model. *Genetics and Molecular Research*, **6**, 1051-1063.

Cheetham, J., Smith, D.A., Dantas, A.D.S., Doris, K.S., Patterson, M.J., Bruce, C.R. and Quinn, J. (2007). A single MAPKKK regulates the Hog1 MAPK pathway in the pathogenic fungus *Candida albicans*. *Molecular biology of the cell*, **18**, 4603-4614.

Cheetham, J., Maccallum, D.M., Doris, K.S., Da Silva Dantas, A., Scorfield, S., Odds, F., Smith, D.A. and Quinn, J. (2011). MAPKKK-independent regulation of the Hog1 stress-activated protein kinase in *Candida albicans*. *Journal of Biological Chemistry*, **286**, 42002-42016.

Cheng, S., Joosten, L.A.B., Kullberg, B. and Netea, M.G. (2012). Interplay between *Candida albicans* and the mammalian innate host defense. *Infection and immunity*, **80**, 1304-1313.

Chi, M. and Craven, K.D. (2016). RacA-mediated ROS signaling is required for polarized cell differentiation in conidiogenesis of Aspergillus fumigatus. *PLoS ONE*, **11**.

Chowdhary, A., Sharma, C. and Meis, J.F. (2017). *Candida auris*: A rapidly emerging cause of hospital-acquired multidrug-resistant fungal infections globally. *PLoS Pathogens*, **13.**

Côte, P., Hogues, H. and Whiteway, M. (2009). Transcriptional analysis of the *Candida albicans* cell cycle. *Molecular biology of the cell*, **20**, 3363-3373.

Da Silva Dantas, A., Patterson, M.J., Smith, D.A., Maccallum, D.M., Erwig, L.P., Morgan, B.A. and Quinn, J. (2010). Thioredoxin regulates multiple hydrogen peroxide-induced signaling pathways in *Candida albicans*. *Molecular and cellular biology*, **30**, 4550-4563.

Dalle, F., Wächtler, B., L'ollivier, C., Holland, G., Bannert, N., Wilson, D., Labruère, C., Bonnin, A. and Hube, B. (2010). Cellular interactions of *Candida albicans* with human oral epithelial cells and enterocytes. *Cellular microbiology,* **12**, 248-271.

Dambuza, I.M. and Brown, G.D. (2015). C-type lectins in immunity: Recent developments. *Current opinion in immunology,* **32**, 21-27.

Danhof, H.A. and Lorenz, M.C. (2015). The *Candida albicans* ATO gene family promotes neutralization of the macrophage phagolysosome. *Infection and immunity,* **83**, 4416-4426.

Dantas, A.S., Day, A., Ikeh, M., Kos, I., Achan, B. and Quinn, J. (2015). Oxidative stress responses in the human fungal pathogen, *Candida albicans*. *Biomolecules,* **5**, 142-165.

Davies, M.J. (2005). The oxidative environment and protein damage. *Biochimica et Biophysica Acta (BBA) - Proteins and Proteomics,* **1703**, 93-109.

De Bernardis, F., Mühlschlegel, F.A., Cassone, A. and Fonzi, W.A. (1998). The pH of the host niche controls gene expression in and virulence of *Candida albicans*. *Infection and immunity,* **66**, 3317-3325.

Duch, A., De Nadal, E. and Posas, F. (2012). The p38 and Hog1 SAPKs control cell cycle progression in response to environmental stresses. *FEBS letters,* **586**, 2925-2931.

Enjalbert, B., Smith, D.A., Cornell, M.J., Alam, I., Nicholls, S., Brown, A.J.P. and Quinn, J. (2006). Role of the Hog1 stress-activated protein kinase in the global transcriptional response to stress in the fungal pathogen *Candida albicans*. *Molecular biology of the cell,* **17**, 1018-1032.

El-Benna, J., Dang, P.M., Gougerot-Pocidalo, M., and Elbim, C. (2005). Phagocyte NADPH oxidase: A multicomponent enzyme essential for host defenses. *Archivum Immunologiae et Therapiae Experimentalis,* **53**, 199-206.

El-Benna, J., Dang, P.M., Gougerot-Pocidalo, M., MARIE, J. and Braut-Boucher, F. (2009). p47phox, the phagocyte NADPH oxidase/NOX2 organizer: Structure, phosphorylation and implication in diseases. *Experimental and Molecular Medicine,* **41**, 217-225.

Ene, I.V. and Brown, A.J.P. (2014). Integration of metabolism with virulence in *Candida albicans*. *Fungal Genomics, 2nd Edition,* **13**, 349-370.

Enjalbert, B., Smith, D.A., Cornell, M.J., Alam, I., Nicholls, S., Brown, A.J.P. and Quinn, J. (2006). Role of the Hog1 stress-activated protein kinase in the global transcriptional response to stress in the fungal pathogen Candida albicans. *Molecular biology of the cell,* **17**,1018-1032.

Erwig, L.P. and Gow, N.A.R. (2016). Interactions of fungal pathogens with phagocytes. *Nature Reviews Microbiology,* **14**, 163-176.

Fairn, G.D. and Grinstein, S. (2012). How nascent phagosomes mature to become phagolysosomes. *Trends in immunology,* **33**, 397-405.

Fernández-Arenas, E., Cabezón, V., Bermejo, C., Arroyo, J., Nombela, C., Diez-Orejas, R. and Gil, C. (2007). Integrated proteomics and genomics strategies bring new insight into *Candida albicans* response upon macrophage interaction. *Molecular & Cellular Proteomics,* **6**, 460-478.

Fidel Jr., P.L. (2002). Immunity to *Candida*. *Oral diseases,* **8**, 69-75.

Filler, S.G. and Sheppard, D.C. (2006). Fungal invasion of normally non-phagocytic host cells. *PLoS Pathogens,* **2**, 1099-1105.

Finn, K., Lowndes, N.F. and Grenon, M. (2012). Eukaryotic DNA damage checkpoint activation in response to double-strand breaks. *Cellular and Molecular Life Sciences,* **69,** 1447-1473.

Fitzpatrick, D.A., Logue, M.E., Stajich, J.E. and Butler, G. (2006). A fungal phylogeny based on 42 complete genomes derived from supertree and combined gene analysis. *BMC Evolutionary Biology,* **6**.

Forman, H.J. and Torres, M. (2002). Reactive oxygen species and cell signaling: Respiratory burst in macrophage signaling. *American Journal of Respiratory and Critical Care Medicine,* **166**, S4-S8.

Fradin, C., De Groot, P., Maccallum, D., Schaller, M., Klis, F., Odds, F.C. and Hube, B. (2005). Granulocytes govern the transcriptional response, morphology and proliferation of Candida albicans in human blood. *Molecular microbiology,* **56**, 397-415.

Fradin, C., Kretschmar, M., Nichterlein, T., Gaillardin, C., d'Eenfert, C. and Hube, B. (2003). Stage-specific gene expression of *Candida albicans* in human blood. *Molecular microbiology,* **47**, 1523-1543.

Frohner, I.E., Bourgeois, C., Yatsyk, K., Majer, O. and Kuchler, K. (2009). *Candida albicans* cell surface superoxide dismutases degrade host-derived reactive oxygen species to escape innate immune surveillance. *Molecular microbiology,* **71**, 240-252.

Ghannoum, M.A., Spellberg, B., Saporito-Irwin, S.M. and Fonzi, W.A. (1995). Reduced virulence of *Candida albicans* PHR1 mutants. *Infection and immunity,* **63**, 4528-4530.

Ghelardi, E., Pichierri, G., Castagna, B., Barnini, S., Tavanti, A. and Campa, M. (2008). *Efficacy of Chromogenic Candida Agar for isolation and presumptive identification of pathogenic yeast species.*

Ghosh, S., Navarathna, D.H.M.L.P., Roberts, D.D., Cooper, J.T., Atkin, A.L., Petro, T.M. and Nickerson, K.W. (2009). Arginine-induced germ tube formation in *Candida albicans* is essential for escape from murine macrophage Line RAW 264.7. *Infection and immunity,* **77**, 1596-1605.

Glory, A., Van Oostende, C.T., Geitmann, A. and Bachewich, C. (2017). Depletion of the mitotic kinase Cdc5p in *Candida albicans* results in the formation of elongated buds that switch to the hyphal fate over time in a Ume6p and Hgc1p-dependent manner. *Fungal Genetics and Biology,* **107**, 51-66.

Gong, Y., LI, T., YU, C. and Sun, S. (2017). *Candida albicans* heat shock proteins and Hsps-associated signaling pathways as potential antifungal targets. *Frontiers in Cellular and Infection Microbiology*, **7**.

Gow, N.A.R., Van De Veerdonk, F.L., Brown, A.J.P. and Netea, M.G. (2012). *Candida albicans* morphogenesis and host defence: Discriminating invasion from colonization. *Nature Reviews Microbiology,* **10**, 112-122.

Gräf, R., Rietdorf, J. and Zimmermann, T. (2005). Live cell spinning disk microscopy. *Advanced Biochemical Engineering Biotechnology*, **95**, 57-75.

Groemping, Y. and Rittinger, K. (2005). Activation and assembly of the NADPH oxidase: A structural perspective. *Biochemical Journal,* **386**, 401-416.

Guillemain, G., MA, E., Mauger, S., Miron, S., Thai, R., Guérois, R., Ochsenbein, F. and Marsolier-Kergoat, M. (2007). Mechanisms of checkpoint kinase Rad53 inactivation after a double-strand break in Saccharomyces cerevisiae. *Molecular and cellular biology,* **27**, 3378-3389.

Guinea, J. (2014). *Global trends in the distribution of Candida species causing candidemia.*

Hall, R.A., De Sordi, L., Maccallum, D.M., Topal, H., Eaton, R., Bloor, J.W., Robinson, G.K., Levin, L.R., Buck, J., Wang, Y., Gow, N.A.R., Steegborn, C. and Mühlschlegel, F.A. (2010). CO2 acts as a signalling molecule in populations of the fungal pathogen *Candida albicans*. *PLoS Pathogens,* **6**.

Hartwell, L.H. and Weinert, T.A. (1989). Checkpoints: controls that ensure the order of cell cycle events. *Science,* **246**, 629-634.

Heinsbroek, S.E.M., Taylor, P.R., Martinez, F.O., Martinez-Pomares, L., Brown, G.D. and Gordon, S. (2008). Stage-specific sampling by pattern recognition receptors during *Candida albicans* phagocytosis. *PLoS Pathogens,* **4**.

Hernández-Santos, N. and Gaffen, S. (2012). Th17 Cells in Immunity to *Candida albicans. Science direct,* **5**, 425- 435.

Hill, B.G., Reily, C., Oh, J., Johnson, M.S. and Landar, A. (2009). Methods for the determination and quantification of the reactive thiol proteome. *Free radical Biology and Medicine*, **47**, 675-683.

Homann, O.R., Dea, J., Noble, S.M. and Johnson, A.D. (2009). A phenotypic profile of the *Candida albicans* regulatory network. *PLoS Genetics,* **5**.

Horn, D.L., Neofytos, D., Anaissie, E.J., Fishman, J.A., Steinbach, W.J., Olyaei, A.J., Marr, K.A., Pfaller, M.A., Chang, C. and Webster, K.M. (2009). Epidemiology and outcomes of candidemia in 2019 patients: Data from the prospective antifungal therapy alliance registry. *Clinical Infectious Diseases,* **48**, 1695-1703.

Hostetter, M.K. (1994). Adhesins and ligands involved in the interaction of *Candida spp*. with epithelial and endothelial surfaces. *Clinical microbiology reviews*, **7**, 29-42.

Hoyer, L.L. (2001). The ALS gene family of *Candida albicans*. *Trends in microbiology*, **9**, 176-180.

Hoyer, L.L., Green, C.B., Oh, S. and Zhao, X. (2008). Discovering the secrets of the *Candida albicans* agglutinin-like sequence (ALS) gene family — a sticky pursuit. *Medical Mycology*, **46**, 1-15.

Huang, H., Ostroff, G.R., Lee, C.K., Wang, J.P., Specht, C.A. and Levitz, S.M. (2009). Distinct Patterns of Dendritic Cell Cytokine Release Stimulated by Fungal β-Glucans and Toll-Like Receptor Agonists. *Infection and immunity*, **77**, 1774-1781.

Hussein, B., Huang, H., Glory, A., Osmani, A., Kaminskyj, S., Nantel, A. and Bachewich, C. (2011). G1/S transcription factor orthologues Swi4p and Swi6p are important but not essential for cell proliferation and influence hyphal development in the fungal pathogen *Candida albicans*. *Eukaryotic Cell*, **10**, 384-397.

Hwang, C., Rhie, G., Oh, J., Huh, W., Yim, H. and Kang, S. (2002). Copper- and zinc-containing superoxide dismutase (Cu/ZnSOD) is required for the protection of *Candida albicans* against oxidative stresses and the expression of its full virulence. *Microbiology*, **148**, 3705-3713.

Ikeh, M.A.C., Kastora, S.L., Day, A.M., Herrero-De-Dios, C.M., Tarrant, E., Waldron, K.J., Banks, A.P., Bain, J.M., Lydall, D., Veal, E.A., Maccallum, D.M., Erwig, L.P., Brown, A.J.P. and Quinn, J. (2016). Pho4 mediates phosphate acquisition in *Candida albicans* and is vital for stress resistance and metal homeostasis. *Molecular biology of the cell*, **27**, 2784-2801.

Jacobsen, I.D., Wilson, D., Wächtler, B., Brunke, S., Naglik, J.R. and Hube, B. (2012). *Candida albicans* dimorphism as a therapeutic target. *Expert Review of Anti-Infective Therapy*, **10**, 85-93.

Jaehnig, E.J., Kuo, D., Hombauer, H., Ideker, T.G. and Kolodner, R.D. (2013). Checkpoint kinases regulate a global network of transcription factors in response to DNA Damage. *Cell Reports*, **4**, 174-188.

Jain, C., Pastor, K., Gonzalez, A.Y., Lorenz, M.C. and Rao, R.P. (2013). The role of *Candida albicans* AP-1 protein against host derived ROS in *in vivo* models of infection. *Virulence*, **4**, 67-76.

Jan, Y., Richardson, J.R., Baker, A.A., Mishin, V., Heck, D.E., Laskin, D.L. and Laskin, J.D. (2015). Vitamin K3 (menadione) redox cycling inhibits cytochrome P450-mediated metabolism and inhibits parathion intoxication. *Toxicology and Applied Pharmacology*, **288,** 114-120.

Kaloriti, D., Jacobsen, M., Yin, Z., Patterson, M., Tillmann, A., Smith, D.A., Cook, E., You, T., Grimm, M.J., Bohovych, I., Grebogi, C., Segal, B.H., Gow, N.A.R., Haynes, K., Quinn, J. and Brown, A.J.P. (2014). Mechanisms underlying the exquisite sensitivity of *Candida albicans* to combinatorial cationic and oxidative stress that enhances the potent fungicidal activity of phagocytes. *mBio*, **5**.

Kaloriti, D., Tillmann, A., Cook, E., Jacobsen, M., You, T., Lenardon, M., Ames, L., Barahona, M., Chandrasekaran, K., Coghill, G., Goodman, D., Gow, N.A.R., Grebogi, C., Ho, H., Ingram, P., Mcdonagh, A., De Moura, A.P.S., Pang, W., Puttnam, M., Radmaneshfar, E., Romano, M.C., Silk, D., Stark, J., Stumpf, M., Thiel, M., Thorne, T., Usher, J., Yin, Z., Haynes, K. and Brown, A.J.P. (2012). Combinatorial stresses kill pathogenic *Candida species*. *Medical Mycology,* **50**, 699-709.

Kasperkovitz, P.V., Khan, N.S., Tam, J.M., Mansour, M.K., Davids, P.J. and Vyas, J.M. (2011). Toll-like receptor 9 modulates macrophage antifungal effector function during innate recognition of *Candida albicans* and *Saccharomyces cerevisiae*. *Infection and immunity,* **79**, 4858-4867.

Kehrer, J.P. (2000). The Haber–Weiss reaction and mechanisms of toxicity. *Toxicology*, **149**, 43-50.

Klaunig, J.E., Wang, Z., Pu, X. and Zhou, S. (2011). Oxidative stress and oxidative damage in chemical carcinogenesis. *Toxicology and applied pharmacology*, **254**, 86-99.

Kos, I., Patterson, M.J., Znaidi, S., Kaloriti, D., Da Silva Dantas, A., Herrero-de-Dios, C.M., d'Enfert, C., Brown, A.J.P. and Quinn, J. (2016). Mechanisms underlying the delayed activation of the Cap1 transcription factor in *Candida albicans* following combinatorial oxidative and cationic stress important for phagocytic potency. *mBio,* **7**.

Krause, K. (2004). Tissue distribution and putative physiological function of NOX family NADPH oxidases. *Japanese journal of infectious diseases*, **57**, S28-S29.

Krysan, D.J., Sutterwala, F.S. and Wellington, M. (2014). Catching Fire: *Candida albicans*, Macrophages, and Pyroptosis. *PLoS Pathogens*, **10.**

Kullberg, B.J. and Arendrup, M.C. (2015). Invasive candidiasis. *New England Journal of Medicine,* **373**, 1445-1456.

Kwiecien, S., Jasnos, K., Magierowski, M., Sliwowski, Z., Pajdo, R., Brzozowski, B., Mach, T., Wojcik, D. and Brzozowski, T. (2014). Lipid peroxidation, reactive oxygen species and antioxidative factors in the pathogenesis of gastric mucosal lesions and mechanism of protection against oxidative stress-induced gastric injury. *Journal of Physiology and Pharmacology,* **65**, 613-622.

Lambeth, J.D. and Neish, A.S. (2014). Nox enzymes and new thinking on reactive oxygen: A double-edged sword revisited. *Annual Review of Pathology: Mechanisms of disease*, 14, 119.

Lehrer, R.I. and Cline, M.J. (1969). Leukocyte myeloperoxidase deficiency and disseminated candidiasis: the role of myeloperoxidase in resistance to *Candida* infection. *The Journal of clinical investigation*, **48**, 1478-1488.

Levine, R.L., Moskovitz, J. and Stadtman, E.R. (2000). Oxidation of methionine in proteins: Roles in antioxidant defense and cellular regulation. *IUBMB life*, **50**, 301-307.

Lewis, L.E., Bain, J.M., Okai, B., Gow, N.A. and Erwig, L.P. (2013). Live-cell video microscopy of fungal pathogen phagocytosis. *Journal of visualized experiments: JoVE*, **71**.

Lewis, L.E., Bain, J.M., Lowes, C., Gillespie, C., Rudkin, F.M., Gow, N.A.R. and Erwig, L. (2012). Stage specific assessment of *Candida albicans* phagocytosis by macrophages identifies cell wall composition and morphogenesis as key determinants. *PLoS Pathogens*, **8**.

Lilic, D., Gravenor, I., Robson, N., Lammas, D.A., Drysdale, P., Calvert, J.E., Cant, A.J. and Abinun, M. (2003). Deregulated production of protective cytokines in response to *Candida albicans* infection in patients with chronic mucocutaneous candidiasis. *Infection and Immunity*, **71**, 5690-5699.

Lo, H., Köhler, J.R., Didomenico, B., Loebenberg, D., Cacciapuoti, A. and Fink, G.R. (1997). Nonfilamentous *C. albicans* mutants are avirulent. *Cell*, **90**, 939-949.

Longhese, M.P., Foiani, M., Muzi-Falconi, M., Lucchini, G. and Plevani, P. (1998). DNA damage checkpoint in budding yeast. *EMBO Journal*, **17**, 5525-5528.

Lorenz, M.C., Bender, J.A. and Fink, G.R. (2004). Transcriptional Response of *Candida albicans* upon internalization by macrophages. *Eukaryotic Cell*, **3**, 1076-1087.

Lowndes, N.F. and Murguia, J.R. (2000). Sensing and responding to DNA damage. *Current opinion in genetics & development*, **10**, 17-25.

Lu, Y., Su, C., Unoje, O. and Liu, H. (2014). Quorum sensing controls hyphal initiation in *Candida albicans* through Ubr1-mediated protein degradation. *Proceedings of the National Academy of Sciences of the United States of America*, **111**, 1975-1980.

Martindale, J.L. and Holbrook, N.J. (2002). Cellular response to oxidative stress: Signaling for suicide and survival. *Journal of cellular physiology*, **192**, 1-15.

Martínez-Esparza, M., Aguinaga, A., González-Párraga, P., García-Peñarrubia, P., Jouault, T. and Argüelles, J.C. (2007). Role of trehalose in resistance to macrophage killing: study with a tps1/tps1 trehalose-deficient mutant of *Candida albicans*. *Clinical Microbiology and Infection*, **13**, 384-394.

Martino, P., Girmenia, C., Venditti, M., Micozzi, A., Santilli, S., Burgio, V.L. and Mandelli, F. (1989). *Candida* colonization and systemic infection in neutropenic patients. A retrospective study. *Cancer*, **64**, 2030-2034.

Mattia, E., Carruba, G., Angiolella, L. and Cassone, A. (1982). Induction of germ tube formation by N-acetyl-D-glucosamine in *Candida albicans*: uptake of inducer and germinative response. *Journal of Bacteriology*, **152**, 555-562.

Mayer, F.L., Wilson, D. and Hube, B. (2013). *Candida albicans* pathogenicity mechanisms. *Virulence*, **4**, 119-128.

Mckenzie, C.G.J., Koser, U., Lewis, L.E., Bain, J.M., Mora-Montes, H.M., Barker, R.N., Gow, N.A.R. and Erwig, L.P. (2010). Contribution of *Candida albicans* cell wall components to recognition by and escape from murine macrophages. *Infection and Immunity*, **78**, 1650-1658.

Medzhitov, R. and Janeway, C.A. (2002). Decoding the Patterns of Self and Nonself by the Innate Immune System. *Science,* **296**, 298-300.

Miramón, P., Dunker, C., Windecker, H., Bohovych, I.M., Brown, A.J.P., Kurzai, O. and Hube, B. (2012). Cellular Responses of *Candida albicans* to phagocytosis and the extracellular activities of neutrophils are critical to counteract carbohydrate starvation, oxidative and nitrosative stress. *PLoS ONE,* **7**.

Miramón, P., Kasper, L. and Hube, B. (2013). Thriving within the host: *Candida spp*. interactions with phagocytic cells. *Medical microbiology and immunology*, **202,** 183-195.

Monod, M., Togni, G., Hube, B. and Sanglard, D. (1994). Multiplicity of genes encoding secreted aspartic proteinases in *Candida species*. *Molecular microbiology,* **13**, 357-368.

Moragues, M.D., Rementeria, A., Sevilla, M.J., Eraso, E. and Quindos, G. (2014). *Candida* antigens and immune responses: Implications for a vaccine. *Expert Review of Vaccines*, **13**, 1001-1012.

Moyes, D.L., Wilson, D., Richardson, J.P., Mogavero, S., Tang, S.X., Wernecke, J., Höfs, S., Gratacap, R.L., Robbins, J., Runglall, M., Murciano, C., Blagojevic, M., Thavaraj, S., Förster, T.M., Hebecker, B., Kasper, L., Vizcay, G., Iancu, S.I., Kichik, N., Häder, A., Kurzai, O., Luo, T., Krüger, T., Kniemeyer, O., Cota, E., Bader, O., Wheeler, R.T., Gutsmann, T., Hube, B. and Naglik, J.R. (2016). Candidalysin is a fungal peptide toxin critical for mucosal infection. *Nature*, **532**, 64-68.

Mühlschlegel, F.A. and Fonzi, W.A. (1997). PHR2 of *Candida albicans* encodes a functional homolog of the pH-regulated gene PHR1 with an inverted pattern of pH-dependent expression. *Molecular and cellular biology*, **17**, 5960-5967.

Mukaremera, L., Lee, K.K., Mora-Montes, H.M. and Gow N.A.R. (2017). *Candida albicans* yeast, pseudohyphal, and hyphal morphogenesis differentially affects immune recognition. *Frontiers in Immunology*, **8**.

Naglik, J.R., Challacombe, S.J. and Hube, B. (2003). *Candida albicans* Secreted aspartyl proteinases in virulence and pathogenesis. *Microbiology and Molecular Biology Reviews,* **67**, 400-428.

Netea, M.G., Brown, G.D., Kullberg, B.J. and Gow, N.A.R. (2008). An integrated model of the recognition of Candida albicans by the innate immune system. *Nature Reviews Microbiology*, **6,** 67-78.

Netea, M.G., Joosten, L.A.B., Van Der Meer, J.W.M. and Kullberg, B.J. (2010). Host defense and susceptibility to *Candida* infections. *Journal of invasive fungal infections*, **4**, 89-95.

Nicholls, S., Leach, M.D., Priest, C.L. and Brown, A.J.P. (2009). Role of the heat shock transcription factor, Hsf1, in a major fungal pathogen that is obligately associated with warm-blooded animals. *Molecular microbiology,* **74**, 844-861.

Nicholls, S., Maccallum, D.M., Kaffarnik, F.A.R., Selway, L., Peck, S.C. and Brown, A.J.P. (2011). Activation of the heat shock transcription factor Hsf1 is essential for the full virulence of the fungal pathogen *Candida albicans*. *Fungal Genetics and Biology,* **48,** 297-305.

Niedergang, F. and Grinstein, S. (2018). How to build a phagosome: new concepts for an old process. *Current opinion in cell biology,* **50**, 57-63.

Nikolaou, E., Agrafioti, I., Stumpf, M., Quinn, J., Stansfield, I. and Brown, A.J. (2009). Phylogenetic diversity of stress signalling pathways in fungi. *BMC Evolutionary Biology,* **9**.

Noble, S.M. and Johnson, A.D. (2005). Strains and strategies for large-scale gene deletion studies of the diploid human fungal pathogen *Candida albicans*. *Eukaryotic Cell,* **4**, 298-309.

Nourshargh, S. and Alon, R. (2014). Leukocyte Migration into Inflamed Tissues. *Immunity,* **41**, 694-707.

Odds, F.C. (1987). *Candida infections*: an overview *Critical reviews in microbiology,* **15**, 1-5.

Odds, F.C., Gow, N.A.R. and Brown, A.J.P. (2001). Fungal virulence studies come of age. *Genome biology,* **2**.

Okai, B., Lyall, N., Gow, N.A., Bain, J.M. and Erwig, L. (2015). Rab14 regulates maturation of macrophage phagosomes containing the fungal pathogen *Candida albicans* and outcome of the host-pathogen interaction. *Infection and immunity,* **83**, 1523-1535.

Olinski, R., Gackowski, D., Foksinski, M., Rozalski, R., Roszkowski, K. and Jaruga, P., (2002). Oxidative DNA damage: assessment of the role in carcinogenesis, atherosclerosis, and acquired immunodeficiency syndrome. *Free Radical Biology and Medicine,* **33**, 192-200.

Omeara, T.R., Veri, A.O., Ketela, T., Jiang, B., Roemer, T. and Cowen, L.E. (2015). Global analysis of fungal morphology exposes mechanisms of host cell escape. *Nature Communications,* **6**.

Pappas, P.G., Kauffman, C.A., Andes, D.R., Clancy, C.J., Marr, K.A., Ostrosky-Zeichner, L., Reboli, A.C., Schuster, M.G., Vazquez, J.A., Walsh, T.J., Zaoutis, T.E. and Sobel, J.D. (2015). Clinical Practice Guideline for the Management of Candidiasis: 2016 Update by the Infectious Diseases Society of America. *Clinical Infectious Diseases,* **62**, e1-e50.

Patterson, M.J., Mckenzie, C.G., Smith, D.A., Da Silva Dantas, A., Sherston, S., Veal, E.A., Morgan, B.A., Maccallum, D.M., Erwig, L. and Quinn, J. (2013). Ybp1 and Gpx3 signaling in *Candida albicans* govern hydrogen peroxide-induced oxidation of the Cap1 transcription factor and macrophage escape. *Antioxidants and Redox Signaling,* **19**, 2244-2260.

Patuwo, C., Young, K., Lin, M., Pardi, V. and Murata, R.M. (2015). The changing role of HIV-associated oral candidiasis in the era of HAART. *Journal of the California Dental Association,* **43**, pp. 87-92.

Peacock, M.E., Arce, R.M. and Cutler, C.W. (2017). Periodontal and other oral manifestations of immunodeficiency diseases. *Oral diseases,* **23**, 866-888.

Pellicioli, A., Lee, S.E., Lucca, C., Foiani, M. and Haber, J.E. (2001). Regulation of *Saccharomyces* Rad53 Checkpoint Kinase during Adaptation from DNA Damage–Induced G2/M Arrest. *Molecular cell*, **7**, 293-300.

Pfaller, M.A., Diekema, D.J., Gibbs, D.L., Newell, V.A., Ellis, D., Tullio, V., Rodloff, A., FU, W., Ling, T.A. and the global antifungal surveillance group. (2010). Results from the ARTEMIS DISK Global Antifungal Surveillance Study, 1997 to 2007: a 10.5-Year Analysis of Susceptibilities of *Candida* species to fluconazole and voriconazole as determined by CLSI Standardized disk diffusion. *Journal of clinical microbiology,* **48**, 1366-1377.

Pfaller, M.A., Moet, G.J., Messer, S.A., Jones, R.N. and Castanheira, M. (2011). Geographic variations in species distribution and echinocandin and azole antifungal resistance rates among *Candida* bloodstream infection isolates: Report from the SENTRY Antimicrobial Surveillance Program (2008 to 2009). *Journal of clinical microbiology,* **49**, 396-399.

Pfaller, M.A., Pappas, P.G. and Wingard, J.R. (2006). Invasive Fungal Pathogens: Current Epidemiological Trends. *Clinical Infectious Diseases,* **43**, S3-S14.

Pizzimenti, S., Toaldo, C., Pettazzoni, P., Dianzani, M.U. and Barrera, G. (2010). The "Two-Faced" effects of reactive oxygen species and the lipid peroxidation product 4-Hydroxynonenal in the hallmarks of cancer. *Cancers,* **2**, 338-363.

Pradhan, A., Herrero-de-Dios, C., Belmonte, R., Budge, S., Lopez Garcia, A., Kolmogorova, A., Lee, K.K., Martin, B.D., Ribeiro, A., Bebes, A., Yuecel, R., Gow, N.A.R., Munro, C.A., Maccallum, D.M., Quinn, J. and Brown, A.J.P. (2017). Elevated catalase expression in a fungal pathogen is a double-edged sword of iron. *PLoS Pathogens,* **13**.

Qian, Q., Jutila, M.A., Van Rooijen, N. and Cutler, J.E. (1994). Elimination of mouse splenic macrophages correlates with increased susceptibility to experimental disseminated candidiasis. *Journal of Immunology,* **152**, 5000-5008.

Ramanan, N. and Wang, Y. (2000). A High-Affinity iron permease essential for *Candida albicans* virulence. *Science,* **288,** 1062-1064.

Rhind, N. and Russell, P. (1998). Mitotic DNA damage and replication checkpoints in yeast. *Current Opinion in Cell Biology*, **10**, 749-758.

Richard Cole (2014) Live-cell imaging, *Cell Adhesion & Migration*, **8**, 452-459.

Richardson, M. and Rautemaa, R. (2009). How the host fights against *Candida* infections. *Frontiers in Bioscience - Scholar,* **1**, 246-257.

Romani, L. (2011). Immunity to fungal infections. *Nature Reviews Immunology*, **11**, 275-288.

Romani, L. (1999). *Immunity to Candida albicans: Th1, Th2 cells and beyond.*

Rossi, D.C.P., Gleason, J.E., Sanchez, H., Schatzman, S.S., Culbertson, E.M., Johnson, C.J., Mcnees, C.A., Coelho, C., Nett, J.E., Andes, D.R., Cormack, B.P. and Culotta, V.C. (2017). *Candida albicans* FRE8 encodes a member of the NADPH oxidase family that produces a burst of ROS during fungal morphogenesis. *PLoS pathogens,* **13**.

Rudkin, F.M., Bain, J.M., Walls, C., Lewis, L.E., Gow, N.A.R. and Erwig, L.P. (2013). Altered dynamics of *Candida albicans* phagocytosis by macrophages and PMNs when both phagocyte subsets are present. *mBio,* **4**.

Ryan, O., Shapiro, R.S., Kurat, C.F., Mayhew, D., Baryshnikova, A., Chin, B., Lin, Z., Cox, M.J., Vizeacoumar, F., Cheung, D., Bahr, S., Tsui, K., Tebbji, F., Sellam, A., Istel, F., Schwarzmüller, T., Reynolds, T.B., Kuchler, K., Gifford, D.K., Whiteway, M., Giaever, G., Nislow, C., Costanzo, M., Gingras, A., Mitra, R.D., Andrews, B., Fink, G.R., Cowen, L.E. and Boone, C. (2012). Global Gene Deletion Analysis Exploring Yeast Filamentous Growth. *Science,* **337**, 1353-1356.

Samaranayake, L.P. (1990). Oral candidosis: an old disease in new guises. *Dental update,* **17**, 36-38.

Sanchez, Y., Bachant, J., Wang, H., Hu, F., Liu, D., Tetzlaff, M. and Elledge, S.J. (1999). Control of the DNA damage checkpoint by Chk1 and Rad53 protein kinases through distinct mechanisms. *Science,* **286**, 1166-1171.

Saville, S.P., Lazzell, A.L., Monteagudo, C. and Lopez-Ribot, J.L. (2003). Engineered Control of cell morphology in vivo reveals distinct roles for yeast and filamentous forms of *Candida albicans* during Infection. *Eukaryotic Cell,* **2**, 1053-1060.

Schaller, M., Borelli, C., Korting, H.C. and Hube, B. (2005). Hydrolytic enzymes as virulence factors of *Candida albicans*. *Mycoses,* **48**, 365-377.

Sheppard, D.C., Locas, M. Restieri, C. and Laverdiere, M. (2008). Utility of the germ tube test for direct identification of *Candida albicans* from positive blood culture bottles. *Journal of clinical microbiology*, **46**, 3508-3509.

Schwartz, I.S. and Patterson, T.F. (2018). The Emerging Threat of antifungal resistance in transplant Infectious Diseases. *Current infectious disease reports,* **20**.

Segal, B.H., Grimm, M.J., Khan, A.N.H., Han, W. and Blackwell, T.S. (2012). Regulation of innate immunity by NADPH oxidase. *Free Radical Biology and Medicine*, **53**, 72-80.

Shapiro, R.S. and Cowen, L.E. (2010). Coupling temperature sensing and development. *Virulence,* **1**, 45-48.

Shapiro, R.S., Uppuluri, P., Zaas, A.K., Collins, C., Senn, H., Perfect, J.R., Heitman, J. and Cowen, L.E. (2009). Hsp90 orchestrates temperature-dependent *Candida albicans* morphogenesis via Ras1-PKA signaling. *Current Biology,* **19**, 621-629.

Shareck, J. and Belhumeur, P. (2011). Modulation of morphogenesis in *Candida albicans* by various small molecules. *Eukaryotic Cell,* **10**, 1004-1012.

Shepherd, M.G., Poulter, R.T. and Sullivan, P.A. (1985). *Candida albicans*: biology, genetics, and pathogenicity. *Annual Review of Microbiology,* **39**, 579-614.

Sherman, F., 2002. Getting started with yeast. *Methods in Enzymology,* **350**.

Sherrington, S.L., Sorsby, E., Mahtey, N., Kumwenda, P., Lenardon, M.D., Brown, I., Ballou, E.R., Maccallum, D.M. and Hall, R.A. (2017). Adaptation of *Candida albicans* to environmental pH induces cell wall remodelling and enhances innate immune recognition. *PLoS Pathogens,* **13**.

Shi, Q., Wang, Y., Zheng, X., Teck Ho Lee, R. and Wang, Y. (2007). Critical role of DNA checkpoints in mediating genotoxic-stress–induced filamentous growth in *Candida albicans*. *Molecular biology of the cell,* **18**, 815-826.

Singh, P., Chauhan, N., Ghosh, A., Dixon, F. and Calderone, R. (2004). Skn7 of *Candida albicans*: Mutant construction and phenotype analysis. *Infection and immunity,* **72**, 2390-2394.

Slutsky, B., Staebell, M., Anderson, J., Risen, L., Pfaller, M. and Soll, D.R. (1987). 'White-opaque transition': A second high-frequency switching system in *Candida albicans. Journal of Bacteriology,* **169**, 189-197.

Smith, D.A., Nicholls, S., Morgan, B.A., Brown, A.J.P. and Quinn, J. (2004). A conserved stress-activated protein kinase regulates a core stress response in the human pathogen *Candida albicans*. *Molecular biology of the cell,* **15**, 4179-4190.

Smith, D.A., Morgan, B.A. and Quinn, J. (2010). Stress signalling to fungal stress-activated protein kinase pathways. *FEMS microbiology letters,* **306**, 1-8.

Sobel, J.D. (2007). Vulvovaginal candidosis. *The Lancet,* **369**, 1961-1971.

Sobel, J.D. (1988). Pathogenesis and epidemiology of vulvovaginal candidiasis. *Annals of the New York Academy of Sciences,* **544**, 547-557.

Sohn, K., Urban, C., Brunner, H. and Rupp, S. (2003). Efg1 is a major regulator of cell wall dynamics in *Candida albicans* as revealed by DNA microarrays. *Molecular microbiology,* **47**, 89-102.

Soll, D.R. (1992). High-frequency switching in *Candida albicans*. *Clinical microbiology reviews,* **5**, 183-203.

Staab, J.F., Bradway, S.D., Fidel, P.L. and Sundstrom, P. (1999). Adhesive and mammalian transglutaminase substrate properties of *Candida albicans* Hwp1. *Science,* **283**, 1538-1538.

Sternberg, S. (1994). The emerging fungal threat. *Science,* **266**, 1632-1634.

Stoldt, V.R., Sonneborn, A., Leuker, C.E. and Ernst, J.F. (1997). Efg1p, an essential regulator of morphogenesis of the human pathogen *Candida albicans*, is a member of a conserved class of bHLH proteins regulating morphogenetic processes in fungi. *EMBO Journal,* **16**, 1982-1991.

Sudbery, P.E. (2011). Growth of *Candida albicans* hyphae. *Nature Reviews Microbiology,* **9**, 737-748.

Sudbery, P., Gow, N. and Berman, J. (2004). The distinct morphogenic states of *Candida albicans*. *Trends in microbiology,* **12**, 317-324.

Sundstrom, P. (1999). Adhesins in *Candida albicans*. *Current opinion in microbiology,* **2**, 353-357.

Swaim, M.W. and Pizzo, S.V. (1988). Methionine sulfoxide and the oxidative regulation of plasma proteinase inhibitors. *Journal of leukocyte biology*, **43**, 365-379.

Tavares, A.H., Bürgel, P.H. and Bocca, A.L. (2015). Turning Up the Heat: Inflammasome Activation by Fungal Pathogens. *PLoS Pathogens,* **11**.

Tongul, B. and Tarhan, L. (2014). The effect of menadione-induced oxidative stress on the in vivo reactive oxygen species and antioxidant response system of Phanerochaete chrysosporium. *Process Biochemistry*, **49**, 195-202.

Torosantucci, A., Angiolella, L., Filesi, C. and Cassone, A. (1984). Protein synthesis and amino acid pool during yeast-mycelial transition induced by N-Acetyl-D-glucosamine in *Candida albicans*. *Journal of general microbiology*, **130**, 3285-3293.

Tripathi, G., Wiltshire, C., Macaskill, S., Tournu, H., Budge, S. and Brown (A.J.P). (2002). Gcn4 co-ordinates morphogenetic and metabolic responses to amino acid starvation in *Candida albicans*. *EMBO Journal,* **21**, 5448-5456.

Urban, C.F., Reichard, U., Brinkmann, V. and Zychlinsky, A. (2006). Neutrophil extracellular traps capture and kill *Candida albicans* and hyphal forms. *Cellular microbiology*, **8**, 668-676.

Uwamahoro, N., Verma-Gaur, J., Shen, H., Qu, Y., Lewis, R., Lu, J., Bambery, K., Masters, S.L., Vince, J.E., Naderer, T. and Traven, A. (2014). The pathogen *Candida albicans* hijacks pyroptosis for escape from macrophages. *mBio*, **5**.

Van de Veerdonk, F.L. and Netea, M.G. (2010). T-cell subsets and antifungal host defenses. *Current Fungal Infection Reports,* **4**, 238-243.

Van de Veerdonk, F.L. and Netea, M.G. (2016). Treatment options for chronic mucocutaneous candidiasis. *Journal of Infection*, **72**, S56-S60.

Van de Veerdonk, F.L., Netea, M.G., Joosten, L.A., Van der Meer, J.W.M. and Kullberg, B.J., 2010. Novel strategies for the preventionand treatment of *Candida* infections: The potential of immunotherapy. *FEMS microbiology reviews,* **34**, 1063-1075.

Van 'T Wout, J.W., Linde, I., Leijh, P.C.J. and Van Furth, R. (1988). Contribution of granulocytes and monocytes to resistance against experimental disseminated *Candida albicans* infection. *European Journal of Clinical Microbiology & Infectious Diseases,* **7,** 736-741.

Verma, A., Wüthrich, M., Deepe, G. and Klein, B. (2015). Adaptive Immunity to Fungi. *Cold Spring Harbor Perspectives in Medicine*, **5**.

Vieira, O.V., Botelho, R.J. and Grinstein, S. (2002). Phagosome maturation: Aging gracefully. *Biochemical Journal*, **366**, 608-704.

Vylkova, S. and Lorenz, M.C. (2014). Modulation of Phagosomal pH by *Candida albicans* promotes hyphal morphogenesis and requires Stp2p, a regulator of amino acid transport. *PLoS Pathogens*, **10**.

Vylkova, S., Carman, A.J., Danhof, H.A., Collette, J.R., Zhou, H. and Lorenz, M.C. (2011). The fungal pathogen *Candida albicans* autoinduces hyphal morphogenesis by raising extracellular pH. *mBio*, **2**.

Wagener, J., Maccallum, D.M., Brown, G.D. and Gow, N.A.R. (2017). *Candida albicans* chitin increases arginase-1 activity in human macrophages, with an impact on macrophage antimicrobial functions. *mBio*, **8**.

Wagener, J., Malireddi, R.K.S., Lenardon, M.D., Köberle, M., Vautier, S., Maccallum, D.M., Biedermann, T., Schaller, M., Netea, M.G., Kanneganti, T., Brown, G.D., Brown, A.J.P. and Gow, N.A.R. (2014). Fungal chitin dampens inflammation through IL-10 induction mediated by Nod2 and TLR9 activation. *PLoS Pathogens*, **10**.

Wang, H., Gao, J., LI, W., Wong, A.H., Hu, K., Chen, K., Wang, Y. and Sang, J. (2012). Pph3 dephosphorylation of Rad53 is required for cell recovery from MMS-induced DNA damage in Candida albicans. *PLoS ONE*, **7**.

Wang, Y. (2013). Fungal adenylyl cyclase acts as a signal sensor and integrator and plays a central role in interaction with bacteria. *PLoS Pathogens*, **9**.

Wang, Y., Cao, Y., Jia, X., Cao, Y., Gao, P., Fu, X., Ying, K., Chen, W. and Jiang, Y. (2006). Cap1p is involved in multiple pathways of oxidative stress response in *Candida albicans*. *Free radical Biology and Medicine*, **40**, 1201-1209.

Wang, E., Babbey, C.M. and Dunn, K.W. (2005). Performance comparison between the high-speed Yokogawa spinning disc confocal system and single-point scanning confocal systems. *Journal of microscopy*, **218**, 148-159.

Weinert, T. (1998). DNA damage checkpoints update: getting molecular. *Current Opinion in Genetics & Development*, **8**, 185-193.

Weinstein, R.A. and Fridkin, S.K. (2005). The changing face of fungal infections in health care settings. *Clinical Infectious Diseases*, **41**, 1455-1460.

Wellington, M., Koselny, K., Sutterwala, F.S. and Krysan, D.J. (2014). *Candida albicans* triggers NLRP3-mediated pyroptosis in macrophages. *Eukaryotic Cell*, **13**, 329-340.

Whibley, N. and Gaffen, S.L. (2014). Brothers in Arms: Th17 and Treg Responses in *Candida albicans* Immunity. *PLoS Pathogens*, **10.**

Wilson, R.B., Davis, D. and Mitchell, A.P. (1999). Rapid hypothesis testing with *Candida albicans* through gene disruption with short homology regions. *Journal of Bacteriology*, **181**, 1868-1874.

Winter, E. (2012). The Sum1/Ndt80 transcriptional switch and commitment to meiosis in *Saccharomyces cerevisiae*. *Microbiology and Molecular Biology Reviews,* **76**, 1-15.

Wisplinghoff, H., Bischoff, T., Tallent, S.M., Seifert, H., Wenzel, R.P. and Edmond, M.B. (2004). Nosocomial bloodstream infections in US Hospitals: Analysis of 24,179 Cases from a prospective nationwide surveillance study. *Clinical Infectious Diseases,* **39**, 309-317.

Woods, J.W., Manning JR., I.H. and Patterson, C.N. (1951). Monilial infections complicating the therapeutic use of antibiotics. *Journal of the American Medical Association,* **145**, 207-211.

Wormley, F.L., STeele, C., Wozniak, K., Fujihashi, K., Mcghee, J.R. and Fidel, P.L. (2001). Resistance of T-Cell Receptor δ-Chain-Deficient Mice to Experimental *Candida albicans* vaginitis. *Infection and immunity,* **69**, 7162-7164.

Wysong, D.R., Christin, L., Sugar, A.M., Robbins, P.W. and Diamond, R.D. (1998). Cloning and sequencing of a *Candida albicans* catalase gene and effects of disruption of this gene. *Infection and immunity*, **66**, 1953-1961.

Yadav, A.K., Desai, P.R., Rai, M.N., Kaur, R., Ganesan, K. and Bachhawat, A.K. (2011). Glutathione biosynthesis in the yeast pathogens *Candida glabrata and Candida albicans:* essential in *C. glabrata*, and essential for virulence in *C. albicans. Microbiology*, **157**, 484-495.

Zavrel, M., Majer, O., Kuchler, K. and Rupp, S. (2012). Transcription factor Efg1 shows a haploinsufficiency phenotype in modulating the cell wall architecture and immunogenicity of *Candida albicans*. *Eukaryotic Cell,* **11**, 129-140.

Zhang, X., De Micheli, M., Coleman, S.T., Sanglard, D. and Moye-rowley, W.S. (2000). Analysis of the oxidative stress regulation of the *Candida albicans* transcription factor, Cap1p. *Molecular microbiology,* **36**, 618-629.

Zheng, X., Wang, Y. and Wang, Y. (2004). Hgc1, a novel hypha-specific G1 cyclin-related protein regulates *Candida albicans* hyphal morphogenesis. *EMBO Journal,* **23**, 1845-1856.

Znaidi, S., Barker, K.S., Weber, S., Alarco, A., Liu, T.T., Boucher, G., Rogers, P.D. and Raymond, M. (2009). Identification of the *Candida albicans* Cap1p regulon. *Eukaryotic Cell,* **8**, 806-820.

8 APPENDIX

8.1 SUPPLEMENTAL DATA

8.1.1 S.1. Transcription factor library (Homann *et al*., 2009).

Strain	*Genotype*
TF001	*sfl1*Δ::*C.d.HIS1*/*sfl1*Δ::*C.m.LEU2 arg4*Δ/*arg4*Δ *leu2*Δ/*leu2*Δ *his1*Δ/*his1*Δ *URA3*/*ura3*Δ::*imm*^{434}*IRO1*/*iro1*Δ::*imm*^{43}
TF002	*hms1*Δ::*C.d.HIS1*/*hms1*Δ::*C.m.LEU2 arg4*Δ/*arg4*Δ *leu2*Δ/*leu2*Δ *his1*Δ/*his1*Δ *URA3*/*ura3*Δ::*imm*^{434}*IRO1*/*iro1*Δ::*imm*^{434}
TF003	*rpn4*Δ::*C.d.HIS1*/*rpn4*Δ::*C.m.LEU2 arg4*Δ/*arg4*Δ *leu2*Δ/*leu2*Δ *his1*Δ/*his1*Δ *URA3*/*ura3*Δ::*imm*^{434}*IRO1*/*iro1*Δ::*imm*^{434}
TF004	*pho4*Δ::*C.d.HIS1*/*pho4*Δ::*C.m.LEU2 arg4*Δ/*arg4*Δ *leu2*Δ/*leu2*Δ *his1*Δ/*his1*Δ *URA3*/*ura3*Δ::*imm*^{434}*IRO1*/*iro1*Δ::*imm*^{434}
TF005	*ctf1*Δ::*C.d.HIS1*/*ctf1*Δ::*C.m.LEU2 arg4*Δ/*arg4*Δ *leu2*Δ/*leu2*Δ *his1*Δ/*his1*Δ *URA3*/*ura3*Δ::*imm*^{434}*IRO1*/*iro1*Δ::*imm*^{434}
TF006	*zcf13*Δ::*C.d.HIS1*/*zcf13*Δ::*C.m.LEU2 arg4*Δ/*arg4*Δ *leu2*Δ/*leu2*Δ *his1*Δ/*his1*Δ *URA3*/*ura3*Δ::*imm*^{434}*IRO1*/*iro1*Δ::*imm*^{434}
TF007	*zcf14*Δ::*C.d.HIS1*/*zcf14*Δ::*C.m.LEU2 arg4*Δ/*arg4*Δ *leu2*Δ/*leu2*Δ *his1*Δ/*his1*Δ *URA3*/*ura3*Δ::*imm*^{434}*IRO1*/*iro1*Δ::*imm*^{434}
TF008	orf19.2730
TF009	*arg83*Δ::*C.d.HIS1*/*arg83*Δ::*C.m.LEU2 arg4*Δ/*arg4*Δ *leu2*Δ/*leu2*Δ *his1*Δ/*his1*Δ *URA3*/*ura3*Δ::*imm*^{434}*IRO1*/*iro1*Δ::*imm*^{434}
TF010	*tac1*Δ::*C.d.HIS1*/*tac1*Δ::*C.m.LEU2 arg4*Δ/*arg4*Δ *leu2*Δ/*leu2*Δ *his1*Δ/*his1*Δ *URA3*/*ura3*Δ::*imm*^{434}*IRO1*/*iro1*Δ::*imm*^{434}
TF011	*hal9*Δ::*C.d.HIS1*/*hal9*Δ::*C.m.LEU2 arg4*Δ/*arg4*Δ *leu2*Δ/*leu2*Δ *his1*Δ/*his1*Δ *URA3*/*ura3*Δ::*imm*^{434}*IRO1*/*iro1*Δ::*imm*^{434}
TF012	*zcf17*Δ::*C.d.HIS1*/*zcf17*Δ::*C.m.LEU2 arg4*Δ/*arg4*Δ *leu2*Δ/*leu2*Δ *his1*Δ/*his1*Δ *URA3*/*ura3*Δ::*imm*^{434}*IRO1*/*iro1*Δ::*imm*^{434}
TF013	*stb5*Δ::*C.d.HIS1*/*stb5*Δ::*C.m.LEU2 arg4*Δ/*arg4*Δ *leu2*Δ/*leu2*Δ *his1*Δ/*his1*Δ *URA3*/*ura3*Δ::*imm*^{434}*IRO1*/*iro1*Δ::*imm*^{434}
TF014	*try5*Δ::*C.d.HIS1*/*try5*Δ::*C.m.LEU2 arg4*Δ/*arg4*Δ *leu2*Δ/*leu2*Δ *his1*Δ/*his1*Δ *URA3*/*ura3*Δ::*imm*^{434}*IRO1*/*iro1*Δ::*imm*^{434}
TF015	*sef1*Δ::*C.d.HIS1*/*sef1*Δ::*C.m.LEU2 arg4*Δ/*arg4*Δ *leu2*Δ/*leu2*Δ *his1*Δ/*his1*Δ *URA3*/*ura3*Δ::*imm*^{434}*IRO1*/*iro1*Δ::*imm*^{434}
TF016	*bas1*Δ::*C.d.HIS1*/*bas1*Δ::*C.m.LEU2 arg4*Δ/*arg4*Δ *leu2*Δ/*leu2*Δ *his1*Δ/*his1*Δ *URA3*/*ura3*Δ::*imm*^{434}*IRO1*/*iro1*Δ::*imm*^{434}
TF017	*zcf19*Δ::*C.d.HIS1*/*zcf19*Δ::*C.m.LEU2 arg4*Δ/*arg4*Δ *leu2*Δ/*leu2*Δ *his1*Δ/*his1*Δ *URA3*/*ura3*Δ::*imm*^{434}*IRO1*/*iro1*Δ::*imm*^{434}
TF018	*gln3*Δ::*C.d.HIS1*/*gln3*Δ::*C.m.LEU2 arg4*Δ/*arg4*Δ *leu2*Δ/*leu2*Δ *his1*Δ/*his1*Δ *URA3*/*ura3*Δ::*imm*^{434}*IRO1*/*iro1*Δ::*imm*^{434}
TF019	orf19.3928
TF020	*sfl2*Δ::*C.d.HIS1*/*sfl2*Δ::*C.m.LEU2 arg4*Δ/*arg4*Δ *leu2*Δ/*leu2*Δ *his1*Δ/*his1*Δ *URA3*/*ura3*Δ::*imm*^{434}*IRO1*/*iro1*Δ::*imm*^{434}
TF021	*grf10*Δ::*C.d.HIS1*/*grf10*Δ::*C.m.LEU2 arg4*Δ/*arg4*Δ *leu2*Δ/*leu2*Δ *his1*Δ/*his1*Δ *URA3*/*ura3*Δ::*imm*^{434}*IRO1*/*iro1*Δ::*imm*^{434}
TF022	*brg1*Δ::*C.d.HIS1*/*brg1*Δ::*C.m.LEU2 arg4*Δ/*arg4*Δ *leu2*Δ/*leu2*Δ *his1*Δ/*his1*Δ *URA3*/*ura3*Δ::*imm*^{434}*IRO1*/*iro1*Δ::*imm*^{434}
TF023	*zcf20*Δ::*C.d.HIS1*/*zcf20*Δ::*C.m.LEU2 arg4*Δ/*arg4*Δ *leu2*Δ/*leu2*Δ *his1*Δ/*his1*Δ *URA3*/*ura3*Δ::*imm*^{434}*IRO1*/*iro1*Δ::*imm*^{434}
TF024	*zcf21*Δ::*C.d.HIS1*/*zcf21*Δ::*C.m.LEU2 arg4*Δ/*arg4*Δ *leu2*Δ/*leu2*Δ *his1*Δ/*his1*Δ *URA3*/*ura3*Δ::*imm*^{434}*IRO1*/*iro1*Δ::*imm*^{434}
TF025	*leu3*Δ::*C.d.HIS1*/*leu3*Δ::*C.m.LEU2 arg4*Δ/*arg4*Δ *leu2*Δ/*leu2*Δ *his1*Δ/*his1*Δ *URA3*/*ura3*Δ::*imm*^{434}*IRO1*/*iro1*Δ::*imm*^{434}

TF026	*zcf20*Δ::*C.d.HIS1*/*zcf20*Δ::*C.m.LEU2 arg4*Δ/*arg4*Δ *leu2*Δ/*leu2*Δ *his1*Δ/*his1*Δ *URA3*/*ura3*Δ::*imm*^{434}*IRO1*/*iro1*Δ::*imm*^{434}
TF027	*cta7*Δ::*C.d.HIS1*/*cta7*Δ::*C.m.LEU2 arg4*Δ/*arg4*Δ *leu2*Δ/*leu2*Δ *his1*Δ/*his1*Δ *URA3*/*ura3*Δ::*imm*^{434}*IRO1*/*iro1*Δ::*imm*^{434}
TF028	*rme1*Δ::*C.d.HIS1*/*rme1*Δ::*C.m.LEU2 arg4*Δ/*arg4*Δ *leu2*Δ/*leu2*Δ *his1*Δ/*his1*Δ *URA3*/*ura3*Δ::*imm*^{434}*IRO1*/*iro1*Δ::*imm*^{434}
TF029	*zcf23*Δ::*C.d.HIS1*/*zcf23*Δ::*C.m.LEU2 arg4*Δ/*arg4*Δ *leu2*Δ/*leu2*Δ *his1*Δ/*his1*Δ *URA3*/*ura3*Δ::*imm*^{434}*IRO1*/*iro1*Δ::*imm*^{434}
TF030	*zcf24*Δ::*C.d.HIS1*/*zcf24*Δ::*C.m.LEU2 arg4*Δ/*arg4*Δ *leu2*Δ/*leu2*Δ *his1*Δ/*his1*Δ *URA3*/*ura3*Δ::*imm*^{434}*IRO1*/*iro1*Δ::*imm*^{434}
TF031	*zcf25*Δ::*C.d.HIS1*/*zcf25*Δ::*C.m.LEU2 arg4*Δ/*arg4*Δ *leu2*Δ/*leu2*Δ *his1*Δ/*his1*Δ *URA3*/*ura3*Δ::*imm*^{434}*IRO1*/*iro1*Δ::*imm*^{434}
TF032	*rml1*Δ::*C.d.HIS1*/*rml1*Δ::*C.m.LEU2 arg4*Δ/*arg4*Δ *leu2*Δ/*leu2*Δ *his1*Δ/*his1*Δ *URA3*/*ura3*Δ::*imm*^{434}*IRO1*/*iro1*Δ::*imm*^{434}
TF033	*cas5*Δ::*C.d.HIS1*/*cas5*Δ::*C.m.LEU2 arg4*Δ/*arg4*Δ *leu2*Δ/*leu2*Δ *his1*Δ/*his1*Δ *URA3*/*ura3*Δ::*imm*^{434}*IRO1*/*iro1*Δ::*imm*^{434}
TF034	orf19.4722
TF035	*lys142*Δ::*C.d.HIS1*/*lys142*Δ::*C.m.LEU2 arg4*Δ/*arg4*Δ *leu2*Δ/*leu2*Δ *his1*Δ/*his1*Δ *URA3*/*ura3*Δ::*imm*^{434}*IRO1*/*iro1*Δ::*imm*^{434}
TF036	*hcm1*Δ::*C.d.HIS1*/*hcm1*Δ::*C.m.LEU2 arg4*Δ/*arg4*Δ *leu2*Δ/*leu2*Δ *his1*Δ/*his1*Δ *URA3*/*ura3*Δ::*imm*^{434}*IRO1*/*iro1*Δ::*imm*^{434}
TF037	*tye7*Δ::*C.d.HIS1*/*tye7*Δ::*C.m.LEU2 arg4*Δ/*arg4*Δ *leu2*Δ/*leu2*Δ *his1*Δ/*his1*Δ *URA3*/*ura3*Δ::*imm*^{434}*IRO1*/*iro1*Δ::*imm*^{434}
TF038	orf19.4972
TF039	*cup2*Δ::*C.d.HIS1*/*cup2*Δ::*C.m.LEU2 arg4*Δ/*arg4*Δ *leu2*Δ/*leu2*Δ *his1*Δ/*his1*Δ *URA3*/*ura3*Δ::*imm*^{434}*IRO1*/*iro1*Δ::*imm*^{434}
TF040	orf19.5026
TF041	*cat8*Δ::*C.d.HIS1*/*cat8*Δ::*C.m.LEU2 arg4*Δ/*arg4*Δ *leu2*Δ/*leu2*Δ *his1*Δ/*his1*Δ *URA3*/*ura3*Δ::*imm*^{434}*IRO1*/*iro1*Δ::*imm*^{434}
TF042	*zcf29*Δ::*C.d.HIS1*/*zcf29*Δ::*C.m.LEU2 arg4*Δ/*arg4*Δ *leu2*Δ/*leu2*Δ *his1*Δ/*his1*Δ *URA3*/*ura3*Δ::*imm*^{434}*IRO1*/*iro1*Δ::*imm*^{434}
TF043	*zcf30*Δ::*C.d.HIS1*/*zcf30*Δ::*C.m.LEU2 arg4*Δ/*arg4*Δ *leu2*Δ/*leu2*Δ *his1*Δ/*his1*Δ *URA3*/*ura3*Δ::*imm*^{434}*IRO1*/*iro1*Δ::*imm*^{434}
TF044	orf19.5326
TF045	*gal4*Δ::*C.d.HIS1*/*gal4*Δ::*C.m.LEU2 arg4*Δ/*arg4*Δ *leu2*Δ/*leu2*Δ *his1*Δ/*his1*Δ *URA3*/*ura3*Δ::*imm*^{434}*IRO1*/*iro1*Δ::*imm*^{434}
TF046	*lys144*Δ::*C.d.HIS1*/*lys144*Δ::*C.m.LEU2 arg4*Δ/*arg4*Δ *leu2*Δ/*leu2*Δ *his1*Δ/*his1*Δ *URA3*/*ura3*Δ::*imm*^{434}*IRO1*/*iro1*Δ::*imm*^{434}
TF047	*efh1*Δ::*C.d.HIS1*/*efh1*Δ::*C.m.LEU2 arg4*Δ/*arg4*Δ *leu2*Δ/*leu2*Δ *his1*Δ/*his1*Δ *URA3*/*ura3*Δ::*imm*^{434}*IRO1*/*iro1*Δ::*imm*^{434}
TF048	*lys14*Δ::*C.d.HIS1*/*lys14*Δ::*C.m.LEU2 arg4*Δ/*arg4*Δ *leu2*Δ/*leu2*Δ *his1*Δ/*his1*Δ *URA3*/*ura3*Δ::*imm*^{434}*IRO1*/*iro1*Δ::*imm*^{434}
TF049	orf19.5651
TF050	*cwt1*Δ::*C.d.HIS1*/*cwt1*Δ::*C.m.LEU2 arg4*Δ/*arg4*Δ *leu2*Δ/*leu2*Δ *his1*Δ/*his1*Δ *URA3*/*ura3*Δ::*imm*^{434}*IRO1*/*iro1*Δ::*imm*^{434}
TF051	*mbp1*Δ::*C.d.HIS1*/*mbp1*Δ::*C.m.LEU2 arg4*Δ/*arg4*Δ *leu2*Δ/*leu2*Δ *his1*Δ/*his1*Δ *URA3*/*ura3*Δ::*imm*^{434}*IRO1*/*iro1*Δ::*imm*^{434}
TF052	*stp3*Δ::*C.d.HIS1*/*stp3*Δ::*C.m.LEU2 arg4*Δ/*arg4*Δ *leu2*Δ/*leu2*Δ *his1*Δ/*his1*Δ *URA3*/*ura3*Δ::*imm*^{434}*IRO1*/*iro1*Δ::*imm*^{434}
TF053	*zcf31*Δ::*C.d.HIS1*/*zcf1*Δ::*C.m.LEU2 arg4*Δ/*arg4*Δ *leu2*Δ/*leu2*Δ *his1*Δ/*his1*Δ *URA3*/*ura3*Δ::*imm*^{434}*IRO1*/*iro1*Δ::*imm*^{434}
TF054	*zcf32*Δ::*C.d.HIS1*/*zcf32*Δ::*C.m.LEU2 arg4*Δ/*arg4*Δ *leu2*Δ/*leu2*Δ *his1*Δ/*his1*Δ *URA3*/*ura3*Δ::*imm*^{434}*IRO1*/*iro1*Δ::*imm*^{434}

TF055	*try4*Δ::*C.d.HIS1*/*try4*Δ::*C.m.LEU2 arg4*Δ/*arg4*Δ *leu2*Δ/*leu2*Δ *his1*Δ/*his1*Δ *URA3*/*ura3*Δ::*imm*^{434}*IRO1*/*iro1*Δ::*imm*^{434}
TF056	*wor2*Δ::*C.d.HIS1*/*wor2*Δ::*C.m.LEU2 arg4*Δ/*arg4*Δ *leu2*Δ/*leu2*Δ *his1*Δ/*his1*Δ *URA3*/*ura3*Δ::*imm*^{434}*IRO1*/*iro1*Δ::*imm*^{434}
TF057	*uga32*Δ::*C.d.HIS1*/*uga32*Δ::*C.m.LEU2 arg4*Δ/*arg4*Δ *leu2*Δ/*leu2*Δ *his1*Δ/*his1*Δ *URA3*/*ura3*Δ::*imm*^{434}*IRO1*/*iro1*Δ::*imm*^{434}
TF058	*rca1*Δ::*C.d.HIS1*/*rca1*Δ::*C.m.LEU2 arg4*Δ/*arg4*Δ *leu2*Δ/*leu2*Δ *his1*Δ/*his1*Δ *URA3*/*ura3*Δ::*imm*^{434}*IRO1*/*iro1*Δ::*imm*^{434}
TF059	*ace2*Δ::*C.d.HIS1*/*ace2*Δ::*C.m.LEU2 arg4*Δ/*arg4*Δ *leu2*Δ/*leu2*Δ *his1*Δ/*his1*Δ *URA3*/*ura3*Δ::*imm*^{434}*IRO1*/*iro1*Δ::*imm*^{434}
TF060	*zcf32*Δ::*C.d.HIS1*/*zcf32*Δ::*C.m.LEU2 arg4*Δ/*arg4*Δ *leu2*Δ/*leu2*Δ *his1*Δ/*his1*Δ *URA3*/*ura3*Δ::*imm*^{434}*IRO1*/*iro1*Δ::*imm*^{434}
TF061	*cup9*Δ::*C.d.HIS1*/*cup9*Δ::*C.m.LEU2 arg4*Δ/*arg4*Δ *leu2*Δ/*leu2*Δ *his1*Δ/*his1*Δ *URA3*/*ura3*Δ::*imm*^{434}*IRO1*/*iro1*Δ::*imm*^{434}
TF062	*try6*Δ::*C.d.HIS1*/*try6*Δ::*C.m.LEU2 arg4*Δ/*arg4*Δ *leu2*Δ/*leu2*Δ *his1*Δ/*his1*Δ *URA3*/*ura3*Δ::*imm*^{434}*IRO1*/*iro1*Δ::*imm*^{434}
TF063	orf19.6874
TF064	*yox1*Δ::*C.d.HIS1*/*yox1*Δ::*C.m.LEU2 arg4*Δ/*arg4*Δ *leu2*Δ/*leu2*Δ *his1*Δ/*his1*Δ *URA3*/*ura3*Δ::*imm*^{434}*IRO1*/*iro1*Δ::*imm*^{434}
TF065	*mac1*Δ::*C.d.HIS1*/*mac1*Δ::*C.m.LEU2 arg4*Δ/*arg4*Δ *leu2*Δ/*leu2*Δ *his1*Δ/*his1*Δ *URA3*/*ura3*Δ::*imm*^{434}*IRO1*/*iro1*Δ::*imm*^{434}
TF066	*uga33*Δ::*C.d.HIS1*/*uga33*Δ::*C.m.LEU2 arg4*Δ/*arg4*Δ *leu2*Δ/*leu2*Δ *his1*Δ/*his1*Δ *URA3*/*ura3*Δ::*imm*^{434}*IRO1*/*iro1*Δ::*imm*^{434}
TF067	*suc1*Δ::*C.d.HIS1*/*suc1*Δ::*C.m.LEU2 arg4*Δ/*arg4*Δ *leu2*Δ/*leu2*Δ *his1*Δ/*his1*Δ *URA3*/*ura3*Δ::*imm*^{434}*IRO1*/*iro1*Δ::*imm*^{434}
TF068	*crz1*Δ::*C.d.HIS1*/*crz1*Δ::*C.m.LEU2 arg4*Δ/*arg4*Δ *leu2*Δ/*leu2*Δ *his1*Δ/*his1*Δ *URA3*/*ura3*Δ::*imm*^{434}*IRO1*/*iro1*Δ::*imm*^{434}
TF069	*mrr1*Δ::*C.d.HIS1*/*mrr1*Δ::*C.m.LEU2 arg4*Δ/*arg4*Δ *leu2*Δ/*leu2*Δ *his1*Δ/*his1*Δ *URA3*/*ura3*Δ::*imm*^{434}*IRO1*/*iro1*Δ::*imm*^{434}
TF070	*cta4*Δ::*C.d.HIS1*/*cta4*Δ::*C.m.LEU2 arg4*Δ/*arg4*Δ *leu2*Δ/*leu2*Δ *his1*Δ/*his1*Δ *URA3*/*ura3*Δ::*imm*^{434}*IRO1*/*iro1*Δ::*imm*^{434}
TF071	*zcf38*Δ::*C.d.HIS1*/*zcf38*Δ::*C.m.LEU2 arg4*Δ/*arg4*Δ *leu2*Δ/*leu2*Δ *his1*Δ/*his1*Δ *URA3*/*ura3*Δ::*imm*^{434}*IRO1*/*iro1*Δ::*imm*^{434}
TF072	*uga3*Δ::*C.d.HIS1*/*uga3*Δ::*C.m.LEU2 arg4*Δ/*arg4*Δ *leu2*Δ/*leu2*Δ *his1*Δ/*his1*Δ *URA3*/*ura3*Δ::*imm*^{434}*IRO1*/*iro1*Δ::*imm*^{434}
TF073	*zcf39*Δ::*C.d.HIS1*/*zcf39*Δ::*C.m.LEU2 arg4*Δ/*arg4*Δ *leu2*Δ/*leu2*Δ *his1*Δ/*his1*Δ *URA3*/*ura3*Δ::*imm*^{434}*IRO1*/*iro1*Δ::*imm*^{434}
TF074	*asg1*Δ::*C.d.HIS1*/*asg1*Δ::*C.m.LEU2 arg4*Δ/*arg4*Δ *leu2*Δ/*leu2*Δ *his1*Δ/*his1*Δ *URA3*/*ura3*Δ::*imm*^{434}*IRO1*/*iro1*Δ::*imm*^{434}
TF075	orf19.217
TF076	*zcf1*Δ::*C.d.HIS1*/*zcf1*Δ::*C.m.LEU2 arg4*Δ/*arg4*Δ *leu2*Δ/*leu2*Δ *his1*Δ/*his1*Δ *URA3*/*ura3*Δ::*imm*^{434}*IRO1*/*iro1*Δ::*imm*^{434}
TF077	*upc2*Δ::*C.d.HIS1*/*upc2*Δ::*C.m.LEU2 arg4*Δ/*arg4*Δ *leu2*Δ/*leu2*Δ *his1*Δ/*his1*Δ *URA3*/*ura3*Δ::*imm*^{434}*IRO1*/*iro1*Δ::*imm*^{434}
TF078	*zcf2*Δ::*C.d.HIS1*/*zcf2*Δ::*C.m.LEU2 arg4*Δ/*arg4*Δ *leu2*Δ/*leu2*Δ *his1*Δ/*his1*Δ *URA3*/*ura3*Δ::*imm*^{434}*IRO1*/*iro1*Δ::*imm*^{434}
TF079	*hap31*Δ::*C.d.HIS1*/*hap31*Δ::*C.m.LEU2 arg4*Δ/*arg4*Δ *leu2*Δ/*leu2*Δ *his1*Δ/*his1*Δ *URA3*/*ura3*Δ::*imm*^{434}*IRO1*/*iro1*Δ::*imm*^{434}
TF080	*hap43*Δ::*C.d.HIS1*/*hap43*Δ::*C.m.LEU2 arg4*Δ/*arg4*Δ *leu2*Δ/*leu2*Δ *his1*Δ/*his1*Δ *URA3*/*ura3*Δ::*imm*^{434}*IRO1*/*iro1*Δ::*imm*^{434}
TF081	*ino4*Δ::*C.d.HIS1*/*ino4*Δ::*C.m.LEU2 arg4*Δ/*arg4*Δ *leu2*Δ/*leu2*Δ *his1*Δ/*his1*Δ *URA3*/*ura3*Δ::*imm*^{434}*IRO1*/*iro1*Δ::*imm*^{434}
TF082	*stp4*Δ::*C.d.HIS1*/*stp4*Δ::*C.m.LEU2 arg4*Δ/*arg4*Δ *leu2*Δ/*leu2*Δ *his1*Δ/*his1*Δ *URA3*/*ura3*Δ::*imm*^{434}*IRO1*/*iro1*Δ::*imm*^{434}
TF083	*skn7*Δ::*C.d.HIS1*/*skn7*Δ::*C.m.LEU2 arg4*Δ/*arg4*Δ *leu2*Δ/*leu2*Δ *his1*Δ/*his1*Δ *URA3*/*ura3*Δ::*imm*^{434}*IRO1*/*iro1*Δ::*imm*^{434}

TF084	*sko1Δ::C.d.HIS1/sko1Δ::C.m.LEU2 arg4Δ/arg4Δ leu2Δ/leu2Δ his1Δ/his1Δ URA3/ura3Δ::imm^{434}IRO1/iro1Δ::imm^{434}*
TF085	*war1Δ::C.d.HIS1/war1Δ::C.m.LEU2 arg4Δ/arg4Δ leu2Δ/leu2Δ his1Δ/his1Δ URA3/ura3Δ::imm^{434}IRO1/iro1Δ::imm^{434}*
TF086	*zcf3Δ::C.d.HIS1/zcf3Δ::C.m.LEU2 arg4Δ/arg4Δ leu2Δ/leu2Δ his1Δ/his1Δ URA3/ura3Δ::imm^{434}IRO1/iro1Δ::imm^{434}*
TF087	*hap2Δ::C.d.HIS1/hap2Δ::C.m.LEU2 arg4Δ/arg4Δ leu2Δ/leu2Δ his1Δ/his1Δ URA3/ura3Δ::imm^{434}IRO1/iro1Δ::imm^{434}*
TF088	orf19.1274
TF089	orf19.1496
TF090	*Opi1Δ::C.d.HIS1/opi1Δ::C.m.LEU2 arg4Δ/arg4Δ leu2Δ/leu2Δ his1Δ/his1Δ URA3/ura3Δ::imm^{434}IRO1/iro1Δ::imm^{434}*
TF091	*zcf7Δ::C.d.HIS1/zcf7Δ::C.m.LEU2 arg4Δ/arg4Δ leu2Δ/leu2Δ his1Δ/his1Δ URA3/ura3Δ::imm^{434}IRO1/iro1Δ::imm^{434}*
TF092	*sef2Δ::C.d.HIS1/sef2Δ::C.m.LEU2 arg4Δ/arg4Δ leu2Δ/leu2Δ his1Δ/his1Δ URA3/ura3Δ::imm^{434}IRO1/iro1Δ::imm^{434}*
TF093	*hap5Δ::C.d.HIS1/hap5Δ::C.m.LEU2 arg4Δ/arg4Δ leu2Δ/leu2Δ his1Δ/his1Δ URA3/ura3Δ::imm^{434}IRO1/iro1Δ::imm^{434}*
TF094	orf19.2088
TF095	*ndt80Δ::C.d.HIS1/ndt80Δ::C.m.LEU2 arg4Δ/arg4Δ leu2Δ/leu2Δ his1Δ/his1Δ URA3/ura3Δ::imm^{434}IRO1/iro1Δ::imm^{434}*
TF096	*crz2Δ::C.d.HIS1/crz2Δ::C.m.LEU2 arg4Δ/arg4Δ leu2Δ/leu2Δ his1Δ/his1Δ URA3/ura3Δ::imm^{434}IRO1/iro1Δ::imm^{434}*
TF097	orf19.2476
TF098	*ume7Δ::C.d.HIS1/ume7Δ::C.m.LEU2 arg4Δ/arg4Δ leu2Δ/leu2Δ his1Δ/his1Δ URA3/ura3Δ::imm^{434}IRO1/iro1Δ::imm^{434}*
TF099	*zcf15Δ::C.d.HIS1/zcf15Δ::C.m.LEU2 arg4Δ/arg4Δ leu2Δ/leu2Δ his1Δ/his1Δ URA3/ura3Δ::imm^{434}IRO1/iro1Δ::imm^{434}*
TF100	*zcf16Δ::C.d.HIS1/zcf16Δ::C.m.LEU2 arg4Δ/arg4Δ leu2Δ/leu2Δ his1Δ/his1Δ URA3/ura3Δ::imm^{434}IRO1/iro1Δ::imm^{434}*
TF101	*gzf3Δ::C.d.HIS1/gzf3Δ::C.m.LEU2 arg4Δ/arg4Δ leu2Δ/leu2Δ his1Δ/his1Δ URA3/ura3Δ::imm^{434}IRO1/iro1Δ::imm^{434}*
TF102	orf19.2961
TF103	*hfl1Δ::C.d.HIS1/hfl1Δ::C.m.LEU2 arg4Δ/arg4Δ leu2Δ/leu2Δ his1Δ/his1Δ URA3/ura3Δ::imm^{434}IRO1/iro1Δ::imm^{434}*
TF104	*czf1Δ::C.d.HIS1/czf1Δ::C.m.LEU2 arg4Δ/arg4Δ leu2Δ/leu2Δ his1Δ/his1Δ URA3/ura3Δ::imm^{434}IRO1/iro1Δ::imm^{434}*
TF105	orf19.3625
TF106	*csr1Δ::C.d.HIS1/csr1Δ::C.m.LEU2 arg4Δ/arg4Δ leu2Δ/leu2Δ his1Δ/his1Δ URA3/ura3Δ::imm^{434}IRO1/iro1Δ::imm^{434}*
TF107	*mig1Δ::C.d.HIS1/mig1Δ::C.m.LEU2 arg4Δ/arg4Δ leu2Δ/leu2Δ his1Δ/his1Δ URA3/ura3Δ::imm^{434}IRO1/iro1Δ::imm^{434}*
TF108	*hap3Δ::C.d.HIS1/hap3Δ::C.m.LEU2 arg4Δ/arg4Δ leu2Δ/leu2Δ his1Δ/his1Δ URA3/ura3Δ::imm^{434}IRO1/iro1Δ::imm^{434}*
TF109	*msn4Δ::C.d.HIS1/msn4Δ::C.m.LEU2 arg4Δ/arg4Δ leu2Δ/leu2Δ his1Δ/his1Δ URA3/ura3Δ::imm^{434}IRO1/iro1Δ::imm^{434}*
TF110	*rob1Δ::C.d.HIS1/rob1Δ::C.m.LEU2 arg4Δ/arg4Δ leu2Δ/leu2Δ his1Δ/his1Δ URA3/ura3Δ::imm^{434}IRO1/iro1Δ::imm^{434}*
TF111	orf19.5249
TF112	*ash1Δ::C.d.HIS1/ash1Δ::C.m.LEU2 arg4Δ/arg4Δ leu2Δ/leu2Δ his1Δ/his1Δ URA3/ura3Δ::imm^{434}IRO1/iro1Δ::imm^{434}*

TF113	*rbf1*Δ::*C.d.HIS1*/*rbf1*Δ::*C.m.LEU2 arg4*Δ/*arg4*Δ *leu2*Δ/*leu2*Δ *his1*Δ/*his1*Δ *URA3*/*ura3*Δ::*imm*^{434}*IRO1*/*iro1*Δ::*imm*^{434}
TF114	*fgr17*Δ::*C.d.HIS1*/*fgr17*Δ::*C.m.LEU2 arg4*Δ/*arg4*Δ *leu2*Δ/*leu2*Δ *his1*Δ/*his1*Δ *URA3*/*ura3*Δ::*imm*^{434}*IRO1*/*iro1*Δ::*imm*^{434}
TF115	*tec1*Δ::*C.d.HIS1*/*tec1*Δ::*C.m.LEU2 arg4*Δ/*arg4*Δ *leu2*Δ/*leu2*Δ *his1*Δ/*his1*Δ *URA3*/*ura3*Δ::*imm*^{434}*IRO1*/*iro1*Δ::*imm*^{434}
TF116	orf19.5910
TF117	*tup1*Δ::*C.d.HIS1*/*tup1*Δ::*C.m.LEU2 arg4*Δ/*arg4*Δ *leu2*Δ/*leu2*Δ *his1*Δ/*his1*Δ *URA3*/*ura3*Δ::*imm*^{434}*IRO1*/*iro1*Δ::*imm*^{434}
TF118	*mnl1*Δ::*C.d.HIS1*/*mnl1*Δ::*C.m.LEU2 arg4*Δ/*arg4*Δ *leu2*Δ/*leu2*Δ *his1*Δ/*his1*Δ *URA3*/*ura3*Δ::*imm*^{434}*IRO1*/*iro1*Δ::*imm*^{434}
TF119	*fgr27*Δ::*C.d.HIS1*/*fgr27*Δ::*C.m.LEU2 arg4*Δ/*arg4*Δ *leu2*Δ/*leu2*Δ *his1*Δ/*his1*Δ *URA3*/*ura3*Δ::*imm*^{434}*IRO1*/*iro1*Δ::*imm*^{434}
TF120	*zfu2*Δ::*C.d.HIS1*/*zfu2*Δ::*C.m.LEU2 arg4*Δ/*arg4*Δ *leu2*Δ/*leu2*Δ *his1*Δ/*his1*Δ *URA3*/*ura3*Δ::*imm*^{434}*IRO1*/*iro1*Δ::*imm*^{434}
TF121	*ssn6*Δ::*C.d.HIS1*/*ssn6*Δ::*C.m.LEU2 arg4*Δ/*arg4*Δ *leu2*Δ/*leu2*Δ *his1*Δ/*his1*Δ *URA3*/*ura3*Δ::*imm*^{434}*IRO1*/*iro1*Δ::*imm*^{434}
TF122	*fcr1*Δ::*C.d.HIS1*/*fcr1*Δ::*C.m.LEU2 arg4*Δ/*arg4*Δ *leu2*Δ/*leu2*Δ *his1*Δ/*his1*Δ *URA3*/*ura3*Δ::*imm*^{434}*IRO1*/*iro1*Δ::*imm*^{434}
TF123	orf19.6888
TF124	*tea1*Δ::*C.d.HIS1*/*tea1*Δ::*C.m.LEU2 arg4*Δ/*arg4*Δ *leu2*Δ/*leu2*Δ *his1*Δ/*his1*Δ *URA3*/*ura3*Δ::*imm*^{434}*IRO1*/*iro1*Δ::*imm*^{434}
TF125	*nrg1*Δ::*C.d.HIS1*/*nrg1*Δ::*C.m.LEU2 arg4*Δ/*arg4*Δ *leu2*Δ/*leu2*Δ *his1*Δ/*his1*Δ *URA3*/*ura3*Δ::*imm*^{434}*IRO1*/*iro1*Δ::*imm*^{434}
TF126	*rim101*Δ::*C.d.HIS1*/*rim101*Δ::*C.m.LEU2 arg4*Δ/*arg4*Δ *leu2*Δ/*leu2*Δ *his1*Δ/*his1*Δ *URA3*/*ura3*Δ::*imm*^{434}*IRO1*/*iro1*Δ::*imm*^{434}
TF127	*isw2*Δ::*C.d.HIS1*/*isw2*Δ::*C.m.LEU2 arg4*Δ/*arg4*Δ *leu2*Δ/*leu2*Δ *his1*Δ/*his1*Δ *URA3*/*ura3*Δ::*imm*^{434}*IRO1*/*iro1*Δ::*imm*^{434}
TF128	*aaf1*Δ::*C.d.HIS1*/*aaf1*Δ::*C.m.LEU2 arg4*Δ/*arg4*Δ *leu2*Δ/*leu2*Δ *his1*Δ/*his1*Δ *URA3*/*ura3*Δ::*imm*^{434}*IRO1*/*iro1*Δ::*imm*^{434}
TF129	*fcr3*Δ::*C.d.HIS1*/*fcr3*Δ::*C.m.LEU2 arg4*Δ/*arg4*Δ *leu2*Δ/*leu2*Δ *his1*Δ/*his1*Δ *URA3*/*ura3*Δ::*imm*^{434}*IRO1*/*iro1*Δ::*imm*^{434}
TF130	*arg81*Δ::*C.d.HIS1*/*arg81*Δ::*C.m.LEU2 arg4*Δ/*arg4*Δ *leu2*Δ/*leu2*Δ *his1*Δ/*his1*Δ *URA3*/*ura3*Δ::*imm*^{434}*IRO1*/*iro1*Δ::*imm*^{434}
TF131	*zcf35*Δ::*C.d.HIS1*/*zcf35*Δ::*C.m.LEU2 arg4*Δ/*arg4*Δ *leu2*Δ/*leu2*Δ *his1*Δ/*his1*Δ *URA3*/*ura3*Δ::*imm*^{434}*IRO1*/*iro1*Δ::*imm*^{434}
TF132	*ahr1*Δ::*C.d.HIS1*/*ahr1*Δ::*C.m.LEU2 arg4*Δ/*arg4*Δ *leu2*Δ/*leu2*Δ *his1*Δ/*his1*Δ *URA3*/*ura3*Δ::*imm*^{434}*IRO1*/*iro1*Δ::*imm*^{434}
TF133	*znc1*Δ::*C.d.HIS1*/*znc1*Δ::*C.m.LEU2 arg4*Δ/*arg4*Δ *leu2*Δ/*leu2*Δ *his1*Δ/*his1*Δ *URA3*/*ura3*Δ::*imm*^{434}*IRO1*/*iro1*Δ::*imm*^{434}
TF134	*sw14*Δ::*C.d.HIS1*/*sw14*Δ::*C.m.LEU2 arg4*Δ/*arg4*Δ *leu2*Δ/*leu2*Δ *his1*Δ/*his1*Δ *URA3*/*ura3*Δ::*imm*^{434}*IRO1*/*iro1*Δ::*imm*^{434}
TF135	*zcf26*Δ::*C.d.HIS1*/*zcf26*Δ::*C.m.LEU2 arg4*Δ/*arg4*Δ *leu2*Δ/*leu2*Δ *his1*Δ/*his1*Δ *URA3*/*ura3*Δ::*imm*^{434}*IRO1*/*iro1*Δ::*imm*^{434}
TF136	orf19.173
TF137	*bcr1*Δ::*C.d.HIS1*/*bcr1*Δ::*C.m.LEU2 arg4*Δ/*arg4*Δ *leu2*Δ/*leu2*Δ *his1*Δ/*his1*Δ *URA3*/*ura3*Δ::*imm*^{434}*IRO1*/*iro1*Δ::*imm*^{434}
TF138	*cph2*Δ::*C.d.HIS1*/*cph2*Δ::*C.m.LEU2 arg4*Δ/*arg4*Δ *leu2*Δ/*leu2*Δ *his1*Δ/*his1*Δ *URA3*/*ura3*Δ::*imm*^{434}*IRO1*/*iro1*Δ::*imm*^{434}
TF139	*gat1*Δ::*C.d.HIS1*/*gat1*Δ::*C.m.LEU2 arg4*Δ/*arg4*Δ *leu2*Δ/*leu2*Δ *his1*Δ/*his1*Δ *URA3*/*ura3*Δ::*imm*^{434}*IRO1*/*iro1*Δ::*imm*^{434}
TF140	*cap1*Δ::*C.d.HIS1*/*cap1*Δ::*C.m.LEU2 arg4*Δ/*arg4*Δ *leu2*Δ/*leu2*Δ *his1*Δ/*his1*Δ *URA3*/*ura3*Δ::*imm*^{434}*IRO1*/*iro1*Δ::*imm*^{434}
TF141	*zcf8*Δ::*C.d.HIS1*/*zcf8*Δ::*C.m.LEU2 arg4*Δ/*arg4*Δ *leu2*Δ/*leu2*Δ *his1*Δ/*his1*Δ *URA3*/*ura3*Δ::*imm*^{434}*IRO1*/*iro1*Δ::*imm*^{434}

TF142	orf19.2315
TF143	orf19.2612
TF144	*zis2*Δ::*C.d.HIS1*/*zis2*Δ::*C.m.LEU2 arg4*Δ/*arg4*Δ *leu2*Δ/*leu2*Δ *his1*Δ/*his1*Δ *URA3*/*ura3*Δ::*imm*^{434}*IRO1*/*iro1*Δ::*imm*^{434}
TF145	*kar4*Δ::*C.d.HIS1*/*kar4*Δ::*C.m.LEU2 arg4*Δ/*arg4*Δ *leu2*Δ/*leu2*Δ *his1*Δ/*his1*Δ *URA3*/*ura3*Δ::*imm*^{434}*IRO1*/*iro1*Δ::*imm*^{434}
TF146	*zcf28*Δ::*C.d.HIS1*/*zcf28*Δ::*C.m.LEU2 arg4*Δ/*arg4*Δ *leu2*Δ/*leu2*Δ *his1*Δ/*his1*Δ *URA3*/*ura3*Δ::*imm*^{434}*IRO1*/*iro1*Δ::*imm*^{434}
TF147	*sfu1*Δ::*C.d.HIS1*/*sfu1*Δ::*C.m.LEU2 arg4*Δ/*arg4*Δ *leu2*Δ/*leu2*Δ *his1*Δ/*his1*Δ *URA3*/*ura3*Δ::*imm*^{434}*IRO1*/*iro1*Δ::*imm*^{434}
TF148	*zcf4*Δ::*C.d.HIS1*/*zcf4*Δ::*C.m.LEU2 arg4*Δ/*arg4*Δ *leu2*Δ/*leu2*Δ *his1*Δ/*his1*Δ *URA3*/*ura3*Δ::*imm*^{434}*IRO1*/*iro1*Δ::*imm*^{434}
TF149	*zcf5*Δ::*C.d.HIS1*/*zcf5*Δ::*C.m.LEU2 arg4*Δ/*arg4*Δ *leu2*Δ/*leu2*Δ *his1*Δ/*his1*Δ *URA3*/*ura3*Δ::*imm*^{434}*IRO1*/*iro1*Δ::*imm*^{434}
TF150	*zcf6*Δ::*C.d.HIS1*/*zcf6*Δ::*C.m.LEU2 arg4*Δ/*arg4*Δ *leu2*Δ/*leu2*Δ *his1*Δ/*his1*Δ *URA3*/*ura3*Δ::*imm*^{434}*IRO1*/*iro1*Δ::*imm*^{434}
TF151	orf19.1577
TF152	*fgr15*Δ::*C.d.HIS1*/*fgr15*Δ::*C.m.LEU2 arg4*Δ/*arg4*Δ *leu2*Δ/*leu2*Δ *his1*Δ/*his1*Δ *URA3*/*ura3*Δ::*imm*^{434}*IRO1*/*iro1*Δ::*imm*^{434}
TF153	*aro80*Δ::*C.d.HIS1*/*aro80*Δ::*C.m.LEU2 arg4*Δ/*arg4*Δ *leu2*Δ/*leu2*Δ *his1*Δ/*his1*Δ *URA3*/*ura3*Δ::*imm*^{434}*IRO1*/*iro1*Δ::*imm*^{434}
TF154	*zcf27*Δ::*C.d.HIS1*/*zcf27*Δ::*C.m.LEU2 arg4*Δ/*arg4*Δ *leu2*Δ/*leu2*Δ *his1*Δ/*his1*Δ *URA3*/*ura3*Δ::*imm*^{434}*IRO1*/*iro1*Δ::*imm*^{434}
TF155	*dal81*Δ::*C.d.HIS1*/*dal81*Δ::*C.m.LEU2 arg4*Δ/*arg4*Δ *leu2*Δ/*leu2*Δ *his1*Δ/*his1*Δ *URA3*/*ura3*Δ::*imm*^{434}*IRO1*/*iro1*Δ::*imm*^{434}
TF156	*efg1*Δ::*C.d.HIS1*/*efg1*Δ::*C.m.LEU2 arg4*Δ/*arg4*Δ *leu2*Δ/*leu2*Δ *his1*Δ/*his1*Δ *URA3*/*ura3*Δ::*imm*^{434}*IRO1*/*iro1*Δ::*imm*^{434}
TF157	orf19.1150
TF158	*rap1*Δ::*C.d.HIS1*/*rap1*Δ::*C.m.LEU2 arg4*Δ/*arg4*Δ *leu2*Δ/*leu2*Δ *his1*Δ/*his1*Δ *URA3*/*ura3*Δ::*imm*^{434}*IRO1*/*iro1*Δ::*imm*^{434}
TF159	orf19.1757
TF160	orf19.2743
TF161	*lys143*Δ::*C.d.HIS1*/*lys143*Δ::*C.m.LEU2 arg4*Δ/*arg4*Δ *leu2*Δ/*leu2*Δ *his1*Δ/*his1*Δ *URA3*/*ura3*Δ::*imm*^{434}*IRO1*/*iro1*Δ::*imm*^{434}
TF162	*stp2*Δ::*C.d.HIS1*/*stp2*Δ::*C.m.LEU2 arg4*Δ/*arg4*Δ *leu2*Δ/*leu2*Δ *his1*Δ/*his1*Δ *URA3*/*ura3*Δ::*imm*^{434}*IRO1*/*iro1*Δ::*imm*^{434}
TF163	*rfx1*Δ::*C.d.HIS1*/*rfx1*Δ::*C.m.LEU2 arg4*Δ/*arg4*Δ *leu2*Δ/*leu2*Δ *his1*Δ/*his1*Δ *URA3*/*ura3*Δ::*imm*^{434}*IRO1*/*iro1*Δ::*imm*^{434}
TF164	*rgt1*Δ::*C.d.HIS1*/*rgt1*Δ::*C.m.LEU2 arg4*Δ/*arg4*Δ *leu2*Δ/*leu2*Δ *his1*Δ/*his1*Δ *URA3*/*ura3*Δ::*imm*^{434}*IRO1*/*iro1*Δ::*imm*^{434}
TF165	*ppr1*Δ::*C.d.HIS1*/*ppr1*Δ::*C.m.LEU2 arg4*Δ/*arg4*Δ *leu2*Δ/*leu2*Δ *his1*Δ/*his1*Δ *URA3*/*ura3*Δ::*imm*^{434}*IRO1*/*iro1*Δ::*imm*^{434}